University of Southampton

Faculty of Engineering and Physical Sciences

Zepler Institute

Rapid point-of-care testing solutions to meet clinical needs

DOI: 10.5258/SOTON/D2308

by

Alice Hannah Iles

ORCID ID [0000-0003-0808-5582]

Thesis for the degree of Doctor of Philosophy

October 2022

University of Southampton

Abstract

Faculty of Engineering and Physical Sciences

Zepler Institute

Doctor of Philosophy

Rapid point-of-care testing solutions to meet clinical needs

by

Alice Hannah Iles

There is increasing demand for point-of-care testing solutions for both the diagnosis and monitoring of diseases. As has been demonstrated during the pandemic, paper-based lateral flow devices are an excellent candidate for rapid and large population testing providing a binary yes or no answer for the presence of a single covid-specific biomarker. For these devices to be most effective and more widely applicable they instead require to be quantitative and deliver multiplexing capabilities, i.e., be able to measure simultaneously more than one disease biomarker.

In this thesis the focus is on the inclusion of the above capabilities into create the next generation of lateral flow devices (LFDs) for wider clinical applications. Using the laser-based direct-write (LDW) technique that implements polymerisation of a photopolymer to produce impermeable barriers within the porous membranes inside a LFD I have demonstrated the use of multiple parallel channels for multiplexed detection whilst removing issues such as cross reactivity and the requirement for tests with larger footprints that ensue a higher cost. This multiple channel flow architecture was also utilised to add semi-quantitative measurement capabilities to the LFD. Further the thesis also explored the use of passive flow control within the LFDs enabled via precise laser-patterning of flow constrictions. The constrictions generate a delay in the flow at given points along the LFD and assist in enhancing their detection capabilities, i.e., their sensitivity.

These techniques were applied to demonstrate a multiplexed screening test for Tuberculosis that meets real world requirements. This thesis presents a rapid detection of blood-based biomarkers: CRP, SAA1, LBP and CFHR5 with a multiplexed lateral flow test that has the capability to distinguish those patients with TB from healthy controls with significant accuracy. The diagnostic competence expressed in the form of area under the curve (AUC) was 0.92 for the best two biomarkers and its sensitivity and specificity meets the WHO guidelines for a TB rule-out screening test. Tuberculosis was responsible for 10 million cases globally in 2019 and despite huge efforts the numbers are still increasing.

Table of Contents

Table of Tables

Table of Figures

Table of Figures

Table of Figures

Table of Figures

Research Thesis: Declaration of Authorship

Print name: Alice Iles

Title of thesis: Rapid point-of-care testing solutions to meet clinical needs

I declare that this thesis and the work presented in it are my own and has been generated by me as the result of my own original research.

I confirm that:

1. This work was done wholly or mainly while in candidature for a research degree at this University;
2. Where any part of this thesis has previously been submitted for a degree or any other qualification at this University or any other institution, this has been clearly stated;
3. Where I have consulted the published work of others, this is always clearly attributed;
4. Where I have quoted from the work of others, the source is always given. With the exception of such quotations, this thesis is entirely my own work;
5. I have acknowledged all main sources of help;
6. Where the thesis is based on work done by myself jointly with others, I have made clear exactly what was done by others and what I have contributed myself;
7. Parts of this work have been published as:-
    - Iles, A.H., et al., Semi-quantitative detection of inflammatory biomarkers using a laser-patterned multiplexed lateral flow device. Talanta, 2022. **237**: p. 122944.
    - Iles, A.H., et al., Optimization of flow path parameters for enhanced sensitivity lateral flow devices. Talanta, 2022: p. 123579.

Signature: ..... Date: ……

Acknowledgements

I would like to start by thanking my supervisors, Dr Collin Sones, Professor Rob Eason and Professor Paul Elkington. Not just for reading my thesis chapters, or my manuscripts or posters or power point presentations, but for their on-going support throughout the PhD; for being understanding, compassionate and human. A special thank you to Peijun He, without whom I would have broken a lot more things and made many more mistakes. Thank you to the wider team, Ioannis Katis, Panos Galanis and Anto John for all their help with using equipment, paper writing and sharing a laugh! Thank you to my friends and family that despite not having undertaken a PhD or really knowing what I do on a daily basis, are my biggest cheer-leaders nonetheless. My parents, who have always encouraged me to do whatever makes me happy, for their continued and generous emotional and financial support. To everyone that has listened to me talk about PhD over the last three and a half years, and to those people I have met along the way that have made the experience such an enjoyable one.

Definitions and Abbreviations

AD ..... Alzheimer's disease

ATB..... Active Tuberculosis

AuNP ..... Gold nanoparticles

BSA..... Bovine serum albumin

CFHR5 ..... Complement factor H related protein 5

CN ..... Cognitively normal

CRP..... C reactive protein

CSF ..... Cerebral spinal fluid

c.w..... Continuous wave

DEM ..... Dementia

DI..... Deionised

ED..... Emergency department

ELISA ..... Enzyme linked immunosorbent assay

HIV ..... Human immunodeficiency virus

ICAM1 ..... Intracellular adhesion molecule 1

IL ..... Interleukin

IPA..... Isopropyl alcohol

LBP ..... Lipopolysaccharide binding protein

LDW ..... Laser direct write

LFA ..... Lateral flow assay

LFD ..... Lateral flow device

LFT..... Lateral flow test

LOC..... Lab-on-chip

LOB..... Limit of blank

LOD ..... Limit of detection

LPS..... Lipopolysaccharide

MDR-TB..... Multidrug resistant tuberculosis

MR-pro-ADM.....Mid regional pro-adrenomedullin

Mtb.....Mycobacterium tuberculosis

NC.....Nitrocellulose

PBS .....Phosphate buffered saline

PCT .....Procalcitonin

POC.....Point-of-care

ROC.....Receiver operating characteristic

SAA1 .....Serum amyloid A1

SEM .....Scanning electron microscope

SSAO.....semicarbazide-sensitive amine oxidase

TB .....Tuberculosis

TB-IRIS .....Tuberculosis-associated immune reconstitution inflammatory syndrome

TNF .....Tumour necrosis factor

USD.....United States dollar

VAP1.....Vascular adhesion protein 1

VCAM1 .....Vascular cell adhesion molecule 1

VEGF.....Vascular endothelial growth factor

WHO.....World Health Organisation

XDR-TB .....Extremely drug resistant tuberculosis

Chapter 1 Introduction

1.1 Motivation

There has been a growing interest in the development of point-of-care (POC) diagnostic solutions. POC testing through rapid and affordable detection of analytes at the patient's bedside is essential to facilitate improved disease diagnosis, monitoring, and triage. This enables timelier decision making, as if a disease can be diagnosed at an early stage and treatments started earlier, it in turn leads to improved health outcomes for patients.

The global POC diagnostic market was expected to grow from USD 23.16 billion in 2016 to USD 36.96 billion in 2021; however, the impact of the COVID-19 pandemic has resulted in an unprecedented demand for POC testing across the globe with this market showing growth of over 86% in 2020. It was valued at USD 41.49 billion in 2021. North America accounts for the largest proportion of the global market, followed by Europe, however the Asia-Pacific's POC market is expected to show the most growth [1].

Lateral flow tests (LFTs) are an excellent candidate for POC testing solutions. LFTs, lateral flow immunoassays (LFIA), lateral flow devices (LFDs), also sometimes referred to as immunochromatographic tests, have been used in clinical diagnostics for over 60 years with one of the most well-known LFTs being the pregnancy test. These devices are simplified formats of more sophisticated biosensors, in which the recognition element is located on the surface of a porous paper-like membrane and the result is visualized within a few minutes through the appearance of coloured lines.

A standard LFT detects a single analyte and only gives a qualitative positive or negative answer for the identification of the analyte in the bodily sample added to the LFT. For the wider implementation of these POC tests for many applications there is the need for detection of multiple analytes with the addition of semi-quantitative or ideally fully quantitative detection. For this reason, part of the ambition for the work carried out in this thesis was the development of LFTs that allow implementation of both semi-quantitative and multiplexed analyte detection. This was explored using a laser-direct write patterning technique that made possible the patterning of the nitrocellulose membrane of the LFT to enable multiple analyte detection on one single LFT, simultaneously detecting three analytes. In addition, using this technique the feasibility of identifying multiple analytes, semi-quantitatively without the requirement for an external reader was also explored.

In addition to the need for the optimisation of current-day paper-based lateral flow tests to have improved sensitivity and detection capabilities (multiplexing and semi-quantitative detection) there is an ever-growing need for such POC testing to be affordable for targeted disease detection. As an example, this is particularly true for the early detection of Tuberculosis (TB) which remains the biggest killer of any infectious disease. TB is largely a treatable disease, however timely and accurate diagnosis, within the community, is crucial to its final eradication. . As outlined by the World Health Organisation (WHO), there is a requirement for TB screening and triage tests that could support early identification of people who may be infected. It is vital that these tests are adequately sensitive to ensure that no one who is infected with *Mycobacterium tuberculosis* (the infection causing pathogen) *Mtb* would be missed. Once the target population has been screened, those that are flagged as positive for TB are then referred for confirmatory diagnostic testing with a more sensitive and specific rapid molecular test, such as Cepheid's Xpert MTB/RIF or Molbio's Truenat MTB. TB triage tests would be required to screen large numbers of people - through the systematic screening programs in communities or routine care in health facilities—these tests must therefore be affordable, and able to be used at the point-of-care [2]. It was a key ambition of this project to thus produce a suitably sensitive and specific 'rule-out' test for use in TB triage. In a similar vein there are other diseases or conditions which could benefit equally from such rapid point-of-care testing, and development of LFTs for other such applications has also been endeavoured in this thesis.

Dementia is an umbrella term for neurodegenerative diseases that leads to memory loss and difficulties with thinking, problem-solving or language and Alzheimer's is the most common cause. Accumulation of plaques in the brain leads to degradation of neuron function which produce the characteristic symptoms. There is currently no single test for a diagnosis of Alzheimer's, but clinicians carry out a range of blood tests, psychiatric assessment of symptoms and CT or MRI brain scans. Of importance is the fact that all these tests detect the presence of damage that has already occurred to the patient's brain. There is now the first licenced treatment by the U.S. Food and Drug Administration (FDA) for Alzheimer's that can slow disease progression [3], and this highlights the need for an early screening tool to identify those individuals that are at high risk of developing Alzheimer's disease for whom treatment can be started as early as possible to give the best patient outcomes. It was therefore the ambition of this project to develop a LFT that could be used as a screening tool that identifies host inflammatory markers that show high correlation with the likelihood of the progression of dementia.

A subsequent objective of this work is the validation of these POC tests as effective real-world clinical diagnostics using human/patient samples. This includes the use of healthy and diseased

patient samples to assess the tests' suitability for clinical use. It was also our ambition to ensure these research outcomes be scaled to enable production of commercial products.

1.2 Outline of the thesis

Chapter 2 is an introduction to the background underlying the concepts discussed throughout this thesis, including the basic principles of lateral-flow devices, how they operate and how they are practically assembled in the laboratory. It will also describe the immunoassays that are implemented onto these LFDs and how their mechanism of action allows for the detection of the desired analytes and how this data is analysed.

Chapter 3 begins by presenting a summary of the techniques and methodology applied throughout this project including the use of the laser direct-write (LDW) patterning technique and the procedure for assembling and testing the LFDs and all the reagents required.

Chapter 4 introduces a novel and exciting solution to guide antibiotic administration via the rapid multiplexed and semi-quantitative detection of two inflammatory biomarkers, C-reactive protein (CRP) and procalcitonin (PCT). This chapter explores how this novel approach utilises the LDW patterning technique to create multiple parallel flow-paths produced via the precise partitioning of the single flow-path of a standard LFD. With no interference or cross-reactivity, each flow path has a unique detection capability which permits tailored detection of CRP and PCT respectively within a predefined cut-off range or above a set threshold. Using the same test footprint ensures the test costs remain low and there is no need for additional volumes of sample or reagents. This multiplexed, semi-quantitative near-patient assay has potential for development into a rapid triage and treatment of patients with suspected pneumonia.

Chapter 5 continues to build on the demonstration of a multiplexed LFD instead for the simultaneous detection of four serum biomarkers, for the development of a 'rule-out' test for tuberculosis. It presents data from the preliminary development for four individual tests, moving thereafter to the multiplexed detection of two and three markers and finally the three-way multiplexed LFD. This too describes the use of the LDW patterning technique to create multiple parallel channels, however in this chapter we explore the use of patterning of the different materials of the LFD to optimally combine the three markers. The chapter first details the initial testing done using a phosphate buffered solution (PBS) to explore the difference between detection of the analytes in plasma and serum, thereafter, moving to the use of healthy human serum and finally, validation of the test with a set of diseased patient samples.

Chapter 6 details the development work that was performed for a POC test for SARS-CoV-2 detection during the height of the pandemic. It shows the use of both the nucleocapsid protein and the spike protein for a multiplexed test that has both high sensitivity and specificity for viral detection with reduced instances of false positives.

Chapter 7 reports the preliminary results collected in the development of a multiplexed lateral flow test for the monitoring of Alzheimer's disease. This work stemmed from the knowledge that chronic inflammation can lead to earlier and more severe disease onset and monitoring these inflammatory markers could allow for earlier interventions. This includes the optimisation of individual LFDs with the aim to combine them in the future and validate their use with patient samples.

Chapter 8 encompasses several different applications of the LDW patterning technique to alter the flow path of a standard LFD to optimise their sensitivity. This includes building upon previous work that implemented a spatial constriction of the flow path to further optimise this method. This included the introduction of a second constriction within the flow path which produced a significant improvement of the device limit of detection (LOD) for the detection of the inflammatory marker procalcitonin. In addition, it looks at the use of a reverse constriction flow-geometry and the implementation of in-line polymer barriers to alter the flow of the sample and therefore modify the binding kinetics taking place at the test line.

Finally, Chapter 9 summarises the work and outcomes described throughout this thesis, which are focused primarily on the further extension of the standard LFD to have more sophisticated capabilities and enhanced sensitivity for the production of paper-based point-of-care diagnostic sensors. It looks at the potential future work that could build on this foundation for the development and ultimately the commercialisation of clinically useful tests.

1.3 Main achievements

The following is a list of the main achievements of the different projects that are reported within the thesis.

1. Demonstrated the use of a three-channel lateral flow device using the laser-based direct-write (LDW) technique. This allowed for the simultaneous detection of two blood-based biomarkers: CRP and PCT with the addition of semi-quantitative capabilities that align with NICE guidelines for clinical applications to pneumonia triage.

2. Development and small-scale clinical validation of individual LFDs and a multiplexed LFD for the detection of blood-based biomarkers: CRP, SAA1, LBP and CFHR5 for a screening

tool for Tuberculosis within the community. It has the capability to distinguish those patients with TB from healthy controls with clear significance showing a combined diagnostic capacity of the test with an AUC of 0.92 with sensitivity and specificity sufficient as set out by the WHO guidelines for a TB rule-out screening test.

3. Investigated the use of additional geometric flow control to include test line position within the flow path and within a constricted region of flow alongside the addition of a second constriction to alter the flow dynamics within the test and shown a significant improvement in the LOD for a PCT assay.

4. Demonstrated the use of plasma and serum on the LFD and shown equal compatibility with both mediums.

5. Shown the utility of a dual-channel LFD for the successful detection of two viral proteins for SARS-CoV-2 and validated the capabilities of the test using deactivated virus samples.

6. Shown the potential for the use of vascular markers VAP-1, ICAM-1 and VCAM-1 for use in monitoring Alzheimer's disease using minimally invasive blood-based testing.

Chapter 2 Background

2.1 Paper-based lateral flow devices

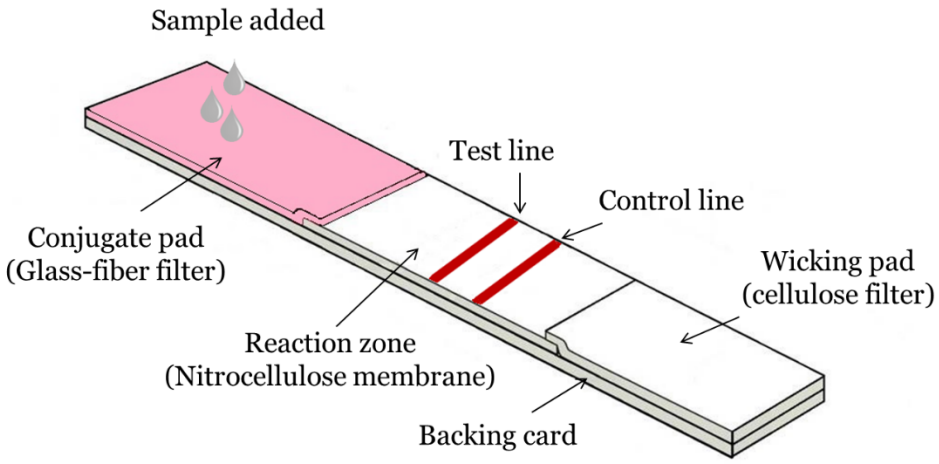

Figure 2.1 - Schematic of a single channel lateral flow POC test with labelled material components.

Lateral-flow devices (immunochromatographic tests) are an ideal platform for POC diagnostics. They are designed such that all reagents required for the completion of the test are already contained within the constituent membranes of a test strip. Contact with a test initiates the fluidic samples movement along the membranes, facilitating specific interactions of immunoreagents that results in the accumulation of signalling molecules within certain zones or regions of the test strip. Although there are many different formats of a lateral flow test, they generally all encompass the key components as seen in Figure 2.1; however, some LFDs may have an additional sample pad or for purely development purposes some LFDs (referred to as half LFD) do not include a conjugate pad:

Sample pad: This is the first component of the test where the sample fluid (blood, urine, saliva) is added. They are generally made of cellulose or cotton linter, and this allows for transport of the sample to the subsequent components of the test. They can, therefore, be used to treat the sample before transportation or include some form of separation mechanism such as a filtering out red blood cells.

Conjugate pad: This is the component of the test that incorporates the labelled biorecognition molecules such as gold nanoparticle-labelled antibodies. These molecules are pre-deposited and dried on the pad. As the liquid sample contacts the conjugate pad it rehydrates the biorecognition molecules and here binding of the tagged antibody to the specific analyte is present in the sample. The conjugate pad is usually made of glass fibre and this material can be highly impactful on the results of the assay as it controls the release of the tagged antibody.

Nitrocellulose membrane: On this membrane is the reaction zone. The test and control lines that constitute the reaction zones are pre-deposited and immobilised on the membrane. There are different types of nitrocellulose membrane with different pore sizes and capillary speeds that can all be incorporated into test's optimisation. The optimal membrane has good binding to the capture probes (antibodies for example) so they are not washed away during the test but also minimal non-specific binding across its surface that could interfere with the results of the assay.

Adsorbent/wicking pad: Placed at the end of the test this final component helps to maintain the liquid flow preventing backflow of sample and ensuring that excess, unbound reagents are removed to ensure the clearest result with no background noise interfering with the test's result.

These components are mounted onto a backing card allowing for easy assembly and increased stability of the test whilst ensuring sufficient contact between the different membranes.

There are generally two assay types that can implemented on a lateral flow test. The sandwich assay format is arguably the most common, as discussed in section 3.2. A primary antibody specific to the target analyte is immobilised on the test line, a secondary antibody against the labelled conjugate antibody is immobilised at the control line. This is so the control line will always appear whether or not the target analyte is present or absent in the sample, confirming that the test has operated correctly.

2.1.1.1 Sample flow

One key feature of the constituent porous materials used as the building blocks for microfluidic devices is their ability to move fluid via capillary action negating the need for additional external pumping devices. Capillary action is the ability of a liquid to travel through a narrow channel without the assistance of, or even in opposition to, an external force such as gravity. It is the movement of liquid through a porous medium guided by the forces of cohesion and surface tension between the channel and the liquid [4]. The fluid velocity slows as it moves further along the length of the test which is due to a progressive depletion of sample volume, which is important information that can influence the positioning of the test line(s) [5].

The transport of the fluid here is one-dimensional and in a porous medium (such as the nitrocellulose membrane) during the wet-out process follows the Washburn equation under two assumptions: 1. A non-limiting source fluid 2. A constant cross-sectional area [6]:

$$L^2 = \frac{\gamma D t}{4\mu} \qquad [2.1]$$

Where L is distance moved by the fluid front along the flow path, γ is the effective surface tension of the fluid, t is time, D is the average pore diameter, and μ is viscosity of the sample [6].

As per the Washburn equation, the velocity of the fluid front decreases over time (L ~$\sqrt{t}$). The surface tension pulls the fluid further along into the membrane, but this force is counteracted by the viscous resistance, which is proportional to the velocity with a coefficient of ($\frac{8\mu L}{D^2}$) that increases over the length of the capillary or column. This results in a decrease in D flow velocity as the fluid penetrates the porous membrane [5].

There are several factors that can influence the flow speed and the assay:

Alignment: The sample flows from one constituent material of the LFD to the next is by contact between the different components of the test. It is therefore crucial that this contact and overlap is sufficient and sustained for the duration of the test. As a finished product the test would be housed in a casing that has specifically designed protruding pinch points that provide compressive force at the points of overlap, ensuring consistent contact critically required between the overlapping materials.

Biochemistry: Some constituents of the assay's biochemistry are free moving, i.e., transported across the test, whilst others remain fixed or immobile. The capture molecules that are deposited at the test and control line are dried and immobilised onto the nitrocellulose membrane and become active within the test as the liquid sample moves over it, accompanied by the labelled detection antibody. The liquid flow path is complex as some of the molecules are on the surface of the membrane and some are within the materials.

Porous materials: The choice of nitrocellulose membrane for the reaction zone and the volume capabilities, shape and wicking speed of the absorbent pad can affect the speed at which the sample travels along the test. Nitrocellulose membrane is available in many different pore sizes, and this allows for customisation of the flow speed.

Test geometry: The overall test geometry can be modified to change the flow rate. For example: the use of in-line barriers, constrictions and shaping of the flow path are all changes that can be made to influence the flow dynamics within the test [7-9].

Sample volume: The sample volume that is added to the LFD is also a key parameter. Not only does the sample contain the analyte of interest and therefore a larger sample volume would imply larger quantities of the analyte, but the sample volume also contributes to the flow rate. When the concentration of analyte within the sample is constant, an increase in sample volume leads to an increase in flow velocity [10]. If the volume of sample is below a certain threshold and is insufficient to fill the LFD, then the flow will stop when the sample is depleted and could result in backflow of the sample. The capture efficiency: the proportion of the antigen that is binding the tagged antibody and the capture antibody at the test line on the LFD, is determined by the antibody binding kinetics but also the flow rate when the sample (and hence the analyte) is moving across the test line. At higher velocity the sample will move through the test line quicker, which reduces the time for interactions between the components (analyte and capture antibodies at the test and control lines) of the immunoassay, ultimately decreasing the test sensitivity. Therefore, a high sample volume can lead to a decrease in test line colour intensity [11]. For this reason, there is an optimal sample volume that should be used for each assay.

Sample medium composition: The type of sample and its contents will affect the way that the assay performs. If the sample is very viscous for example this might lead to flow issues within the capillary system of the membrane. Additionally, the hydrophobicity of the sample will affect how it interacts with and moves along the membrane. Another way the sample might affect the assay is components of the sample that directly interact with the other reagents, for example some blood products such as haemoglobin are very sticky and therefore some pre-sample treatment might be required.

Signal intensity: The intensity of the signal seen at the test line is a function of several relevant concentrations namely that of the capture molecule, detection molecule and the analyte. The sensitivity is also affected by the flow rate of the sample along the test. A faster flow leads to a reduction in test sensitivity due to reduced binding opportunity. Only the analyte that flows ahead of, or in tandem with the detection reagent can contribute towards the signal at the test line.

Chromatography: The process of chromatography is used to separate substances based on their affinity to either the stationary or mobile phase. In this instance, the sample acts as the mobile phase with the membrane acting similarly to the stationary phase. Molecules of different, size, ionic strength and hydrophobicity will interact with the phases differently and can lead to separation along the course of the lateral flow. Therefore, these properties must be considered when choosing the sample type and appropriate reagents.

As seen in Figure 2.2, the capillary size and arrangement within the nitrocellulose membrane is not completely uniform, and this means that the flow of the reagents is dynamic and changes throughout the course of the test. The flow rate of the sample is determined by multiple factors, as discussed in section 2.1.1.1, but the easiest to control is the capillary speed of the nitrocellulose membrane used for the test. The flow rate dictates how much time there is for the sample to interact with the test line. If the flow is slower, the sample has a greater interaction time with the antibodies deposited at the test line, which in a sandwich assay format leads to an increase in test sensitivity. However, for the competitive assay, discussed in detail in section 3.2, where the antigen is deposited at the test line, this has an inverse outcome. By extending the interaction time of the sample with the molecules at the test line, there is a reduction in the test line colour intensity.

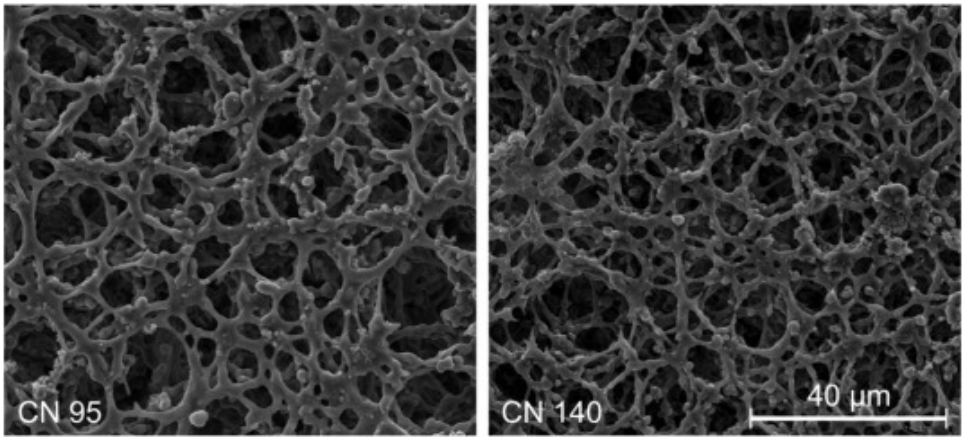

Figure 2.2 - SEM-micrographs of untreated membranes, left: CN 95 with 10 µm nominal pore size; Right: CN 140 with 8 µm nominal pore size, taken from [12]

Alternatively, as described in Chapter 8, the introduction of geometric alterations to the flow path can be used to alter the flow front velocity of the sample in the test by changing the cross-sectional area of the device. This is a useful tool as it can lead to increased sensitivity and signal enhancement.

2.1.2 Signalling

Although lateral-flow tests are a lightweight, low-cost diagnostic solution, there is constant demand for higher sensitivity solutions which is the main challenge associated with conventional lateral flow devices. Currently, the detection of extremely low concentrations such as those markers that fall in the picogram range is difficult to achieve. However, the development of high sensitivity devices is becoming a favoured trend [13]. One solution is integrating more efficient labelling particles, and there are several available, including latex beads [14], carbon nanoparticles

[15], quantum dots [16] and colloidal gold nanorods [17]. However, the most widely used elements are still gold nanoparticles (AuNPs) as they have the capability to add colour to the test line to allow for a visual readout, unlike fluorescence tags that require a reader to be able to be visualised, and they must do this without hindering the flow of the sample through the nitrocellulose membrane. Gold is inert and possesses excellent optical properties making it easy to visualise without the need for sophisticated equipment, and it is highly stable whilst dried or in a liquid state and is easy to conjugate to antibodies.

How the AuNPs interact with light is dependent on the environmental conditions (such as pH) but also the size of the particles. A light ray that is propagating near a AuNP can interact with the free electrons leading to the oscillation of electron charge that is in the resonance of the frequency of visible light. These oscillations are called surface plasmons and for smaller particles, such as those around 30 nm in size, these phenomena cause absorption of light in the blue-green spectrum around 450 nm and emission around 700 nm, which leads to red light being reflected, and subsequently the red colour seen at the test line. As the particle size increases, the wavelength of absorption shifts to longer, redder wavelengths and here the red light is absorbed, and the visible reflected light is blue or purple. Changing the size of the AuNPs used can aid in adjusting the sensitivity of the assay.

2.1.3 Antibody-based diagnostics

Antibodies are serum immunoglobulins, see structure in Figure 2.3, that have a binding affinity for a particular antigen. Specifically, they bind an epitope which is the immunogenic part of the antigen and could a chain of 5-7 amino acids for example. They are used extensively in a wide range of medical applications from biomedical research to diagnostic testing and therapeutics. Both monoclonal and polyclonal antibodies are used but both require the use of animals for their production.

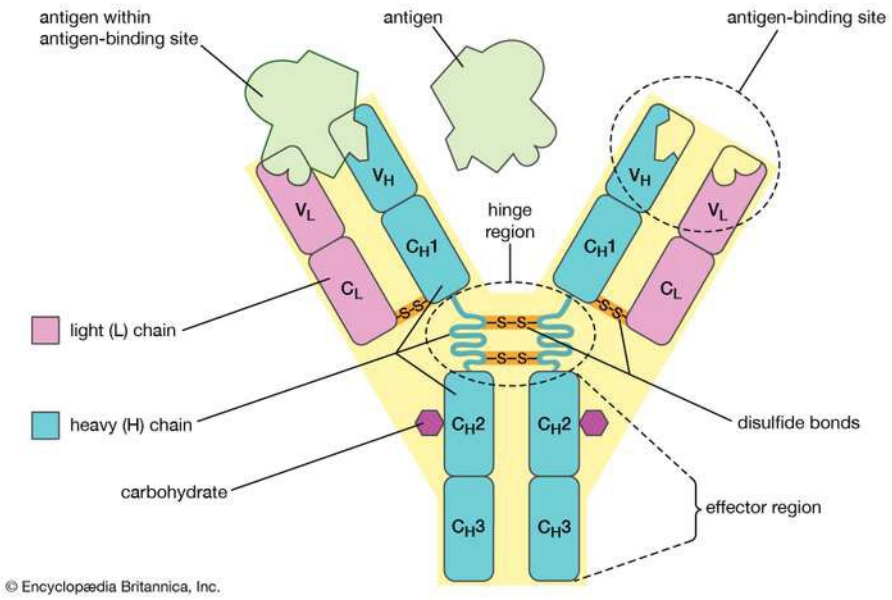

Figure 2.3 - Schematic of the four-chain structure of an antibody. It is composed of two light chains and two heavy chains bound by disulfide bonds to create the characteristic 'Y' shape. Each chain has a variable and constant region. Taken from [18].

Part of the optimization process for the development of a lateral flow device is the choice of immunoassay that will be implemented for the chemical detection of the target analyte. The performance of these immunoassay components is critical for the sensitivity and specificity of the test. There are options of aptamers and other reagents for this however antibodies are the primary reagent used in lateral flow tests and are what have been used throughout this thesis as they are sufficiently sensitive and specific for the successful detection of low concentrations of the targeted analytes.

Antibodies are proteins that are produced in both humans and animals by the adaptive immune system in response to an infection with antigens such as bacterial, viral or other chemical compounds. Although antibodies typically have a weight of 150 kDa (compared to a molecule of water at 18 Da) and are around 13.7 nm x 8.4 nm in their dimensions there is variability between different batched or different manufacturers antibodies, and this can lead to some issues with reproducibility of LFDs. Each antibody is unique which makes them ideal for highly specific detection and use in diagnostics however in the process of assay development and implementation onto the LFD there is a large amount of optimisation required. This process involves the selection of the antibodies for either a sandwich or competitive assay, the conjugation process to tag the antibodies with AuNPs, the correct volume of conjugated antibody necessary and the concentration of antibody deposited at the test line, and this can make the process of LFD development time-consuming and more challenging.

Initially when the analyte of interest has been identified there is a decision whether to use polyclonal or monoclonal antibodies for detection.

For the production of polyclonal antibodies, animals are injected with an antigen or a mixture of antigen and adjuvant to induce an immune response. Polyclonal antibodies are a mix of antibodies produced by B-cells, although they recognise the same antigen each antibody is specific for a different epitope of that antigen. As they are a heterogeneous mix of antibodies, they are highly representative of the body's natural immune response however there can be a higher batch-to-batch variation and therefore can result in more unspecific binding than monoclonal antibodies, limiting their use in lateral flow testing. Immunisation of an animal with monoclonal antibodies induce specific B cells that must then be obtained from the animal's spleen or lymph nodes. Monoclonal antibodies are produced from a single B cell parent and are clones, therefore identical. They recognise a single epitope per antigen meaning higher specificity, correct conformation of the epitope for binding is crucial. The B cells can be immortalised via fusion to a hybridoma cell which gives excellent long-term production of consistently identical antibodies.

When choosing between the use of polyclonal or monoclonal antibodies the application, the time and money available must all be considered. Polyclonal antibodies are produced in up to 8 weeks and are cheaper to produce than monoclonal antibodies that can take 6 months to produce [19]. There are also recombinant antibodies that are produced *in vitro* utilising synthetic genes. This means the sequences can be chosen and controlled which can optimise the epitope binding and leads to better reproducibility than hybridoma fusion.

There are different advantages and disadvantages associated with using either monoclonal or polyclonal antibodies for a lateral flow test. As monoclonal antibodies give less variability, they can be favoured to conjugate to the AuNPs in addition to their high specificity and decreased risk of cross-linking the nanoparticles. This can happen when several conjugated antibodies are binding different epitopes of the same analyte, these particles can form aggregates which can lead to the particles becoming trapped in the pores of the nitrocellulose membrane and not reaching the test line to bind to the capture antibody. Polyclonal antibodies can bind to multiple epitopes meaning using them at the capture site can be advantageous as there is greater chance of binding the analyte as it flows past, however due to their variability they can make reproducibility of the performance of a test problematic. It is possible to use two monoclonal antibodies for a sandwich assay assuming they bind different epitopes on the analyte, but all antibodies must be thoroughly tested to ensure no cross-reactivity can occur. A summary of

advantages and disadvantageous of both monoclonal and polyclonal antibodies can be seen in the table below.

Table 1 - Advantages and disadvantages of monoclonal vs polyclonal antibodies for use in LFDs

	Advantages	Disadvantages
Monoclonal	• Constant renewable resource • Higher consistency • Very high specificity for low concentration analyte detection • Less background signal compared to polyclonal • Homogeneity leads to repeatable results	• More expensive and time-consuming to produce • Cover a single epitope • High specificity might limit their ability to detect across a range of species
Polyclonal	• More economical pricing • High affinity binding • Ability to recognize multiple epitopes • Preferred method for detection of denatured proteins • High tolerance to changes in antigen such as protein glycosylation	• Greater batch to batch variation • Produce large amounts of non-specific antibodies that can lead to background signal • Multiple epitope binding can lead to cross-reactivity

Selecting the most effective antibodies is critical to the performance of the LFD and this is largely defined by the affinity of the antibodies used in the assay to bind to the analyte being detected. However, the avidity is also important, this is not just the likelihood that the antibody will bind to the analyte but how strong the bond between them is. Affinity can be quantified by using the K_D which is equilibrium dissociation constant, a ratio between the K_{on} and the K_{off} between the antibody and antigen. The K_D relates to the amount of antibody required for a particular experiment, so if there is high affinity for the antigen then only a small amount of antibody is needed, meaning the K_D and affinity are inversely proportional.

Antibody specificity is a key component when selecting the optimal antibodies for a test. It is important that they do not react with other components of the sample (if using blood or plasma for example) or bind to similar structured analytes. Insufficient specificity can lead to false positive results during clinical testing and therefore it is necessary to investigate this with cross-reactivity testing earlier in the antibody screening or selection process. In the context of a sandwich assay, where two antibodies bind the analyte simultaneously, it is important that these

antibodies target two distinct immunogenic epitopes. This means that each antibody will bind a slightly different part of the analyte to ensure that they are not directly competing for binding.

Antibodies can be acquired from commercial sources or custom-made by raising them against a particular antigen. Commercial availability of antibodies varies and is largely dependent on the current trends in the market. When initially screening the antibodies, it is beneficial to examine as many antibodies as possible and in the case of a sandwich immunoassay to determine which antibodies function as the most effect pairing for analyte detection.

To test the antibodies in all possible configurations a matrix is produced to test each antibody as both the capture antibody which is immobilized at the test line, and the detection antibody that is conjugated to the gold nanoparticle. An example is shown in the table below:

Table 2 – An example of an antibody testing matrix

	Capture				
Detection	Antibody #1	Antibody #2	Antibody #3	Antibody #4	Antibody #5
Antibody #1		1 x 2	1 x 3	1 x 4	1 x 5
Antibody #2	2 x 1		2 x 3	2 x 4	2 x 5
Antibody #3	3 x 1	3 x 2		3 x 4	3 x 5
Antibody #4	4 x 1	4 x 2	4 x 3		4 x 5
Antibody #5	5 x 1	5 x 2	5 x 3	5 x 4	

Most commercially available antibodies are developed for use in an enzyme linked immunosorbent assay (ELISA) or Western Blot and therefore some of the information available about the antibodies such as the assay's limit of detection (LOD) may not be accurate for use in a different application such as on a LFD. In an LFD the antibody must be able to function after conjugation to the signalling molecule and after drying onto the nitrocellulose membrane as well as have the capacity to be effectively rehydrated from the conjugate pad during transport of the liquid sample. ELISA and Western Blot techniques incorporate longer incubation periods as part of the protocol whereas during the lateral flow assay the antibody's binding at the capture line may have less than a second for this to occur and therefore the binding kinetics of the antibodies have an impact of the assay outcome.

In all assays it is important to include a second capture line that functions as a control. This line will produce a signal independent of the presence of the analyte and serves as assurance to the user that the test has been performed correctly and the results are valid. This control line uses an antibody that is a specific to the species used for the detection antibody. For example, if the detection antibody used is a Goat anti-mouse antibody, then the control line could use mouse IgG as then the detection antibody would always bind at the control line, independent of the analyte being present in the sample.

2.2 Enzyme-linked immunosorbent assay (ELISA)

Enzyme-linked immunosorbent assay (ELISA) is one of the most commonly used diagnostic tool for biochemical detection. It uses antibodies and colorimetric detection to indicate the presence of antigens which could be the products of the host immune response or a pathogen specific marker, and these assays have very high detection sensitivity [20]. ELISAs are performed in polystyrene plates, typically in 96-well plates that are coated to allow high strength binding to the analyte/protein of interest. It is this assay that has been adapted and applied throughout this thesis for the detection of a selection of biomarkers. There are several broad stages to the ELISA process:

1. Firstly, coating, where depending on the type of ELISA the antigen or antibody is coated onto the wells of the plate.
2. Blocking where an agent, typically bovine serum albumin (BSA) is added to reduce non-specific binding.
3. Detection, where a substrate is added that can add colour for example gold nanoparticles or fluorescence particles for example.
4. Then this result is read generally using a reader as this can also be used to quantify the amount of the antigen present in the sample.

There are several different types of the assays as described in Figure 2.4. Which was adapted from [20].

In a **direct ELISA** a tagged detection antibody directly binds to the antigen of interest. This ELISA can be advantageous as by removing secondary antibodies it removes the chance of any antibody cross-reactivity and reduces the number of steps needed which reduces the time implications, however it does also reduce the sensitivity compared to the other types of ELISA.

An **indirect ELISA** requires an antibody that is enzyme-linked in addition to the primary antibody. The enzyme-linked antibody is added after washing and then incubated the same as a direct

ELISA. The indirect ELISA gives a higher sensitivity readout compared to a direct ELISA and is generally less expensive as there is more flexibility over the antibodies that can be used but it does introduce the risk of cross-reactivity between the two antibodies.

A **sandwich ELISA** is quite different from the direct and indirect ELISAs where firstly a capture antibody is coated onto the plate. The name 'sandwich' comes from the antigen being sandwiched between a capture antibody deposited onto the well and the tagged detection antibody. The antigen is first incubated with the capture antibody before the detection antibody is added and further incubation and washing is required before the addition of the enzyme-linked antibody. This method of ELISA gives the highest sensitivity however it can be costly and more difficult as a matching antibody pair is required, the additional antibody and steps also add further to the time taken to complete the assay.

Finally, the **competitive ELISA** utilises two antibodies one that is enzyme-linked and the other that is used to test for the presence of an antigen specific antibody in the sample. The idea is that combining two antibodies creates competition for binding to the antigen. Therefore, in this case, an absence of colour is indicative of a positive result in contrast to the other types of ELISA. This type of ELISA has low specificity however there is little sample pre-processing required and it can be used for a large range of antigens in one sample, especially small antigens.

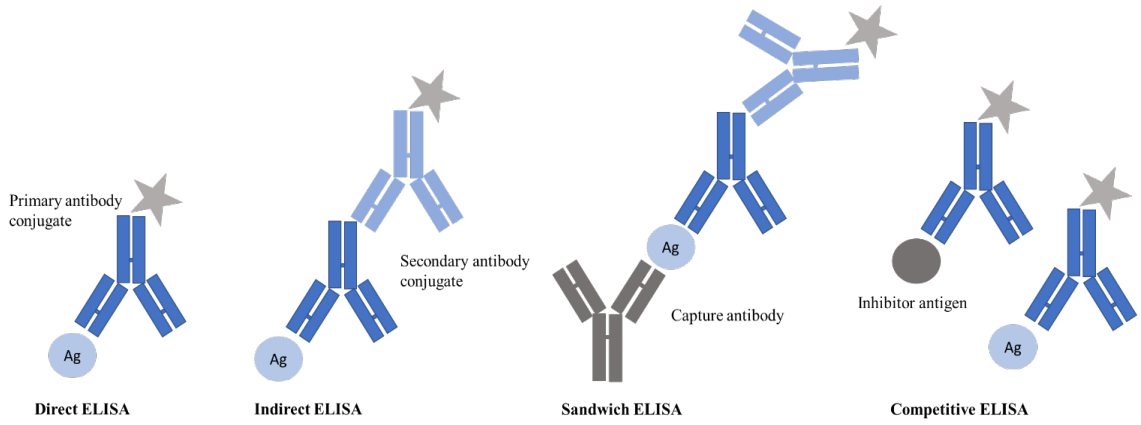

Figure 2.4 - Schematic describing four different ELISA assay types; Direct, Indirect, Sandwich and Competitive.

These assays although designed for use in the ELISA plate format can be implemented on an LFD for use in diagnostics. However, in the assays reported in this thesis, the detection or secondary antibody is directly conjugated to the colour producing substrate and not an enzyme-linked antibody.

2.3 The Laser direct write technique

Laser direct write (LDW) is a patterning technique previously reported by the team at the ORC to achieve several modifications and optimisations including flow control, the creation of in line filters, multiplexing technologies and increased sensitivity of LFDs [7, 9, 21-27]. The method has several advantages over other similar methods to modify the flow path without damaging the nitrocellulose and it can also be used in conjunction with immunoassay reagents. This technique provides good precision to allow for the production of minimally sized devices as the technique can be used to create barriers that are 100 µm in thickness meaning the overall footprint of the device can remain < 2 mm. There are three main components to the laser patterning system, consisting of the laser source, the delivery system, and the substrate being deposited.

Specifically, in this additive patterning approach, to structure the desired porous material (e.g., the nitrocellulose membrane) with specifically defined flow paths, material is added to the (nitrocellulose membrane), as opposed to laser ablation where material is removed [8]. The initial step is the local deposition of a photo-polymer onto the nitrocellulose membrane or other porous substrate at specifically designed positions. The polymer is then exposed to laser light at a 450 nm that will lead to its polymerisation and solidification of the polymer within the membrane. This technique allows for the creation of precise hydrophobic structures within the membrane. The polymer is photosensitive meaning its properties can be altered by exposure to light. The liquid photo-polymer is a mixture of monomers, oligomers and photoinitators which are activated when exposed to a particular wavelength leading to a change in properties. The exposure induces decomposition of the photoinitators into reactive species that trigger the polymerisation of the functional groups of the oligomers to the monomers leading to the formation of cross-links between the elements of the polymer and an additional free radical that continues the reaction, ultimately causing a change in the physical properties and transformation from a liquid phase to a solid state.

There are other polymerisation processes such as thermally cured polymerisation however photo-polymerisation allows for precise and local curing which is able to give superior spatial resolution and higher rates of polymerisation. Subsequently, this photo-polymerisation technique coupled with photo-curable materials are a popular choice for numerous applications including but not limited to medical diagnostics, and imaging [28].

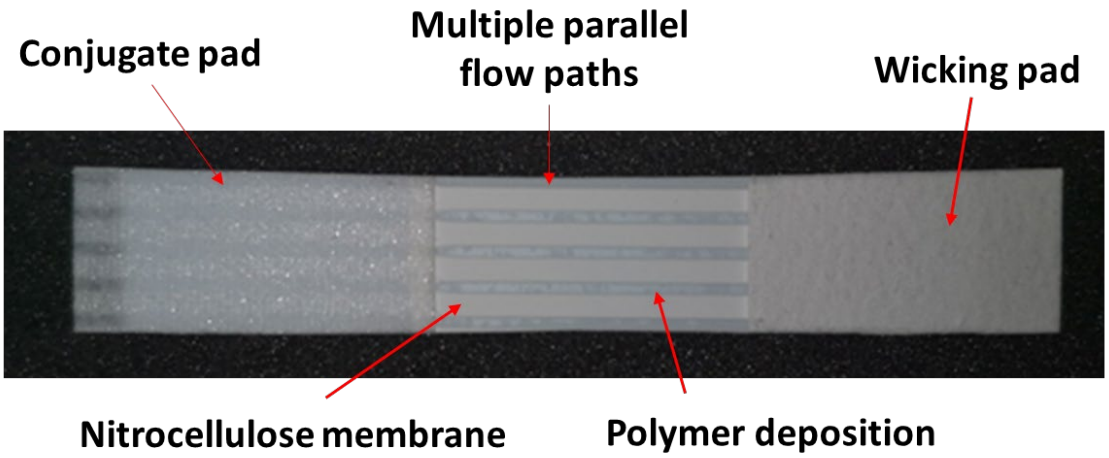

Figure 2.5 - Image of a four parallel flow path multiplexed device

There are several other methods that have been reported for the patterning of membranes in the production of paper-based microfluidics; including photolithography [29], wax printing [30-33], inkjet printing [34], laser cutting or ablation [12, 35, 36], flexographic printing [37] and plasma treatment [38, 39]. Below is a summary of some of the other reported patterning techniques and their advantages and disadvantages in Table 3. In comparison, the LDW method exhibits key advantages: it does not need expensive and fixed patterning masks, custom equipment, specialist chemicals or inks which can also be hazardous, does not create debris, does not require a solid or backed support or supporting cards as it uses lower power and processes faster, and it overcomes the limitation of lateral spreading of the hydrophobic material used to form the fluidic channel walls extending through the thickness of the membrane with barrier dimensions below 100 µm. Most significantly it is suitable for scale-up to mass-production on a roll-to-roll basis through incorporation into an LFD production line.

Table 3 - Summary of patterning techniques

Reported Technique	Advantages	Disadvantages	References
Photolithography	Low-cost mass production.	Requires expensive equipment and complex steps for fabrication [23].	[29]
Wax printing	High throughput production and requires only a commercial printer and a heating source [40].	Dissolvable in organic solvents, subject to cracking if bend or damaged, and has temperature-dependent properties.	[30-33, 41]
Inkjet printing	Can be used to deposit a range of substrates, relatively low cost [42].	Requires ink to be low viscosity and low surface tension to print [43].	[34, 44-46]
Laser cutting/ablation	Using a laser for structuring with NC is comparatively difficult because of the low flash point of the material [12].	High investment costs, lasers need a considerable amount of energy, cause debris.	[8, 12, 36]
Flexographic printing	Highly versatile for use in different substrates.	Flexographic printing equipment is quite complex and due to the setup and plate making cost it is preferable for medium to large volumes of printing only.	[37, 47]
Plasma treatment	Can alter the surface structure of polymers without changing the bulk properties of the treated material [48].	Some polymers are susceptible to plasma-induced degradation.	[38, 39]

Comparing the unit cost of the above methods is challenging but one advantage of the LDW technique is that it is cost efficient for small batches such as during the development phase and the initial setup is affordable and scalable.

2.4 Analysis

2.4.1 Calibration Curves

Calibration curves are used frequently as part of the work carried out in this thesis and provide critical information for LFD development and optimisation. A calibration curve or standard curve is used to determine the concentration of an unknown sample by comparing the unknown sample concentration to those of a set of standard samples of known concentration. The calibration curve importantly also gives information about the dynamic range, sensitivity, LOD, limit of quantification (LOQ) and the limit of linearity (LOL). The LOD is the lowest analyte concentration that can be distinguished from the limit of blank (LOB) whereas the LOQ is the lowest concentration at which the analyte can be detected by the means of the given analytical procedure with its accuracy and precision. The LOQ will therefore be different depending on whether the result of the test is being read by eye or by an electronic reader, but the LOD will remain the same for the test.

Below, in Figure 2.6 is an example calibration curve for the marker serum amyloid A1 (SAA1). There are seven concentrations for which the test line colour intensity is measured, including a control where the concentration of the analyte is 0 µg/ml. On the graph is labelled the LOD which is the lowest concentration where a visible test line can be seen and this was assessed visually, giving a LOD of 0.25 µg/ml, this is indicated on the graph with a blue line. Next is the LOQ which is indicated using the purple line and gives a value of 0.5 µg/ml, the LOQ here is the value that can be reliably and repeatedly detected. The red line on the graph shows the concentration that represents the LOL of 4.0 µg/ml, where the increase in intensity stops being as linear and starts to plateau, here an aspect of the assay is becoming saturated, and the test line colour intensity can not increase anymore even as more analyte is added. Further details of the testing protocol can be found in section 3.4.

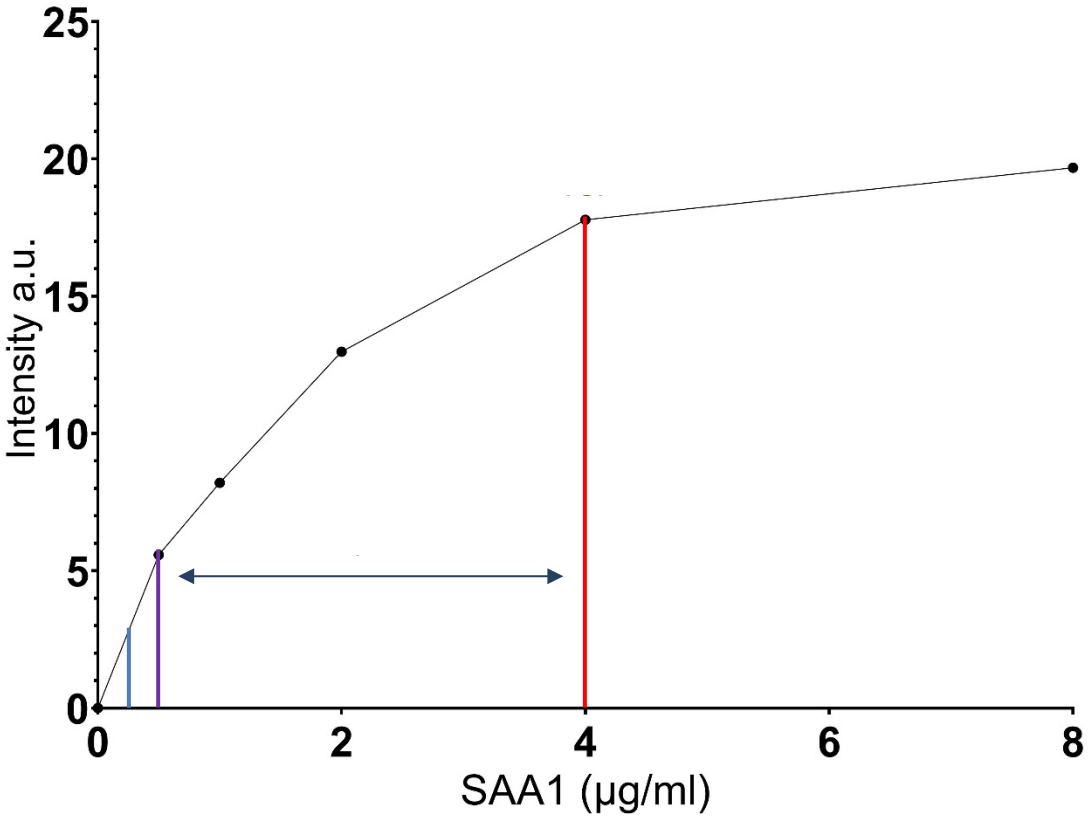

Figure 2.6 -Calibration curve for the test line colour intensity vs the concentration of SAA1 in µg/ml. Labelled with LOD (blue line), LOQ (purple line) and LOL (red line). Mean plotted from three technical replicates.

2.4.2 The Hook Effect

The hook effect occurs when there is a large amount of analyte in the sample and therefore this binds to the capture antibodies at the test line and this blocks the binding sites. In order for the analyte in the sample to be seen as present in the sample it must bind a tagged antibody that can be visualised when it binds at the capture site. This leads to a decrease in the test line colour intensity as the concentration increases above a certain point, an example of this can be seen in the graph below.

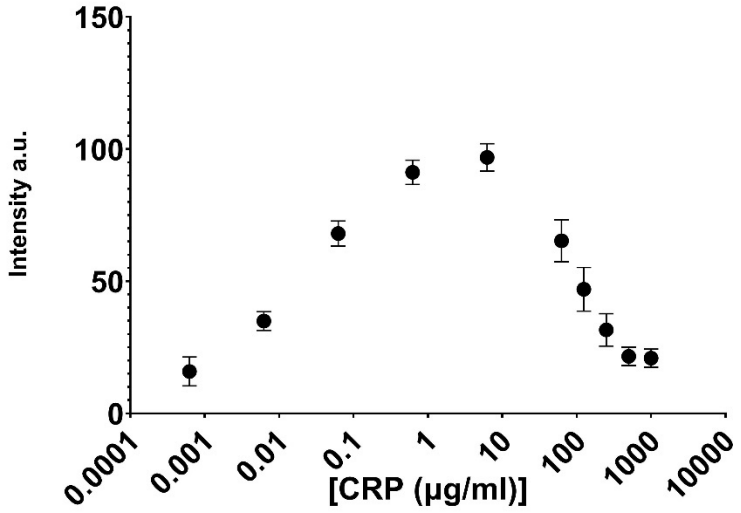

Figure 2.7 – CRP calibration curve showing the mean plotted with error bars representing the standard deviation for three repeat measurements, highlighting the Hook effect.

2.5 Key terminology

Below are some of the key terms that are used throughout the thesis and their individual definitions for clarity as these terms are used interchangeably although they are all unique.

Biomarker: A 'biomarker' can be virtually any biological compounds, such as a protein or fragment thereof, a peptide, lipoprotein, carbohydrate, lipid, nucleic acid, organic or inorganic or small molecule that is present in the biological sample and can therefore be isolated and measured in the sample. Furthermore, a biomarker can be any entire molecule or a part that be functionally recognised. A biomarker is informative if a measurable aspect or characteristic of that marker is associated with a given disease state such as infection with TB. A measurable aspect may include, for example, the presence, absence or concentration of the biomarker.

Analyte: Is a compound or substance that is of analytical interest and is the constituent being identified or measured.

Antigen: Is a foreign substance that can bind to a specific antibody or T-cell receptor to elicit an immune response within the human body.

Chapter 3 Techniques and Methodology

3.1 Laser Direct write (LDW) Patterning

To create the impermeable structures within the NC membranes of lateral flow tests have used a previously demonstrated laser direct-write (LDW) approach [22, 23, 49]. This has already shown the versatility and usefulness of this LDW technique in the patterning of diagnostic devices in porous materials such as cellulose [21, 25] and nitrocellulose membranes [23]. It has been demonstrated that it can be used to create impermeable barriers that do not allow liquid to migrate across the multiple channels of the diagnostic sensors therefore eliminating cross-reactivity between the multiple assay reagents [22].

A liquid photopolymer is first locally deposited onto the porous NC membrane with a deposition nozzle at locations pre-defined by the device design, and in this case of a multiplexed LFD, this is in the form of straight lines that extend along the length of the LFD. A laser beam subsequently follows the deposition head and illuminates the deposited line pattern(s) thereby inducing photo-polymerization of the polymer, transforming it into a fully solidified polymeric wall that extends throughout the full depth of the membrane. The schematic in figure 3.1 describes the laser patterning protocol.

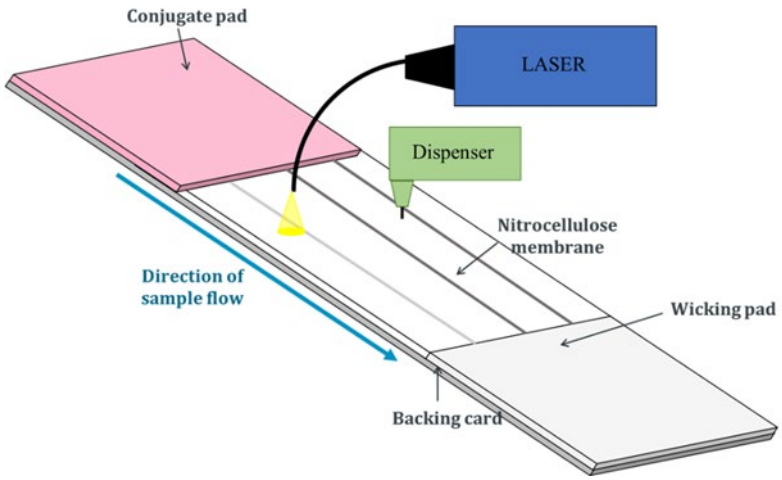

Figure 3.1 - Schematic of LDW patterning of the NC membrane of lateral flow device to create four parallel flow channels. These impermeable barriers mean there is no interference or cross reactivity between the assays used to detect the multiple markers within the parallel channels of a single LFD.

This technique creates precise hydrophobic polymer structures within the membrane. The polymer is photosensitive therefore its properties can be altered by exposure to light. The liquid polymer is an amalgamation of monomers, oligomers and photo-initiators which when exposed to a particular wavelength leads to decomposition of the photo-initiators into reactive species that trigger the polymerisation of the functional groups of the oligos to the monomers which precedes the formation of cross-links between the elements of the polymer and an additional free radical that continues the reaction, ultimately causing a change in the physical properties and transformation to a solid state. A schematic of this can be seen in Figure 3.2.

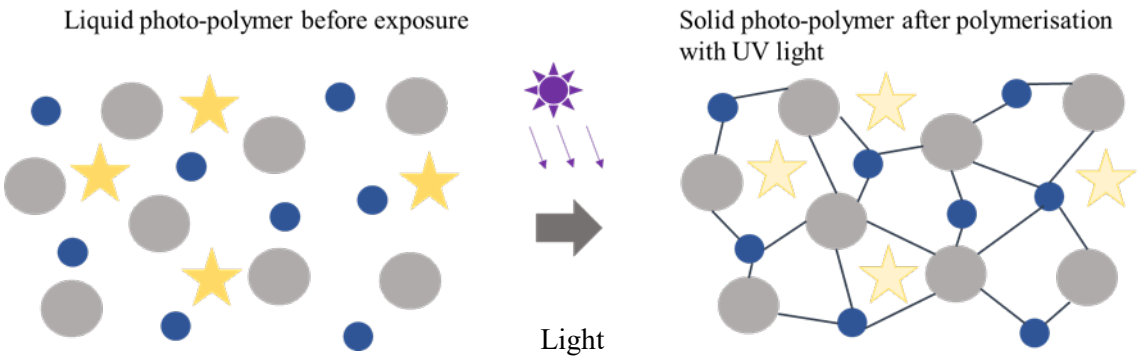

Figure 3.2 - Schematic of the light-induced photo-polymerization process showing the formation of cross-links between the monomers (dark blue small circles) and oligomers (large grey circles) triggered by photo-initiators (stars) after exposure to blue light.

The polymerized line patterns (with ~500 µm width) define the fluidic wall(s) that serve as impregnable demarcating barriers that define the boundaries between parallel channels and serve to confine and transport the liquids within the channels of the porous membrane. The speed used for deposition of the polymer lines on the porous membrane was 50 mm/s and the laser speed used to illuminate (and thereby polymerize) the polymer was 50 mm/s. A time delay of 15 seconds was introduced between the deposition of the polymer and the illumination by the laser light, to allow the polymer to extend throughout the thickness of the porous membrane. The membrane was 3.5 cm from the deposition head and the subsequent laser was at a distance of 0.5 cm. These parameters have been previously optimised to ensure complete penetration and full polymerization of the polymer of the polymer within the NC membrane. The fabrication conditions including the photopolymer deposition speed, the laser scanning speed and the time delay that we used for the device processing herein are sufficient to fully polymerize the photopolymer producing impermeable polymeric structures.

The photopolymer used was Desolite 3471-3-14 from DSM Desotech, Inc., Elgin, IL, USA, which is an acrylate-based photopolymer with a viscosity of 10,000 mPa·s at 25°C. Composition: 10-15% multifunctional acrylate, 10-25% glycol ether acrylate, 1-5% photo-initiators, <1% additives and <1% monomer. It has a density of 1110 kg · m^{-3}, refractive index of 1.5 and surface tension of 25 dynes cm^{-1} when measured at room temperature (~23°C). The Desolite is stored in an opaque container to avoid light exposure and kept at room temperature, resulting in a shelf life of 18 months as dictated by the manufacturer. The dispensing platform used for the deposition of the

photopolymer onto the nitrocellulose membrane was a PICO® PµlseTM system from Nordson EFD, UK. It is designed to dispense micro-droplets of 0.5 nL through a tip of 100 µm diameter at a frequency of 100 Hz. The laser used for the LDW patterning process was a 405 nm continuous wave diode laser (MLDTM 405 nm, Cobolt AB, Stockholm, Sweden) with an output power of 70 mW. The numerical aperture of the laser is 0.075 and the beam divergence is <1.1, beam quality (M^2) is <1.2; additionally, the beam has circular symmetry >0.9:1 and is non-collimated and is used without a focusing lens and therefore the beam propagates in free space.

The speed at which the dispenser is moving dictates the volume of photo polymer that is deposited per unit area of the substrate and defines the areal density of polymer, and this can range from 30 – 90 mm/s depending on the requirement. It is also crucial that the polymer has sufficient time to penetrate through the entire thickness of the membrane before it is polymerised to ensure a solid barrier has been formed that would prevent the motion of any liquid across the boundary between adjacent channels. For this reason, there is a time delay between the deposition of the polymer and the polymerisation with the laser. This time was optimised for this polymer however the use of an alternative polymer with different physical properties would require further optimisation to establish the appropriate delay time.

3.2 Antibody deposition

To implement the immunoassay onto the LFD firstly the capture molecule (either analyte for a competitive assay or antibody for a sandwich assay) was locally deposited to form a test line on the NC membrane of a single-channel LFD. The test and control line deposition were performed using a XYZ3210 dispense platform from Biodot (Irvine, CA, USA) which allows for precise and consistent antibody distribution, more information can be found on this in Appendix B. The machine is programmed to deposit 20 nl droplets every 0.25 mm in quick succession to create a test line constituted of the capture molecules. The NC with deposited antibodies was then left to dry overnight at room temperature in a desiccator cabinet with humidity < 60%.

3.3 Building the LFD

3.3.1 Conjugate pad treatment

The conjugate pad was fully immersed in the treatment solution (0.05% Tween 20 and 5% BSA in DI water) and dried at 60 °C for one hour followed by further drying overnight at room temperature in a desiccator cabinet with humidity < 60%.

3.3.2 Device assembly

All the materials; the NC membrane, absorbent/wicking pad and conjugate pad were procured as large reels. The NC membrane was a Unisart CN 95 membrane obtained from Sartorius Stedim Biotech GmbH, Germany with a thickness of 140 – 170 µm, a pore size of 15 µm and a capillary flow speed of 90-135 s/40 mm. The absorbent pad was a Whatman™ CF4 obtained from GE Healthcare with a thickness of 480 µm. The conjugate pad was obtained from Ahlstrom-Munksjö, Finland was grade 6614 with a weight of 75 g/m^2, a wicking rate of 5 s/2cm, water absorption of 57 mg/cm^2 and made of polyester fibres with binder.

The first stage is the LDW patterning of the NC membrane, followed by antibody deposition via the biodot system. The NC is left overnight before use to ensure the antibodies have been dried onto the membrane and will not be washed away upon use. Next the conjugate pad is treated and then dried at 60°C for one hour then left over night before use. Once dried the individual components are assembled onto the backing card (from Kenosha, Netherlands). Firstly, the NC is applied to the backing card followed by the absorbent pad which is placed on top of the NC with a 2 mm overlap. The conjugate pad is then placed on top again with a similar overlap. A clear tape is then placed over the entire card and all components to ensure the device is protected and that contact between the materials is maintained. The final stage is cutting the materials into individual LFDs of predetermined width using the CM5000 guillotine cutter (Biodot).

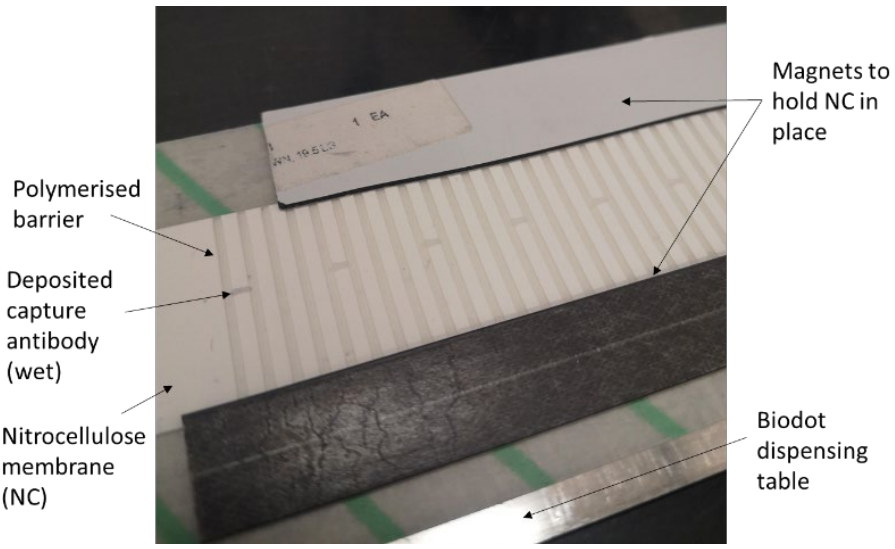

Figure 3.3 – Photograph of a multi-channel device with antibodies deposited on the NC in every fourth channel using the biodot dispensing system, to make a four-channel LFDs. with antibody deposited in every fourth channel on the NC, using the biodot dispensing system.

3.3.3 Preparation of the conjugate

For the antibodies bound at the capture line to be detectable they must be tagged with a coloured signalling label. In this thesis gold nanoparticles were used throughout; however different types of antibody conjugation labels can be used.

3.3.4 Streptavidin-biotin conjugation

This conjugation method relies on the strong binding between streptavidin and biotin. The antibody being used for the conjugation must be biotinylated, i.e., have a biotin molecule added. Then the gold molecule is decorated with streptavidin which has high affinity for the biotin molecule, and this joins the antibody to the gold nanoparticle (AuNP). The popularity of this particular method of conjugation is primarily due to two factors. The first is that both the biotin and streptavidin molecules are relatively small which gives rise to superior binding opportunities to other molecules such as antibodies, without limiting their ability to bind their antigen. The second is the high specificity with which these molecules bind to each other, as well as the

strength of the bond, which is the strongest type of non-covalent bond with a dissociation constant (K_D) of approximately ~10-14 mol/L. This means the binding occurs very quickly and is highly stable over a wide pH range (4-9) and can withstand, temperature up to ~70°C and interactions with solvents [50]. As seen in Figure 3.4, one streptavidin molecule can bind up four biotin molecules allowing for amplification of weak signals to improve the sensitivity of diagnostic assays. The streptavidin decorated gold used in this thesis was Streptavidin Gold Conjugate (40nm, 10 OD) (ab186864) from Abcam, UK.

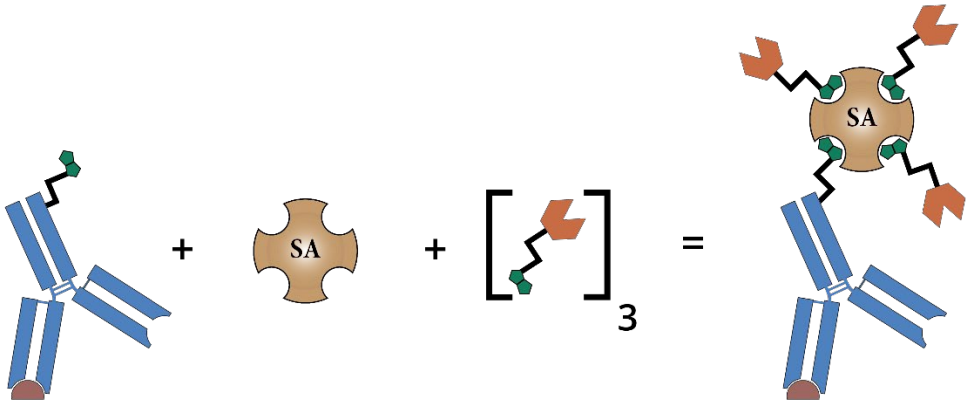

Figure 3.4 – Schematic of biotin-streptavidin binding complex [51]

3.3.5 NanoCompsix gold conjugation

The following commercially available kit was used for the conjugation of the antibodies to the AuNPs; NanoComposix PEG-Carboxyl conjugation kit contains a lipoic-dPEG12-COOH ligand that's covalently bound to the gold nanoparticle with a dithiol which forms a strong, stable bond to its surface. The acid group provides a negatively charged surface for further functionalization and these carboxyl surfaces can be used to bind molecules that have free amines such as antibodies to their surface. An amide bond between the acid surface and the free amine is formed using EDC/NHS chemistry. The BioReady materials are provided to use EDC/NHS chemistry to covalently link the antibodies to the AuNPs. The conjugate was prepared as per the manufacturers protocol for BioReady carboxyl 80 nm gold particles, 20 OD AUZR80-10M obtained from nanoComposix, CA, USA.

3.4 Device testing

The devices detailed in this thesis encompass two types of LFD, the half and full LFD. The half LFD which is does not include the conjugate pad and is sometimes used to save time and cost in the early development stage. The full LFD has the conjugate pad attached and represents a commercially available LFD

3.4.1 Half LFD

Sometimes for early-stage development a half LFD that does not include the conjugate pad is used initially. Use of the conjugate pad is an additional step that required optimisation of reagents and therefore additional development and time and therefore not used at this preliminary or feasibility study stage. For use of the half LFD however, the conjugate was mixed with the sample in the well of a 96-well plate and the NC membrane was introduced directly to this mixture. The test was allowed to run for several minutes, until all the fluid had been taken up by the LFD and moved to the outer edge of the absorbent pad.

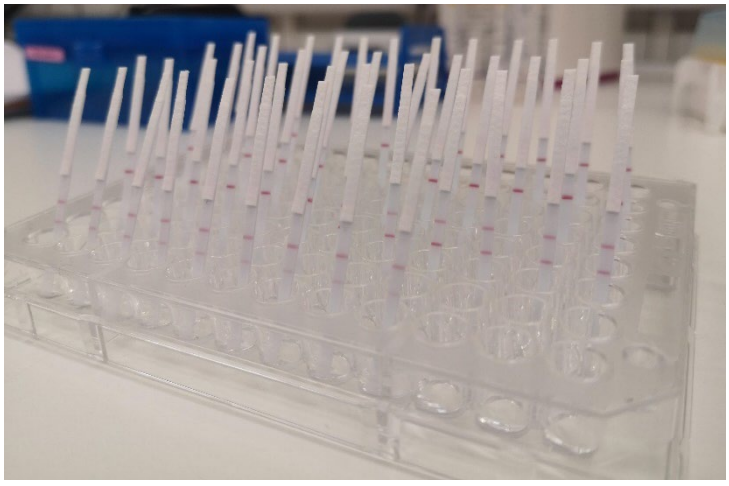

Figure 3.5 – Photograph of individual 2 mm half LFDs being tested in a 96-well plate

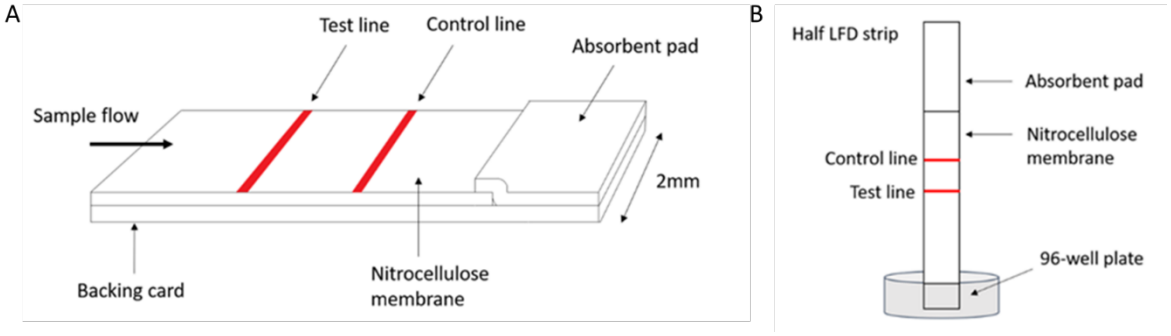

Figure 3.6 - A) Schematic of the half LFD with components labelled, B) Testing procedure of the half LFD in a 96-well plate.

After the test has completed and the entirely of the sample has been wicked up into the test, finished the half LFD was then moved into a new well containing 50 µl of PBS to clear any background colour. For multiplex devices where the footprint of the device is greater, a proportionally larger volume of PBS in used.

3.4.2 Full LFD

The full LFD instead includes the conjugate pad. Before use, the conjugate (gold tagged antibodies) for the assay was pipetted onto the conjugate pad and allowed to dry for 1 hour; the volume of conjugate used was assay-dependent. The sample was then pipetted into the well of a 96-well plate and the test was inserted, conjugate pad first. The sample rehydrates the dried conjugate to allow the sample to bind to the tagged antibody and flow along the test. For the 2 mm LFD 80 µl of sample was used and no post-wash step was necessary.

3.5 Results analysis

For the collection of the experimental data, the intensities of the test line were measured during the initial development stage using a scanner (Epson Perfection V800 Photo A4 Flatbed Scanner). The images captured using the scanner were processed with the ImageJ software (National Institutes of Health, USA) to extract the respective red colour intensities produced at the test line. Using its RGB function the software measures the mean colour intensity of the pixels at the test line and the colour intensity value for the control device was subtracted from the measured value to account for any background. The control device is a LFD tested with no analyte and therefore represents a negative result.

3.5.1 Limit of Detection

An important aspect of assay analysis during optimisation is calculation of the limit of detection (LOD) of the assay, which is defined as the lowest quantity of the analyte that can be detected but still distinguished from a blank value (control) within a stated confidence limit,[52]. There are different ways to assess the LOD depending on the assay, and these include visual evaluation, a signal-to-noise approach and standard deviation estimation.

A simple visual evaluation could be relevant for use with LFDs as the LOD is determined by establishing the minimum concentration of analyte that can be detected reliably by eye. Alternatively, the signal-to-noise ratio can be used to determine LOD by comparing the signal obtained for samples with a known concentration of an analyte with the signal from the blank which will give the minimum concentration at which the analyte can be reliably detected with a given confidence factor. The limit of blank (LOB) is another important parameter which determines the LOD of an assay. LOB describes the highest measurement result that is likely to be observed (with a stated probability) for a blank or negative sample. The assumption in the determination of the LOB is that values exceeding the 95th percentile of the distribution of values on truly blank or negative samples deviate significantly from blank or negative measurements. When a sample produces an observed value that exceeds the 95th percentile, it may contain a concentration of analyte that is above zero [53]. Given a Gaussian distribution of blank or negative values, this limit corresponds to:

$$\text{LOB} = \mu B + 1.645 SDB \qquad [3.1]$$

where μB and SDB are the mean and standard deviation of the blank or negative measurements respectively. LOD is the lowest analyte concentration likely to be reliably distinguished from the LOB and at which detection is feasible. To calculate the LOD, a minimum of 10 individual samples with concentrations ranging from the LOB to approximately 4xLOB should be tested at least 10 times by at least two technicians in a minimum of two days or runs. A pooled estimated standard deviation of the sample distribution at a low level (SDS) can be derived from repeated measurements. Finally, an estimated LOD is then obtained as:

$$\text{LOD} = \text{LOB} + 1.645 SDS \qquad [3.2]$$

Finally, LOD can also be determined based on the standard deviation of the response and the slope. The detection limit (DL) may be expressed as:

$$\text{LOD} = 3.3\ \sigma\ S \qquad [3.3]$$

where σ is the standard deviation of the response and S is the slope of a linear calibration curve. The above definition is only restricted within the cases of linear calibration (S=constant), however, for most of the competitive immunoassays, the calibration curves are curvilinear (S=variable) and the LOD cannot be estimated simply from this equation.

3.5.2 Statistical analysis

All the data collected was processed and stored in GraphPad Prism 9, including all statistical analysis except the receiver operating characteristic curve (ROC) curve which was performed in IBM SPSS Statistics software. For ROC curve analysis the raw data was first labelled with an outcome, in this instance this was either 0 = negative or 1 = positive for the samples. This data was then analysed using binary logistic regression, which predicts the probability that the observation (test line colour intensity) falls into one of the two defined categories (either positive or negative for TB). It is these predicted probabilities that are then plotted onto the ROC curve which is a graphical plot that shows the diagnostic capability of a binary classifier system as the discrimination threshold is varied, in this case that is the test line colour intensity. The outcome is an AUC that gives the sensitivity and specificity of the variable at different thresholds to establish at what point the test line colour intensity value has best discriminatory power to differentiate healthy from TB patients.

All other analysis, including t-tests, is dependent on the data set being investigated.

Chapter 4 Semi-quantitative and multiplexed detection

4.1 Introduction

In vitro diagnostics influence over 60% of clinical decisions yet account for only 2% of healthcare funding despite the fact that effective diagnostics reduce overall spending by reducing unnecessary hospitalisations and treatment [54].

The lateral flow device (LFD) market was valued at 11.4 billion USD in 2021 and with a compound annual growth rate (CAGR) of 7.7% it is expected to reach a value of 12.6 billion USD by 2026 [55]. LFDs are an attractive solution for point-of-care (POC) testing because they are cheap, easy to use and do not require skilled personnel or expensive equipment to operate. They do have two inherent inadequacies however: most commercially available LFDs are limited in their multiplexing capabilities and are generally designed to detect a single biomarker and furthermore the result presented is largely binary with a yes/no output [56].

Multiplexing, or the simultaneous measurement of multiple biomarkers using a single LFD has significant potential in increasing the diagnostic efficiency [57], and this is even more pertinent when the multiple biomarkers that need to be detected also need to be quantified simultaneously to guide the treatment of a disease are inter-dependent [58]. Consequently, the demand for POC multiplexed diagnostic assays has seen a dramatic increase. The simultaneous detection of several biomarkers provides valuable information to improve the efficiency of analysis and decreases the chance of false negative and false positive results, increasing tests sensitivity and specificity [59]. Multiplexing can help when the sample volume is limited as one sample can be used to test for multiple biomarkers, reduce time for analysis as only one single test has to be run and finally helps reduce the overall cost of the testing. Thus, this advanced POC testing solution could lead to a great enhancement in the ability to respond to public health crises.

4.1.1 Multiplexing technologies

The current methodologies for the implementation of multiplexing on LFDs can broadly be divided into the following categories:

- Strip architecture modifications/lamination

- Spatial separation
- Barcode design
- Cross-reaction antibody
- Distinct signal transducers
- Molecular logic encoding

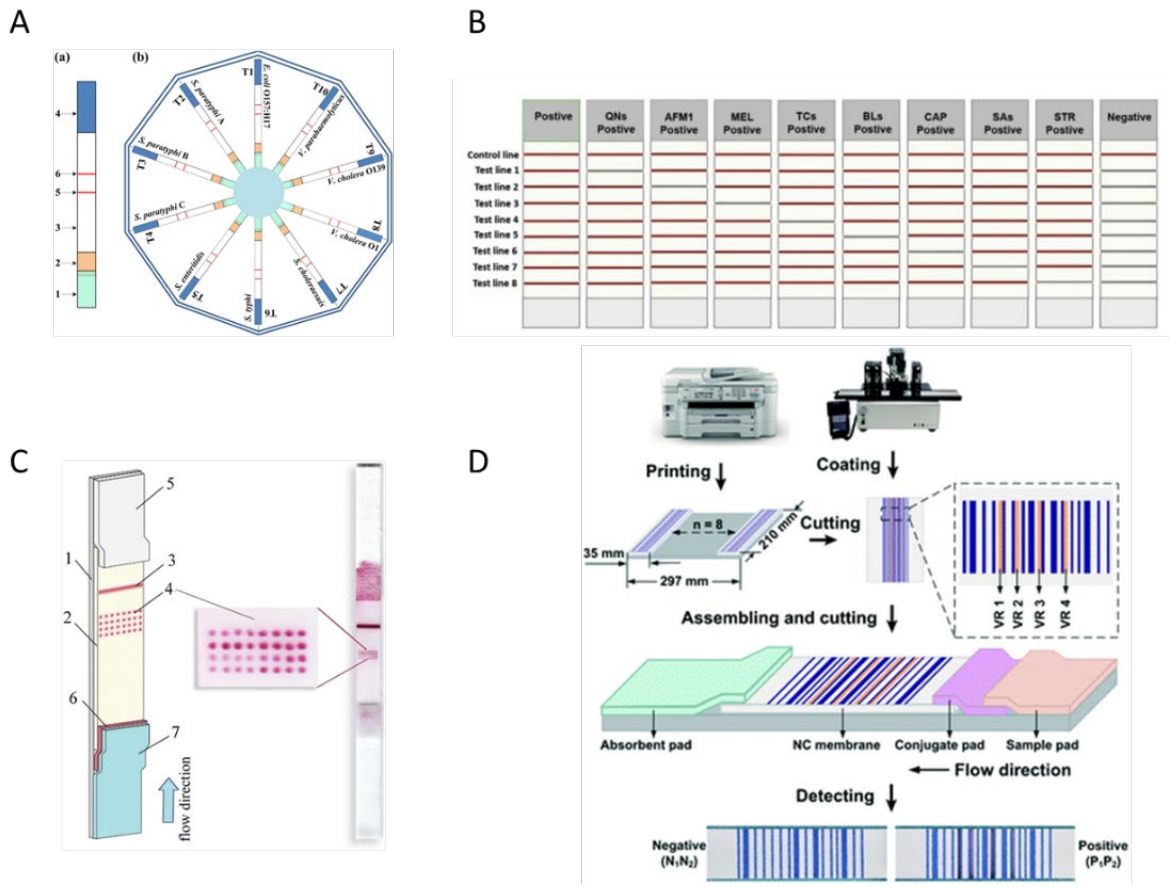

Figure 4.1 – Images showing examples of different methods of multiplexing on lateral flow devices using A) lamination of multiple LFDs [60] B) spatial separation of test lines in the same flow path [61], C) use of a microarray [62] and D) a bio-barcode implemented on a LFD with a reader for quantification [42].

Strip architecture/lamination

Modification of the strip architecture or lamination of LFDs is the simplest method for multiplexing. As the sample flow on the test is separated it eliminates any interference or cross-reactivity between the different assays [63]. However, the test's footprint, cassette and volume of sample required all increase proportionally with the number of analytes being detected leading to increased costs, processing time and basic complexity of taking the test [64, 65].

There have been a variety of test architectures including "fork sign", "disc" and "origami" with both 2D and 3D geometries. In such cases, multiple test strips are combined by the sharing of a single cassette and sample pad. One such example is the detection of multiple markers from urine in an "origami" orientation [66]. Li et al compared the efficiency of a selection of different architectural designs including the "fork" and "peace sign" [67]. Their results showed that the "peace sign" with a common triangular center sample pad, was the most effective geometry for the detection of whole-cell bacteria, namely *Pseudomonas aeruginosa* and *Staphylococcus aureus.* This has been further developed by several researchers for the antibody profiling against Yersinia pestis, foodborne pathogens and nucleic acids using the disc-type multiplexing architecture [65, 68]. This method has also been used for rapid detection of blood components for blood grouping [69].

This assembly of multiple tests forms an effective method of multiplexed analyte detection however there are limitations. Typically, these larger devices require up to 100 µl of sample and this increases as more tests are added to the assembly. This means these devices are suitable for analysis of biomarkers for which sample media is abundant such as water, urine, or saliva, however, in hotter countries the collection of both saliva and urine can be problematic, furthermore these tests are less appropriate for biological fluid that is harder or more invasive to collect, such as a finger-prick which delivers < 5 µl of sample. Additionally, the distribution of the sample across each test should be investigated carefully as the sample volume can have an impact on the sensitivity and accuracy of the test.

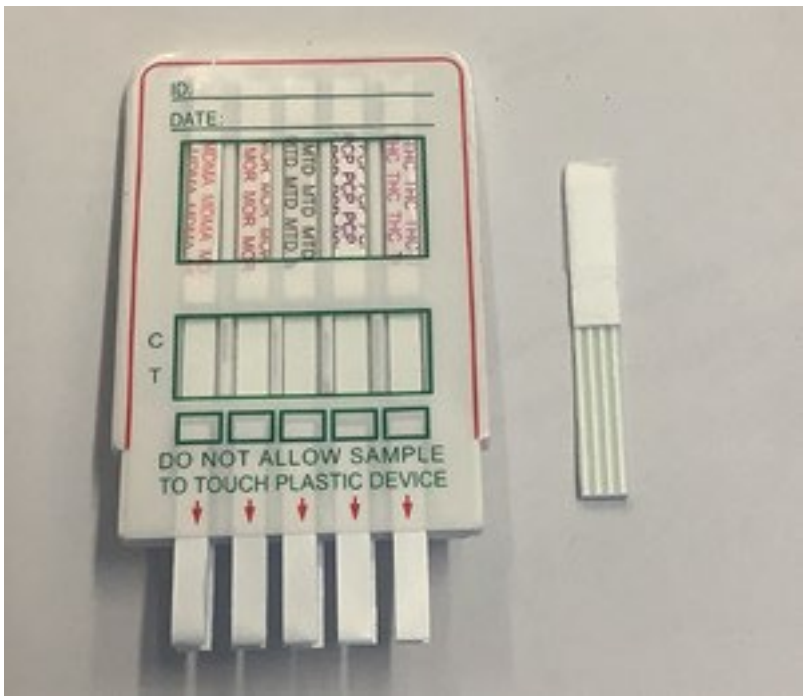

Figure 4.2 - Comparative photo showing a commercially available multiplex LFD wherein multiple LFDs have been laminated and assembled into a cassette (left) and LDW patterned multiplex LFD (right).

Spatial separation

This method of multiplexed detection uses independent detection zones for individual analytes which can be detected using the same or different signal labels. Spatial separation dramatically increases the number of markers that can be detected by using multiple test lines or dots (often referred to as a microarray). Han et al demonstrated the capacity for eight spatially separated test lines in a single flow path for the detection of antibiotics and aflatoxin M_1 in milk [61], however the AuNPs used in the labelling and therefore the detection had insufficient brightness and therefore the test had low sensitivity. Silver enhancement signal amplification has been implemented to improve on these results [70] and additionally the use of carbon nanoparticles (CNPs) has shown higher sensitivity for the detection of four Shiga toxin-producing *Escherichia coli* genes [71] and three *Fusarium* mycotoxins [72].The use of a microarray has been reported many times[62, 73-76]. This method has been used to achieve the detection of thirty-two analytes simultaneously for drug testing within 10 minutes [62]. Although this method can circumvent the

issues of sample volume and physical limitations seen with strip lamination, the increased complexity of the design may introduce flow variation over the different detection zones and interference may occur. There is also the question of interpreting such a complex interface and the requirement for a reader to obtain the results from this type of sensor. This is problematic for several reasons; firstly, the use of a reader and interpretation may require specific training and secondly the development of a reader and the upfront cost of the unit further increase the cost of the sensor and reduce accessibility. This also does not account for the requirement for power and the test being limited to use where a reader is available and working.

Alternatively, luminescence can provide a higher sensitivity alternative to colored labels due to their intense emission [77]. The use of Fluoro-Max nanoparticle detection can successfully differentiate four hepatitis B virus (HBV) genotypes using a multiline lateral flow geometry [78]. Due to their high performance, there is increasing use of luminescent materials for detection on LFDs, including dye-doped nanoparticles [79, 80], quantum dots [81], up-converting nanoparticles [60, 65] and gold nanoclusters [82].

Barcode design

A barcode can both encode information and store data through the pattern of dark bars and spaces between them of different widths [83]. This information can then be decoded using a barcode scanner and is analogous to the 'yes/no' output of LFD diagnostics. The efficiency of the barcode technology can be utilized for multiplexing applications, and this has been implemented by several groups for the detection of protein biomarkers, blood typing, pathogens, and drugs [42].

The information encoding and storage capacity of the barcode has led to accelerated development of multiplexed LFDs. They can be interpreted with a simple and affordable barcode reader that gives a highly precise and accurate readout. However, the initial step to encode the barcodes is highly complicated and requires skilled technicians and this would influence the production of such devices or POC testing.

Cross-reaction antibody

Conventionally LFDs implementing multiplexing use multiple specific signal probes that can identify a specific target. However, there is an option to use signal probes that are broadly specific

to a class or group of compounds. There is an interest in the development of broadly specific antibodies through genetic engineering and chemical crosslinking [84] to have specific cross-reactivity for the measurement of several analytes and this has been shown successfully for the detection of twelve *Listeria* species and provides a suitable alternative for a multiplexed LFD with a single test line [85]. They have also been implemented on a single test line device for detection of twenty-seven sulfonamides in foodstuffs and can be visualized with the naked eye within 10 minutes [86].

This technique is one of the simpler methods for introducing multiplexing. However, the production of these broad-spectrum antibodies is complicated and production with high purity and repeatability would require expensive production initially. As this method is only suitable for some applications and the detection of a group or class of molecules, the affinities of each antibody for the individual components would vary and therefore it would be important to ensure equal sensitivities across all potential target analytes of the group. This method would not be applicable for all testing requirements, although it could be highly appropriate for certain applications.

Distinct signal transducers

Integrating multiple test lines into a single LFD is a straightforward method of adding multiplexed capacity. However, these LFDs are only several centimeters in length and therefore are limited by spatial availability. The length of the LFD could be extended to accommodate significantly more test lines but the 'wet-out' velocity of a fluid travelling in the dry porous membrane is inversely proportional to the length squared travelled and therefore increasing the length means it will take longer for the test to complete [6]. Additionally, to maintain a non-depleted sample over a longer distance of membrane would require a large starting sample volume. So as an alternative method, multiple signaling labels could be combined into a single test line. Compared to the multiple line model or microarray, the use of a single test line can reduce the assay time, cost and non-specific binding or interference that can occur with multiple detection sites in the same flow path. The use of this method has been demonstrated for the detection of two mycotoxins by combining blue and red AuNPs as signaling molecules. A single test line was used in a competitive assay format and therefore in the absence of the target molecules a purple test line (combination of blue and

red AuNPs) was formed, if both were present there was no line shown, and they could be distinguished with the appearance of either a blue or red test line if only one molecule was present in the sample. Quantitative analysis was achieved through the use of a smartphone reader [87]. The same principle can be applied to quantum dots as they have unique photophysical properties, such as broad absorption bands and narrow emission spectra which can be tailored for the precise identification of multiple analytes in the same test line [88-90]. This can be combined with Surface Enhanced Raman Spectroscopy (SERS) for increased sensitivity and has been used for the development of LFDs for detection of viruses, bacteria, and cardiac markers [91-93].

For this method to be successful the signal from the labels must be clearly distinct with high resolution and there can be no cross-reactivity between the labels. Due to this it could limit the number of analytes that can be detected this way unless the detection is incredibly sensitive, but this is likely to involve the use of more expensive and specialist equipment which limits accessibility. Furthermore, this accumulation of multiple labels at the same test line could lead to steric hindrance whereby the analytes cannot bind to the biorecognition element.

Molecular logic encoding

Logic gates use 1, equal to ‘true’ (positive) and 0, equal to ‘negative’ (false) as data inputs, and this information can be converted into data outputs through various logic operations. These logic gates simplify the process of data processing and have been applied to biological and chemical molecules. Here these inputs are processed to give outputs such as a colorimetric, fluorescent, or chemiluminescent signal for example. This principle has been applied to biosensing and LFDs as a means of extending their capacity to include multiplexing. They have been shown to detect an array of analytes including proteins, DNA, bacteria, and small molecules [94, 95].

This method circumvents the issues of spatial and physical limitations seen when multiplexing and can therefore immensely increase capability, whilst simplifying data analysis. This is an area of interest that is still developing to increase the complexity of the operations.

Lamination is a relatively simple method, and reduces the risk of interference between assays, however the costs of fabrication, the test footprint, cassette (LFD housing) and volume of sample required all increase proportionally with the number of tests combined, leading to increased overall cost and processing time. The spatial separation approach involves the inclusion of

multiple test lines and therefore requires little modification to the device architecture. However, the interpretation of the results is challenging due to the proximity of multiple test lines and their mutual cross-interference. This can be mitigated to some extent by increasing the distance between the different test lines, but this in turn translates into an increased footprint in the same manner as for the lamination method. Microarrays allow for more biomarkers to be detected in a smaller test footprint however this is at the expense of the test's robustness. The smaller detection sites are susceptible to flow variability and subsequent signal generation. Additionally, due to the higher number of detection sites in a small space a reader is required to interpret the results accurately.

In recent years the development of rapid multiplexed biosensing has seen increasing interest due to the need for POC diagnostics that can compete in terms of sensitivity and specificity with laboratory-based techniques. The increased capacity for multiplexed detection has increased the applicability of LFDs in food and environmental monitoring as well as clinical diagnostics. Nevertheless, there are still several challenges being faced in this area at the current time to ensure that testing remains affordable and simple enough for use in the field.

4.1.2 Semi-quantitative technologies

The current methodologies for the implementation of quantitative or semi-quantitative detection on LFDs can broadly be divided into the following categories:

- Spatial separation
- Introduction of a reader
- Standard/reference line
- Tailoring specific cut-off values

Spatial separation

As with the multiplexing technique, the use of multiple detection zones or test lines within the same flow path can also be used to implement semi-quantitation onto LFDs. This technique utilizes multiple test lines in a 'ladder' format where each contains capture antibodies against the analyte. The underlying principle here is the consumption of the labeled antibody-antigen

complex as it moves along the test and interacts with the capture antibodies immobilized at the separate test lines. The test line colour intensity and the number of visible test lines is directly proportional to the concentration of the analyte that is present in the sample. This has been applied to many assays [96-99]

Alternatively, using the same format, both competitive and sandwich assay formats can be combined to allow for a similar effect of multiple visible test lines, however in this case the number of test lines may not be directly proportional to the concentration of analyte in the sample but may represent a pre-defined range of concentration [100, 101].

Introduction of a reader

Imaging and readout hardware is available to covert a standard qualitative LFD into a quantitative-biosensors however this technology is not always suitable for in-the-field testing and adherence to the POC testing, as set out in the ASSURED criteria defined by the WHO, requirements and therefore smartphone readers have been developed to bridge the gap. Although these have been shown to be successful, they mostly require additional attachments, such as black boxes, to ensure that the ambient lighting conditions do not affect the read out or additional treatment to the LFD for analysis [102-105]. More recently, alternatives have been proposed that require less sophisticated add-ons for operation such as using a simple black cardboard box as an enclosure [106].

Quantitative evaluation of the measured biomarker is known but relies on the use of readers [107, 108] and such measurement of the biomarker using a LFD, without a reader, is not only a prudent choice for many under-resourced countries across the world but is also a critical requirement. Smartphones are cheaper alternatives to proprietary readers for quantitation of paper-based sensors [109]; however, they still necessitate the use of the same adapted phone model by all end-users, which would not be practical in real-world settings. In addition, specifically designed add-on tools/holders are required to adapt/align the LFD to the smartphone's camera for imaging. As an example, smartphones could possibly be transformed into LFD readers for rapid, affordable, and early detection of pneumonia in a developing nation such as India where pneumonia is the leading cause of mortality in children and accounts for 20% of the deaths [110]. However, as late as 2018 only 26% of the Indian population had a smartphone and this was only projected to rise to 31.7% in 2020 [111].

Use of standard or reference line

Semi-quantitation can also be achieved by comparing the test line to a standard or reference line. For example, using the control line, the concentration of the analyte in the sample could be determined within a pre-defined range. Whether the test line is darker in colour, the same as, or lighter in colour than the control line can be an indication of the concentration range of the analyte [76, 101].

Tailoring specific cut-off values

As an alternative to having multiple test lines, another solution could be a single test line that has tailored cut-off values to adhere to clinical diagnostic requirements. In this case the presence or absence of the test line will correlate directly to a predetermined concentration threshold, which is highly relevant for clinical applications as well as regulatory such as drugs testing [26, 62, 112-115].

Despite the recent advances in the areas of multiplexed and semi-quantification of LFDs there are still challenges to overcome to further broaden the use and applicability of LFDs in clinical diagnostics as well as environmental and regulatory testing.

4.1.3 Biomarkers for pneumonia triage

Pneumonia is an inflammation of the lungs that can be caused by a multitude of different organisms and is a leading cause for hospitalisations and death in developed countries [116]. Although bacterial infection is the most common cause of community-acquired infection, viruses account for two-thirds of childhood infections and 13% of adult cases [117]. The diagnosis is generally made by the combination of a chest x-ray and blood tests. The chest x-ray highlights the presence of the infection but cannot distinguish the causative agents and the blood tests require further analysis of the immune cells. Differentiating between bacterial or other infections is crucial for providing the correct treatment facilitating both the patient's recovery and avoiding administering of antibiotics for non-bacterial infections.

Host protein biomarkers can be used in the diagnosis of disease and identification. C-reactive protein (CRP) is a generic inflammatory marker produced by the body in response to an infection.

It must travel to the site of infection where it works to induce the complement pathway and increase phagocytosis and removal of harmful pathogens from the body. As it is present in the blood, it is readily accessible and hence its measurement is very easy and minimally invasive. As LFDs require only a small sample volume, a finger prick of blood would be sufficient to measure CRP. CRP has been shown to be an excellent marker of infection, giving a better indication than body temperature and white blood cell count alone [118]. CRP is normally present in very low concentrations in healthy individuals (<8 μg/ml) [118] but rises significantly for unwell patients to values greater than 500 μg/ml [119]. A quantitative measurement of CRP in the bloodstream can provide valuable information for the diagnosis and treatment of a patient, and because CRP is non-specific marker, CRP detection is broadly used in the primary care setting in conjunction with testing for other biomarkers. For patients with suspected pneumonia the National Institute for Health and Care Excellence (NICE) in the U.K. specify the following treatment guidelines: where CRP ≤ 20 μg/mL, no antibiotics should be given; for CRP ranging between 20 μg/mL and 100 μg/mL, a delayed prescription should be provided at a later date if their symptoms do not improve; if the level of CRP is ≥ 100 μg/mL then antibiotics should be given immediately.

In addition to CRP, blood serum procalcitonin (PCT) is a useful marker that can guide the initiation and duration of an antibiotic treatment because PCT offers good sensitivity in differentiating between bacterial and viral infections. PCT has also been approved by the US FDA for guiding treatment of pneumonia as when measured in healthy patient serum it ranges from <0.1 ng/mL to 0.5 ng/mL [120], but increases above 0.5 ng/mL during a systemic infection [121-124]. Furthermore, the levels of PCT can also be used as an antimicrobial stewardship tool for respiratory infections with levels above 0.5 ng/mL indicating a very likely bacterial infection [122, 125]. In addition, the levels of PCT have been shown to have predictive power of disease prognosis and likelihood of hospitalization for community acquired pneumonia as well as death [126, 127]. Patient serum PCT levels, at hospital admission, have a strong association with their APACH II score (a detailed description of this can be found in Appendix C), which is an ICU mortality prediction score [128]. Although these are not the only biomarkers associated with pneumonia, there is abundant evidence to support their use to influence treatment and patient care when compared to other less significant markers such as IL-6, which are also mentioned in the literature [129].

Therefore, the combination of these two markers could serve as an excellent screening test for the identification of firstly the causative agent of the pneumonia infection and secondly the severity of the infection; both pieces of information that are crucial to making an accurate and timely diagnosis and treatment plan whilst helping to reduce the development of antimicrobial resistance caused by over-prescription of unnecessary or incorrect antibiotics.

The group in the ORC has previously reported the use of LFDs with parallel flow-paths to circumvent the above-described multiplexing-related limitations [24]. This multiplexing technology maintains the overall device footprint to that of a standard LFD and therefore not only maintains the size of the required sample volume, but also saves money on the reagents, cassette (housing), packaging, and shipment of the devices, with each LFD costing in the order £1 to manufacture. Herein, is extended the multiplexing concept reported by He et al [24], to demonstrate, for the first time reader-less, multiplexed, semi-quantitative detection of two inflammatory markers, CRP and PCT, using multiple parallel channels created within a single LFD.

The novel device is an LFD with three-parallel channels created in the nitrocellulose membrane section of the LFD, as seen in Figure 4.3. Channel 1 and Channel 2 are for the detection of CRP with Channel 1 having a cut-off value of 20 µg/ml and Channel 2 having a cut-off value for detection of 100 µg/ml to produce a semi-quantitative measurement and these two channels implement the format of a competitive assay. Channel 3 is for the detection of PCT specifically with a cut-off of 0.5 ng/ml using a sandwich assay format. The details of these two immunoassay types will be described in section 4.2. For this initial development work that we are reporting here, we have chosen to use a simplistic device which does not include a conjugate pad; LFDs are often developed without the sample and conjugate pad during a research-phase study, and these are added later for the development of a commercial product. While developing this LFD, the use of a simpler device geometry is purely to save resources, as the need for large amounts of detection antibody dried onto the conjugate pad can make the development work prohibitive to undertake. In the future this can be added of course, as part of additional modifications that would be required for future commercialisation.

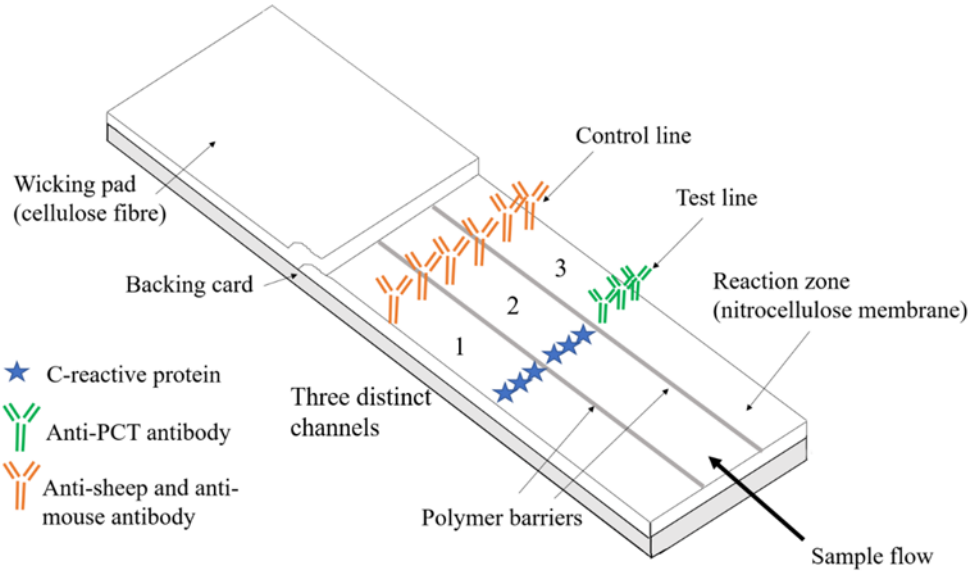

Figure 4.3 - Schematic of the three-channel multiplexed device for simultaneous detection of CRP and PCT with polymer barrier and assay components indicated.

4.2 Assays

The semi-quantitative lateral flow for detection of CRP and PCT uses a combination of two immunoassay types, the sandwich immunoassay and competitive immunoassay.

4.2.1 Sandwich immunoassay

Although there are several immunoassay formats that can be implemented on LFDs, the two most used are the sandwich assay and the competitive assay [130], and their general principles of operation can be seen in Figure 1 (in the background). For the sandwich immunoassay format, a monoclonal antibody is deposited onto the nitrocellulose membrane creating the test line and a further non-specific antibody is deposited on the same membrane to constitute the control line. The conjugate mixture that would be required for the initial analyte/target capture and its detection later in the assay sequence contains the detection antibody bound to a coloured signalling label, commonly a gold nanoparticle. When the sample is added to the conjugate mixture the analyte biomarker (PCT in this case) in the sample will bind with the labelled antibody and forms an analyte-detection antibody complex. This sample-conjugate mixture is then introduced to the LFD and when the analyte-detection antibody complex reaches the test line the

analyte will bind to the pre-deposited antibody at the test line creating a sandwich of two antibodies with the analyte biomarker bound in-between. As the detection antibody is labelled, the result can be visualized by the appearance of a coloured test line. In the simplest format the presence of the test line indicates a positive result. The control line will appear in every test and the absence of this line indicates a void test. In the sandwich format, the colour intensity of the test line is proportional to the concentration of biomarker in the sample.

4.2.2 Competitive immunoassay

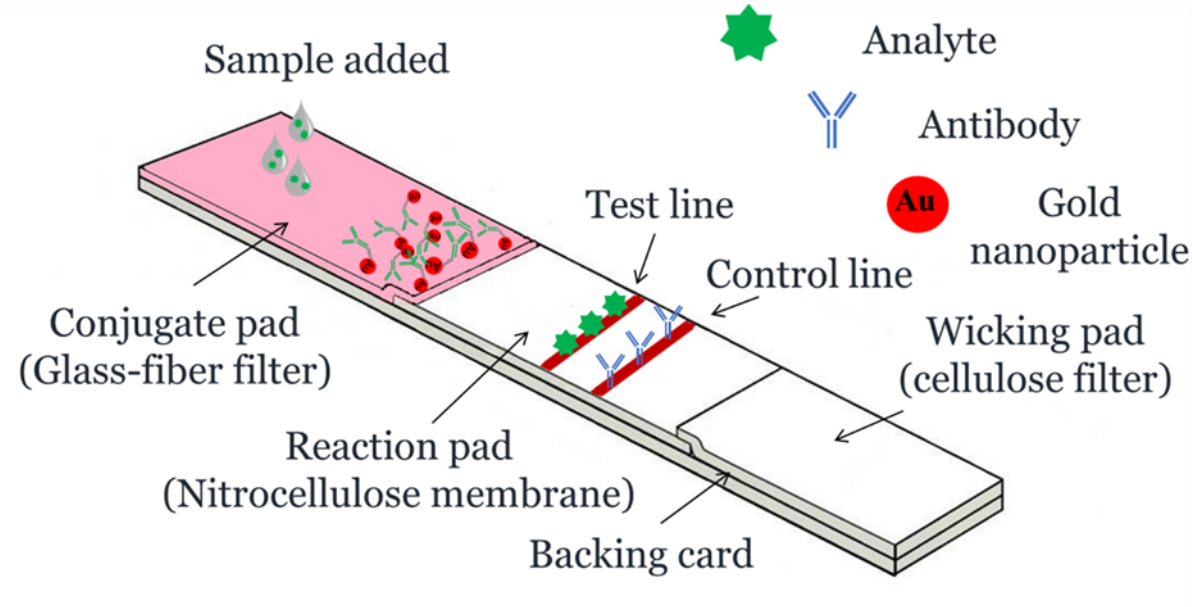

Figure 4.4 - Schematic of lateral flow device with labelled components and assay for competitive format.

As it is less sensitive, the competitive assay format can be preferable when the concentration of the analyte of interest is high. For this assay, as shown schematically in Figure 4.4, instead of a capture antibody, an antigen (the targeted biomarker CRP) is pre-deposited onto the membrane to produce the test line. The analyte (also CRP in this case) in the sample then directly competes with that antigen for binding to the tagged detection antibody. In the absence of the biomarker (CRP) in the sample, the gold-tagged detection antibody will bind directly with the immobilized antigen on the test line thereby producing a strong signal, and therefore in this case, the test line's colour intensity is inversely proportional to the concentration of biomarker in the sample.

The usual control line is also present to validate that the test has worked correctly. Here we have utilized the competitive assay format to overcome the Hook effect which can result from a biomarker with a high and wide physiological range such as CRP [100, 131].

This chapter presents the implementation of immunoassays for CRP and PCT on a single LFD for the semi-quantitative detection of these markers for potential use for rapid POC triaging of pneumonia. To our knowledge this is the first report of semi-quantitative and multiplexed detection of pneumonia-related markers using an LFD, without the need of a proprietary readers. This novel lateral flow device has three parallel channels in the nitrocellulose membrane section of the LFD.

4.3 LFD design and fabrication

4.3.1 Materials

The fluidic channels that define the multiplexed LFD were fabricated within backed nitrocellulose membrane purchased from Sartorius (UniSart CN95). The membrane thickness is 240-270 µm with an average pore size of 0.45 µm, the CN95 has a capillary speed of between 65-115 s/40mm. The absorbent pads were cellulose-based filter papers from GE Healthcare (CF4). For the CRP assay the capture antibody deposited at the test line was recombinant human C-reactive protein expressed in E. Coli (Sigma Aldrich C1617). The biotinylated anti-CRP detection antibody used was obtained from R&D systems (BAM17072). The antibody used to produce the control line was an anti-mouse Goat IgG from R&D Systems (AF007). The streptavidin-conjugated gold nanoparticles (AuNPs), 40nm, 10 OD, were obtained from Abcam (ab186864). The BSA and PBS used in the solutions were obtained from Sigma Aldrich (A2058, P3813). The capture and detection antibody for the PCT assay and the analyte were from the Human Procalcitonin DuoSet ELISA kit from R&D system (DY8350). The control line was donkey anti-sheep IgG antibody from R&D systems (BAF016). The samples were prepared using sterile filtered human serum obtained from Sigma Aldrich (H4522).

4.3.2 Laser direct-write patterning

To combine the two assays and produce one compact multiplexed LFD (schematically described in Figure 4.3) we used the laser direct-write (LDW) approach [22, 23, 49] as discussed in detail in Chapter 2.

4.3.3 Device assembly

Initially the detection of CRP and PCT was investigated separately using individual single channel LFDs 2 mm in width and 45 mm in length. The CRP assay was investigated using both the competitive and sandwich assay however it was finally developed in the competitive assay format whereas for PCT we used the sandwich assay format. The capture molecule (either CRP or anti-PCT antibody) was locally deposited to form a test line on the nitrocellulose membrane of a single-channel LFD. The test and control line deposition were performed using a XYZ3210 dispense platform from Biodot (Irvine, CA, USA) which allows for precise and consistent antibody distribution, described in section 3.2. Finally, the LFDs were left to dry at room temperature overnight.

Firstly, the components (cellulose wicking pad and LDW-patterned nitrocellulose membrane reaction pad) of the lateral flow devices were prepared and then assembled onto a backing card for stability. An appropriate (2-3 mm) overlap between these components ensured for an uninterrupted fluid movement. The devices were then cut to size using a CM5000 guillotine cutter (Biodot). To evaluate the LFD, it was dipped into a mixture of the sample, the detection antibody and the streptavidin-modified 40 nm AuNPs in the wells of a 96-well microtiter plate as shown in Figure 3.6. The LFD was then left to stand for 3 minutes until all the solution in the well had been wicked into the device and reached all the way to the end of the absorbent pad. The device was finally dipped into 20 µL of PBS solution for another 5 min to allow the rest of the unbound reagent to be wicked through to the reaction pad, thereby minimizing or eliminating any background colour that might develop across the device.

4.3.4 Results analysis

Although the test does not require the use of a reader, the intensities of the test line were measured during the initial development stage, using a scanner (Epson Perfection V800 Photo A4 Flatbed Scanner). The images captured using the scanner were processed with the ImageJ software (National Institutes of Health, USA) to extract the respective red colour intensities produced at the test lines. Using the RGB function the program measures, the mean colour intensity of the pixels of a fixed area at the test line and the colour intensity value for the control device was subtracted from the measured value to account for any background.

4.4 Calculation of Limit of Detection

The LOD was calculated as per the equations below [132]:

$$LoD = LoB + 1.645\sigma s \quad [4.1]$$

Where the limit of the blank (LoB) is defined as:

$$LoB = \mu B + 1.645\sigma B \quad [4.2]$$

Here the μB is the mean LFD signal colour intensity value for the negative control samples, σB is the corresponding standard deviation, and σs is the standard deviation for the lowest detectable concentration. The corresponding concentration and associated 95% confidence intervals were then calculated using the fitted curve.

4.5 Results

The ambition was to create a cut-off point where the test line was no longer detectable so the test could be semi-quantitative without the requirement for a reader for the detection of CRP. Changing the parameters within the sandwich assay for CRP did not give a suitable ‘cut-off’ effect as the test line only increased/decreased proportionally. There were a number of optimisation processes investigated which can be seen below. Ultimately it was decided to use the competitive assay format for the final test for the detection of CRP. Due to the lower concentration of PCT being tested the sandwich assay format was used.

4.5.1 CRP parameter testing

To align with the NICE guidelines, The concentration range required for this semi-quantitative test for CRP was <20 µg/ml -100 µg/ml. For the sandwich assay a signal can only be visualised if the analyte is bound to the tagged detection antibody. Analyte (without the detection antibody) that binds to the capture antibody at the test line will prevent subsequent binding and also does not produce a signal, so when the concentration of analyte is very high it can lead to a decreased signal at the test line as the unbound analyte blocks the binding sites. The first step was investigating how different parameters affected the test line intensity and how each of these could be optimised.

4.5.1.1 Test line antibody concentration – Sandwich Assay

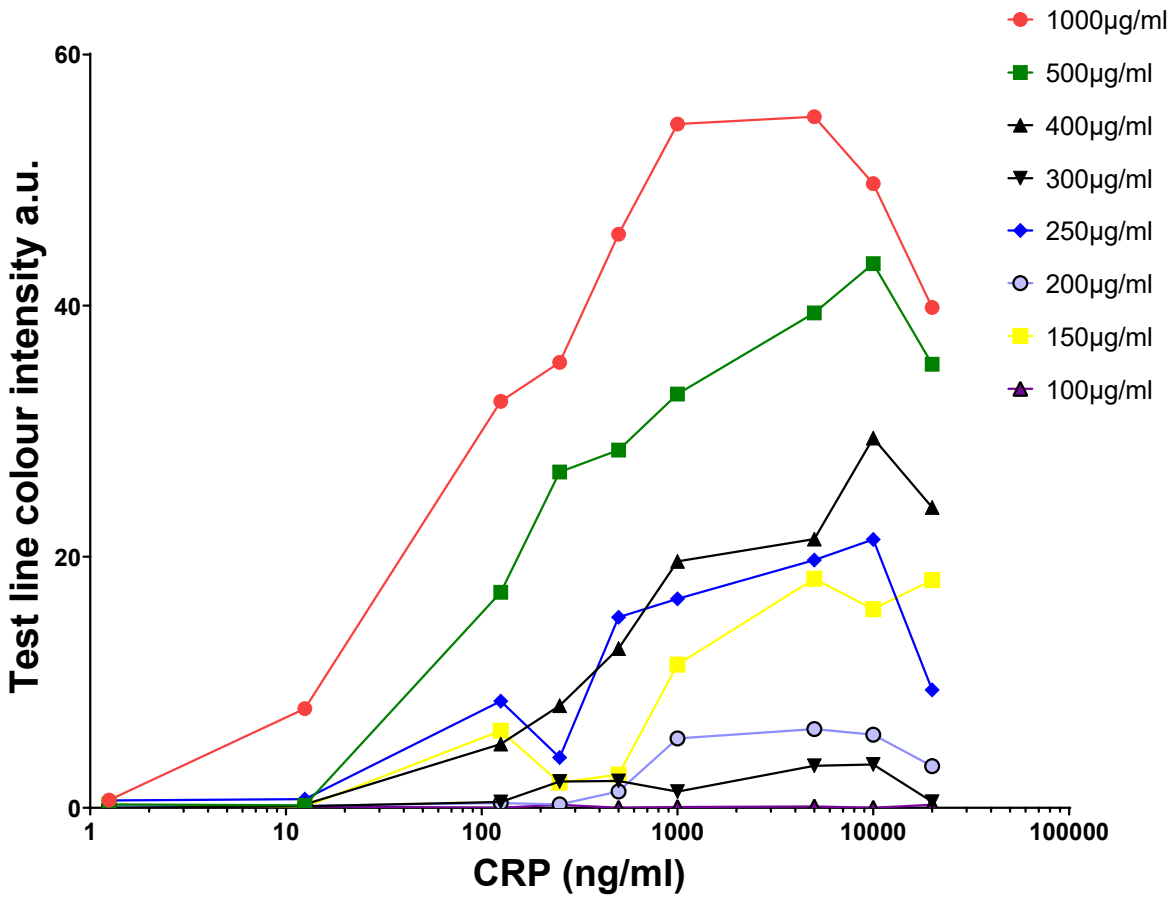

Figure 4.5 – Graph showing the test line colour intensities for nine concentrations of CRP (1.25 – 20000 ng/ml) using different capture antibody concentrations at the test line (100 – 1000 µg/ml). For 1 µl of sample each point is the mean value for three repeat measurements.

The results in Figure 4.5 show that as the capture antibody concentration increases, so does the test line colour intensity, as there are more capture sites for labelled detection to bind. However, what can also be seen is the 'Hook' effect. This is seen where the test line colour intensity starts to decrease at the higher concentrations, such as for the capture concentration of 1000 µg/ml, the intensity peaks at 5000 ng/ml of CRP and then begins to decrease. Although the test line colour intensity decreases with the decrease in capture concentration there is no real difference in the LOD of the test until 100 µg/ml where the capture concentration is so low that there are insufficient binding sites for a visual signal to be seen. For this reason, and the 'Hook' effect,

altering the capture antibody concentration is not an optimal method to alter the detection capabilities of an LFD. There is also some irregularity at the lower capture concentrations such as <200 µg/ml which shows lower colour intensity than 150 µg/ml. This could be because at the lower concentrations there is a large dilution and therefore there may be decreased uniformity of the antibody within the solution, therefore when the antibody is deposited there are likely to be some area with a higher concentration of antibody than others.

4.5.1.2 Reference line – Sandwich assay

As previously mentioned in section 1.1, one alternative method of quantitation is the use of a reference or standard line as part of the LFD, which the test line can be compared against to establish if the concentration of the target analyte is high or low for a semi-quantitative analysis. As shown above in Figure 4.5, changing the capture concentration for the sandwich assay was not the optimal way to distinguish the concentration of CRP as per the NICE guidelines. As the control line is an integral part of the test and requires no additional processing or reagents, it was decided to trial the use of the control line as a reference line to establish a semi-quantitative measurement of CRP in the sample. The results from the experiment using this method can be seen in Figure 4.6, 4.7 and 4.8.

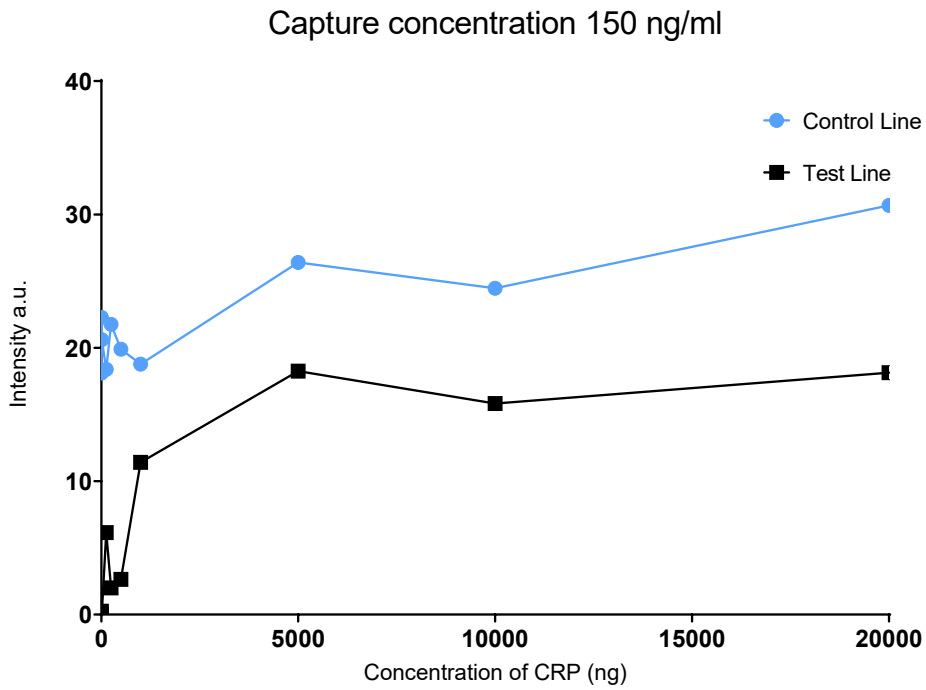

Figure 4.6 - Graph showing the test and control line colour intensities vs the concentration of CRP (ng/ml) for the test line (shown in black) and the control (shown in blue) for the capture antibody concentration 150 ng/ml. For 1 µl of sample each point is the mean value for three repeat measurements.

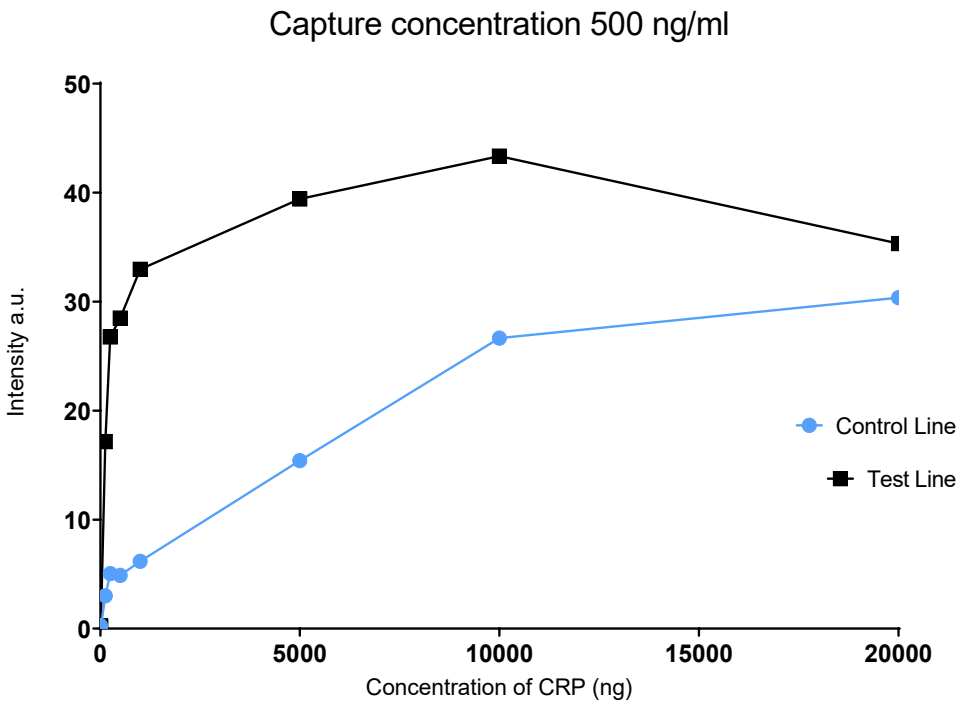

Figure 4.7 - Graph showing the test and control line colour intensities vs the concentration of CRP (ng/ml) for the test line (shown in black) and the control (shown in blue) for the capture antibody concentration 500 ng/ml.

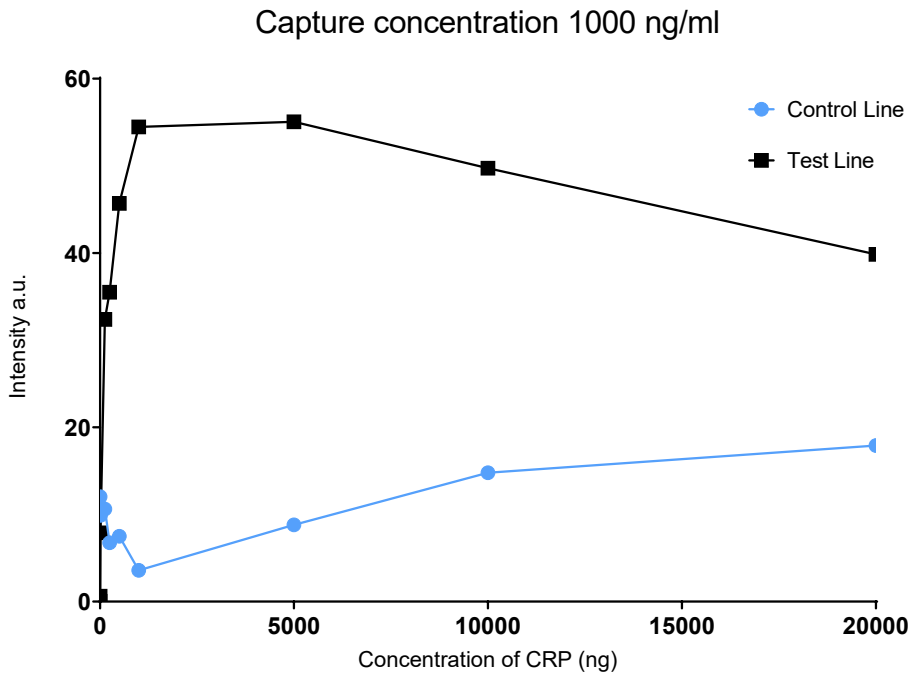

Figure 4.8 - Graph showing the test and control line colour intensities vs the concentration of CRP (ng/ml) for the test line (shown in black) and the control (shown in blue) for the capture antibody concentration 1000 ng/ml.

The results for 1000 ng/ml capture antibody concentration show that the test line colour intensity values for the control and the test line are inversely proportional, as the intensity for one line increases it decreases for the other. If there is insufficient conjugate introduced to the test, then there will not be enough available to bind completely at the control line as it will have been depleted at the test line if there is high analyte concentration in the sample. At 500 ng/ml capture antibody concentration the test and control line follow the same trend but the intensity values for the control line are lower, so the relationship between the two is not significant enough to be of use to establish a strict cut-off detection value. For the 150 ng/ml capture antibody concentration as the concentration is very low there is reduced capture binding capacity and as expected the test line colour intensity is reduced. In this case the control line has a higher intensity than the test line as there is surplus conjugate that will continue past the test line and bind at the control line. Although this method was investigated there was not seen to be a significant relationship over all between the test and control line colour intensities that would be discriminatory for different antigen concentrations and therefore this method was not carried forward. The occurrence of the Hook effect can also be seen as the concentration of CRP increases: initially the

test line intensity increases until a certain point and thereafter decreases again as the binding sites are saturated with untagged analyte and this is different for each capture concentration.

The results from the sandwich assay were not promising as a robust assay for semi-quantitative detection of CRP with the pre-defined cut-off value. For this reason, the next step of the development of this test was the exploration of a competitive assay format. There are several parameters it was important to investigate to ensure an optimised assay; membrane type according to flow rate, sample volume, conjugate volume and capture molecule concentration.

4.5.1.3 Flow rate – Competitive Assay

The flow rate of the sample is determined by multiple factors but the easiest way to control it is the capillary speed of the nitrocellulose membrane used for the test. The flow rate dictates how much time there is for the analyte in the sample to interact with the antibody at the test line. If the sample flow is slower, the analyte has a greater interaction time which in a sandwich assay format leads to an increase in test sensitivity however as the competitive assay has an inversed outcome, extending the interaction time of the analyte with the test line antibody leads to a reduction in the test line intensity.

As seen previously in Figure 2.2 (background) the CN140 membrane has smaller pore structures leading to a slower flow rate for the sample when compared to that for CN95.

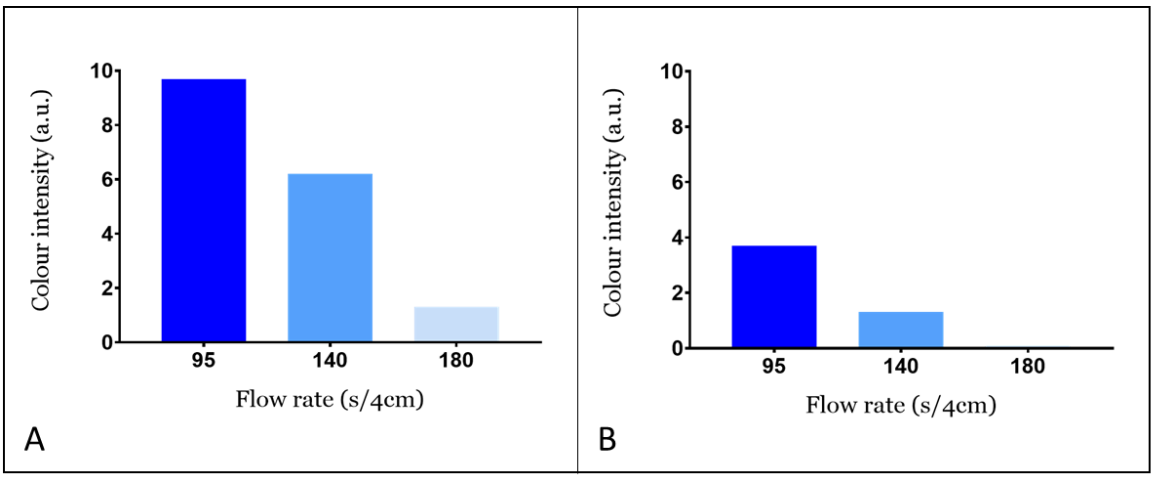

Figure 4.9 – Graphs showing the effect of three membranes with different flow rates on the test line intensity at concentrations of CRP A) 20 µg/ml and B) 100 µg/ml using LFDs in the competitive assay format.

As seen in Figure 4.9 the intensity is much higher on all membrane types at the lower concentration of 20 µg/ml as the assay is in the competitive format. This test was designed to have a strict detection cut off values. For instance, using CN95 the LFD with a concentration of CRP of 20 µg/ml has a high intensity, that without the use of a reader would indicate a negative result as it is in the competitive assay format. This means that 20 µg/ml was not readily detectable whereas the 100 µg/ml using CN180 had no test line at all which indicates a clear positive result. As the aim was to create a cut-off value below which the test would not detect, the test sensitivity needed to be reduced. As CN95 has the fastest capillary rate, it reduces the time available that the pre-deposited capture molecule has to react with the conjugate, additionally the CN180 can be subject to false positive results and non-specific binding due to the reduced flow speed.

4.5.1.4 Sample volume – Competitive Assay format

When changing the volume of the test sample, although the concentration of the analyte does not change, by increasing the volume the absolute number of analyte particles flowing through the test will be more. A very small volume may also be insufficient to fill the capillary space of the test which is important to ensure uniform distribution of the analyte throughout the test and to achieve a uniform test line, as without a sufficient sample the rate at which the sample is pulled

through the membrane will be reduced and some of the sample may not reach the test line to bind the capture antibodies.

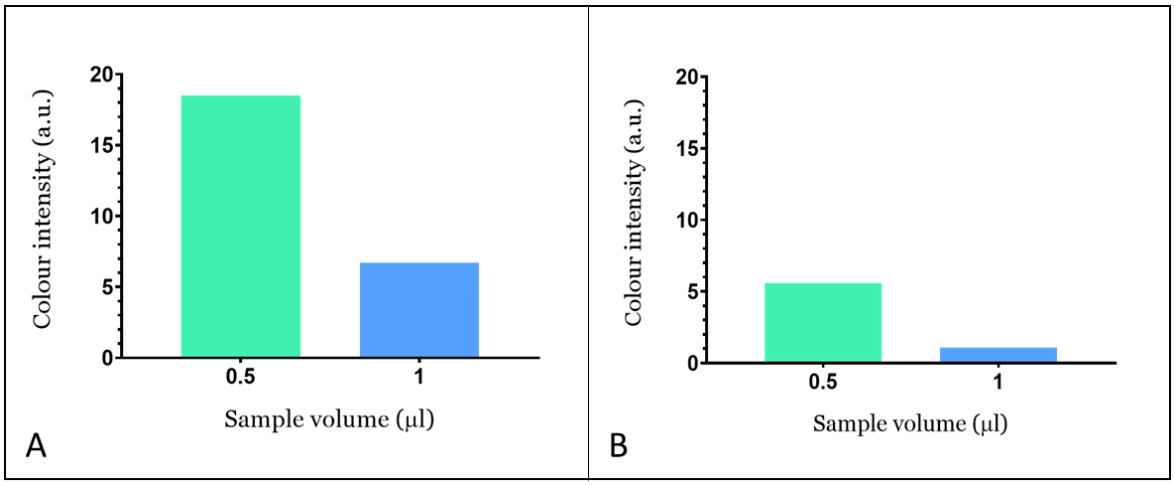

Figure 4.10 – Graphs showing the effect of sample volume (µl) on the colour intensity of the test line for CRP concentrations A) 20 µg/ml and B) 100 µg/ml using LFDs in the competitive assay format.

As seen in Figure 4.10 the smaller the sample volume the fewer number of analytes available to bind to the conjugate meaning more unbound conjugate is available to bind to the pre-deposited capture molecule at the test line. The colour intensity for 20 µg/ml was the highest with 0.5 µl meaning that this was more desirable to reduce the detection capabilities of the test however 0.5 µl is a very small volume to pipette accurately and therefore is impractical for a POC test. It was decided that the use of 1 µl sample volume, as obtained from a finger prick test, would provide a more user-friendly solution.

4.5.1.5 Conjugate volume – Competitive Assay

Similarly, the volume of the conjugate (detection antibody and gold nanoparticles) also changes the actual number of molecules available to bind and is therefore part of the optimisation process for the desired detection range.

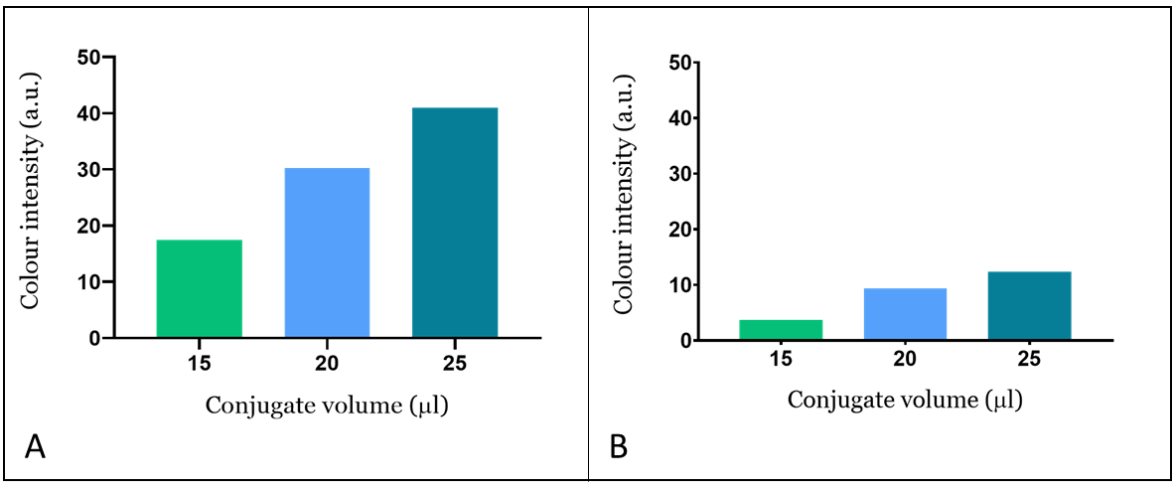

Figure 4.11 - Graphs showing the effect of three different conjugate volumes (µl) on the test line intensity at concentrations of CRP A) 20 µg/ml and B) 100 µg/ml using LFDs in the competitive assay format.

As seen in Figure 4.11, as the conjugate volume increases so does the intensity of the test line. This is because free conjugate is available to bind to the pre-deposited analyte at the test line. Although the conjugate volume does influence the test line colour intensity for the different concentrations of CRP A) 20 µg/ml and B) 100 µg/ml, there is a proportional decrease in the test line colour intensity for the higher concentration and therefore it is not a suitable parameter to use to create a cut-off for semi-quantitative detection.

4.5.1.6 Capture antigen concentration - Competitive assay

To tailor the detection capability of the CRP test to allow for different LOD in each channel the capture antigen concentration that is pre-deposited and dried was changed. The concentration of the capture antigen affects how many tagged CRP molecules can bind at the test line to produce the visible signal. Therefore, modifying this concentration could be used to control the detection capabilities of that channel.

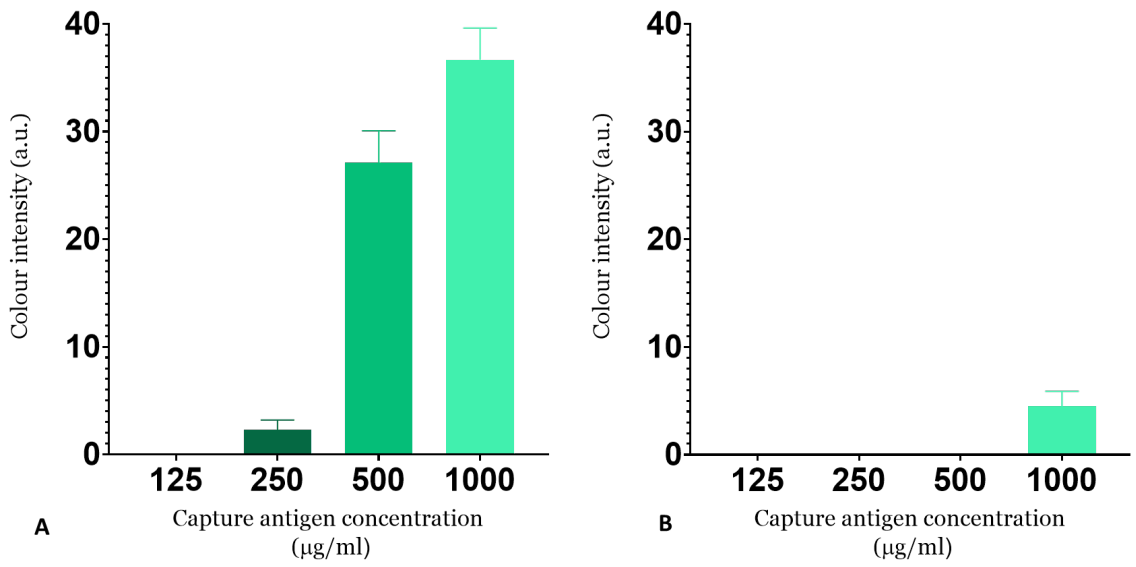

Figure 4.12 - Graphs showing the effect of the capture antigen concentration (µg/ml) on the test line intensity at concentrations of CRP A) 20 µg/ml and B) 100 µg/ml using LFDs in the competitive assay format.

A completely negative result would be inferred from a strong test line colour intensity, therefore as the concentration of what increases from 20 µg/ml to 100 µg/ml the test line colour intensity decreases across all the capture concentrations. The higher the capture concentration the more capture sites there are available to bind to the free CRP in the sample, therefore, the lower capture concentrations < 1000 µg/ml become saturated first and therefore at the highest sample CRP concentration of 100 µg/ml, there is no visible test line at any capture concentration other than 1000 µg/ml and even this is very faint. This shows that the capture antigen concentration can be altered to allow for the tailored detection of specific sample concentrations.

The initial experiments conducted were aimed at optimising the single CRP LFD with the competitive assay format to create specific detection values for the test to align with the NICE diagnostic guidelines for pneumonia. As seen in Figure 4.12A, with capture antigen concentration of 20 µg/ml, gives the assay a detection limit of above 20 µg/ml, as below 20 µg/ml the test is unable to detect the presence of the analyte indicated by a strong test line. In Figure 4.13B, the test can only detect values of at least 100 µg/ml meaning the concentration of the analyte must be at least 100 µg/ml for the test to detect it. The distinct difference between the tests which

allows for the modification of the detection limit is the concentration of CRP that is pre-deposited at the test line. The tests shown in Figure 4.12A have 250 µg/ml of CRP deposited compared to Figure 4.13B where the concentration is 1 mg/ml. The higher concentration of analyte at the test line creates more competition for binding and therefore increases the limit of detection of the test.

4.5.2 CRP LFD

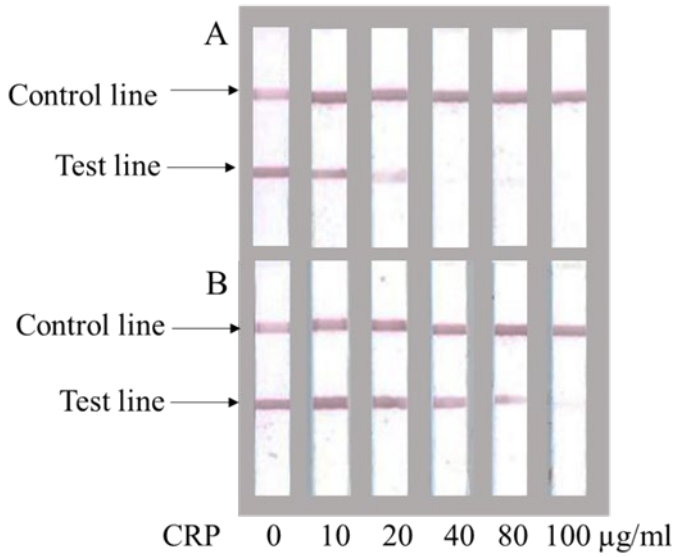

Figure 4.13 – Scanned images showing standard single channel CRP LFDs that implement a competitive CRP assay. The capture concentration of CRP deposited at the test line is as follows A) 250 µg/ml and B) 1 mg/ml. Representative images of five repeated

.

Figure 4.13 shows the individual LFDs initially developed for the competitive CRP assay. It can be seen that as the concentration of CRP increases the test line colour intensity decreases. For Figure 4.13A, with the lower capture antigen concentration of, the test line stops being visible above 20 µg/ml, however for Figure 4.13B, the capture concentration is much higher and therefore the test line is visible (meaning no analyte) up until 100 µg/ml. This allowed for the creation of a 'cut-off' for semi-quantitative detection.

The next step was to combine the two individual channels for CRP into a dual channel LFD.

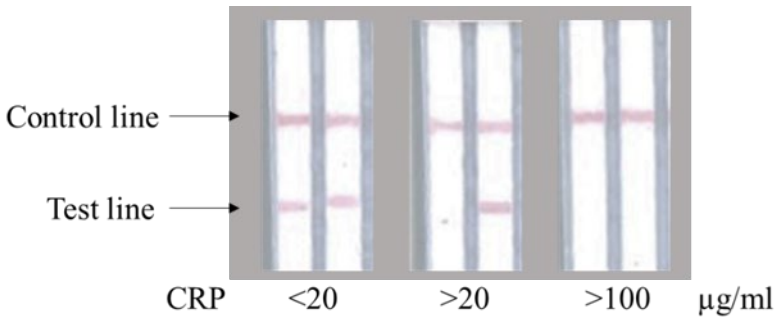

Figure 4.14 – Scanned images showing three examples of the dual LFD for semi-quantitative detection of CRP with CRP concentrations labelled.

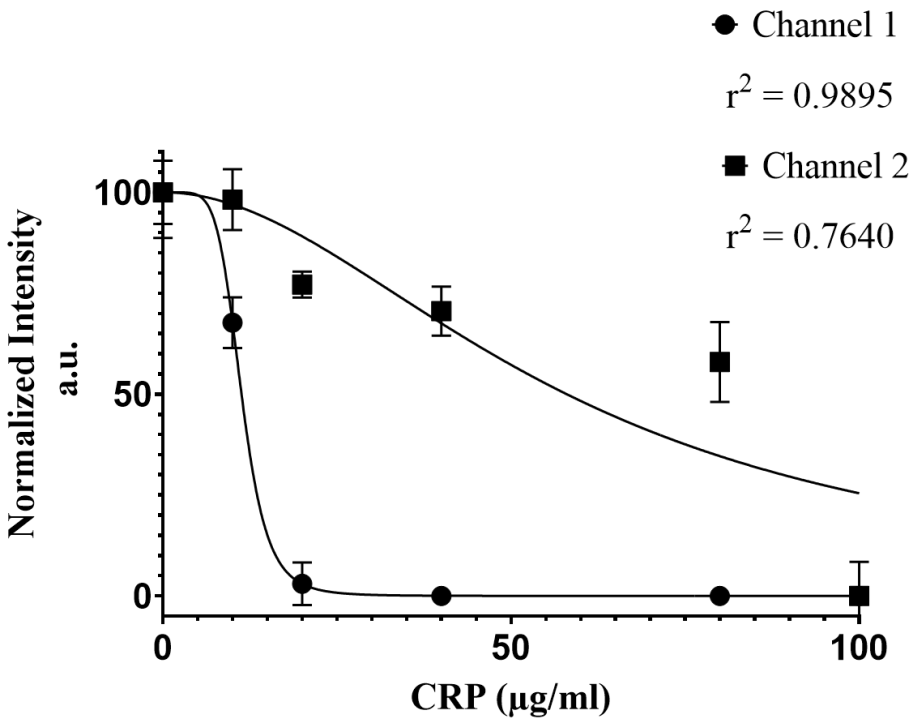

Figure 4.15 - Calibration curve of both channels of the LFD for five repeat measurements showing the mean and error bars representing the relative standard deviation.

The same capture concentrations from the single-channel LFDs were used but now the two channels run in parallel while separated by the LDW patterned polymer barrier. The dual channel device utilizes the same reagents. The antigen was deposited into the channels at concentrations of 250 µg/ml and 1mg/ml respectively, hence enabling the two channels to have different cut offs

at 20 μg/ml and 100 μg/ml. The interpretation of the results is clear and can be analysed quickly. Where both test lines are visible, the tagged detection antibody has bound to the capture CRP indicating that the concentration of CRP in the sample is less than or equal to 20 μg/ml; when only the second channel has a visible test line present, the concentration is greater than 20 μg/ml but must be less than 100 μg/ml; finally, the absence of any visual test line in either channel indicates that the concentration of CRP in the sample must be at least 100 μg/ml as it has bound all the tagged detection antibody leaving none remaining to bind at the test line. The control line is also an integral part of the test as its absence indicates an invalid test. Figure 4.15 shows the calibration curve with its relative standard deviation, while the small size of the error bars show that the measurements are precise and repeatable. After undergoing non-linear regression analysis, performed in GraphPad prism, the dual channel LFD channels had an r^2 = 0.9895 and 0.7640 respectively. There is still a strong relationship between the test line intensity and the CRP concentration in the sample after combining the channels.

4.5.3 PCT

Alongside the development of the single and dual channel for CRP detection a successful single-channel LFD for the detection of PCT was also developed. A sandwich assay format test was designed to only detect PCT concentrations of 0.5 ng/ml and above. The AuNPs used to label the detection antibody were used at a ratio of 2:1 to the detection antibody, which was used at a concentration of 3 μg/ml after optimization experiments were carried out. The capture antibody deposited to form the test line was initially trialled at different concentrations from 100 μg/ml and 1 mg/ml to access the detection capabilities of each concentration. After optimization, the capture antibody concentration used was at 1 mg/ml, and this allowed for the detection of PCT down to 0.5 ng/ml but any values below this would not be detected by the test. This can be seen in the calibration curve in Figure 4.16. This was designed to keep the detection limits within the clinically relevant range for pneumonia triage. Figure 4.17 shows such example devices with detection of different concentrations of PCT from 0 ng/ml to 50 ng/ml. The limit of detection was found to be 0.5 ng/ml, and this can be seen in Figure 4.17 on the fifth test from the left, as below this concentration there is no visible test line present.

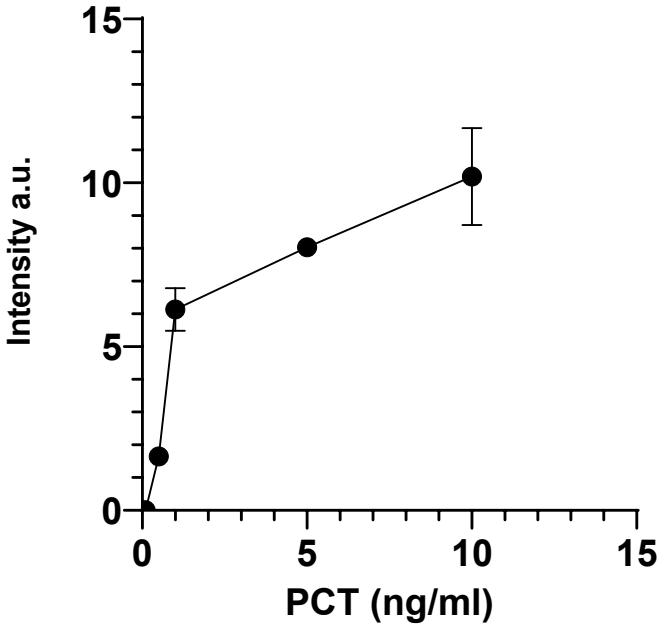

Figure 4.16- Calibration curve for procalcitonin carried out in spiked PBS. Graph shows mean and standard deviation for three repeat measurements.

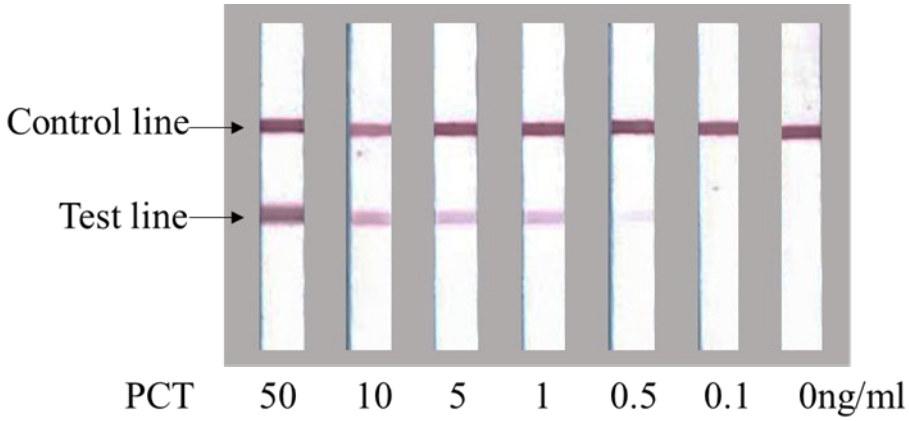

Figure 4.17 – Images of single channel LFDs showing the detection of PCT with concentrations ranging from 50 to 0 ng/ml. Representative images of five repeated measurements.

After statistical analysis the LOD of the single LFD for PCT was found to be 0.54 ng/ml (95% CI of 0.117 ng/ml to 1.031 ng/ml). After undergoing non-linear regression, dose-response [agonist] vs

normalized response – variable slope, it shows good strength of relationship between the concentration of PCT in the sample and the test line intensity and the relative standard deviation error bars are small which indicate good precision of data and repeatability. All statistical analysis was conducted in GraphPad Prism and can be seen in the graph in Figure 4.18.

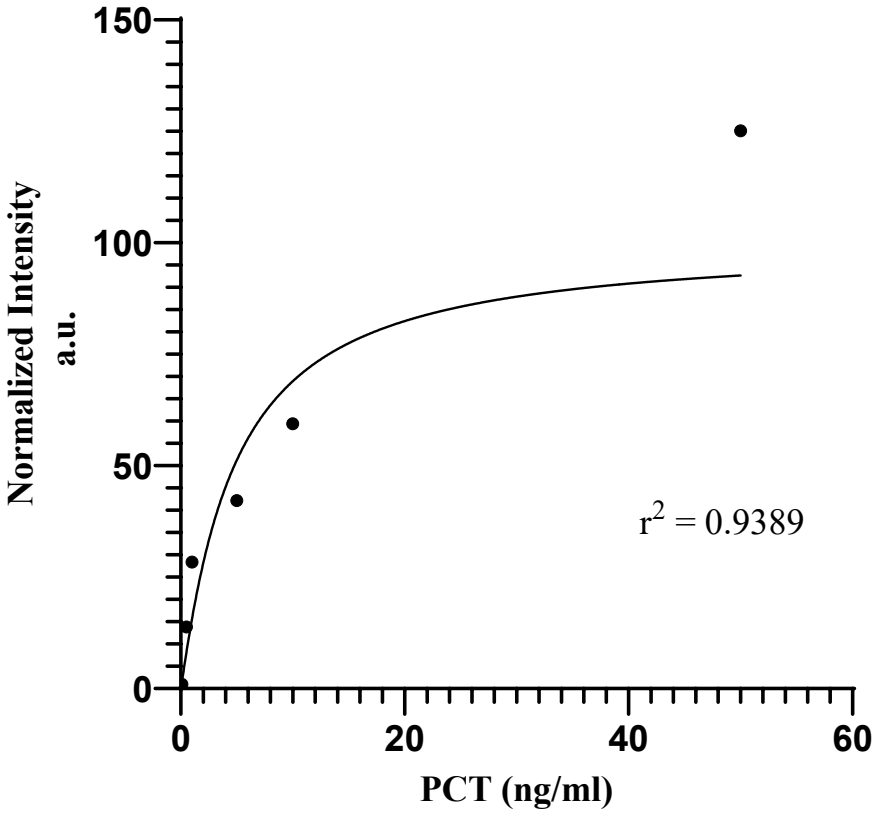

Figure 4.18 - Graph showing the normalised test line colour intensity for the individual LFDs for PCT for the different concentrations of PCT. Non-linear regression analysis and best fit performed in GraphPad prism.

4.5.4 Multiplexed semi-quantitative LFD

The final stage of the multiplexed test development was combining the dual channel CRP LFD with the single channel PCT LFD for the simultaneous and semi-quantitative detection of CRP and PCT. In order to ensure the control line would appear in every channel both the anti-goat and anti-mouse antibodies were combined and deposited at the control line. It was then necessary to optimise the volume of reagents needed for a three-channel test. The final conjugate mixture

added to the three-channel test consisted of 20 µl of AuNPs diluted at 1:15 and 5 µl of anti-CRP detection antibody and 10 µl of anti-PCT detection antibody.

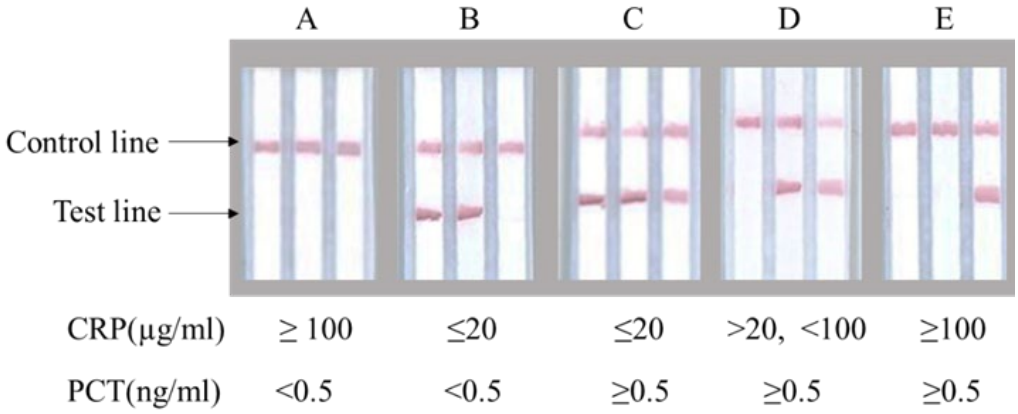

Figure 4.19 - Scanned images showing multi-channel LFDs that measure both CRP and PCT respectively within adjoining parallel flow paths created using the LDW procedure. The respective CRP (µg/ml) and PCT (ng/ml) concentrations in the samples used to test device A -E are the following: ≥100, <0.5; ≤20, <0.5; ≤20, ≥0.5; >20, <100, ≥0.5; ≥100, ≥0.5.

The final multiplexed LFD can be seen in Figure 4.19. These multi-channel devices measure both CRP and PCT within parallel flow paths that were created using the LDW technique. The three-channel multiplexed device provides a clear and unambiguous result for the concentration range of the analytes present in the sample. As seen in Figure 4.19A-E there is a clearly visible control line in each of the three channels of the LFDs, indicating that the testing has worked correctly in all cases. For the LFD in Figure 4.19A there are no visible test lines in any of the three channels, and this indicates the sample had a concentration of CRP greater than or equal to 100 µg/ml and a concentration of PCT below 0.5 ng/ml. Figure 4.19B shows an LFD with visible tests lines in the first two channels. This indicates that the concentration of CRP in the sample is less than or equal to 20 µg/ml and no visible test line in the third channel means the concentration of PCT is less than 0.5 ng/ml. For the LFD in Figure 4.19C with visible test lines in all of it three channels, the CRP concentration is less than or equal to 20 µg/ml and that for PCT is at least 0.5 ng/ml. Figure 4.19D shows an LFD with no visible test line in the first channel indicates that the CRP concentration is greater than 20 µg/ml; however, test lines in the second and third channel

indicate that the concentration of CRP is less than 100 µg/ml and that for PCT must be at least 0.5 ng/ml. Finally, for the LFD in Figure 4.19E, the first two channels have no visible test lines and therefore the CRP concentration is greater than or at least 100 µg/ml and PCT is at least 0.5ng/ml. The results in Figure 4.19 demonstrates that; a) the control line appears in every channel independently of the results for the test line and b) each channel acts as one individual LFD as the assays and (therefore their results) in one channel are not affected by those implemented in the adjacent channels. An advantage over other semi-quantitative tests using the 'barcode' style test is that, as the channels are physically distinct and separated, there is no interference between them. There is also no opportunity for cross-reactivity between the different analytes and their antibodies leading to more reliable results. In addition, each channel has a separate control line to ensure the test has been completed and the results are valid.

4.6 Discussion

The key to successful pneumonia treatment is quick and accurate diagnosis facilitated by rapid POC testing that can be performed at the patient's bedside. Currently, the available technology is insufficient to cater for the complexity of pneumonia triage, which requires both multiplexed biomarker detection and quantification. The results presented in this chapter show clear potential to fill the gap within this research field, especially in low resource countries where pneumonia is a huge problem and healthcare facilities are limited.

As has been demonstrated in this study, a simple single 3-channel device - one channel for PCT detection and two for CRP detection is sufficient for rapid diagnosis of these two highly relevant biomarkers. The tests showed excellent correlation between the test line colour intensity and the biomarker concentration in the sample for the relevant clinical concentration ranges, and thus provides the necessary confidence and level of evidence that a single test delivering multiple separate results is of real value in the diagnostic sector.

Of critical importance is the fact that the above can be implemented with a straightforward LDW patterning technique in which multiple independent tests can be performed with no cross-reactivity or interference, and this was the motivation for undertaking this research for application to the area of pneumonia diagnosis in this case. The presented results clearly demonstrate that: 1) the control line appears in every channel independently of the result for the test line. 2) Each channel acts as an individual, single LFD and the results in one channel are not

affected by those in the adjacent channels. 3) The use of human serum for the experiment which increases the chance of successful transfer of the LFD from the laboratory to clinical use. Human serum is a complex matrix with multiple components and here we have demonstrated the capability of the LFDs to detect within this complex matrix without any cross-reactivity.

Although presented here are the results for a partial LFD (without the conjugate pad), the next step for this research would be the introduction and optimisation of the conjugate pad to complete the test. After initial testing with human serum in the laboratory the next step is to validate the complete test with patient samples for the diagnosis of pneumonia.

4.7 Conclusion

In conclusion, presented herein is a novel strategy for the multiplexed and semi-quantitative detection of the inflammatory markers CRP and PCT using parallel flow channel within a single LFD. The demonstration of a successfully developed dual channel LFD that allows for the detection of CRP, below 20 µg/mL, above 20 µg/mL and above 100 µg/mL, as per the NICE guideline, defining the clinically relevant range for pneumonia. These results have been concurrently reported alongside the development and demonstration of a single channel LFD that measured PCT down to a cut-off of 0.5 ng/mL, providing a rapid testing pathway that allows distinguishing between viral and bacterial causative agents. Combining these two markers into a single POC diagnostic test that can be used by healthcare professionals would not only improve the speed and accuracy of treatment for patients with pneumonia but would also assist in the campaign for prudent antimicrobial stewardship. Finally, as a proof of principle, these tests have been successfully developed into a multiplexed LFD for the detection of both CRP and PCT for use in future pneumonia triage. The multiple parallel flow-paths within the multichannel CRP-PCT LFD allows for not only the individual detection of different analytes but also their detection at different concentrations without any cross-interference. This LFD has an excellent potential as a diagnostic tool. Future work will be required for the clinical validation of this test to triage patients with suspected pneumonia and determine the effect on outcome and antibiotic use.

Chapter 5 Developing a proof-of-concept rule-out screening test for Tuberculosis

5.1 Introduction

5.1.1 The global TB pandemic

Tuberculosis (TB) is a communicable disease which typically affects the lungs and is caused by the bacillus, *Mycobacterium tuberculosis (Mtb)*. It is spread when those who are sick with TB expel bacteria into the air, for example, by coughing and these droplets are inhaled by someone else. It is estimated that about a quarter of the world's population is infected with *Mycobacterium tuberculosis* [133]. That is not to say that these people are ill but that they carry the bacteria in a latent infection and there is a 10 % chance that those people will go on to develop the infectious disease at some point in their lives. In 2019, globally, an estimated 10.0 million people fell ill with TB and was the cause of an estimated ~1.2M deaths and is one of the ten leading causes of death worldwide. TB cases were reported in 198 countries and territories across the world in the World Health Organisation's (WHO's) 2020 global TB report [133].

TB is both preventable and treatable with a 6-month drug regimen. Since 2000, TB treatment has averted more than 60 million deaths [133]. However, to treat people effectively, it is crucial to find those within the population who are infected with TB before their symptoms become severe and begin spreading the disease. Treatment, therefore, has the additional benefit of curtailing onward transmission of infection and without early and accurate diagnosis and rapid linkage to care, TB continues to spread in households and communities [134].

There are a number of techniques including the PCR based, GeneXpert and smear microscopy currently used in the diagnosis of TB however these are largely insufficient or not fit for purpose for mass testing [135]. The GeneXpert is a cartridge-based nucleic acid amplification test used around the world for the diagnosis of TB. In addition to the identification of the disease it also assesses the patient for Rifampicin resistance, a front-line drug used for the treatment of TB. Although the equipment is expensive and requires trained personnel to operate, it has shown itself to be an excellent diagnostic tool, able to identify disease where the sputum smear test is negative and identify rifampicin resistance without the need for bacterial cell culture [136]. By the

end of 2016, 23 million cartridges for the diagnosis of TB had been purchased by the public sector [137]. However, smear microscopy remains the most widely used method for TB diagnosis [138].

Diagnosis by smear microscopy requires the collection of a sputum sample from the patient that is first fixed thinly on a glass slide and then stained using the Ziehl-Neelsen acid fast bacilli (AFB) stain and finally visually isolated (record the number or organism. i.e., the bacterial load to grade the disease severity) by a highly trained microscope user. Despite being the most used method, it is highly insensitive, requiring at least 10,000 bacilli per millilitre of sputum to be visually identifiable by even the most trained pathologist and therefore the results are subjective [139]. Sputum culture can lead to more sensitive results, however as *Mtb* is a slow-growing pathogen and it can take weeks before a result can be seen. In addition, young children and those infected with HIV, who present as the most vulnerable groups, often cannot give sputum samples or the bacterial load in the sample is too small to detect [140]. Handling infected sputum samples is very hazardous as this is where the bacteria are carried, and therefore requires a Biosafety Level 3 facility which is not always available in less developed regions. A less hazardous blood-based test would be advantageous, particularly in high burden areas [141].

Effectively diagnosing TB is the most challenging aspect of TB care and 1/3rd of the 10 million people who were found to have TB in 2019, were not diagnosed [142]. This is because currently available diagnostics do not sufficiently meet the needs of people or of health systems in terms of accuracy, time to results, affordability, and appropriateness for use at the point-of-care [143, 144].

Better tools are necessary to enable low-cost, rapid, and accurate TB screening and diagnosis closer to the point-of-care [135]. TB screening and triage tests are needed to test a large number of people —through systematic screening programs in communities or routine care in health facilities—so it is very important for these tests to be simple, affordable, and able to be implemented at the point-of-care [144].

The latest Global Tuberculosis Report issued from the WHO outlines the milestones that were previously set out in relation to TB diagnosis, treatment, and reduction and how these have been greatly affected by the COVID-19 pandemic. Unfortunately, in 2020 the number of people being diagnosed with TB was reduced and therefore fewer people received treatment including preventative treatments and ultimately this led to an increase in the number of deaths as a result of TB infection, when compared to pre-pandemic levels. The cumulative number of people that were treated for TB between 2018 and 2020 was 19.8 million, which accounts for just 50 % of the target for 2018-2022 of 40 million [133]. TB fell second only to COVID-19 as the leading cause of death by a single infectious agent. The pandemic was naturally a non-anticipated set back to the

TB goals with further disruption anticipated and increasing deaths predicted into 2021 and 2022. This has led to global targets falling short; however, the immediate actions are to try and mitigate the impact that COVID-19 on TB cases and provision of care. Figure 5.1 [133] highlights the distribution of incidence around the world in 2020.

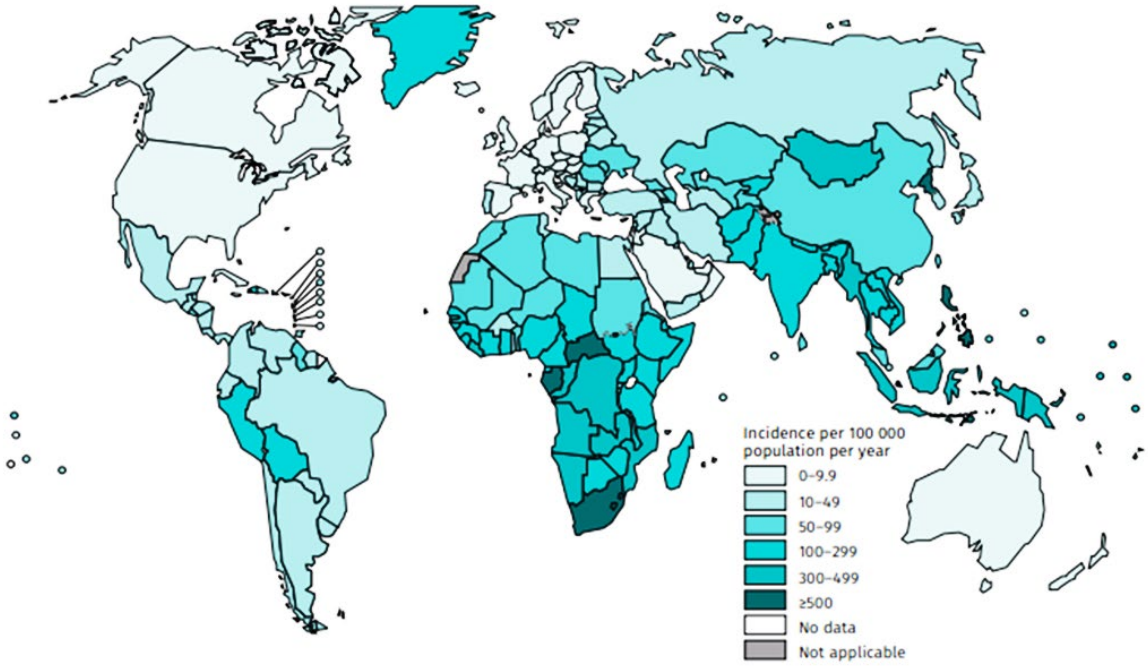

Figure 5.1 – Global map showing the distribution incidence per 100,000 population per year for Tuberculosis.

5.1.2 Requirements for a near patient TB diagnostic

Member States of the WHO and the United Nations (UN) have committed to ending the TB epidemic, through their adoption of WHO's 'End TB Strategy' and the UN Sustainable Development Goals (SDG Target 3.3). The WHO together with Foundation for Innovative New Diagnostics (FIND) have already identified a set of target product profiles (TPPs) to help with the development of any new TB diagnostics.

The suggested TPP for Tests for TB screening and triage, as recommended by the WHO are below:

- It should be a **point-of-care non-sputum-based test** capable of detecting all forms of TB by identifying characteristic **biomarkers**.
- A POC test should be a **simple, low-cost test that can be used by first-contact health-care providers to identify those who need further testing**.

- These tools need to be very sensitive so that people with TB do not get missed and those people that screen as positive for TB are referred for further confirmatory diagnostic tests with higher sensitivity and specificity.
- All tools must adhere to the WHO ASSURED criteria [135].

There are a number of current triage and screening tests, however this all have limitations to their use.

1. **Four-symptom screen**, this is the most widely used screening tool and tests for the signature symptoms of TB: cough, fever, weight loss, and night sweats; ~77 % sensitive and 68 % specific for detecting TB from these symptoms. The symptom-based approach to TB screening requires *a priori* knowledge of the patient's HIV status to be sufficiently sensitive therefore this is not as useful if used in isolation and has poor specificity for active TB in the high-risk groups of individuals such as those that have HIV infection where the specificity drops to 5- 61% [144, 145]. It is also not as sensitive among people who have more recently contracted the infection as the onset of symptoms is triggered by damage to the lungs and therefore in the early stages, the symptoms may not be present or may be mild. It is only once the symptoms are visible that the individual is spreading the disease to others and therefore this is quite late to be recognising individuals.
2. **Chest X-ray** is another available screening and triage tool for pulmonary TB with 87-98 % sensitivity and 75 % specificity. It can detect TB infection earlier than the four-symptom screen. However, due to the cost and low portability of X-ray machines and the requirement for trained personnel to carry out and interpret the images they are not the most feasible method for large scale screening in low- and middle-income countries [146].
3. **One way to overcome the issues with a standard X-ray is the use of: Light-weight and portable X-rays systems and computer aided detection (CAD) software.** This can be used at the community level and assists healthcare workers with the interpretation of the X-ray images where a radiologist is not available. This is still a work-in-progress, but it has so far shown similar performance to humans and could provide an initial screening tool whereby those individuals flagged as high risk of having TB go on for further molecular testing. With the potential for integration into cloud systems, although the devices could be used offline, it could be used to follow up with patients at a later time. It is still under investigation by the WHO [147].
4. **Breath Test** detects the presence of biomarkers indicative of TB in lungs and this is currently under development. The test is projected to cost < $10 but does require a reader that would cost around $2000, which would be a relatively high set-up cost

and the use of the test would be limited to the availability of a reader (Aeonose from The eNose Company, 81% sensitivity and 60% specificity) [148]. This concept has also been explored in the use of face-masks to sample patients to identify active TB cases [149].

The solution explored and presented here is a POC triage test for rapid and affordable screening via biomarker signature detection.

1. **Multiplexed lateral flow test**
2. **Detects four significant non-sputum-based biomarkers found through an in-depth unbiased analysis of plasma from TB-infected patients [150].**

A screening test, such as is documented in this chapter, would rule-out TB in the majority of patients without disease (sensitivity ≥ 90%) and limit referrals for the more costly confirmatory testing (*e.g.*, Xpert and/or culture) to only patients with a high likelihood of having TB (specificity ≥ 70%). A test with these characteristics that is also low-cost and can be performed by front-line health workers has been ranked among the highest priority needs for TB diagnostics, a summary of the requirements for both a screening test for training and a non-sputum-based biomarker test are outlined in Table 4.

Table 4 – Requirements for a screening test and a non-sputum biomarker test as set out by the WHO [142].

Test for screening and triage	Optimal	Minimal
Sensitivity	>95%	>90%
Specificity	>80%	>70%
Level of use	Community	Health post
Time to results	<5 mins	<30 mins
Price per test	<$1	<$2
Non-sputum biomarker test	**Optimal**	**Minimal**
Sensitivity	>98%	>98%
Specificity	>98%	>98%
Level of use	Health post	Primary care clinic with lab
Time to results	<20 mins	<1 hour
Price per test	<$4	<$6

Sensitivity is a higher priority than specificity for a screening test as the key aspect is to ensure that the diagnosis of any person with TB is not missed.

One issue that cannot directly be solved by a diagnostic device is patient compliance in relation to seeking medical assistance and correctly taking any prescribed medication. However, a POC test that can be used within the community would hopefully encourage those who show as being high risk of being infected with TB to go and seek further testing at a medical facility. The serological tests (serum based) that are currently in existence have been criticised by the WHO due to their low accuracy levels (WHO, Commercial Serodiagnostic Tests for Diagnosis of Tuberculosis 2011). The ideal test would be specific for the identification of TB and would provide high sensitivity so those with low bacterial load can still be identified.

5.1.3 Host protein-based TB diagnostics

The challenge of a host-based diagnostic designed to identify proteins is the lack of the protein's specificity to one pathogen. Most protein markers that are currently under investigation are indicative of a host's immune response to a foreign body and are therefore largely generic for a bacterial or viral infection for example [150-158]. However, these do indicate that indicate that

the production of host markers in response to infection with Mtb can be used to distinguish those infected with TB from patients with other respiratory illnesses and from healthy individuals.

However, the use of several, selectively chosen proteins could provide enough confidence in the presence of Mtb when compared to other pathogens also causing respiratory illness. The WHO has stated that they are looking for a 'community-based triage or referral test' where the test could provide a 'rule-out' result for those that do not have TB and a 'further testing' verdict for those with suspected TB infection. The test must use a readily available sample such as blood from a finger prick and it must be cheaper and easier to use than the current methods. The minimum performance specification is set to a sensitivity of 90% with specificity of 70% [2].

The next step forward to improve TB treatment and prevention is to develop a readily accessible triage test that is simple and affordable [153]. The detection of one or multiple biomarkers indicative of a Mtb infection could provide an ideal diagnostic solution. These biomarkers can be divided into several categories: (1) Components of Mtb (2) antibody response to components of Mtb (3) non-specific cellular immune responses to infection (4) 'omics' approaches including transcriptomics and proteomics.

The work carried out by our collaborators, Garay-Baquero et al [150] was the first stage of this process. This study describes the development and implementation of a non-depletion-based proteomic methodology for deep profiling of plasma and identification of novel biomarkers. It describes a bioinformatic pipeline for discovery and selection of candidates for verification that utilizes both statistical and bioinformatic analysis.

They report numerous novel analytes (biomarkers) that have the potential to be translated for clinical diagnostic. The plasma samples were separated into four segments for the mass spec analysis, and in this manuscript, they report comprehensive analysis of segment 4 [150]. The group verified a subset of biomarkers from segment 4 by independent antibody-based assays to generate a preliminary diagnostic panel, and similar interrogation of the other three segments is likely to generate further novel biomarkers. Taken together, developing assays for these host biomarkers and then combining them into a multiplex lateral flow assay presents itself as a potential near-patient TB rule-out test that fulfils the WHO product characteristics. Such an assay could be a powerful tool to address the global TB pandemic.

A wide spectrum of proteins may provide useful biological signatures of physiological status during homeostasis or its disruption. Given their phenotypic relevance and stability under specific circumstances, proteins have been proposed as viable diagnostic candidates. Among the different

proteins found in the plasma matrix those involved in tissue leakage, providing systemic information about specific immunopathologic event, such as destruction of lung tissue are relevant to active TB. In addition, plasma protein signatures can be translated to create rapid tests, and this technology is rapidly evolving. Examples include colorimetric gold nanoparticles placed on paper-based devices, label-free biosensors, and disposable nanofluidic chips. TB has undergone extensive proteomic discovery research. Although new diagnostic markers have been identified for the active disease [151, 159-164] and progression from a latent state [165], an optimal diagnostic panel has yet to be identified.

5.1.4 Biomarkers studied in this panel

There is a large amount of literature to support the use of the markers highlighted in this study in TB diagnosis. C-reactive protein (CRP) is an acute phase reactant, the levels of which increase in response to IL-6 mediated infections such as active TB. There are a multitude of studies that have consistently shown CRP to have high sensitivity for TB [150, 166-177] and that TB-associated elevations in CRP levels are independent of HIV status [175, 178]. However, CRP alone has not fulfilled the WHO criteria and so is likely to be needed to be studied in combination with other biomarkers.

Analyses of numerous plasma markers by Albuquerque et al, identified a biosignature of 10 biomarkers capable of distinguishing individuals between three clinical groups: healthy control, pulmonary TB and extra-pulmonary TB, simultaneously. Machine-learning decision trees indicated that CRP and lipopolysaccharide-binding protein (LBP) were amongst the markers that, when combined, displayed the highest accuracy in distinguishing extra-pulmonary TB from pulmonary TB in children [152].

CRP shows potential to meet the requirements of an effective triage test. A study in Uganda [177] showed POC CRP had 89% sensitivity and 72% specificity for sputum culture-confirmed TB. Although this is slightly below the WHO suggested values when GeneXpert was used as the reference value, the sensitivity of POC CRP and a symptom screen test were incredibly similar, i.e. 94% vs 99%.

Another study in Africa identified CRP, amongst other markers, to determine TB infection in both HIV positive and negative patients. When used in combination, this seven marker biosignature had a sensitivity of 93.8% and a specificity of 73.3%. This shows that there is potential for a biomarker-based POC care diagnostic for TB, however it would need to include multiple markers for sufficient sensitivity and specificity [154].

It has also been identified that LBP could also be a useful marker for the detection of TB-associated immune reconstitution inflammatory syndrome (TB-IRIS)[179]. It is estimated that over a third of people living with HIV are also infected with TB and although the administration of antiretroviral therapy (ART) has greatly improved prognosis for HIV infection there is a risk of other complications. During ART HIV and TB co-infected patients can develop more severe TB symptoms which leads to TB-IRIS [180, 181].

Serum amyloid A1 (SAA1) is an acute phase protein, and its production is triggered by infection or identification of pathogens. It is also associated with the circulating concentration of high-density lipoprotein as it modulates lipid trafficking and immune responses. It is the precursor protein in a process called reactive amyloidosis, which can lead to complications in cases of TB, therefore it works as a marker of disease activity [182]. SAA1 and CRP were also identified among a panel of markers that showed strong association with disease severity and smear microscopy grading and they were also modulated by antibody treatment [183]. Furthermore, the discovery and validation of a six-marker panel found SAA1 to have the largest mean fold change after 8 weeks of TB therapy and CRP and LBP were among the top 5 markers with the biggest fold change [158].

Complement Factor H Related 5 (CFHR5) is a novel marker for the diagnosis of TB identified by Garay-Baquero et al. This protein plays a part in regulating part of the immune response called the complement system. This system works to destroy and remove foreign bodies such as bacteria by triggering inflammation and therefore the levels are increased during infection with TB.

The current biomarker studies published to date explore a large range of markers which could have diagnostic potential however these studies can be difficult to compare as each focus on specific geographic regions as well as varying in the number of participants and co-morbidities.

In summary, current TB diagnostic tests are insufficient. One key product required is a near-patient triage test that can identify those with possible active TB who then go on to more expensive and specific tests such as CXR and GeneXpert. Although the ideal biomarker panel is still under investigation, this work sought to demonstrate that protein biomarkers could be developed into a multiplex assay with potential for use as a triage test, basing the panel on the published literature and the work of Garay-Baquero.

5.2 Methods and Materials

The antibodies used for the assays were as follows:

- CRP: Capture and detection antibody was Human C-Reactive Protein/CRP Antibody (MAB17071), from R&D Systems, USA. Standard was C Reactive Protein human (C1617-1MG) from Sigma Aldrich, Germany.
- SAA1: Antibodies and standard used were from the Human Serum Amyloid A1 DuoSet ELISA (DY3019-05) from R&D Systems, USA.
- LBP: Antibodies and standard used were from the Human LBP DuoSet ELISA (DY870-05) from R&D Systems, USA.
- CFHR5: Capture antibody, Human Complement Factor H-related 5/CFHR5 Antibody (MAB3845), detection antibody, Human Complement Factor H-related 5/CFHR5 Antibody (AF3845), standard, Recombinant Human Complement Factor H-related 5/CFHR5, CF (3845-F5) from R&D Systems, USA.
- The control line was a combination of Goat anti-mouse IgG from (AF007) and Donkey anti-goat IgG (AF109) all from R&D Systems, USA. Gold nanoparticles for antibody conjugation were BioReady carboxyl 80 nm gold particles, 20 OD AUZR80-10M obtained from nanoComposix, CA, USA.

5.2.1 Blood collection

5-6 10 ml EDTA tubes BD vacutainers purple blood collection tubes were venesected. The tubes were then centrifuged at 1500 xg for 15 minutes at 4°C. The plasma was then removed and pooled in a falcon tube, kept on ice, mixed with a stripette and aliquoted into the eppendorfs.

5.2.2 LFD testing – Individual LFDs

Each device was assembled as per the methodology reported in Chapter 3 for a full LFD. The first stage was the development and optimisation of individual LFDs for each of the four biomarkers under investigation. The prepared devices (all membranes attached) were cut to 2 mm width LFDs. The antibodies were conjugated using the BioReady carboxyl 80 nm gold particles. The volume of conjugate pipetted onto the conjugate pad varied for each marker and this was investigated and optimised. The individual LFDs were tested with 80 µl of pre-diluted sample.

5.2.3 LFD testing – Multiplexed LFD

For the production of the multiplexed LFD initially the NC membrane was patterned using the LDW method outlined in section 3.1. Polymer lines were deposited at 2.5 mm intervals to allow for a flow path of 2 mm for each channel taking into account the width of the polymer barrier. Next, the antibodies were deposited into the channels and each antibody was deposited in turn into every fourth channel and to avoid any cross-contamination, the Biodot dispensing machine was thoroughly cleaned between each of the four antibody-deposition cycle. The devices were clean cut into the four-channel device along the middle of the polymer barrier and assembled with the wicking and conjugate pad. The conjugate for each assay was then pipetted into the individual channels of the conjugate pad for each biomarker.

5.2.4 Patterning the conjugate pad

As outlined in section 3.1 the LDW technique was used to pattern the conjugate pad. The deposition speed was varied as part of the investigation.

5.2.5 Clinical details and ethics

- Plasma samples were collected from patients attending the Ubuntu TB clinic in Cape Town between May 2012 and December 2013 in a cohort collected and described by Walker N et al. (https://www.ncbi.nlm.nih.gov/pubmed/28475709), with approval from by the University of Cape Town Research Ethics Committee (HREC REF 516/2011). Active pulmonary TB was confirmed microbiologically by sputum smear and culture positivity and radiologically by chest radiograph. Healthy controls were sputum smear and culture negative. All the patient samples tested were HIV negative.

- Serum samples were collected as part of the UK collected MIMIC (Multi-functional Integrated Microsystem for rapid point-of-care TB identification) study is a Government and Industry–funded UK cohort collected from three UK centres: Southampton, UCL and Edinburgh. All patients in this study are HIV negative. Active TB was microbiologically confirmed by sputum culture positivity. Healthy controls were asymptomatic and IGRA (interferon gamma release assay) negative. Dr Marc Tebruegge (University of Southampton) is a co-PI on this study.

- Ethics for analysing these blood samples to develop novel diagnostic tests for tuberculosis has been approved by the University of Southampton Faculty of Medicine Ethics Committee (ERGO II: 17758 & ERGO II 14291)

5.3 Results

The development and optimisation process involved several steps. Firstly, the development of individual LFDs which were tested in PBS before moving to healthy serum. The individual LFDs were then tested using patient samples for HC and TB positive cases and finally a number of the individual LFDs were combined into a multiplexed device that was also tested for proof of concept on a limited number of patient samples.

5.3.1 Testing Analytes in PBS

The first stage of the development process was the optimisation of four individual LFDs for the markers (CRP, SAA1, LBP, CFHR5). The LFDs were initially tested using PBS to establish their initial LOD and detection range capabilities. The results of these are shown in the calibration curves of Figure 5.2, plotting the intensity of the test line against the concentration of the analyte for each of the four markers (CRP, SAA1, LBP and CFHR5). A number of parameters were examined at this stage including the volume of conjugate and the volume of sample required for each test. From previous experimentation by the team, it was established that 80 µl was an adequate sample volume to not only ensure that there was continuous flow but also ensure that the entirety of the sample was able to be removed by the wicking pad.

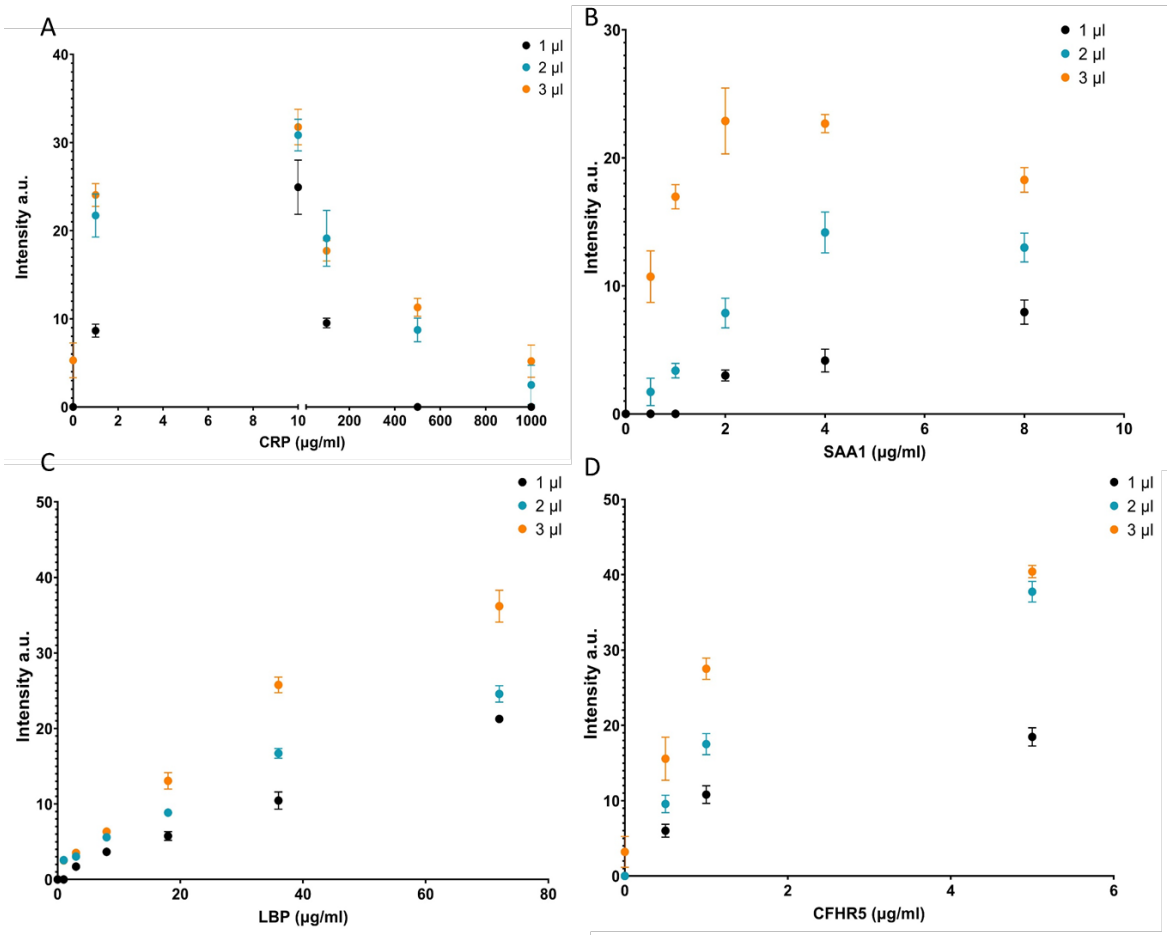

Figure 5.2 – Graphs showing the mean test line colour intensity (for 3 repeat measurements) against the analyte concentration for three different conjugate volumes (1 µl, 2 µl and 3 µl) for the four biomarkers A) CRP, B) SAA1, C) LBP and D) CFHR5. The error bars represent standard deviation for three repeat measurements.

As can be seen in Figure 5.2 above, as the conjugate volume increases so too does the sensitivity of the assay as there is more tagged detection antibody to bind to the analyte in the sample. However, at a certain point the amount of conjugate can lead to false positive signal as there can be some non-specific binding at the capture site. For CFHR5 there is a small visible signal at 0 µg/ml (control) when using 3 µl of conjugate however the signal was reduced when only using 1 µl of conjugate, therefore it was decided to continue forward with 2 µl. For LBP the peak of test line colour intensity was at 3 µl, and there was no false positive seen so to maximise sensitivity 3 µl was used. For CRP, where the assay is highly sensitive, a higher volume of conjugate increases the onset of the Hook effect occurring at lower concentrations and therefore for this assay a lower volume was used. For instance, as can be seen in Figure 5.2A, the lower the conjugate volume, the more severe the Hook effect is. When only 1 µl of conjugate is used there is no visible signal at 500 µg/ml or 1000 µg/ml CRP, however, at 3 µl there is an increased signal at the higher

concentrations of CRP but there is also some visible signal at 0 µg/ml (control) showing a slight false positive signal, therefore 2 µl of conjugate was used for this assay.

Once the individual assays for LFDs were working, commercially available standards of the biomarkers of interest were spiked into PBS and tested producing the calibration curves with optimised conjugate and sample volumes as seen in Figure 5.3.

The purpose of this is to establish the dynamic range of each of the LFDs and to establish whether the resolution of the test is sufficient to be able to detect the change in analyte concentration from Healthy control (HC) to TB. The initial calibration curves were produced using commercial analyte standard spiked into PBS before introducing plasma as a more complex matrix for the assay. The calibration curves show the Hook effect occurring for the CRP assay which has already been established for this assay when testing for higher concentrations of the analyte. There are several ways to overcome this phenomenon which are detailed in the section 5.3.4 below.

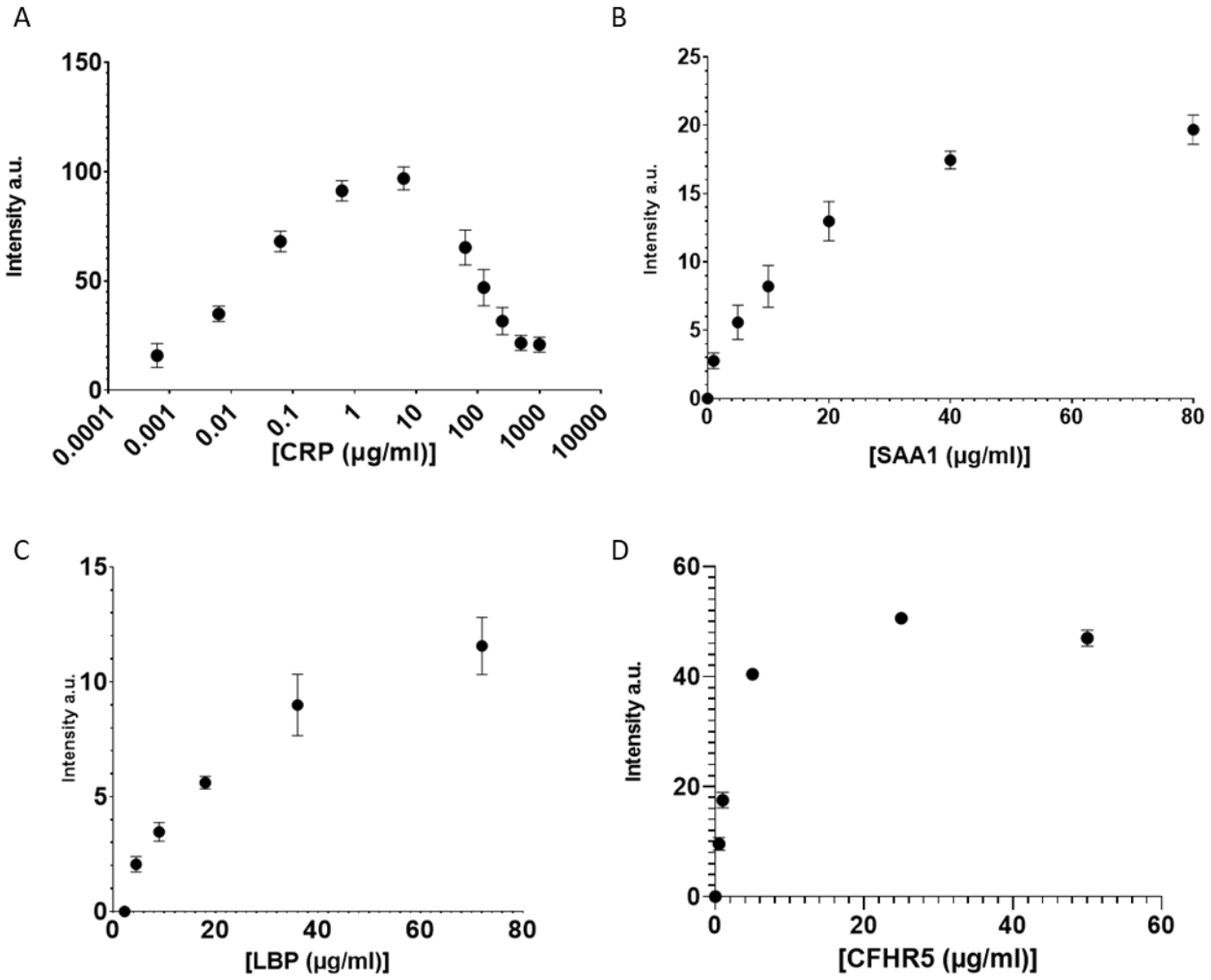

Figure 5.3 – Calibration curves showing the test line colour intensity against concentration for all four biomarkers. Mean plotted with error bars representing standard deviation of three repeat measurements.

Overall, the calibration curves show an increase in test line colour intensity with an increase in the concentration of marker and this was as anticipated. There is no visible signal for 0 µg/ml (control) for any of the markers which means that there were no false positive results due to any of the assay components or reagents.

In the calibration curve for CRP in Figure 5.3A, the Hook effect can be seen very clearly. The test line colour intensity increases with the concentration until it reaches a peak around 10 µg/ml where it then decreases as the concentration increases further. A very slight Hook effect can be seen in Figure 5.4 - Photo of six LFDs for the detection of CFHR5 across a range of concentrations from 0 – 50 µg/ml. Figure 5.4, showing six individual LFDs for CFHR5 detection and the highest concentration (50 µg/ml) shows a slight decrease in test line intensity.

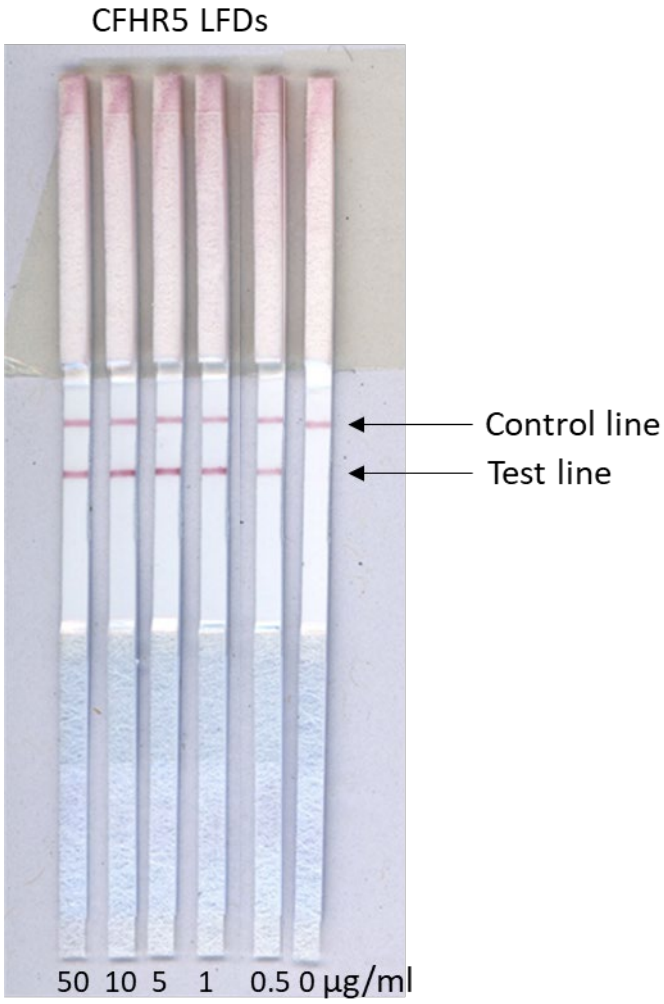

Figure 5.4 - Photo of six LFDs for the detection of CFHR5 across a range of concentrations from 0 – 50 µg/ml.

5.3.2 Comparison of plasma versus serum

Fibrinogen and blood clotting factors, present in blood along with red and white blood cells and nutrients, cause blood to clot when exposed to air or extracellular matrix outside the blood vessels, helping prevent excessive bleeding following injury. These components can be prevented from working however, with the addition of anti-coagulants. Plasma and serum are two types of preparations of blood that are created depending on whether an anticoagulant is added to the blood sample at the point of collection [184]. The addition of anti-coagulants to prevent clot formation is essential, for example, if the blood sample is cultured.

Plasma: When an anticoagulant is added to whole blood shortly after collection, coagulation is prevented, and all components are kept in suspension. If this whole blood suspension is centrifuged then all the heavier cellular components will sediment, the heavier red blood cells settle first at the bottom and this is followed by the white blood cells and platelets that form a buffy coat layer above the bottom layer of red blood cells, leaving a clear liquid at the top. Plasma is this clear upper layer of blood that is made up of all blood components including fibrinogen which is one of the twelve clotting factors is retained in the plasma, the blood cells are not part of the plasma.

Serum: If no anti-coagulant is added to the whole blood, the clotting factors cause the blood to clot. The fibrinogen-containing clots do an efficient job of removing red blood cells from the blood in the form of solid masses. In research, serum is most widely used since it makes up a larger proportion of blood than plasma does. It generates more volume per unit of blood at least in part because it removes primarily the unwanted red blood cells more efficiently.

For the development of a non-sputum-based test the use of both plasma and serum was investigated as potential medium. It was important to ascertain which would give the most reliable results or whether both could potentially be used on the LFD. As proof of concept the comparison between plasma and serum was only made for the CRP assay.

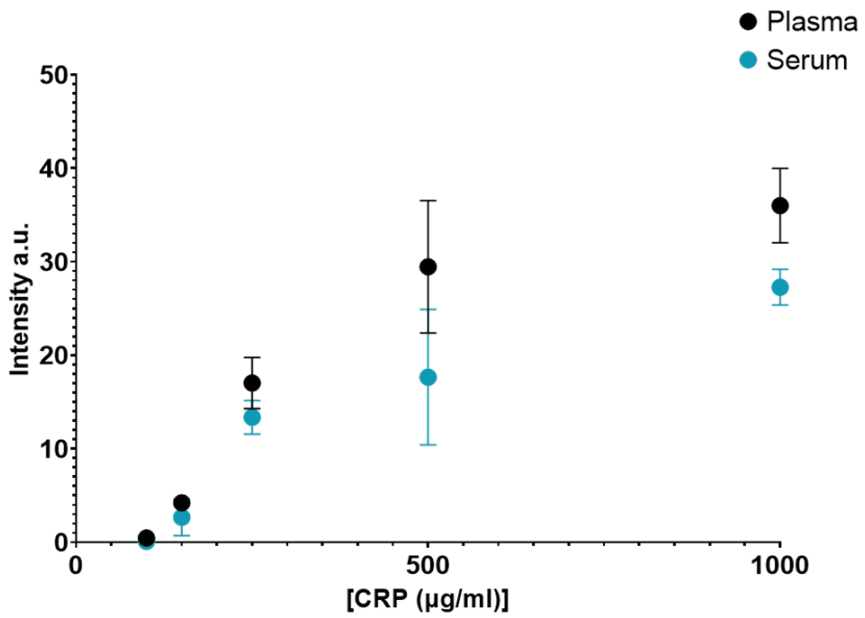

Figure 5.5 - Graph showing the test line colour intensity for 5 different capture antibody concentrations of CRP showing results for testing plasma (black) and serum (blue). Mean plotted with error bars representing the standard deviation of three repeat measurements.

Statistical analysis, in the form of an unpaired t-test performed in GraphPad Prism, showed that there is no significant difference between the test line colour intensities for testing with serum or plasma. That being said, there is arguably a reduction in the hook effect for the plasma as the intensity value for 1000 µg/ml is higher, although the difference is small and for the other concentrations there is an overlap in the intensity values for plasma and serum. For the future implementation of this POC test this information is important as it increases the versatility of the test if there is greater flexibility because of the different sample types that can be used for testing. For the majority of the development work reported in this chapter, plasma was used for the investigation however there were a small number of patient samples included in the later analysis that used serum samples.

5.3.3 Testing in plasma

All of the markers investigated as part of this work are host inflammatory markers and therefore are always present in the plasma, but the concentration increases during infection. The first stage was to establish baselines for the concentrations of markers found in healthy individuals. Firstly, a single healthy plasma sample was taken and serially diluted. Each marker was measured in the plasma for each dilution and the results can be seen in Figure 5.6.

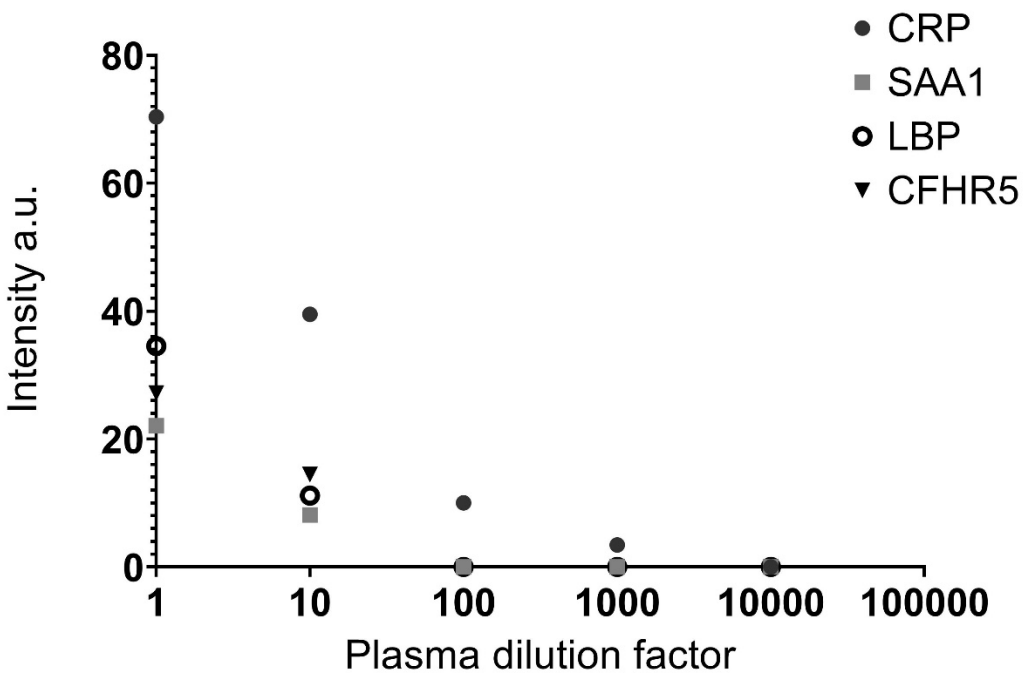

Figure 5.6 – Shows the test line colour intensity for individual LFDs developed for CRP, SAA1, LBP and CFHR5, at five different healthy plasma dilutions.

As can be seen in Figure 5.6, there is a decrease in test line colour intensity for all markers as the dilution factor increases (1 being whole undiluted plasma). This shows that the LFDs are able to detect the decrease in the biomarkers as the dilution factor increases and there is less analyte in the sample. It also shows that the medium of plasma works successfully on the LFD, with no flow issues which shows potential for future use with actual patient samples.

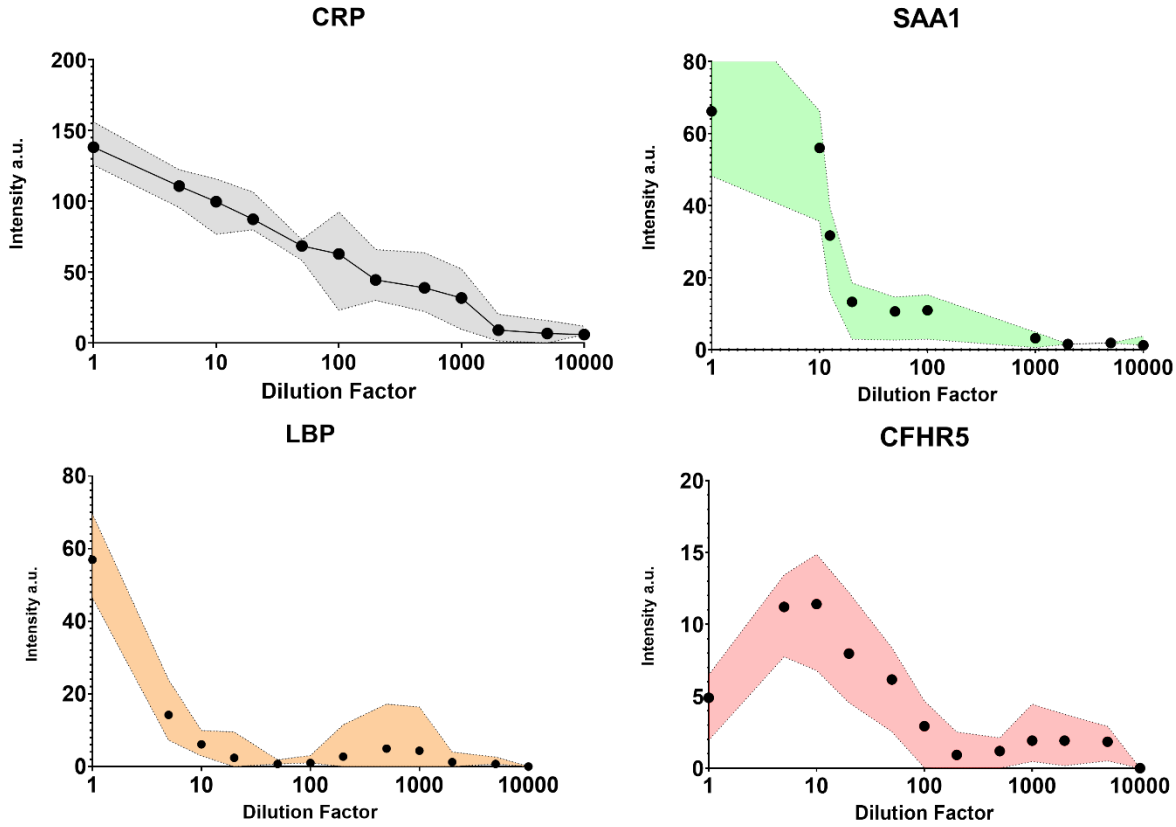

Figure 5.7 – Graphs showing the test line colour intensity for a serial dilution of healthy plasma for A: CRP, B: SAA1, C: LBP and D: CFHR5. The mean is plotted with the shaded area representing the range of the data across five different healthy patient samples.

The graphs in Figure 5.7 give an indication of the range of intensity that might be found across five healthy individuals although with sample number of five (n = 5) there are limited conclusions that can be drawn from it. Despite this, the graphs do show a relatively small range across the data which indicates that being able to differentiate TB from HC might be possible at this stage. For graph 5.6 D, which plots the results of CFHR5, there is a slight dip at the plasma concentration is higher (1 = whole plasma). This could be due to the Hook effect but will be taken into consideration when deciding on the dilution factor to use for the final test. There is also an observable increase in the intensity for LBP and CFHR5 around the 1:1000 dilution, that is non-characteristic of a dilution series, this could be caused by increased variability with a larger dilution due to insufficient mixing of the solution. The raw data suggests that there is one patient sample that is skewing the data in this way, and this could be due to the sample processing. Some of the samples had been stored in the freezer for a prolonged period of time and this may have affected how they performed when introduced to the LFD. There is also human error that can affect the samples and over a small sample number this is likely to be more prominent. Statistically, the sample in question was not considered an outlier and therefore was not removed from the analysis.

At this stage there is no reason to believe that the plasma or products in the plasma are affecting the assay. This is supported by comparing the test line intensity for those obtained in PBS with those from the plasma as seen in Figure 5.8.

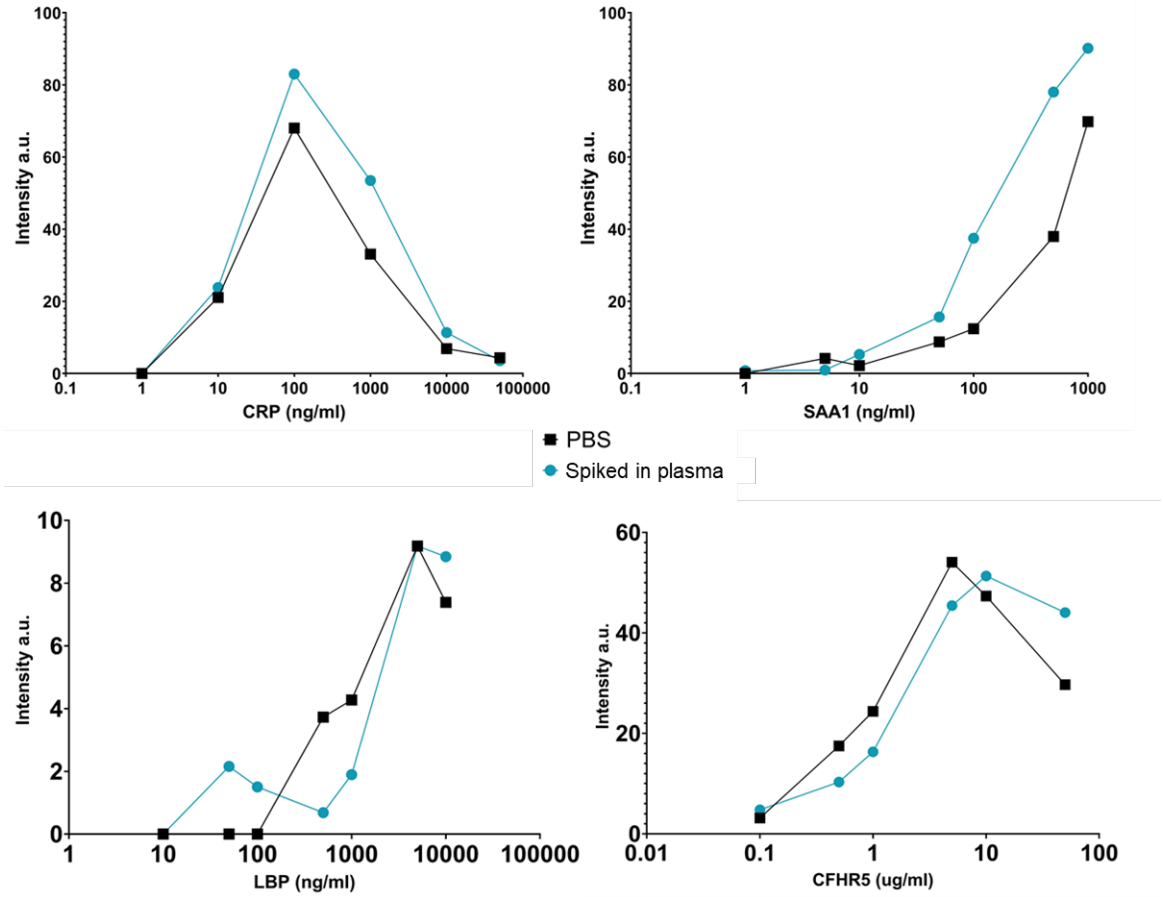

Figure 5.8 – Graphs showing the test line colour intensity for different concentrations of analyte spiked in PBS (black squares) and plasma (blue circle) for CRP, SAA1, LBP and CFHR5.

In perhaps greater detail, there is a degree of variation between the results for testing in PBS and plasma for LBP, however these results were obtained using just one plasma sample and as seen in Figure 5.7 there is some variation between healthy plasma levels of these markers which could have influenced the results. Despite this the results are consistent enough to give confidence that there is nothing in the plasma interfering with the assays to a significant enough level to affect the results.

5.3.4 CRP: Combined Sandwich and Competitive Assay

As can be seen from the calibration curves for CRP, this assay is subject to the Hook effect, described in section 2.4.2. There are several ways to overcome the Hook effect on an LFD, namely;

1. Add an additional capture line that can help to remove excess CRP from the assay before the sample reaches the second or subsequent 'designated' test line.
2. Add an antigen line to create a hybrid assay that contains one test line in a competitive assay format and one that utilises the sandwich assay format. These two lines allow the distinction between low concentrations and high concentrations where the Hook effect occurs.
3. Add more conjugate to the system so there is enough gold and detection antibody to bind all the analyte in the sample.
4. Dilute the sample to reduce the concentration of analyte in the sample.

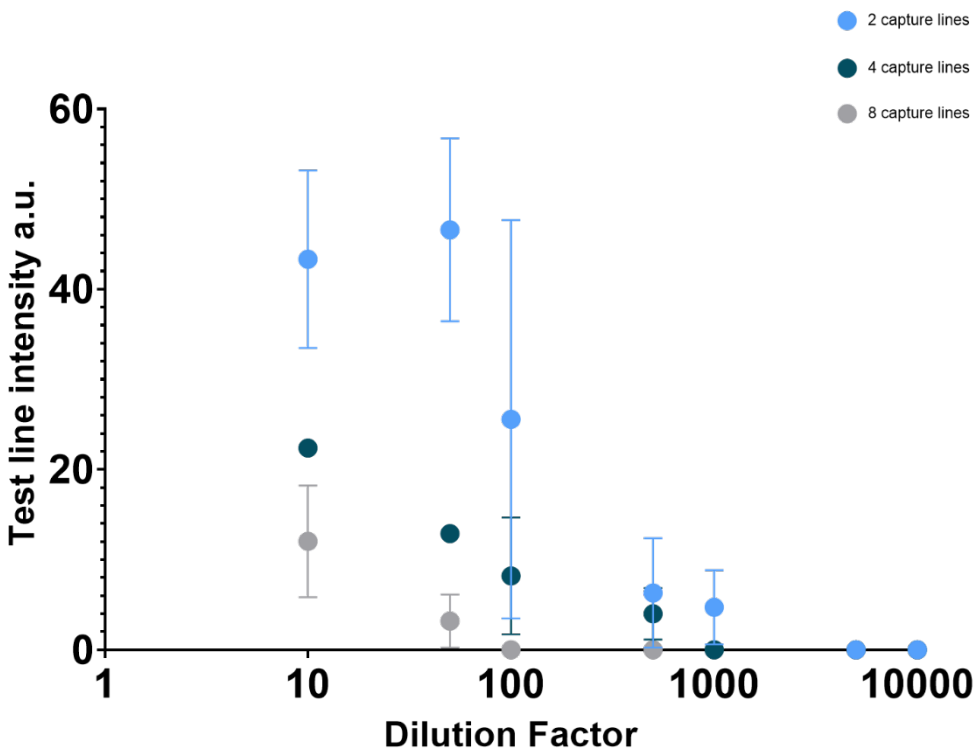

Figure 5.9 – Graph showing the test line colour intensity for CRP with three different numbers of pre-test capture lines for four different plasma dilutions. Mean plotted with error bars showing standard deviation of three repeat measurements.

The graph shown in Figure 5.9 shows the results for the use of multiple capture lines that are placed in front of the designated test line, and the test line colour intensity is then plotted on the graph against the plasma dilution using pooled healthy plasma. As the number for additional capture lines increases the designated test line's intensity decreases which is the expected result. As a clear example, for CRP, especially where the dilution factor is higher (concentration of analyte is lower) the analyte, CRP is depleted after it has passed two or four capture lines before reaching the actual test line.

Another alternative method to allow for semi-quantitative detection whilst compensating for the Hook effect seen with the CRP assay is the use of a hybrid test that combines the sandwich and competitive assay formats. This method has been previously reported [185, 186] . Here there is the usual test line but then the LFD also has a second capture site referred to as the overload line that is made up of pre-deposited CRP analyte. A schematic of the different lines and the completed devices can be seen in Figure 5.10.

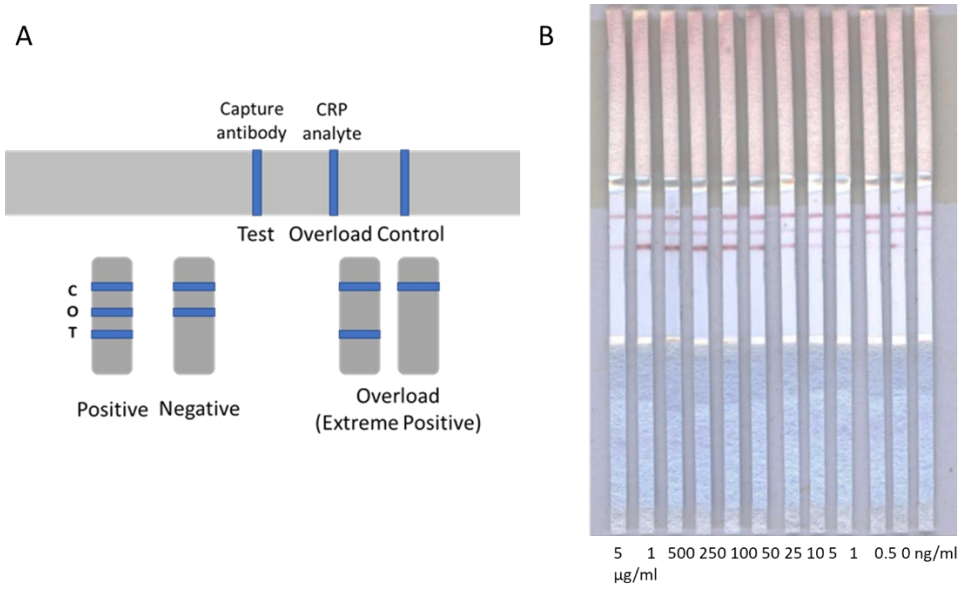

Figure 5.10 – A) Shows a schematic of the combined sandwich and competitive assay on a single LFD in the same flow to distinguish low results from very high where the Hook effect occurs and B) shows a scanned image of the individual LFDs with this combined assay implemented.

The images of the full LFDs in Figure 5.10 B show that the first line the sample reaches in the flow path is the test line with capture antibody. This increases in colour intensity as the concentration of CRP increases up until ~100 ng/ml where it starts to decrease down to 0 ng/ml until when there is no visible test line. The second line is the antigen line, when the concentration of CRP increases this line decreases so at 0 ng/ml there is a strong line but at 5 µg/ml there is no visible line. The combination of these two lines allows for the distinction between low and high CRP concentrations where the Hook effect occurs. The results for the test line colour intensity extracted for the test for both lines can be seen in the graph below in Figure 5.11.

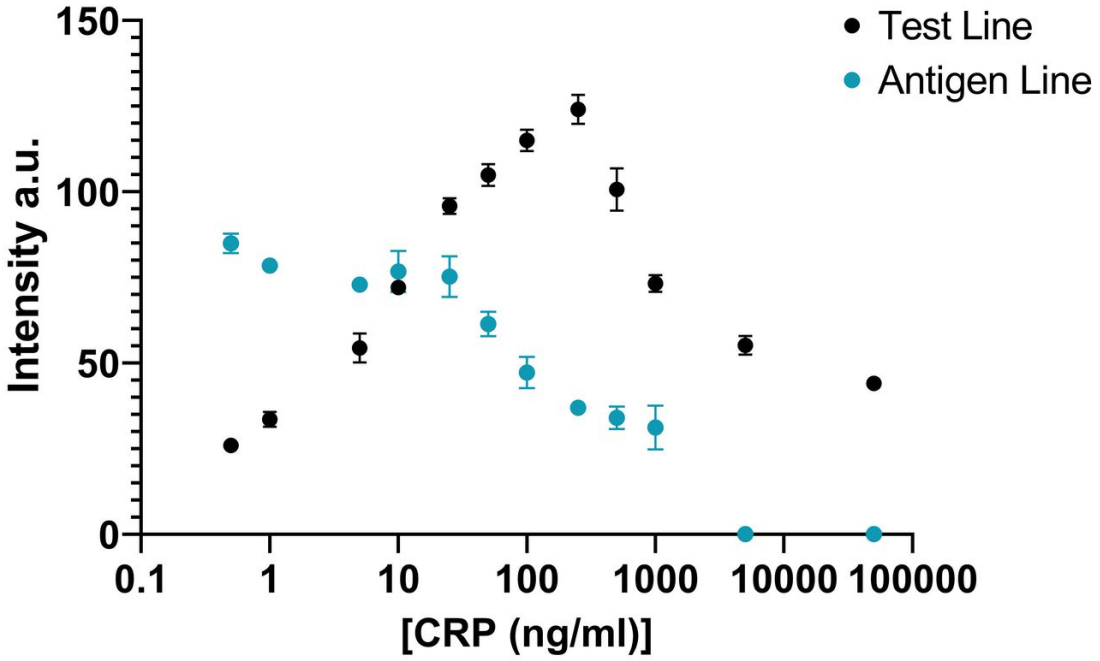

Figure 5.11 -Graph showing the normalised colour intensity of the test line (black) and antigen line (blue) for concentrations of CRP from 0-50000 ng/ml. Mean plotted with error bars representing standard deviation for three repeat measurements.

The results in Figure 5.11 show the relationship between the test line and the antigen line. Generally, they show an inverse relationship as one increases the other decreases which allows for the distinction in concentration in the sample for a semi-quantitative analysis. Although this is a useful method and shows good results and promise as a technique that can allow for semi-quantitative detection in addition to overcoming the Hook effect, to keep the cost of the test as low as possible and to ensure that the readout from the test would be user friendly, the easiest method to reduce the Hook effect is to use a pre-sample dilution step. This method can be implemented in a user-friendly POC test as has been seen in the COVID-19 testing with the use of pre-prepared tube of buffer that the sample is added directly to, before adding it to the LFD.

5.3.5 Testing patient samples: Individual LFDs

After the initial optimisation of each individual LFD for the markers (CRP, SAA1, LBP and CFHR5) using PBS and spiked healthy serum, these LFDs were tested using patient samples. These samples were obtained from patients from South Africa and the UK. They were a mixture of TB-confirmed patients, healthy patients and pools of these samples mixed together, although the majority of the samples were plasma samples there were several serum samples that were included in the testing, plasma for TB (n = 9) for HC (n = 10) and serum TB (n=2) for HC (n=2).

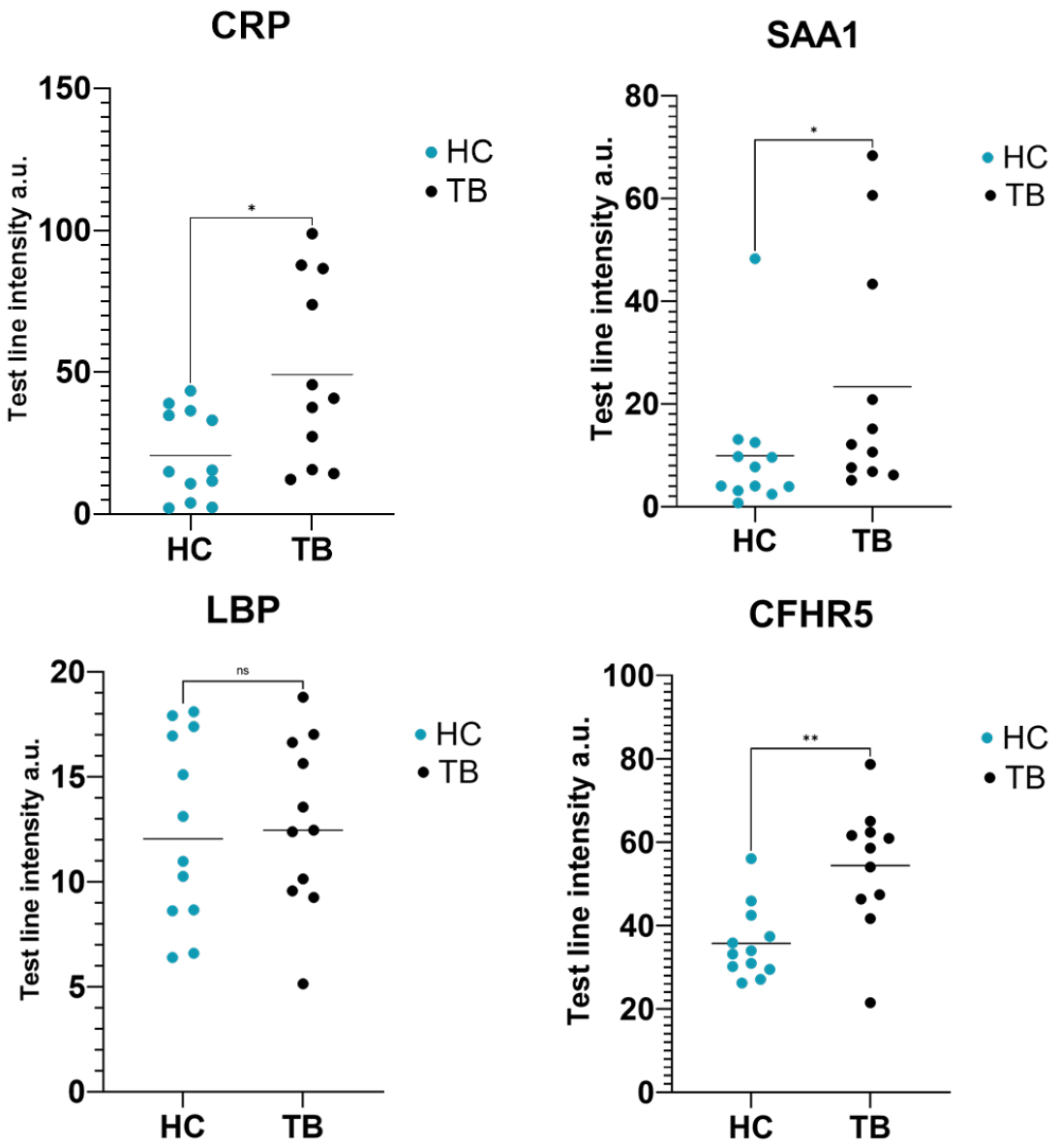

Figure 5.12 – Shows scatter plots with individual and the median values of test line colour intensity extracted from the individual LFDs for a) CRP b) SAA1 c) LBP and d) CFHR5. 11 plasma samples from TB patients and 12 healthy controls were analysed including 2 master pools (of several patient samples). Differences were considered significant when $P < 0.05$.

The graphs in Figure 5.12 show the ability of each marker to distinguish the HC from the TB patients via the test line colour intensity. The master pools used were patient samples pooled together for use in the initial optimisation of experiments due to the limited available of sample volumes. The test line colour intensity for each test, for each sample was plotted for each of the four markers. The analysis performed on the sample data was done in GraphPad Prism and these underwent a Mann-Whitney t-test which gives a P value that equates to the level of difference between the test line colour intensity results obtained for the HC samples vs the TB samples, and the results from this analysis are summarised in Table 5.

Table 5 – Summary of Mann-Whitney analysis results

MARKER	P VALUE	SIGNIFICANT DIFFERENT (P < 0.05)	P VALUE*	SIGNIFICANT DIFFERENT (P < 0.05)
CRP	0.0156	Yes	0.0115	Yes
SAA1	0.0439	Yes	0.1230	No
LBP	0.9279	No	0.8534	No
CFHR5	0.0022	Yes	0.0068	Yes
ALL MARKERS COMBINED	0.0005	Yes	0.0019	Yes

*serum samples removed

The results summarised in Table 5 show that the test line colour intensity of the LFD is significantly different between the HC and TB samples for CRP, SAA1 and CFHR5 however the tests for LBP showed no ability to statistically differentiate HC from TB. However, when the data from all four markers was combined, using the normalised test line colour intensity the result showed a highly significant difference. There were only 2 serum samples used for each of the HC and TB patients for each marker however when these results were removed from the analysis as seen in in third column of Table 5, the P value is altered for the markers. Although the change was minimal for CRP, LBP and CFHR5 the change in SAA1 took the P value from being significant (<0.05) to not, however when combined the markers still provide a highly significant result. Although this is an interesting finding, as there were only 2 serum samples for each data set this cannot be taken to be conclusive to support the use of serum or plasma specifically for the test in the future. The results do show the potential of these markers to be used as a rule-out triage tool for TB. However significant, the ultimate goal was to combine these four markers into a panel that could be used together on a LFD. Therefore, the combined results for all the markers were plotted on the graph in Figure 5.13 showing the combined test line intensity for all the HC vs TB for all markers.

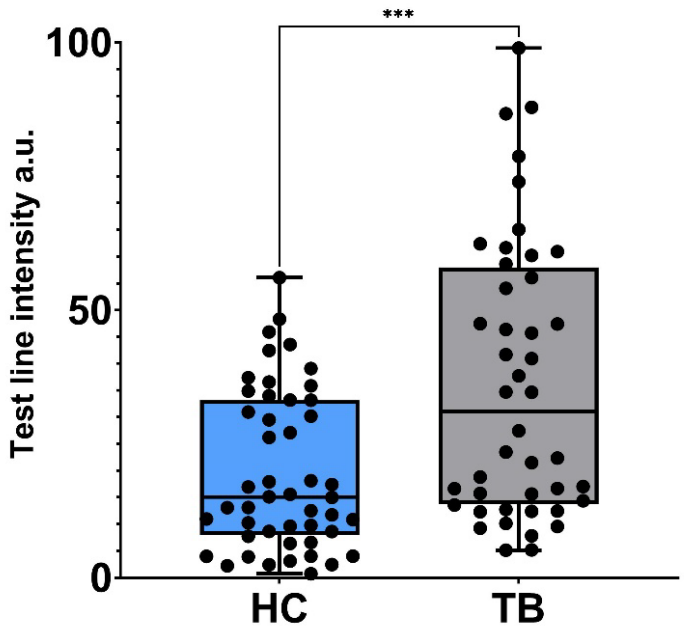

Figure 5.13 – Box and whisker plot for each patient sample for all four markers, CRP, SAA1, LBP and CFHR5.

Mann-Whitney statistical analysis of the data in Figure 5.13, shows a superior statistically significant difference between the intensities obtained for the HC compared to TB (P = 0.0005) when all the marker data is combined. This shows that combining the markers into a panel gives better differentiating power for HC and TB than using the biomarkers individually. The data does show that there is a considerable overlap between the intensity values obtained from the HC with those from the TB samples, although the highest TB values were significantly higher than those for HC.

As the results for an individual LFD for LBP these results were removed to see what effect this had on the significance of the data. Mann-Whitney statistical analysis of the data in Figure 5.14, shows a P = <0.0001 showing very a very significant difference between the intensity for HC and TB, which is superior to that of all four markers combined. For this reason, only three markers (CRP, SAA1 and CFHR5) were carried forward to the development of the multiplexed device.

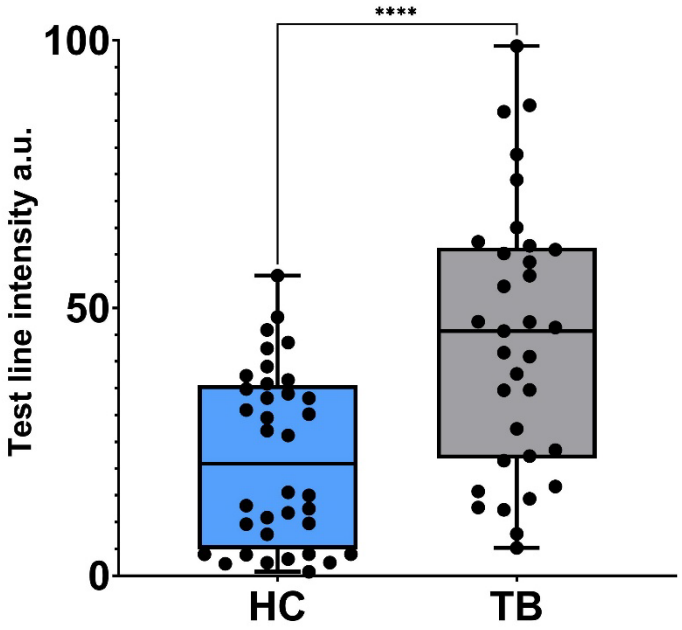

Figure 5.14 - Box and whisker plot for each patient sample for three markers, CRP, SAA1 and CFHR5.

As these are host markers, there is variation in biomarker levels between individuals and therefore an amount of overlap was anticipated. It highlights the importance of setting an appropriate cut-off value for the intensity that can be used to determine whether the sample is classed as HC or TB in a field setting.

5.3.6 Luminex intensity vs Lateral flow intensity

The biomarker panel used here was initially discovered and validated using a Luminex assay, the details of which can be found in the published methods of Garay-Baquero et al [150]. The Luminex assay is an antibody detection system that is based on spectrally encoded beads that allows for multiplexed protein analysis. Although the Luminex assay did not provide quantitative analysis of the analytes in the patient samples in this case, it gave a relative fold change observed between the healthy controls and the TB positive patients.

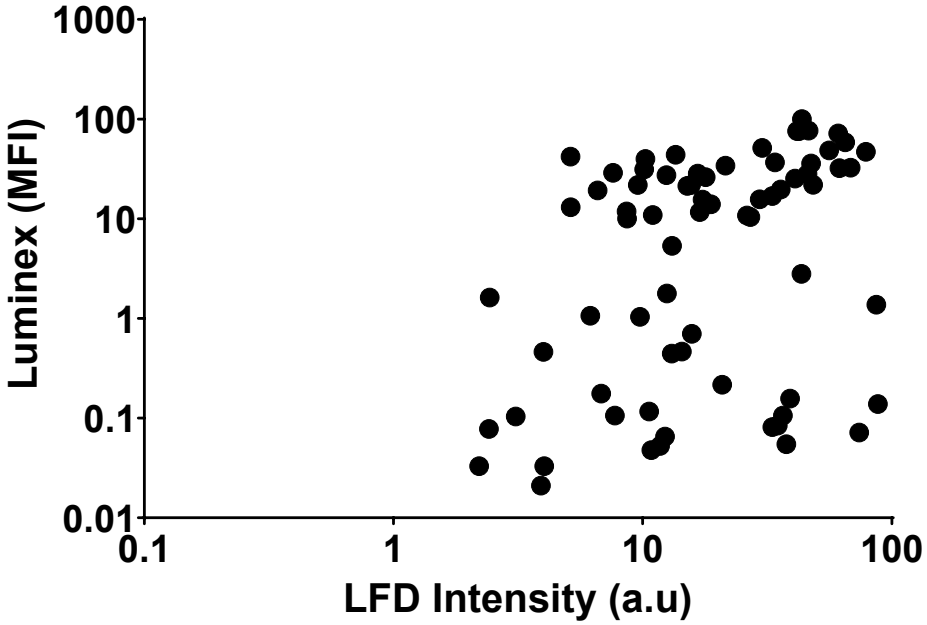

Figure 5.15 – Graph showing the normalised mean fluorescence intensity (MFI) obtained from the Luminex assay plotted against the normalised test line intensity obtained from the LFD for the 11 plasma samples from TB patients and 12 healthy controls.

Spearman's analysis was used as the two variables are non-parametric and do not adhere to normal distribution. The r value (r = 0.4351) suggests that although the points align linearly but with a lot of variability, the P value (P = 0.0001) (which is considered significant when $P < 0.05$) suggests a highly significant relationship between the intensity obtained from the Luminex assay and the intensity extracted from the LFD test line.

The intention of this study was not to assess the LFD as compared to the Luminex assay but to evaluate the LFD as a diagnostic test. The gold standard for comparison would be an ELISA performed on the samples that would give a quantitative analysis of the biomarker concentrations as the Luminex assay here only gives the Median Fluorescent Intensitys (MFI)s for the HC vs TB patients and does not quantify the results as a standard curve was not performed on the assay.

5.3.7 Receiver operating characteristic (ROC) Analysis

A ROC analysis for the above work was conducted as per section 3.5.2. Each of the markers were initially analysed individually and plotted on the ROC curve alongside the combined results for all four markers and the reference line.

The purpose of the ROC curve is to decide where to draw the line between the positive and negative results. If all control values were lower than the patient values there would be a clear cut-off, however as these two distributions overlap it is not as simple. As the aim of this project

was to create a rule-out test, sensitivity is more important than specificity and therefore making the threshold very low means that no cases of TB would be missed however there will be a high rate of false positive results. GraphPad Prism tabulates and plots the sensitivity and specificity of the test at various cut-off values from the ROC curves.

Sensitivity: The percentage of patients with the disease that the test correctly identifies to be positive.

Specificity: The percentage of patients without the disease that the test correctly identifies as negative.

Prism calculates the sensitivity and specificity using each value in the data table as the cut-off value and this generates many pairs of sensitivity and specificity. There must be a balance to ensure the best sensitivity and specificity.

The area under the ROC curve is called the concordance statistic or C-index and it quantifies the ability of the test to discriminate between individuals with the disease from healthy controls, a perfect test would have an area of 1.00. The area is the probability that a patient selected at random would have a higher intensity value for that marker than a healthy control.

In addition to the AUC GraphPad Prism also calculates a P value for each analysis that tests the null hypothesis that the AUC is equal to 0.50 (that the test has the same distinguishing capacity as flipping a coin). If the obtained P value is small, then it can be assumed that the test is able to successfully distinguish between disease patients and healthy controls [187].

ROC curves were produced for the individual markers and for combinations of the best performing markers as can be seen in Figure 5.16, the accompanying AUC and P values produced by the analysis can be found in Table 6.

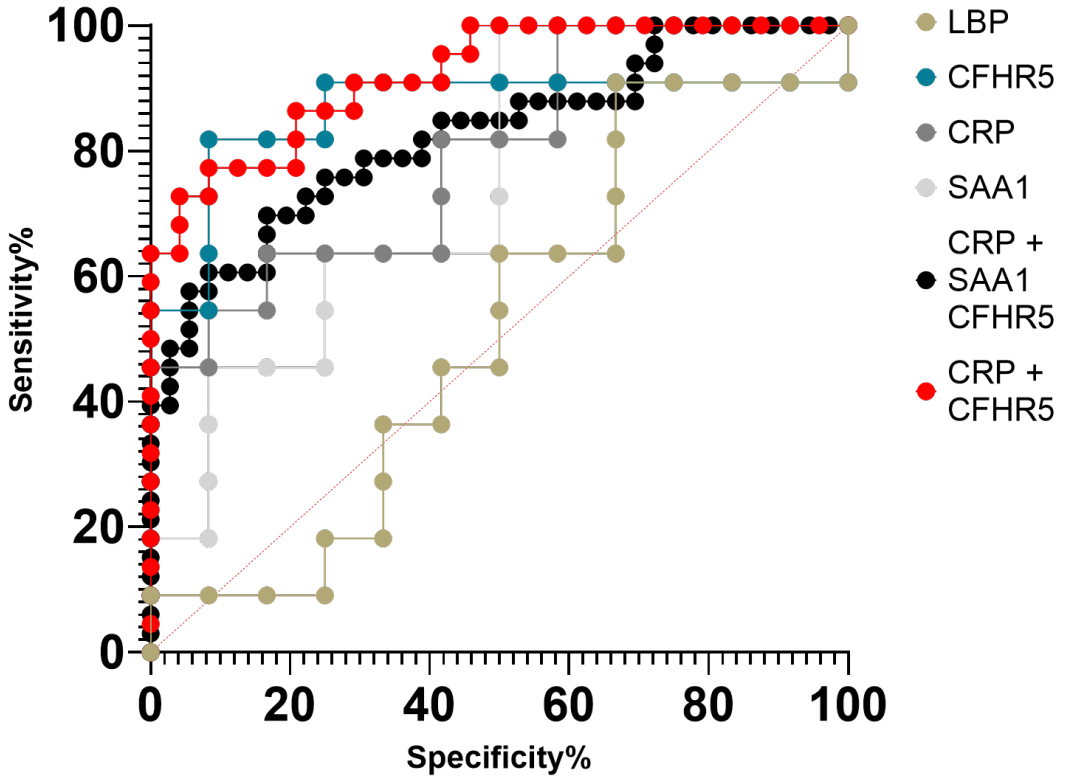

Figure 5.16 – ROC curve produced in GraphPad Prism v.9. TB positive was set as the positive test outcome and the test direction such that larger test result indicates a more positive test.

The ROC curve shown in Figure 5.16 shows the discriminatory power of CFHR5 to be 0.8636 however when this is combined with CRP this increases to 0.9205 giving superior ability to distinguish HC from TB patients.

Table 6 – Results for AUC from the ROC analysis

Marker	AUC	P Value
CRP	0.7955	0.0164
SAA1	0.7500	0.0423
LBP	0.5152	0.9020
CFHR5	**0.8636**	**<0.0001**
CRP+SAA1+CFHR5	**0.8249**	**<0.0001**
CRP+CFHR5	**0.9205**	**<0.0001**

The results in Table 7 detail the ROC curve analysis that was obtained for the combination of CRP and CFHR5. The analysis gives the sensitivity and specificity of the test at different cut-off values. For example, where the test line colour intensity is greater than 15.66 the sensitivity is 90.91

(72.19%-98.38%) and the specificity is 70.83 (50.83% - 85.09%). This is the best combination for this particular marker combination.

Table 7 – Results from ROC analysis for sensitivity and specificity for the combination of CRP and CFHR5 taken from GraphPad.

	Sensitivity%	95% CI	Specificity%	95% CI
> 2.320	100.0	85.13% to 100.0%	4.167	0.2137% to 20.24%
> 3.230	100.0	85.13% to 100.0%	8.333	1.481% to 25.85%
> 4.540	100.0	85.13% to 100.0%	12.50	4.344% to 31.00%
> 5.825	100.0	85.13% to 100.0%	16.67	6.679% to 35.85%
> 7.225	100.0	85.13% to 100.0%	20.83	9.245% to 40.47%
> 9.095	100.0	85.13% to 100.0%	25.00	12.00% to 44.90%
> 10.45	100.0	85.13% to 100.0%	29.17	14.91% to 49.17%
> 10.70	100.0	85.13% to 100.0%	33.33	17.97% to 53.29%
> 11.23	100.0	85.13% to 100.0%	37.50	21.16% to 57.29%
> 11.69	100.0	85.13% to 100.0%	41.67	24.47% to 61.17%
> 11.77	100.0	85.13% to 100.0%	45.83	27.89% to 64.93%
> 11.97	100.0	85.13% to 100.0%	50.00	31.43% to 68.57%
> 12.23	100.0	85.13% to 100.0%	54.17	35.07% to 72.11%
> 12.81	95.45	78.20% to 99.77%	54.17	35.07% to 72.11%
> 13.84	95.45	78.20% to 99.77%	58.33	38.83% to 75.53%
> 14.68	90.91	72.19% to 98.38%	58.33	38.83% to 75.53%
> 15.06	90.91	72.19% to 98.38%	62.50	42.71% to 78.84%
> 15.35	90.91	72.19% to 98.38%	66.67	46.71% to 82.03%
> 15.66	90.91	72.19% to 98.38%	70.83	50.83% to 85.09%
> 15.78	86.36	66.67% to 95.25%	70.83	50.83% to 85.09%
> 16.57	86.36	66.67% to 95.25%	75.00	55.10% to 88.00%
> 19.42	86.36	66.67% to 95.25%	79.17	59.53% to 90.76%
> 24.46	81.82	61.48% to 92.69%	79.17	59.53% to 90.76%
> 30.29	77.27	56.56% to 89.88%	79.17	59.53% to 90.76%
> 34.02	77.27	56.56% to 89.88%	83.33	64.15% to 93.32%
> 35.71	77.27	56.56% to 89.88%	87.50	69.00% to 95.66%
> 37.13	77.27	56.56% to 89.88%	91.67	74.15% to 98.52%
> 38.39	72.73	51.85% to 86.85%	91.67	74.15% to 98.52%
> 40.00	72.73	51.85% to 86.85%	95.83	79.76% to 99.79%
> 41.30	68.18	47.32% to 83.64%	95.83	79.76% to 99.79%
> 42.62	63.64	42.95% to 80.27%	95.83	79.76% to 99.79%
> 44.63	63.64	42.95% to 80.27%	100.0	86.20% to 100.0%
> 46.02	59.09	38.73% to 76.74%	100.0	86.20% to 100.0%
> 46.87	54.55	34.66% to 73.08%	100.0	86.20% to 100.0%
> 50.72	50.00	30.72% to 69.28%	100.0	86.20% to 100.0%

Despite the promising results, a sensitivity of 90.91 (72.19%-98.38%) and specificity of 70.83 (50.83% - 85.09%) is not sufficient to meet the WHO requirements for a screening and triage test of sensitivity > 95% and specificity <80%. The values are however close and show potential, the markers would need further validation with an increased pool of patient samples to accurately assess their ability to discriminate diseased patients from healthy controls.

5.3.8 Patterning the conjugate pad

The multiplex four-channel LFD has four parallel channels inscribed in the NC membrane using the LDW technique. The four separate assays that are to be implemented in these four independent

channels require their own conjugated antibodies to be deposited onto the conjugate pad. If all four are mixed together, this could lead to the following issues: 1) This increases the risk of cross-reactivity occurring between the assays and 2) more conjugate needs to be added to account for loss into the other channels (assuming 25% of the conjugate will flow into each channel), and this increases the volume of reagents and the cost. One way to overcome this issue is to also pattern the conjugate pad to ensure that each conjugate is kept separate. Previously the patterning of the conjugate material had not been investigated, therefore the deposition speed was varied to establish at which point the polymer line is solid and there is no liquid leaking from the barrier, as can be seen in Figure 5.17, and the results from the deposition speed which can be seen in Table 8.

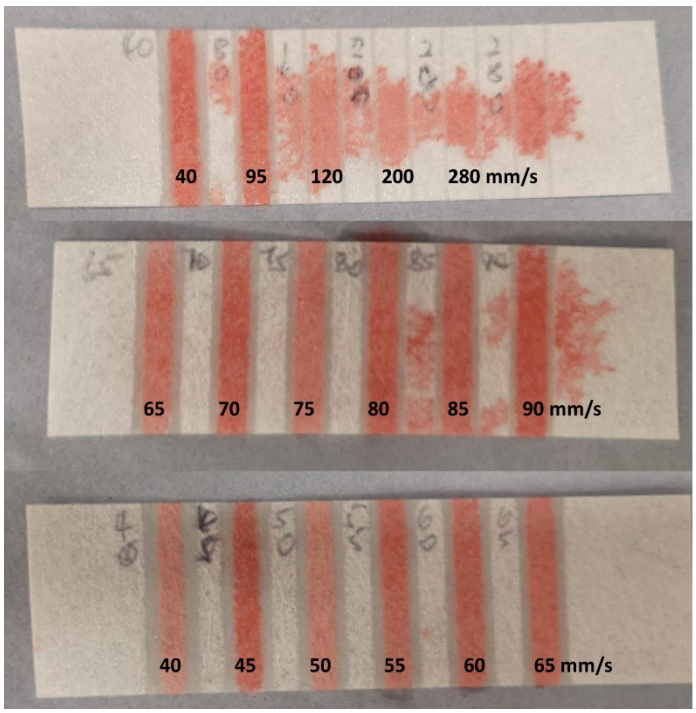

Figure 5.17 - Images of the conjugate pad patterned using different deposition speeds and then tested for leakage using red coloured ink. Ink can be seen within and leaking from the channels under all non-optimal conditions of speeds > 75 mm/s.

Table 8 – Results for the effect of deposition speed of polymer on barrier integrity created in the conjugate pad.

DEPOSITION SPEED (MM/S)	VISIBLE LEAKAGE FROM THE BARRIER (YES/NO)	MEAN BARRIER THICKNESS (MM)
280	Yes	0.4
200	Yes	0.4
120	Yes	0.6
95	Yes	0.7
90	Yes	0.7
85	Yes	0.8
80	Yes	0.9
75	No	1.0
70	No	1.1
65	No	1.2
60	No	1.3
55	No	1.7
50	No	1.8
45	No	2
40	No	2.1

As the speed of deposition decreased the integrity of the polymer line increased however the barrier thickness also increases proportionally as the slower speed means there is more polymer deposited per unit of area. The ambition of patterning the conjugate pad was to allow for a reduction in waste of conjugate and therefore if the barrier line separating the channels was 2.1 mm (as for 40 mm/s) the conjugate pad would be much wider than the NC membrane. It was decided that the barrier must have complete integrity but be the thinnest possible and therefore the deposition speed of 65 mm/s was chosen and repeated to ensure that there would be no leakage from one channel to the next. The images in Figure 5.17 show the results for a conjugate membrane with barriers (that form the walls of the patterned channels) patterned at different deposition speeds and then tested for its integrity using colour ink.

5.3.9 Multiplexed test

The results obtained for the individual LFD for LBP were not as expected and did not show that LBP was able to distinguish healthy controls from TB patients when used in the LFD format. Therefore, LBP was not included in the multiplex device. The multiplexed test is the combination of three individual marker assays implemented on a single LFD to detects the presence of CRP, SAA1 and CFHR5 simultaneously within a single sample. The use of the LDW patterning technique of the conjugate pad in addition to the nitrocellulose membrane means that each assay runs in parallel but completely independently of one another, with no cross-reactivity. The three-channel device can be seen in Figure 5.18. Although the ROC analysis showed that CFHR5 was the marker with superior discrimination power, followed by the combination of CFHR5 and CRP the production of a three-way multiplexed device was an important step in the process to ensure that if other markers were identified in the future the platform would be able to support multiple markers successfully.

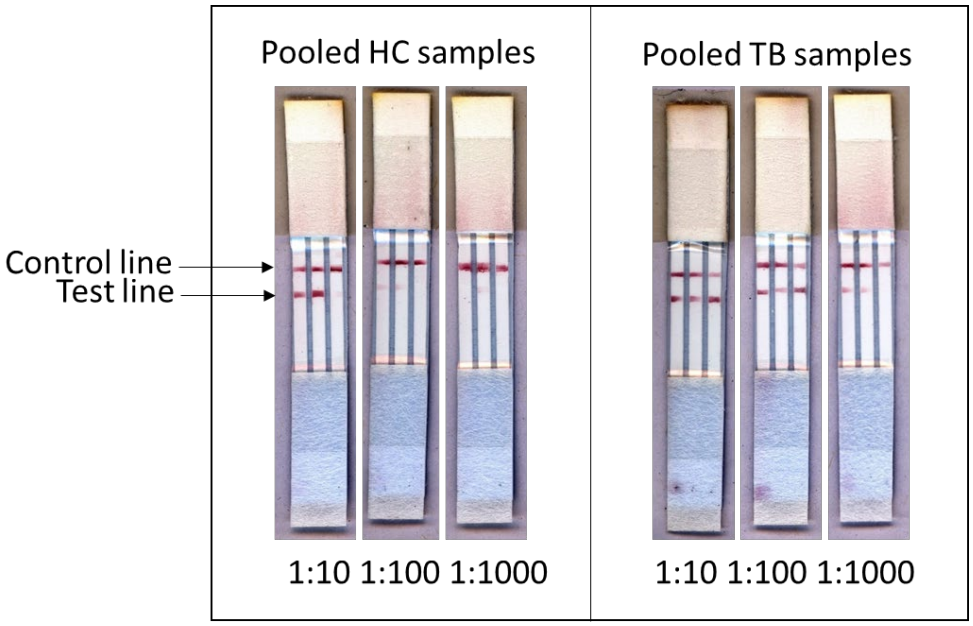

Figure 5.18 – Scanned images of three channel multiplexed LFDs for the detection of CRP, SAA1 and CFHR5. The devices were tested with pooled HC samples and pooled TB samples, both of which were tested at 1:10, 1:100 and 1:1000 dilutions.

As can be seen in Figure 5.18 the image on the left which is the device(s) tested using the HC samples shows a much fainter test line across the markers than the image on the right which shows the LFD tested using the TB positive samples.

Due to patient sample exhaustion the healthy and TB samples were pooled for a comparison between the average test line colour intensities. Additionally, the samples were processed using a 10-fold dilution due to the wide physiological range that the markers span.

5.4 Discussion

A multiplex lateral flow screening test has significant potential, as if developed to become the first POC screening tool that meets the WHO requirements for a non-sputum based TB screening test, it could help to identify those with TB in the community who are not being picked up until they have already spread the disease further [135, 188]. This means further treatment would be received quicker and treatment can be started sooner, and this is crucial as TB is treatable but involves a long antibody drug regimen for six months [134].

The multiplexed LFD that was created as part of this project has shown high applicability to the WHO criteria for the development of a non-sputum-based rule-out test for TB [142]. The protein biomarker immunoassays that are implemented on the LFD have shown potential and capability to distinguish those patients that are healthy controls from those with a confirmed TB infection. There is, however, notably overlap between the intensity values that were extracted from the LFDs for the HC and TB patients. This means that a definitive rule-out cannot be given from the results of this particular test, and this is largely due to inherent heterogenicity in host immune responses. There was also the issue that the LFD for LBP did not show any capacity to differentiate HC from TB. This was not an expected outcome as the assay appeared to be performing successfully using the standard samples. There are several reasons why this could have happened; although every effort is made to ensure that the materials used are all stored and used as per the manufacturer's instructions there is the possibility that some external factor impacted on the efficacy of the antibodies being used. Due to time constraints of the project, it was not possible to repeat the experiments to rule out these types of issues. Additionally, there was an impact on the statistical significance of the results when the serum samples were removed from the analysis. Although this is a significant finding, there were only two serum samples for each marker (HC and TB) and there were only 12 HC and 11 TB samples tested in total. Therefore, the removal of two samples will have a larger impact on the data than if there had been a larger total number of samples and therefore although it is worth keeping this finding in mind, a larger cohort of samples would need to be analysed before any real conclusions could be made. The minimum number of samples required for a diagnostic study can be calculated, depending on the prevalence of the disease in the population and the sensitivity/specificity of the test [189]. In future this would need to be explored however for this study the limitation was availability of samples.

The markers that have been selected were chosen as part of a proteomics analysis that was completed by our collaborators within the Faculty of Medicine and the markers highlighted as significant were the best from a much larger pool [150]. However, this pool was also part of an

even larger analysis with some areas of this protein discovery and validation incomplete, therefore in the future there could be additional markers that could provide superior diagnostic power. The multiplexed LFD is optimised for the use of CRP, SAA1 and CFHR5 however, additional markers could be added to this panel or others substituted with little inconvenience or additional time requirements.

Despite a robust development and optimisation process and validation of the LFD using patient samples there are limitations to this study.

The samples that were used to validate these LFDs were a smaller cohort with 11 TB samples and 12 HC and this is not a large number of samples from which to draw definitive conclusions, especially, as the host marker concentrations vary between people, however this was the available remit of this project. The other limitation is the samples were a mixture of cohort from the UK and Africa and this does not represent all geographical populations where TB is high burden. For instance, India and South America would also be interesting regions in which to explore the validity of the test. In addition to this, the diagnostic value of the test was measured by its ability to distinguish patients with TB from HC but not patients with other respiratory diseases (ORDs). ORDs are a highly important cohort that should be investigated for a TB diagnostic test and although the identified protein biomarkers were investigated for ORDs during the proteomics discovery and validation, their diagnostic capabilities were not explored when the corresponding assays were implemented on a LFD. However, arguably for a rule-out test as opposed to a rule-in test, the specificity is not as important as the sensitivity of the test for highlighting those individuals who are infected with TB.

Finally, this LFD uses host inflammatory biomarkers that are always present at low levels even in healthy individuals and therefore the presence or absence of these markers is not sufficient but instead their quantification is required for diagnosis, and this therefore necessitates a requirement for a reader. During the optimisation process a scanner and desktop computer was used for all the analysis however in the context of a POC test this would be inappropriate. There are numerous commercially available readers that can be purchased and programmed for the use with LFDs or alternatively a specific reader could be developed, and this would be part of the future work of this project. Other groups have developed a test without the requirement for a reader [190]. Although in terms of cost this is advantageous, there is additional sample processing steps that are required for this to work that a) increases the time taken to complete the assay and b) increases the likelihood of user error affecting the results. Readers in the form of smartphones or adaptations to smartphones have been used to increase the sensitivity of the lateral flow devices which is a viable option [102, 105, 106, 109, 191]. However, in the context of TB and the

prevalence of the disease in less developed countries there are still places where a lower percentage of the population have a smartphone [192]. Additionally, they can be subject to variability in the user or environmental lighting conditions. To keep the cost low but the testing accurate a purpose-built reader that can be kept at central hubs would likely provide an appropriate solution.

Other groups have aimed to develop protein-based biomarker panels that are able to distinguish HC from TB and in some cases ORD, with mixed levels of success. One group was able to establish a six-protein biomarker panel from a larger group of 74 biomarkers, using a Luminex assay. This panel was able to detect active pulmonary TB with 100% sensitivity and 89% specificity when compared to culture methods, for 55 patients, independent of HIV status [193]. Another study, also using a Luminex assay utilised machine learning to identify a panel of four host proteins and an antibody (Ag85B) to detect TB. They tested in a larger cohort of 583 patients and achieved a sensitivity of 86% and specificity of 69% which is close to the WHO TPP criteria. Despite these successful findings, translating these highly technological laboratory based tests such as the Luminex assay into a POC testing solution is incredibly challenging and for this reason, the research has not progressed to commercialisation of a product [155].

Lipoarabinomannan (LAM) has also been explored for use as a biomarker for TB diagnosis in a non-sputum-based (urine) test, and a commercial test is available, Alere Determine TB LAM Ag kit from Abbott Laboratories that was endorsed by the WHO to assist in TB diagnosis. With sensitivity of 61% and specificity of 81% it no longer meets the WHO criteria for a non-sputum-based test and despite a low cost of $3.50 its wider use has been limited by budget availability [135, 194, 195]. This highlights the challenges that are faced in the production of non-sputum-based biomarker tests, even those that make it to commercialisation.

One review of biomarkers used for TB diagnostics [155] summarised the work on a selection of proposed biomarkers. This was an analysis of 443 publications including several different types of biomarkers (antibodies, cytokines etc). Forty-four biomarkers were identified in total that met the TPP set out by the WHO, of these twenty-four utilised a multiplexed biosignature. There is no meta-analysis that can support the results obtained between research groups and therefore there is no independent confirmation of any of these biomarkers. Furthermore, very few of these identified at the research stage, progress through to clinical validation however the information that was taken as part of this publication is being used by FIND to set up a database for biomarker development and this could help research groups in the future target areas with more potential [155].

Although this was not explored through the course of the project there is the potential that this screening test could be used as part of community testing and screening programmes that are already established and therefore utilise the infrastructure that is already in place for the identification of other diseases to implement this screening tool into the population.

5.5 Conclusion

I have demonstrated the potential for multiplex LFTs to be developed as screening tests for TB. The comprehensive proteomics analysis that was carried out to identify the biomarkers investigated in this chapter (CRP, SAA1, LBP and CFHR5) was a part of a larger cohort analysis which is as yet, incomplete. This means that there is the possibility that other protein biomarkers could be identified that show the ability to distinguish patients with TB from healthy controls, a major strength of this methodological approach. One option would be to expand the current biomarker panel to incorporate further markers and extend the LFD to detect six or more markers simultaneously, but this would present some manufacturing challenges. Alternatively, if newer markers are identified that provide superior differentiating power, then, any of the current markers could be replaced. The LFD platform is established and can be easily modified to accommodate further markers or substitute markers with little difficulty, and this could be an option for the future.

In addition to the development of the individual markers a multiplexed lateral flow for the detection of three host markers simultaneously was produced. Although the results from the individual biomarker testing did not necessarily support the use of SAA1 alongside CRP and CHFR5 as previously mentioned, other markers may yet be identified, and successful development of a three-way test allows for future alterations to the biomarker panel being used without the requirement for extensive optimisation. This is the focus of ongoing work within the group, once the optimal new biomarkers have been identified.

Chapter 6 SARS COVID-19

6.1 Introduction

SARS-CoV-2 was first identified in China in late 2019 and by early 2020 was quickly found in countries all around the world [196, 197]. With 6,605,406 deaths globally as of November 6th 2022, the pandemic has highlighted the unprecedented need for rapid diagnostic testing to monitor and halt the spread of disease not just for this pandemic but for other inevitable subsequent pandemics in the future. Although most cases of COVID-19 presented mild symptoms some patients developed pneumonia and flu-like symptoms and some severe and even fatal respiratory diseases such as severe acute respiratory distress syndrome (SARS) [198]. SARS-CoV-2 is primarily spread through person-to-person contact via the exchange of droplets from coughing and sneezing, however contamination of surfaces with these droplets can also lead to transmission. Studies have since suggested that asymptomatic patients could be responsible for high transmission and therefore there was and still is a requirement for rapid detection of SARS-CoV-2 the virus responsible of COVID-19 infection [199] [200].

The primary diagnostic tool that was employed for COVID-19 testing in the early stages of the pandemic, was reverse transcription polymerase chain reaction (RT-PCR), which can have good sensitivity and excellent specificity. Unfortunately, implementation costs and logistical problems with reagents during the global SARS-CoV-2 pandemic hindered its universal on-demand adoption. When cases were at their highest in the UK, RT-PCR was unable to keep up with high demand due to its relative expense and requirement for trained personnel and laboratory access [201].

Paper-based LFDs are an excellent candidate for POC rapid diagnostics. With sufficient sensitivity and specificity, they can provide results in 15-30 minutes and circumvent the need for the expensive and more complicated RT-PCR testing, which could be especially useful in low- and middle-income countries (LMICs) and at sites with high footfall and turnover such as at an airport and large venues. At the time of development, this was early on in the pandemic and only a small number of antigen-detecting LFDs for POC testing had been developed with limited sensitivity and clinical validation. Initially the only LFD tests for the detection of SARS-CoV-2 were in the form of serology tests which detect the presence of host antibodies in response to the viral infection. Although antibody-based testing could provide additional diagnostic capacity, antibody production by the body takes time and therefore these antibodies are not present in the early

stage of infection when diagnosis is crucial. In the case of SARS-CoV-2 infection, it was shown that the seroconversion time of IgG and IgM antibodies was achieved by 100% of patients within 20 days after symptom onset the median day of seroconversion for both IgG and IgM was 13 days post symptom onset [202-204]. Within this time, an infected individual could have already spread the disease further before they would give a positive test. One such test, VivaDiag IgM/IgG Rapid Test from QIAGEN, Germany, was assessed for use in the emergency department where patients were being admitted with flu-like symptoms and/or fever. Of the patients that were tested 38 patients were deemed positive for COVID-19 when tested with real-time RT-PCR. However, only seven showed a positive serology for IgM and/or IgG, which gives this serological test a sensitivity of 18.4% for the detection of SARS-Cov-2 in this diagnostic setting [205]. Additionally, once the vaccination programme had begun those who had received the vaccine had circulating antibodies against SARS-CoV-2 and it was no longer possible to differentiate active infection. Therefore, antibody-based serological assays/tests cannot assist with accurate and useful early disease diagnosis. This is particularly important for the SARS-CoV-2 outbreak as it is reported that transmission of the virus from one person to another occurs in the very early stages of the disease development [206].

Viral antigen detection could provide an alternative strategy to improve the volume and turnaround time of sample testing for early diagnosis of SARS-CoV-2 infection. The nucleocapsid protein (NP) is one of the predominantly expressed structural proteins and has previously been shown as a suitable target for early diagnostic detection in SARS-CoV-1 infection [207], which is genetically very similar to SARS-CoV-2 [208]. There are several viral proteins that could potentially be of significant use in diagnostics, however the NP was shown to be the superior antigen for early detection of SARS-CoV-1 as detection was possible up to 1 day before the onset of clinical symptoms occurred [209]. During the SARS-CoV-1 outbreak in 2004 similar antigen detecting ELISAs were previously developed with a LOD of 50 pg/ml indicating that an LFD with detection capabilities around this range would be clinically relevant. They also reported levels of NP in the patient sera from 100 pg/ml to 3.2 ng/ml, therefore there is the potential for use of an LFD to not only circumvent the need for expensive and molecular diagnostic expertise but also nasopharyngeal aspirate collection [210]. The spike glycoprotein (SP) is an alternative protein that could be used for diagnostics. It is anchored onto the virus envelope and is a protein made up two domains, S1 and S2 that interact with cell receptors allowing the virus to fuse to host cells. Some regions of the S-protein of SARS-CoV-2 such as S2 domain remain highly conserved despite the high selection pressure, and this means there is less chance of cross-reactivity with other viruses and the efficacy of the test is less likely to be affected by viral mutations. The S-protein is antigenic and therefore can be used for serological assays for diagnosis [204]. As seen in Figure

6.1, the (SP) is found on the viral cell surface unlike the NP which can only be accessed once the virus has been cleaved, making the (SP) easier for antibodies to bind and removes issues associated with access to the NP when viral cleavage may be incomplete.

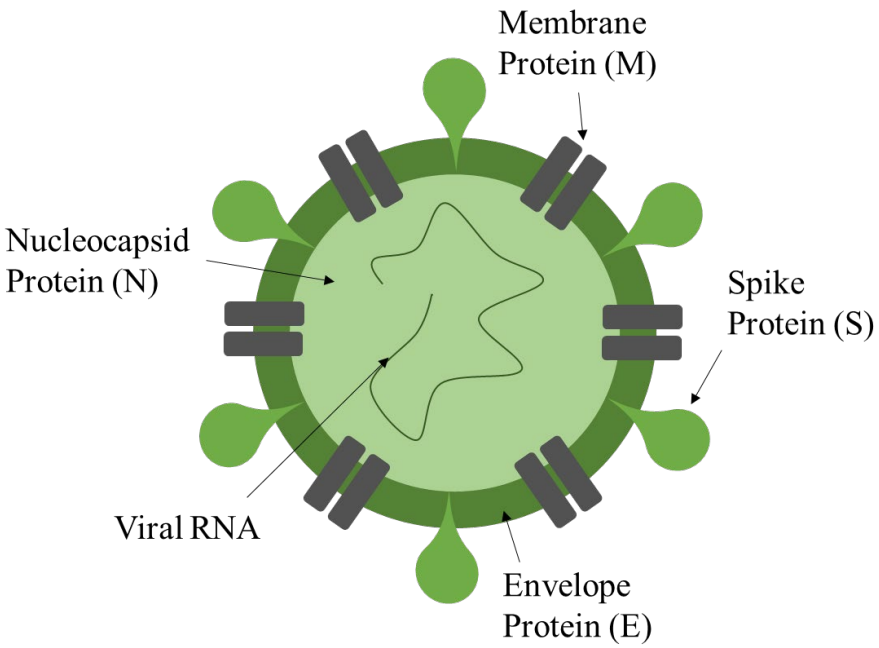

Figure 6.1 – Schematic of SARS-CoV-2 structure and its component parts.

A LFD test can provide an inexpensive solution to the problem of large population testing for diagnosis and population monitoring of SARS-CoV-2 infection. LFDs are already implemented for the diagnosis of other viral infections including dengue fever and foot and mouth disease [211, 212]. LFDs may provide reduced sensitivity when compared with RT-PCR however they can still be of huge clinical relevance.

This chapter presents the development of a half-strip LFD using commercially available antibodies for the detection of SARS-CoV-2. This dual channel multiplexed LFD detects both the SP and NP to ensure high sensitivity and specificity for SARS-CoV-2 testing. The test showed no cross-reactivity with other coronaviruses as well as a variety of other common respiratory organisms. The LOD in terms of $TCID_{50}$ quantifies the number of infectious virus particles in a sample. It is evaluated by adding serial dilutions of the virus containing samples to cells in a 96-well plate. The type of cell used is dependent on the virus and the cytopathic effects being observed. The cells are incubated with the virus particles and then the cells are inspected for any cytopathic effects, such as changes in cell morphology, and they are then classified as being infected with the virus or not, which can be done using visual or colorimetric readouts. The dilution of the virus for which 50% of the wells show infected cells is used to define the $TCID_{50}$ and the viral titre is then expressed as $TCID_{50}$/ml [213].

The half LFD format is frequently utilised as the first step in assay development before the full commercialisation. Such an LFD does not feature the sample or conjugate pad and so the sample and conjugate mixture are mixed in a 96-well plate before the LFD is introduced into wells of a plate. This creates a test with fewer variables for optimisation and facilitates rapid test development. The assay described herein provides an option to be used as a successful antigen test for detecting SARS-CoV-2 and with further development it could be quickly commercialised for production on the large scale.

6.2 Materials and Methodology

For the assay, a total of 18 commercial monoclonal antibodies from different suppliers were screened. The initial antibody screening was performed as in **Table** 2 – An example of an antibody testing matrix by trialling all possible antibody pairings and tested with a nucleocapsid protein-spiked sample at concentrations of 100 ng/ml and 50 ng/ml. The signal intensity from all antibody combinations were extracted and then based on the comparison, the best performing pair was selected for the further development and optimization work as shown in this chapter. The capture and detection antibodies selected were monoclonal mouse SARS-CoV-2 NP antibody (40143-MM08) and monoclonal rabbit SARS-CoV-2 NP antibody (40143-R004) from Sino Biological, China. The control line antibody was a donkey anti-rabbit IgG (D-301-C-ABS2) from R&D Systems. The gold conjugation kit used for tagging of the detection antibody was 80nm conjugation kit from Abcam (ab154876). The SARS-CoV-2 recombinant nucleocapsid protein and inactivated viral supernatant were obtained from the Faculty of Medicine at University of Southampton. Nucleocapsid proteins for other common human coronaviruses including HKU1, 229E, NL63 and OC43 were also provided by the Faculty of Medicine at University of Southampton. Recombinant MERS-CoV NP was obtained from Sino Biological, China (40068-V08B). For a more comprehensive cross-reactivity testing, the Respiratory Verification Panel 2 (NATRVP2-BIO) from ZeptoMetrix, US was used. Sodium tetraborate, Tween 20, Triton X 100, bovine serum albumin (BSA) and phosphate-buffered saline (PBS) were obtained from Sigma Aldrich, UK.

6.2.1 Device Fabrication

The antibodies for the test and control line were first deposited on the nitrocellulose membrane at concentrations of 1 mg/ml and 0.75 mg/ml respectively using a XYZ3210 dispense platform from Biodot (Irvine, CA, USA). The membrane was then left to dry at room temperature overnight. The detection antibody conjugation with gold nanoparticles was then performed using an Abcam conjugation kit as per the manufacture's protocol. After the conjugation, the gold-antibody

conjugate was blocked overnight with 40 mM borate and 3% BSA, pH 8.5. 0.5% Tween 20 in PBS was used for dilution of the conjugate as needed.

6.2.2 Assay Operation Protocol

For use with the 2 mm-wide LFD, 40 µl of sample (either antigen spiked in PBS or deactivated virus samples) and 1 µl of 1:2 diluted conjugate (10 OD NPs bound to antibody diluted in PBS) were used. The result was read after 20 minutes of dipping of the LFD into the mixture as per the methodology outlined in Chapter 3.

The buffer used for sample dilution and/or for both testing with recombinant nucleocapsid protein and inactivated virus was 1% Triton X 100 in PBS, which was used to better evaluate our test performance with all reagents that would be required for use in a clinical setting, where a lysis step is required for breaking apart the virus that makes the target antigen available for detection. The efficiency of the lysis step was evaluated and hence the 1% Triton X 100 in BSA was selected as the lysis buffer and 15 minutes as the time required for the lysis.

6.3 Results and Discussion

The initial testing was conducted using recombinant nucleocapsid protein spiked in different buffers. The purpose of this early phase development was to optimise the sample and conjugate volumes that would give the best sensitivity for the test. The test was then further evaluated using deactivated virus supernatant (SN) samples. Finally, a series of cross-reactivity checks were performed to show that the test had no lack of specificity or cross-reactivity problems.

6.3.1 Recombinant nucleocapsid protein testing

The first stage of the investigation was conducted with recombinant NP that was spiked into the samples. A stock recombinant nucleocapsid protein of 10^8 pg/ml was diluted in 1% Triton X 100 in PBS to a series concentration and run on the half LFD. The results are plotted in Figure 6.2, which shows the relationship between colour intensity of the test lines and the corresponding sample concentrations. This shows good correlation and therefore demonstrates that the LFD is able to distinguish different concentrations of the recombinant NP and it is unlikely there is a false positive or negative result occurring due to cross-reactivity with the reagents.

To analyse the results, the four-parameter dose response curve was generated in GraphPad Prism. Using the LOD equation described in section x non-linear regression was used to calculate

the interpolated concentration values that corresponded with the measured intensity and associated 95% confidence intervals were then calculated using GraphPad Prism. The limit of detection of the half LFD for recombinant protein is 25 pg/ml (95% CI of 20.44 pg/ml to 31.23 pg/ml).

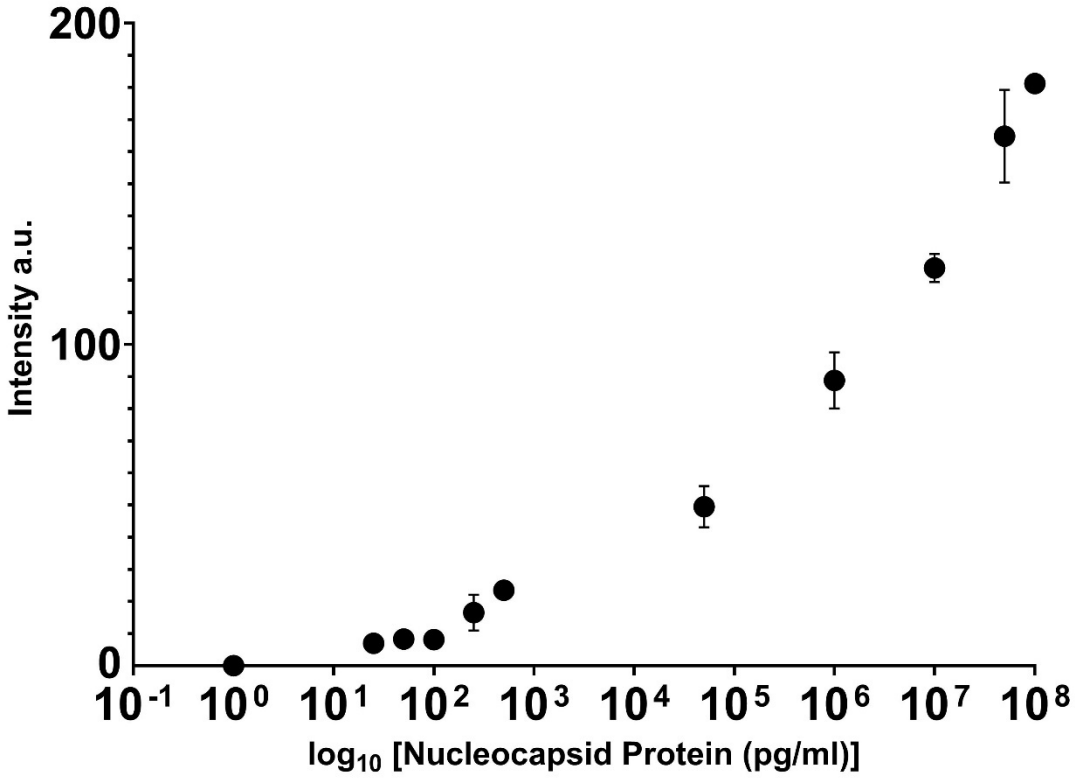

Figure 6.2 - Calibration curve plotting the mean intensity of the test line for samples with different concentration of recombinant NP spiked in 1% Triton X 100 in PBS; the error bars represent the standard deviation of the mean for five repeat measurements and the NP concentration has been plotted on a $\log_{10}$ scale to account for the large concentration range that was tested.

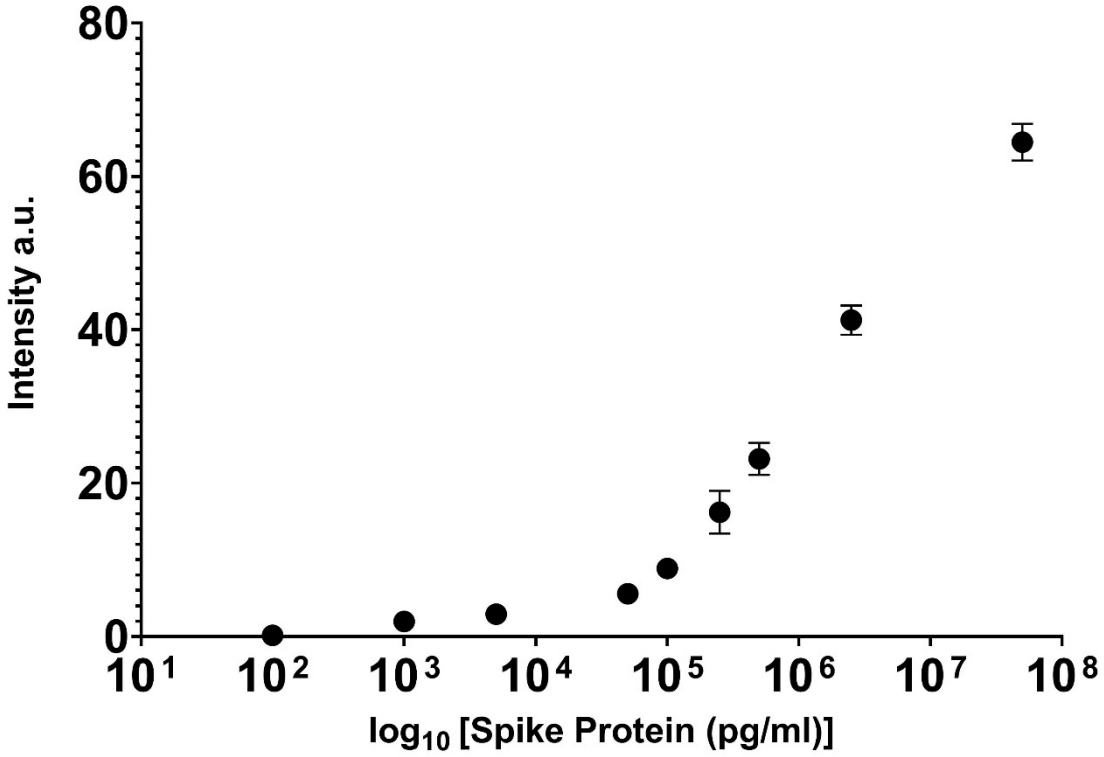

Figure 6.3 - Calibration curve plotting the mean intensity of the test line for samples with different concentration of recombinant SP spiked in 1% Triton X 100 in PBS; the error bars represent the standard deviation of the mean for five repeat measurements and the NP concentration has been plotted on a log10 scale to account for the large concentration range that was tested.

To analyse the results, the four-parameter dose response curve was generated in GraphPad Prism. Using the LOD equation described in section 3.5.1 non-linear regression was used to calculate the interpolated concentration values that corresponded with the measured intensity and associated 95% confidence intervals were then calculated using GraphPad Prism. The limit of detection of the half LFD for recombinant protein is 109.99 pg/ml (95% CI of 60.01 pg/ml to 159.87 pg/ml).

6.3.2 Inactivated virus testing

After the study with recombinant NC protein, inactivated virus was also used to evaluate the test's performance in a more clinically relevant way as the inactivated virus is what would be detected from patient samples. These evaluations have been done with three batches of

inactivated viral supernatants (SN) from three individual cultures. The stock concentration of these three SNs were $5.5x10^5$ (SN1), 1.8×10^6 (SN2) and 10^5 (SN3) PFU/ml respectively (PFU/ml =0.7 x $TCID_{50}$/ml) [213]. To perform the testing with these SNs, each SN was diluted in 1% Triton X 100 in PBS into different concentrations and left for 15 minutes at room temperature to allow the lysis reaction. These diluted SN samples were then used to perform the assay.

The results in Figure 6.4 show the test line colour intensity of individual LFDs for the detection of the SP and NP. The NP, shown in blue on the graph, has a much lower LOD than the SP as seen in green. The SP can only be detected at 500 $TCID_{50}$/ml whereas the NP can be detected down to 15 $TCID_{50}$/ml.

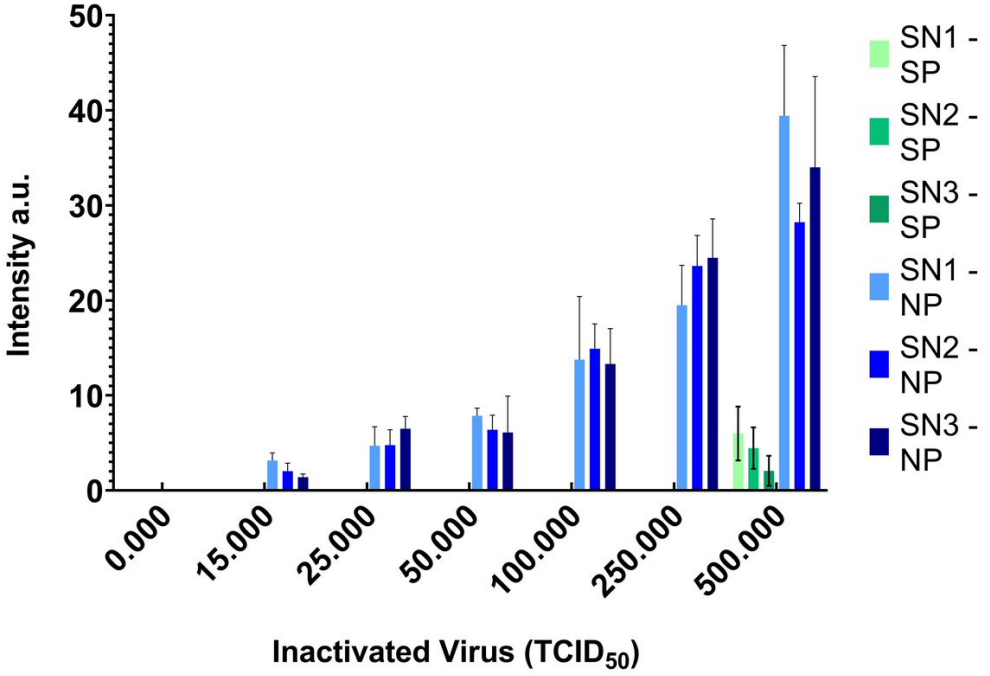

Figure 6.4 - Bar chart showing the test line colour intensity for different concentrations of deactivated virus (0 – 500 $TCID_{50}$) for spike protein as seen in green SN1 (light green), SN2 (medium green) and SN3 (dark green) and for nucleocapsid protein as seen in blue SN1 (light blue) SN2 (medium blue) SN3 (dark blue). Mean plotted with the upper and lower limits for five repeat measurements.

The LOD was calculated as per section 3.5.1. The LOD was calculated for each SN sample and for the detection of both the SP and NP and the results are summarised in Table 9.

Table 9 – Summary of LOD from inactivated virus testing for SN1, SN2 and SN3

Protein	Limit of detection ($TCID_{50}$/ml)		
	SN1	SN2	SN3
Nucleocapsid	10.13 (95% CI 6.94 – 38.35)	17.85 (95% CI 7.78 – 49.50)	11.00 (95% CI 8.43 – 45.31)
Spike	491.64 (95% CI 49.96 – 851.27)	515.13 (95% CI 42.36 – 856.33)	532.59 (95% CI 99.09 – 944.69)

6.3.3 Cross reactivity

To complete the evaluation, we have also performed a comprehensive cross-reactivity study of our half LFD to ensure that the test is specific for SARS-CoV-2.

6.3.4 Other coronaviruses (HKU1, 229E, NL63, OC43 and MERS)

Firstly, the half-strip LFDs were tested against NP proteins of other four common coronaviruses namely HKU1, 229E, NL63, OC43, as well as MERS. For these experiments, different recombinant NPs were diluted in 1% Triton-X 100 in PBS at 0 ng/ml, 10 ng/ml, 100 ng/ml and 500 ng/ml and tested using the half LFDs. As shown in Figure 6.5, the test shows no cross- reaction with any of the NP for concentration up to 500 ng/ml.

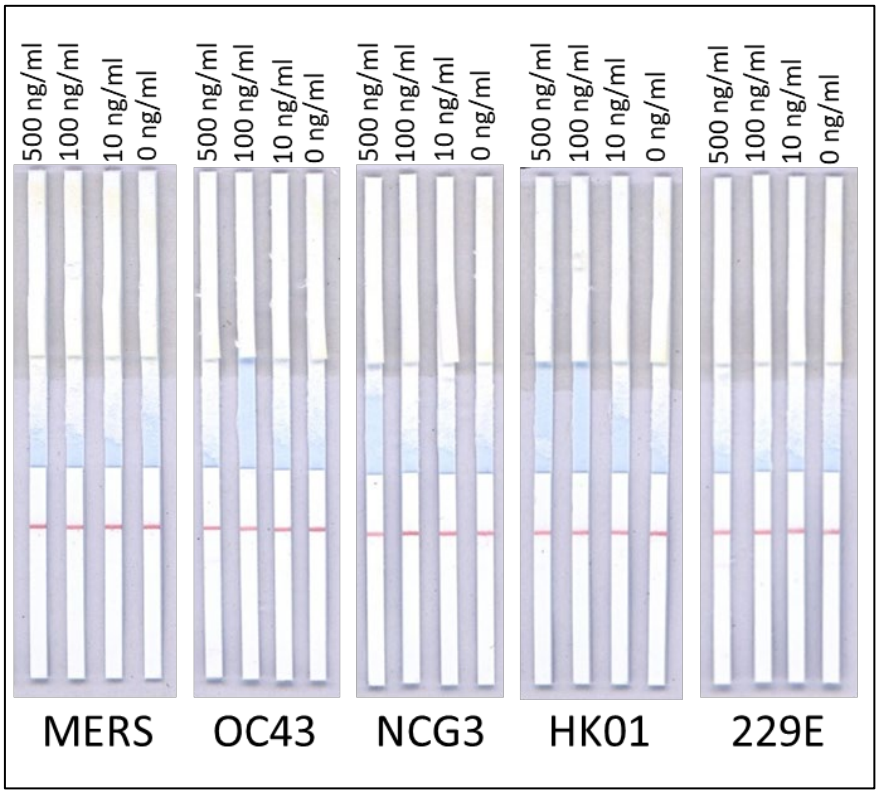

Figure 6.5 – Images of half LFDs tested to evaluate their cross-reactivity with MERS, OC43, NCG3, HK01 and 229E at concentrations of 0 ng/ml, 10 ng/ml, 100 ng/ml and 500 ng/ml. As clearly shown in the non-appearance of test lines in each case there is no cross reactivity to other coronaviruses for the nucleocapsid protein.

6.3.5 Respiratory Panel

To further complete the performance evaluation of our half-strip LFDs, a cross-reactivity check was also performed with a respiratory verification panel from ZeptoMetrix that included a total of 22 viral and bacterial NATtrol™ (Nucleic Acid Testing Control) targets. The results show no cross-reaction with any of the organisms at their stock concentration, a summary of the results can be seen in Table 10.

Table 10 – Summary of respiratory panel testing

Name of the organism	Result	Name of the organism	Result
B. pertussis A639	Neg	Parainfluenza Type 4	Neg
B. parapertussis A747	Neg	RSV Type A2	Neg
C. pneumoniae CWL-029	Neg	Adenovirus Type 1	Neg
M. pneumoniae M129	Neg	Adenovirus Type 3	Neg
Coronavirus HKU-1 Recombinant	Neg	Adenovirus Type 31	Neg
Coronavirus NL63	Neg	Influenza A H1 A/New Cal/20/99	Neg
Coronavirus OC43	Neg	Influenza A H3 N2 A/Brisbane/10/07	Neg
Coronavirus 229E	Neg	Influenza A 2009 H1N1pdm A/NY/02/2009**	Neg
Human Metapneumovirus Type 8 Peru6-2003	Neg	Influenza B B/Florida/02/06	Neg
Rhinovirus Type 1A	Neg	Parainfluenza Type 1	Neg

6.3.6 Dual channel LFD

The final stage of development was to combine these two individual half-strip LFDs into a single dual channel half-strip LFD that simultaneously detects SP and NP within a single sample. The results from this testing can be seen via the image of representative LFDs shown in Figure 6.6 below. Each channel works independently of each other with no movement of sample from one channel to the next. From the image the LOD can be obtained by visual assessment.

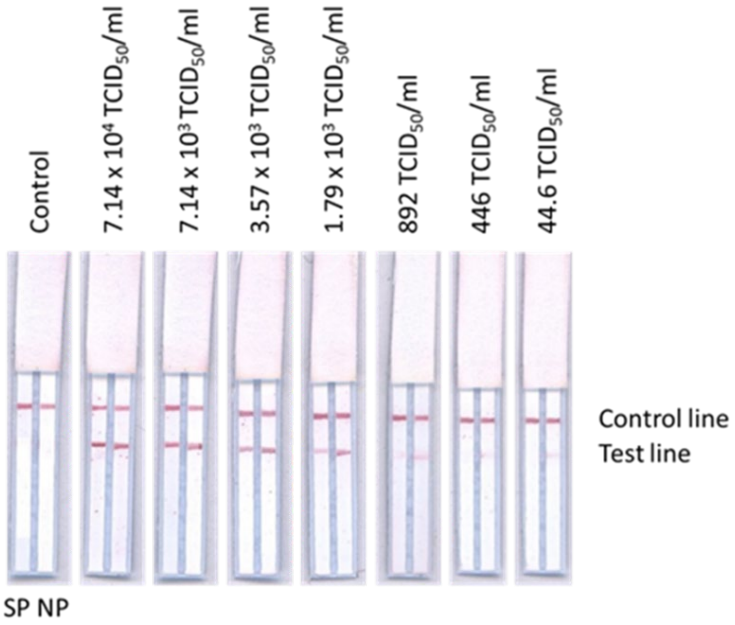

Figure 6.6 - Scanned images of dual channel half-strip LFDs tested using samples with seven different $TCID_{50}$/ml concentrations. The LOD as determined by visual assessment, and these were 44.6 $TCID_{50}$/ml and: 892 $TCID_{50}$/ml for the NP and the SP respectively.

The quantitative results of the test line colour intensity that were extracted using the reader can be seen plotted in Figure 6.7. As can seen from the dual channel device compared to the individual LFDs, the LOD is lower, this is likely due to some of the conjugate from one antibody being drawn into the wrong flow path and therefore the signal is slightly reduced. This could be over-come in the future by adding further conjugate to the system or by the addition of the conjugate pad and patterning it so ensure that the conjugate remains in its corresponding channel as discussed in Chapter 5.

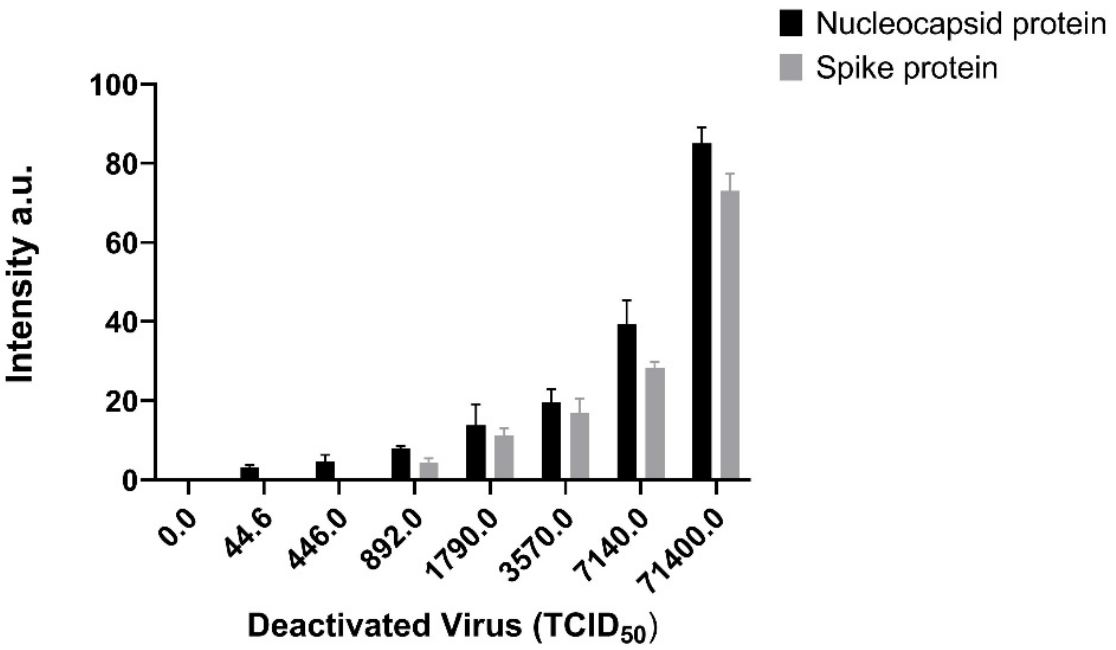

Figure 6.7 - Graph showing test line colour intensity results for the half-strip LFDs tested with deactivated virus at 7 different concentrations from 44.6 $TCID_{50}$ - 71400 $TCID_{50}$/ml for both NP (black bars) and SP (grey bars). Error bars show SD for 5 measurements.

The NP has higher sensitivity for the detection of the coronavirus and can therefore be detected in much lower viral titres, down to 44.6 $TCID_{50}$/ml unlike the SP which can only be detected down to a level of 892 $TCID_{50}$/ml. As can be seen in the scanned image above, the signal for SP at this level is incredibly weak and cannot guarantee correct interpretation, especially if the test is being used by untrained personnel such as members of the public.

6.4 Conclusions

In this chapter a half test LFD was presented for the detection of both the NP and the SP of SARS-CoV-2. It has been demonstrated that the test has high sensitivity for both sample types – samples with the proteins spiked in a buffer as well as the sample within deactivated virus. The LFD showed an extremely low LOD of 25.00 pg/mL for the NP with recombinant protein and 10.44 $TCID_{50}$/ml with inactivated virus. The test has also demonstrated great specificity for SARS-CoV-2 that has shown no cross-reaction with other coronaviruses as well as other common respiratory organisms. Despite this, the low LOD was largely achieved using the NP and there was no necessity shown here for the use of the spike protein, however it demonstrated the usefulness of the dual channel LFD and the future application of this technology. The next step would have been to carry out clinical validation and further commercialisation of this test, however, the availability to scale up the manufacture of this test in time for validation within the timescale of

the pandemic was restricted to companies that already had established infrastructure and the capability to produce their own antibodies. Therefore, it was not commercially viable to pursue this test any further for this specific application, but it showed promise for use in the future.

Chapter 7 Alzheimer's Disease

7.1 Introduction

Alzheimer's Disease (AD) is characterized by the irreversible progressive decline of cognitive function, affecting memory and thinking that eventually leads to the inability to conduct everyday tasks. It is the most common form of dementia world-wide and in most people, symptoms will begin to appear in the mid-60s [214]. It is estimated, that as of 2019, 40 million people in the world have AD and due to increasing life expectancy this is only expected to rise [214]. Without early detection and disease-altering therapies AD will pose a significant problem to global health and welfare.

It has been established that the accumulation of Amyloid β (Aβ) deposits within the neural tissue leads to the pathogenesis of Alzheimer's disease [215]. These Aβ oligomers accumulate leading to hyperphosphorylation of tau proteins. This in turn triggers production of neurofibrillary tangles, neurotoxicity and ultimately cognitive dysfunction [216].

Currently, the only validated methods for the identification of amyloid-β deposition in the brain to characterise the pathology of Alzheimer's disease, are amyloid-β positron-emission tomography (PET) imaging or measurement of amyloid-β in cerebrospinal fluid (CSF). Although this is one of the earliest signs of AD, it stagnates as the disease progresses, and therefore is not suitable as a marker for monitoring disease progression. Additionally, the measurement of tau protein accumulation using PET radiotracers has shown promising results to date but has not been widely validated [217]. As the current methods are insufficient, a minimally invasive, cost-effective blood-based biomarker test, if available, will highlight the presence of AD pathology in the earliest stages and provide a method for monitoring the disease progression [218].

It was recently discovered that the levels of amyloid β (specifically three peptides, Aβ1-38, Aβ1-40 and Aβ1-42) could be measured in patients' serum [219] and this would negate the requirement for use of CSF. For our current lateral flow testing platform, serum is an ideal sample medium meaning we can measure the presence/levels of peptides in the blood. The identification of this marker can be seen up to 20 years prior to the onset of clinical symptoms of cognitive decline [220] so a quick screening test that could be rolled out on a large scale would be hugely beneficial.

Both Aβ and tau protein have shown prognostic potential as they are able to distinguish subjects with mild cognitive impairment (MCI) who progressed to AD from those who did not [219, 221, 222]; however, to measure these markers requires analysis of CSF. The lumbar puncture, which is the procedure whereby CSF is collected is considered to be highly invasive in some countries and there is a negative perception of the procedure which affects patient compliance [223, 224]. There is also a risk that sampling multiple times in order to monitor the disease onset or treatment can impact the levels of these biomarkers [225]. It is crucial to identify patients that have a high probability of disease progression as early as possible to ensure that treatments can be commenced before the damage to the neurones becomes too severe [226].

Data has shown that the pathology precedes the onset of clinical symptoms by years, and clinical outcomes show significant variation [227]. It is, therefore, the ambition of the clinical community, to establish blood-based markers of microvascular pathology that can be measured in plasma or serum that could provide a more clinically accessible tool for initial population screening, for early prediction and detection of the disease as well as ongoing monitoring of AD progression [228].

The biggest challenge to identifying biomarkers is their correlation with the progression of the disease. In addition to help with disease monitoring, the identification of these markers could also lead to advances in disease-modifying treatments that are desperately sought after. There is therefore a pressing need for inexpensive and minimally invasive biomarker tests that can be used for serial measurements that could provide a cost- and time-effective method of identification and monitoring of disease progression [228].

The devlopemnt of AD is a complex and multifaceted process that is thought to also involve chronic inflammation caused by bacterial infections [229-234]. Research in this area is growing and suggests that bacteria may play a role in the initiation of inflammaotry cascases of the central nervous system by activation of pro-inflammatory cytokines and cell death as seen in Figure 7.1. These infections as seen in tooth decay [235] could be a risk factor for the cognitive changes seen in AD. This is an important finding and reinforces the need to measure inflammatory markers for potential indicator of AD development.

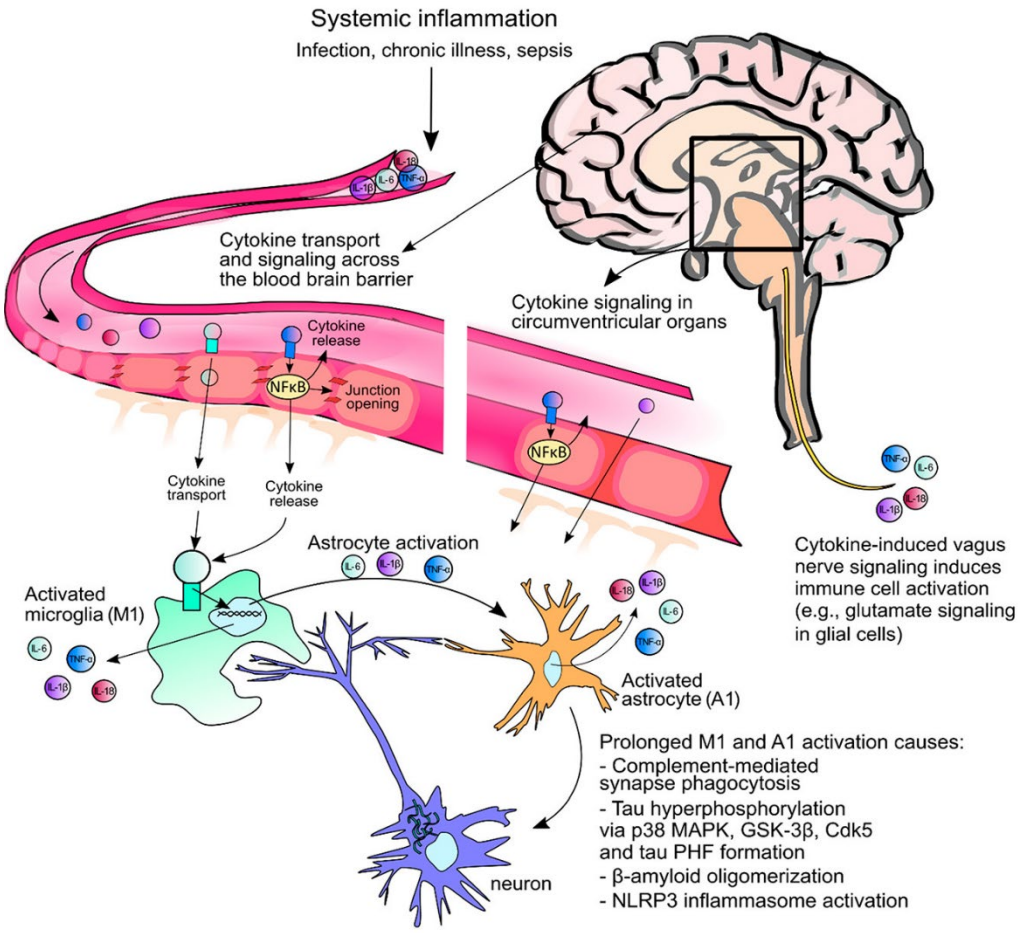

Figure 7.1 – Schematic showing the pathways leading from systemic inflammation to the induction of Alzheimer's-specific pathways [234].

Intercellular adhesion molecule 1 (ICAM-1) and vascular cell adhesion molecule 1 (VCAM-1) are endothelial CAMs that are a part of the immunoglobulin (Ig) family. They play a crucial role in the adhesion of leukocytes (white blood cells) to the surface of endothelial cells during inflammation both acute and chronic [236, 237]. Vascular adhesion protein-1 (VAP-1) is another inflammation-induced molecule that mediates the entry of leukocytes to points of inflammation [238].

There is growing evidence that serum levels of vascular markers ICAM-1 and VCAM-1 correlate with AD and provide potential for use as an early screening blood-based biomarkers [239-241]. In addition, VAP-1 also referred to as semicarbazide-sensitive amine oxidase (SSAO), has shown importance in the pathology of Alzheimer's disease and its inhibition leads to anti-inflammatory benefits which could provide a treatment of dopamine neuron dysfunction caused by acute inflammation in the brain [242].

Therefore, in this study is presented the use of microfluidic devices created on a low-cost paper platform for multiple rapid immunoassays for the detection of ICAM-1, VCAM-1 and VAP-1 for the screening and monitoring of disease progression of dementia.

7.2 Materials and Methods

This work was conducted in collaboration with partners at the Faculty of Medicine of the University of Southampton. They collected the patient samples and processed them for quantification of the inflammatory markers CRP, SAA1, VCAM-1 and ICAM-1.

7.2.1 Work conducted by the Faculty of Medicine, University of Southampton

Human serum samples collected via two cohorts were centrifuged, aliquoted and stored at -80°C.

To measure the inflammation and vascular marker levels, ELISAs were used to detect antibodies in serum samples from a study cohort:

- PERINFLAM – patients with mild or moderate AD with or without active periodontitis, to correlate inflammatory markers with cognitive decline and periodontitis

The PERINFLAM cohort was made up of patients with mild or moderate AD with or without active periodontitis, to correlate inflammatory markers with cognitive decline and periodontitis. consisted of 50 non-smoking individuals, all over 65 years-old, diagnosed with mild to moderate AD. Patients either did or did not have periodontitis that had been untreated for at least 6 months at the time of blood sampling. Cognitive state was measured with the Alzheimer's Disease Assessment Scale-Cognitive Subscale (ADAS-Cog) and the standardised Mini-Mental State Examination (sMMSE) immediately before blood sampling for baseline, and a 6 months time-point. Participants fully consented in compliance to the UK Medical Research Council guidance https://mrc.ukri.org/documents/pdf/medical-research-involving-adults-who-cannot-consent/. Ethics were approved by National Research Ethics Service (NRES) Committee South Central – Southampton B (11/SC/0422).

7.2.2 Mesoscale multiplex system for CRP, SAA, ICAM-1 and VCAM-1

The MSD® MULTI-SPOT Assay System - V-PLEX Vascular Injury Panel 2 Human Kit (Meso Scale Diagnostics, Rockville, Maryland, USA) was used following manufacturer's instructions with the contents provided to measure CRP, SAA, sICAM-1, and sVCAM-1 serum concentrations simultaneously. This technology combines electrochemiluminescence and microarrays in combination with MULTI-SPOT plates, for precise quantitation of multiple analytes in a single sample requiring less time and effort than other assay platforms. The plate was washed three times with wash buffer prior to the addition of 25 µl diluted human serum (1:1000) or calibrator dilution to individual wells, then incubated for 2 hours at 600 rpm. Wells were washed three times with wash buffer, and 25 µl detection antibody solution was added to each well and

incubated at 600 rpm for 1 hour. Wells were washed three times with wash buffer, and 150 µl of read buffer was added to each well. Protein concentrations were directly measured using the MSD® QuickPlex SQ 120 plate reader.

7.2.3 Development of the LFD and assay implementation

The capture antibodies for the test and control lines were first deposited on the nitrocellulose membrane at concentrations of 1 mg/ml and 0.5 mg/ml respectively using a XYZ3210 dispense platform from Biodot (Irvine, CA, USA). The test and control lines were located at 14 mm and 18 mm from the upstream edge of the nitrocellulose membrane. The membrane was then left to dry at room temperature overnight.

Antibodies for the amyloid β assay, detection: Biotin anti-β-Amyloid, 17-24 Antibody (800704) was obtained from BioLegend, CA, USA. Capture antibody 3D6mf2a produced by the FoM. Peptide standards: Aβ1-42 (C01LB-2), Aβ1-40 (C00OA-2) and Aβ1-38 (C00NZ-2) obtained from MSD, London, UK.

The antibodies used for the VCAM assay were from the Human VCAM-1/CD106 DuoSet ELISA kit from R&D systems, the control line was anti-sheep IgG antibody from R&D systems. Capture antibody used at 1 mg/ml, detection used at 12 µg/ml (5 µl of AuNPs + 5 µl of detection antibody added to the test) with 5 µl of sample added. The antibodies used for the ICAM-1 assay were from the Human ICAM-1/CD54 DuoSet ELISA kit from R&D systems. Capture antibody used at 1 mg/ml, detection used at 12 µg/ml (5 µl of AuNPs + 5 µl of detection antibody added to the test) with 5 µl of sample added. The antibodies used for the VAP-1 assay were Human VAP-1 Antibody Pair - BSA and Azide free (ab256639) obtained from Abcam. The AuNPs used were Streptavidin Gold Conjugate (40nm, 10 OD) (ab186864) from Abcam, UK.

For quantitative accurate analysis, the intensity of the test line was measured using a scanner (Epson Perfection V800 Photo A4 Flatbed Scanner). The scanned images were then processed with the ImageJ software (National Institutes of Health, USA) to extract the respective red colour intensity produced at the test lines. Using the RGB function of the program the mean colour intensity of the pixels of the test line was measured and the colour intensity value for the test line of the control LFD (for a control sample the area where the test line would be should it have appeared) was subtracted from the value to account for any background colour on the LFD.

7.2.4 Testing the LFDs

For the Aβ assay the half LFD was used. A single LFD format was used, with the same capture and detection antibodies to test all isomers. The isomers were spiked into PBS in a range of concentrations and tested individually.

For the patient sample testing procedure, the human samples were thawed at room temperature and agitated before use. A single LFD was used for each patient sample, for each marker being tested (each sample was tested four times).

7.3 Results

The first step that was investigated as part of this experimentation was the use of a LFD for the detection of amyloid-β as the link between AD and Aβ levels is well documented in the literature. This was followed by the development of individual LFDs for a panel of vascular markers that have been investigated by collaborators at the Faculty of Medicine in Southampton.

7.3.1 Amyloid-β

Amyloid-β occurs in different isoforms and it is also thought that the ratios between these different isoforms is significant for diagnosis and severity of AD. Herein LFDs were developed for the detection of three different isoforms 38, 40 and 42 of Amyloid-β. The concentrations of Aβ that are typically found in the plasma of patients is very low of 288.0 pg/ml, 272.4 pg/ml and 30.13 pg/ml for Aβ38, Aβ40 and Aβ42 respectively [219]. As the LFD platform did not provide sensitivity down to this level and therefore the detection of amyloid-β was deemed to be more suited to higher sensitivity testing rather than the POC alternative. It was then decided to investigate the detection of the inflammatory markers CRP, SAA1, ICAM-1 and VCAM-1 instead as these were found in a more suitable concentration ranges that would allow their detection using a LFD.

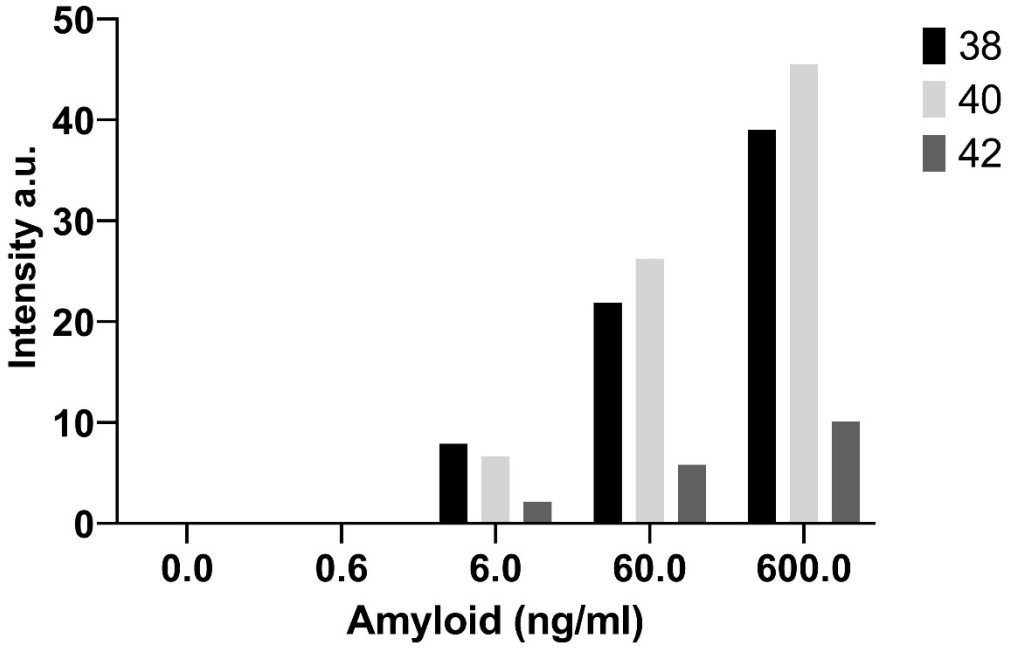

Figure 7.2 – Graph showing the test line colour intensity for three concentrations of amyloid-β for individual LFDs for three different isomers (Aβ38, Aβ40 and Aβ42).

The sensitivity of the LFD was not particularly high as can be seen in Figure 7.2, the lowest concentration that shows a visible test line for all three isomers is 6 ng/ml. The concentrations of Aβ-42 in the CSF range from ~600 pg/ml for cognitive normal and ~300 pg/ml for AD and these concentrations would be even lower for blood [243], therefore the sensitivity seen here would be insufficient for the detection of Aβ for clinical use. This could have been due to the antibodies used however and in order to enhance this LFD's sensitivity a constriction was added to the flow path. Additionally, Aβ aggregates which leads to the characteristic accumulation of plaques in the brain and in this aggregated state, it could be potentially easier to visualise on the LFD however the state of the amyloid here is unknown in terms of aggregation status.

In an attempt to improve the sensitivity of the devices a constriction was added to the flow path and contained the test line, which was previously published by the team [9] and is described in greater detail in Chapter 8. The constriction allows for a larger number of detection antibodies to bind, per unit area, of the test line creating a darker test line which can allow for visualisation of the lower concentrations. The results for the three Aβ isomers with a constriction can be seen in Figure 7.3.

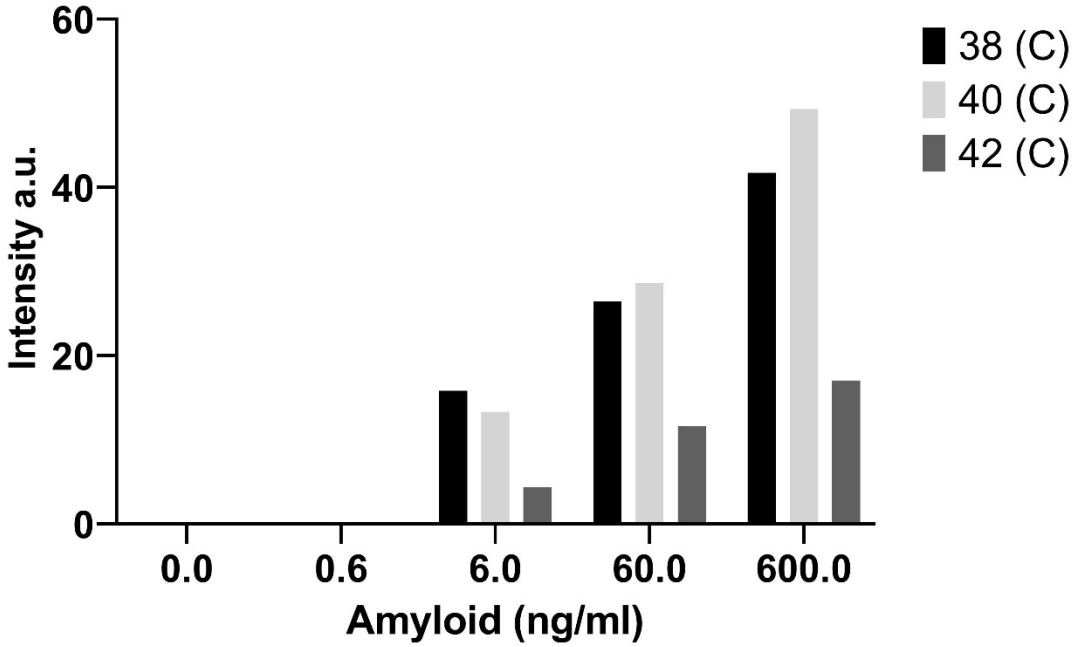

Figure 7.3 - Graph showing the test line colour intensity for three concentrations of amyloid-β for individual LFDs with a constriction for three different isomers (38, 40 and 42).

Although the constriction shows a small increase in sensitivity it is unlikely that this would be sufficient to a) measure the concentrations of Aβ in CSF or blood and b) distinguish levels between cognitively normal (CN) and AD. Therefore, it was again decided to move the focus to the detection of inflammatory markers VCAM-1, ICAM-1 and VAP-1.

7.3.2 Vascular markers

The next investigation was developing individual LFDs for the vascular markers VCAM-1, ICAM-1 and VAP-1.

Our collaborating staff at the Faculty of Medicine at the University of Southampton, investigated the link between vascular injury, periodontitis and cognitive decline. To do this, a MESOSCALE multiplex system was used to simultaneously measure the concentrations of four vascular injury markers (CRP, SAA1, ICAM-1, and VCAM-1) in the serum samples of patients from the PERINFLAM cohort. CRP, SAA1, sICAM-1, and sVCAM1 were all significantly associated with each other in this cohort and the levels SAA1, ICAM-1, and VCAM-1 showed a negative correlation with cognitive decline. CRP positively correlated with antibody titres against two bacterial species that are associated with gum disease (P. gingivalis and T. denticola) [244].

In addition to these markers, an LFD was also developed for the detection of VAP-1.

7.3.3 Testing with analytes spiked in PBS

Initially the LFDs were tested using in PBS spiked with the analytes to produce calibration curves, and evaluate the detection capabilities and limit of detection (LOD) for each vascular marker; VCAM-1, ICAM-1 and VAP-1. The testing was conducted as described in section 3.4.1.

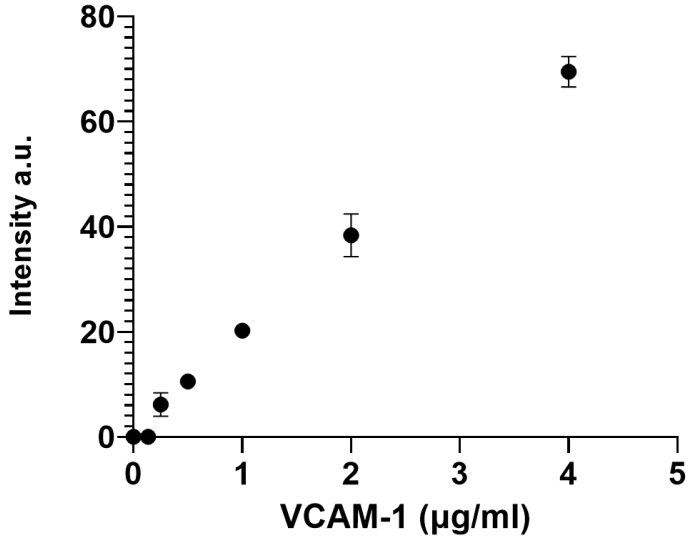

Figure 7.4 - Calibration curve of VCAM-1 spiked in PBS using a range of concentrations from 0 – 4 µg/ml. The mean is plotted with error bars showing standard deviation of the mean from three repeat measurements.

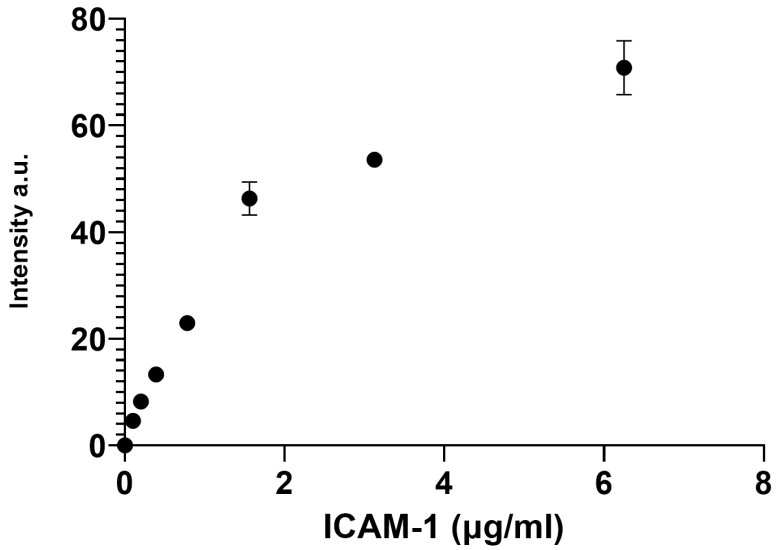

Figure 7.5 - Calibration curve of ICAM-1 spiked in PBS using a range of concentrations from 0 – 6.25 µg/ml the mean is plotted with error bars showing standard deviation of the mean from three repeat measurements.

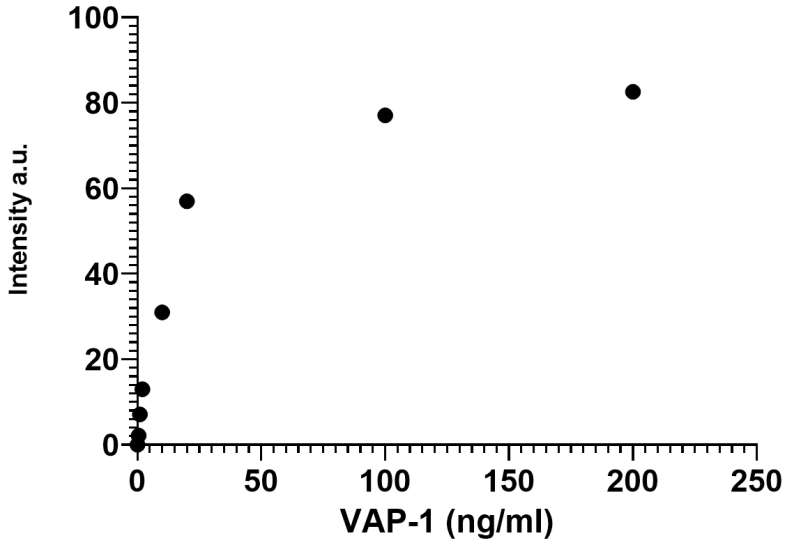

Figure 7.6 - Calibration curve of VAP-1 spiked in PBS using a range of concentrations from 0 – 200 ng/ml the mean is plotted with error bars showing standard deviation of the mean from three repeat measurements.

The calibration curves established the detection range for the assay, and it was decided that these met the required concentrations that would be measurable in patient samples and therefore the assays were carried forward for further testing using patient samples.

7.3.4 Testing with patient samples

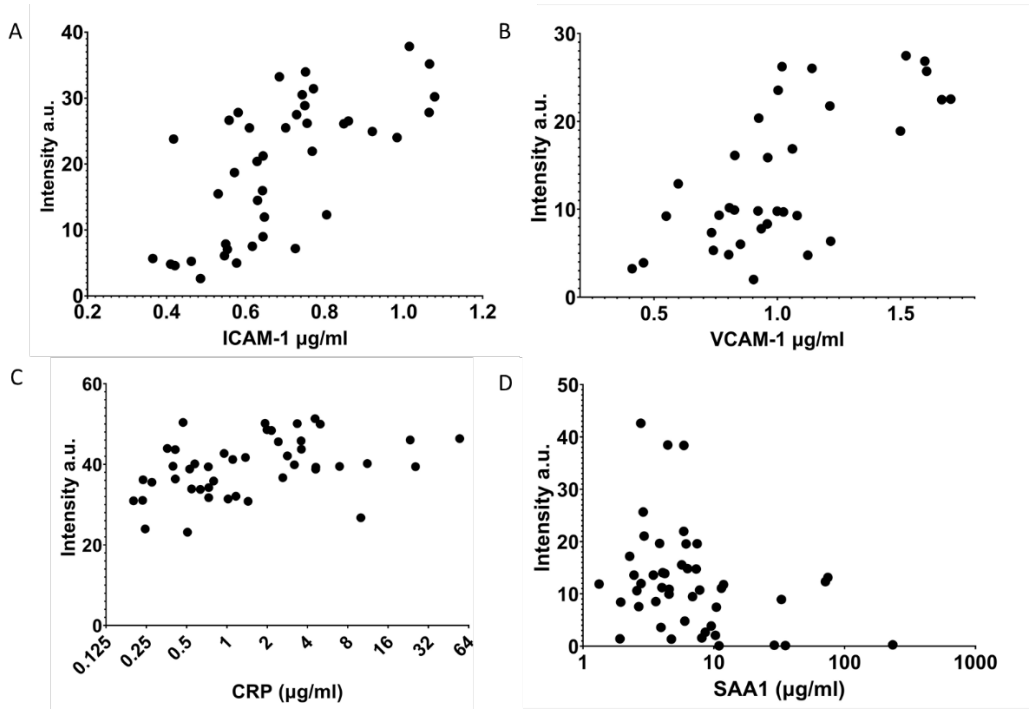

Figure 7.7 – Graphs showing the test line colour intensity obtained from the LFD for each patient sample for A) ICAM-1 and B) VCAM-1 C) CRP and D) SAA1. Concentrations were obtained from the MESOSCALE plate.

The quantitative results obtained from the MESOSCALE plate were plotted against the test line colour intensity for the LFD for each of the samples tested for VCAM-1, ICAM-1, CRP and SAA1 for the PERINFLAM cohort can be seen in Figure 7.7. An r value equal to 1 indicates perfect correlation with the points, and the value decreases as the association weakens. An r value above 0.7 is generally considered to be strong correlation and the above evaluated values that are close to 0.7 would suggest a good correlation. The P value, however, denotes if that corelation is statistically significant and the results of the statistical analysis can be seen in Table 11. There is a visible positive correlation trend shown in Figure 7.7 with the data showing that the intensity does increase as the concentration of the analyte increases for ICAM-1 and VCAM-1, however there are some patient data points that show a higher concentration and lower intensity. For CRP the r value was 0.4541 which shows some positive correlation however this is not a strong link and a P value of 0.0032 which shows statistical significance even if the correlation is weaker. For SAA1 however, as can be seen from the graph 7.7D, there is no correlation between the concentration obtained from the MESOSCALE and that for the test line intensity obtained from the LFD, statistical analysis suggests a negative correlation, but it is likely that there is no clear relationship between the measurements for this marker.

Table 11 – Results of Spearman correlation analysis

MARKER	R VALUE	P VALUE
ICAM-1	0.6755	<0.0001 (****)
VCAM-1	0.6932	<0.0001 (****)
CRP	0.4541	0.0032 (**)
SAA1	-0.3393	0.0211 (*)

Previously the individual LFDs were trialled and optimised with the range of concentrations that have been tested with the patient samples and therefore the Hook effect is unlikely to be the source of this irregularity. One possible reason is the samples were tested using the Mesoscale assay were frozen and then thawed at a later time for measurement with the LFDs and this could have disrupted the integrity of the markers leading to a weakened intensity on the LFD compared to the previous Mesoscale assay measurements.

7.4 Discussion

Dementia, more specifically Alzheimer's disease is growing and with increasing life expectancy this is not going to slow down. Current diagnostic methods rely largely on the on-set of symptoms as a trigger for investigation, unfortunately that means that cognitive damage has already occurred. Therefore, an early screening and monitoring test could be used to highlight those individuals that are at high risk due to the presence of chronic inflammation. This would allow for timely commencement of treatment and therapy to ultimately improve the patient's quality of life and as treatments become more readily available could assist in the eradication of the disease. There is extensive evidence to support the use of Aβ in its various isoforms as a diagnostic marker for AD however in the context of the LFD platform the sensitivity was shown to be insufficient in this case although the detection of all three isoforms on separate LFDs was successfully demonstrated and this does give potential for further enhancement in the future.

The detection of vascular markers was very successful on the LFD platform when using spiked PBS in the preliminary investigation. The concentrations of the markers had been measured and quantified using an ELISA at a previous time, the same patient samples were used to measure the vascular markers using the LFD platform. When the results obtained from the LFDs was compared to those from the ELISA there was a weak correlation for ICAM-1 and VCAM-1 but the results for CRP and SAA1 were mixed. As the results were collected by different operators at different times there is a possibility that during the knowledge transfer process these results became obscured and therefore it is impossible to draw any real conclusions from the work conducted using the patient samples. However inconclusive, there is the potential for these markers to constitute a panel that could be used for screening and monitoring of AD and therefore it was the ambition to repeat these measurements however due to the time constraints of the project this was not possible.

Chapter 8 Geometric flow control

8.1 Introduction

Although there has been significant research aimed at developing LFDs with enhanced performance, showing both increased sensitivity and lowered LOD, their optimization has largely been directed towards improvements and modifications of the biochemistry of the assay, use of membranes with different porosity, and the antibody labelling system, rather than specific attention to local flow control. The conventional LFD design has not evolved for many years and in this traditional configuration the flow rate of the LFD is defined largely by the membrane porosity and cross-sections of the membrane indicate that the analyte in the sample will spend a matter of seconds at the test line which leaves little time for binding of the analyte to the capture antibody. Another alternative would be to increase the capture antibody concentration, but this means that the cost becomes correspondingly higher [245]. The efficiency of all such modifications remains limited by the basic unaltered architecture of the LFD and there is, therefore, a real need to identify fundamental architectural modifications that enhance both the LFD sensitivity and LOD and also keep the modifications minimal to therefore introduce further complications at the time of manufacture.

The work carried out in this area to date has addressed several strategies that alter the architecture of the standard LFD to increase sensitivity. These can broadly be divided into the three following categories:

1. Narrowing of the flow path
2. Introducing obstructions to the flow path
3. Modifications to the sample or conjugate pad generally by the addition of further membranes

Narrowing of the flow path

Narrowing the flow path, or more specifically part of the flow path that contains the test line, can have an effect that is two-fold. In the first instance modifying the flow path can alter the flow front velocity such that there is an increased time for the assay components to bind to increase the sensitivity of the device and this can be achieved via several methods. These include laser ablation [8] and deposition of polymer barriers into the membrane [9] tapering the device or

simply cutting the nitrocellulose membrane [246, 247]. Eriksson et al demonstrated a comprehensive exploration of flow control parameters including the width, length, and the input and output angles of a narrowing constriction.

Introducing obstructions to the flow path

The addition of in-line barriers that introduce an obstruction to the flow can help to reduce the flow rate and increase the sensitivity of the test. Rivas et al has reported the use of wax-printed pillars in the flow path to slow the flow and enhance the test's sensitivity [33]. However, wax printing has its drawbacks and there have been other methods demonstrated such as a strategy involving incorporating a paper-based shunt accompanied by a polydimethylsiloxane (PDMS) barrier to the flow path that can achieve optimum fluidic delays and therefore signal enhancement, resulting in 10-fold signal enhancement over an unmodified LFD [248]. The same group also report a strategy to create a hybrid substrate by incorporating agarose into the test strip to achieve flow control that allows for optimal biomolecule interactions [211].

Modifications to the sample or conjugate pad

Alternative methods for the performance enhancement of a standard LFD are the modification of the sample or the membranes in some form [246, 249]. The use of aqueous two-phase systems (ATPSs) can be used to enhance LFD detection, whereby the sample is concentrated by the integration of a polyethylene glycol–potassium phosphate ATPS at the front of the device. This can be used to improve sensitivity for low concentration biomarkers [250]. Additionally, paper pumps can be used to control the flow rate of the sample within the membrane, they require modification to the flow path and are currently limited by the speed they can achieve due to the geometry and size of the devices [249].

A "stacking pad" configuration can also be used that adds an additional membrane between the conjugation pad and test pad. The effect is the accumulation of the antibody and antigen on the stacking pad and thereby extension of the time that the analyte and antibody have to interact and bind to enhance the detection sensitivity [251]. This group have taken this concept further to create a multiplexed detection LFD with the "stacking pad" enhanced sensitivity [56].

The work reported here builds upon the previous work carried out by the team at the ORC, which explored the use of a narrowing constriction within the flow path to control the flow and subsequently improve the sensitivity of the test [9]. This work now reports, a more comprehensive exploration of the parameters that affect the sensitivity of the device to further optimize the use of a single constriction as well as building on this to the use of multiple constrictions within the flow path of the LFD. These constrictions are constructed via the precise

laser-patterning as outlined in section 3.1. The patterning of the NC membrane to produce a high-sensitivity LFD is demonstrated by its implementation of the immunoassay for the detection of procalcitonin (PCT). PCT is an inflammatory marker that can be used for differentiating between bacterial and viral infections, making it a useful triage marker to guide the initiation and duration of antibiotic treatment. PCT has been approved by the US FDA for antimicrobial stewardship in the context of suspected sepsis as timely diagnosis and treatment is crucial for patient survival [121-124]. PCT can be measured in healthy patient serum with a range from <0.1 ng/mL to 0.5 ng/mL; [120] increasing above 0.5 ng/mL during systemic infection; levels of PCT above 0.5 ng/mL indicate that bacterial infection is very likely [122, 125]. In addition, the levels of PCT have been shown to have predictive power of disease prognosis and likelihood of hospitalization of community-acquired pneumonia as well as death [126, 127]. Patient PCT levels on their admission to hospital have a strong association with their APACH II score which is an ICU mortality prediction score [128].

8.2 Methods

To create the high-sensitivity LFDs, the flow path was constricted to a defined shape (schematically described in Figure 8.1) using the LDW approach that has been discussed in detail in section 3.1. The constricted flow path is shaped such that its inlet gradually reduces in width over ~ 1 mm followed by 8 mm of constant width leading to a 1 mm angled outlet where the flow path returns to the standard 4.5 mm width.

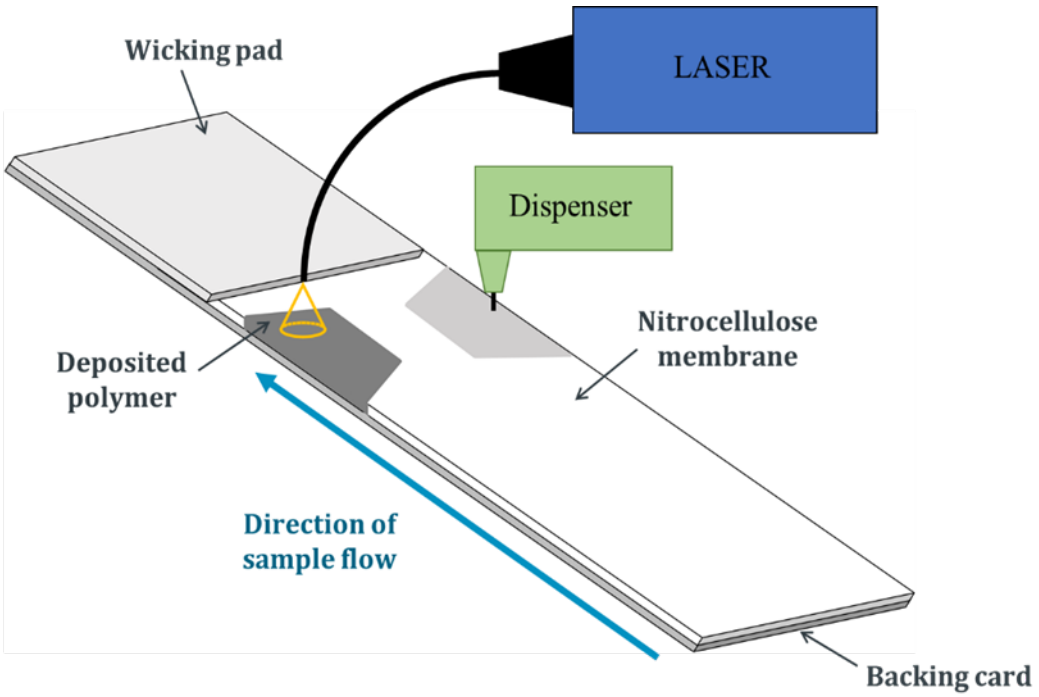

Figure 8.1 - Schematic of the laser-direct write (LDW) patterning technique on the nitrocellulose membrane of a lateral flow device.

8.2.1 Measuring the flow

For the initial flow experiments, to measure the time taken for the flow front to traverse the LFD, a coloured dye was used for ease of visualisation and the entirety of the flow was filmed using a smartphone, and a photo of this can be seen in Figure 8.2. The video was recording the entire experiment for each LFD from the time it was introduced to its respective well separately. T_0 was taken when the bottom of the LFD touched the dye in the well and this was recorded for each test. This data was then analysed using an onscreen ruler to assess when the flow front had reached a designated point, 5 mm from the front end of the LFD.

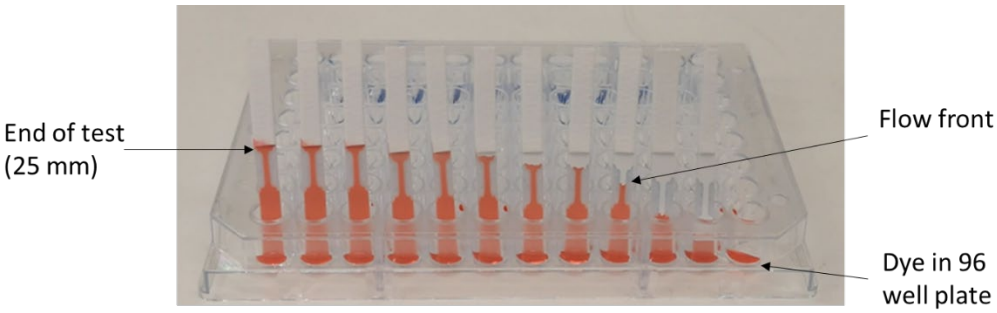

Figure 8.2 – Photograph showing the flow of the red dye within the constricted devices placed within in a 96 well plate.

8.3 Results

Here is reported the results from several parameters investigated in the optimization of a constriction for lateral flow devices with enhanced sensitivity. The following parameters that were investigated are detailed below:

Parameter 1: Position of the constriction within the flow path.

As shown in Figure 8.3 the distance of the constriction from the sample inlet was changed and the time taken for the flow front to travel across the device was measured. These measurements were taken at 5 mm intervals along the length of the device until the flow front reached the end of the test – defined as the end of the nitrocellulose membrane where it meets the wicking pad. Then the test line colour intensity was measured for each constriction position and the results compared.

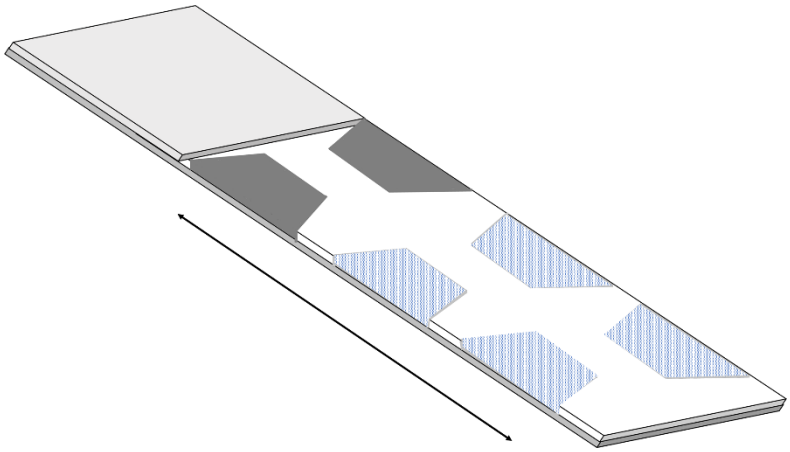

Figure 8.3 -Schematic showing the different positions of the constriction within the flow path, potential positions indicated in shaded grey.

Parameter 2: Position of the test line within the flow path.

As shown in Figure 8.4, the position of the test line within the flow path was investigated, without the use of constriction on these devices. Several test line positions were investigated, and the test line colour intensity was recorded for each position.

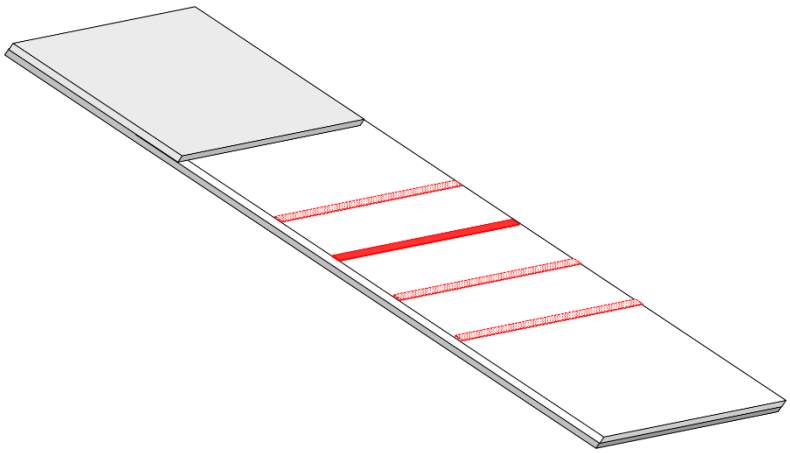

Figure 8.4 - Schematic showing the different positions of the test line within the flow path, potential positions indicated in shaded red.

Parameter 3: Position of the test line within the constriction,

As shown in Figure 8.5, the test line colour intensity was recorded for each test line positioned within the constriction at 1 mm intervals, including within the angled openings at either end of the constriction.

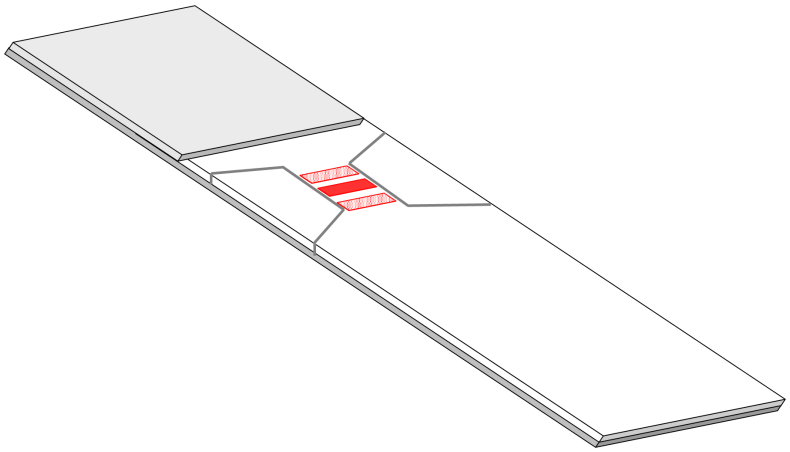

Figure 8.5 - Schematic showing the different positions of the test line within the constriction, potential positions indicated in shaded red.

Parameter 4: Use of a double constriction.

Finally, the use of a second constriction was investigated, as shown in Figure 8.6. With the first constriction placed at the optimal position to control the flow rate, as determined from Parameter 1, the second constriction to contain the test line as determined by Parameters 2 and 3. The time taken for the flow front to reach the end of the test and the test line colour intensity

were recorded for multiple concentrations of PCT and compared to both devices with a single constriction and one with no constrictions.

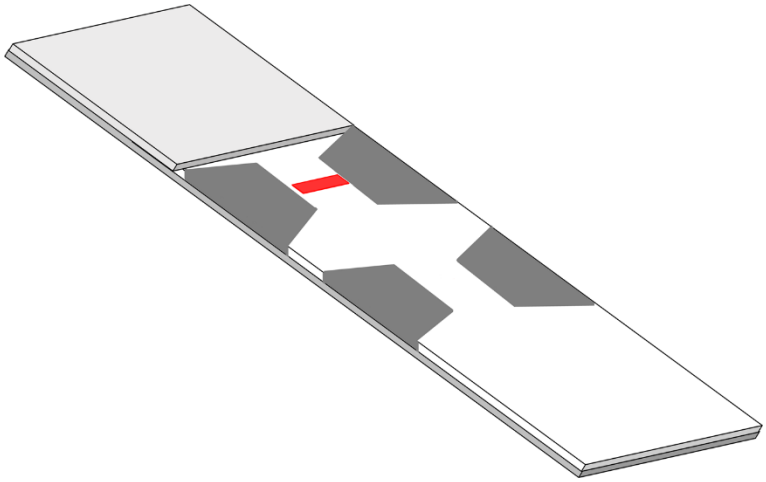

Figure 8.6 - Schematic showing a LFD with a double constriction with a test line in the constriction furthest from the sample inlet.

8.3.1 Parameter 1 - Position of the constriction within the flow path

As previously reported, the addition of a constriction to an LFD can enhance the sensitivity of the assay [9]. Therefore, the first parameter investigated was the position of the constriction relative to the inlet point. There were two outcomes that were recorded, namely what effect the constriction position has on a) the speed of the flow front and therefore the time taken for the test to complete and b) the resultant colour intensity of the test line which is used to infer the sensitivity of the test.

The position of the constriction was systematically changed with respect to the sample inlet of the device and seven different constriction positions were trialed. Figure 8.7 shows a schematic of the devices tested, labelled from ‘a’ to ‘g’ where the start of the constriction is at a distance of 13 mm to 1 mm from the sample inlet respectively, decrementing by 2 mm for each subsequent device (‘b’ to ‘f’). The subsequent Figure 8.8, shows a scanned image of the real devices for reference.

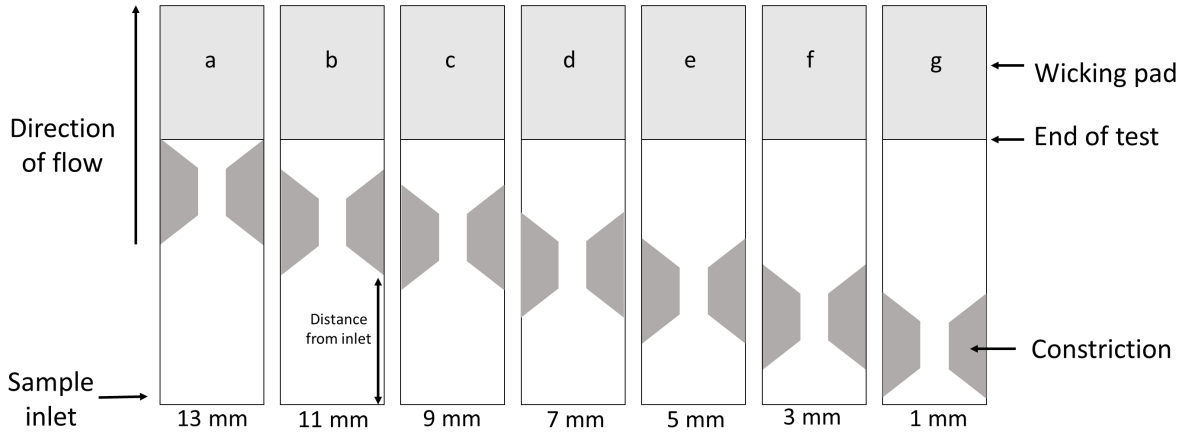

Figure 8.7 – Schematic of seven LFDs showing the different positions of the constriction labelled a-g.

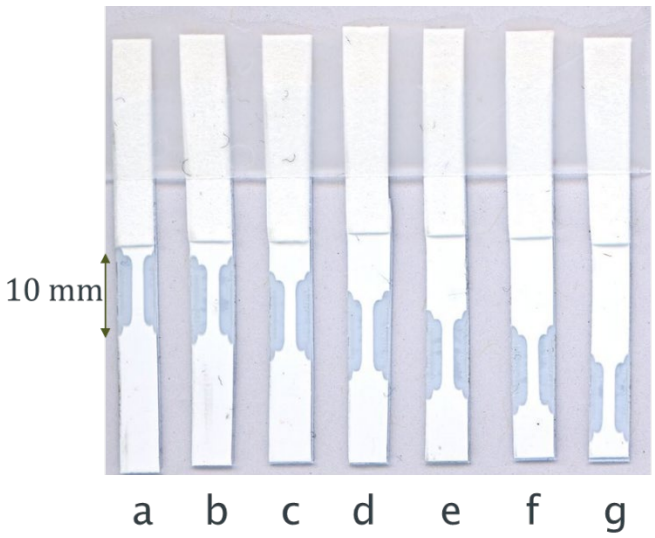

Figure 8.8 - Scanned image of seven LFDs showing the different positions of the constriction labelled a-g.

The results for the time taken for the flow front to reach pre-defined points along the LFD (10 mm, 15 mm, 20 mm and 25 mm) can be seen below in Figure 8.9. The black line shows the results obtained for a standard LFD with no constriction (NC) and this acts as the reference measurement for comparison with other measurements to evaluate the effect that the constriction position has on the time taken by the flow front to travel to the specified end point.

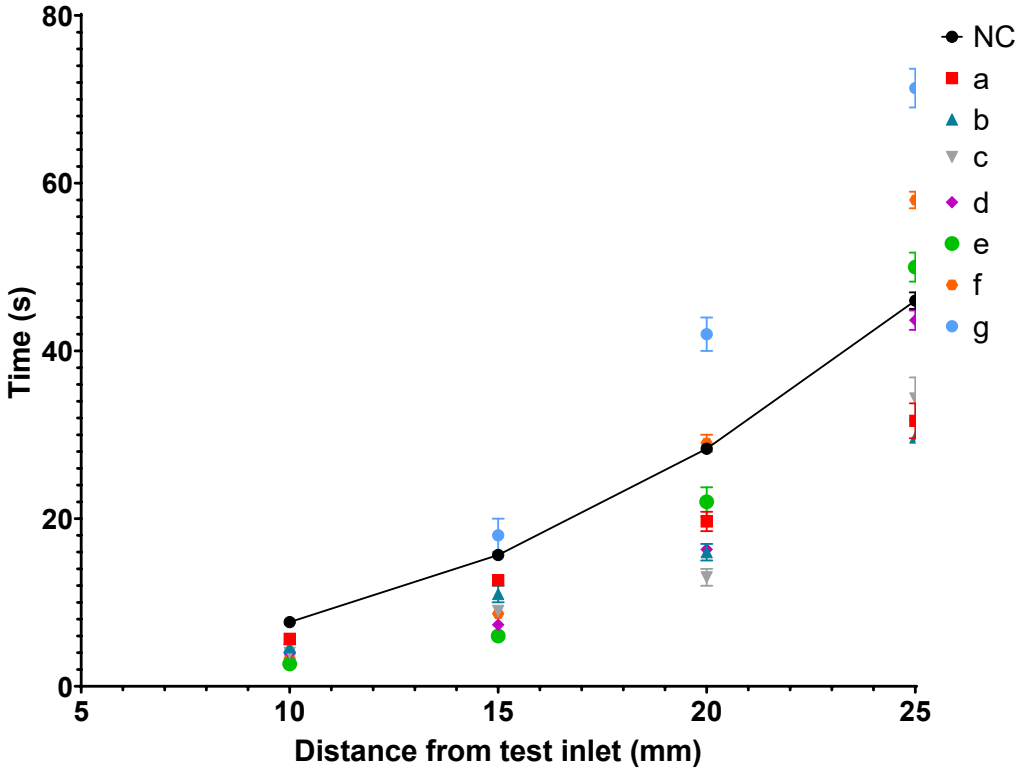

Figure 8.9 – Graph showing the time taken for the flow front to travel 10, 15, 20 and 25 mm from the test inlet within the LFDs with the seven different constriction positions, as well as for an LFD with no constriction (NC) for reference. The plotted point shows the mean and error bars representing standard deviation for three repeat measurements.

The hypothesis under investigation was that the position of the constriction will affect the flow rate of the sample and reagents. This is important as it means that the time available for the components of the immunoassay to bind will vary for each different constriction position. The binding kinetics of the antibodies are crucial for the LOD of the assay and therefore this is a parameter that must be optimized to enhance the test sensitivity.

It was observed that over the length of the LFD the disparity in time between the different constriction positions became more significant as the flow front moved closer towards the end of the device, where the nitrocellulose membrane meets the wicking pad (at a distance of 25 mm). The constriction in position ‘g’, which was closest to the sample inlet, showed the greatest increase in time taken for the test to complete compared to the other positions and also when compared to a test with no constriction (NC). As seen in Figure 8.9, the black line represents the

reference time of a device with no constriction, with the time for some constriction positions falling above and some below this line. At a distance of 25 mm from the inlet, the constriction positions closest to the sample inlet, ‘e’, ‘f’ and ‘g’ are above this line and therefore show that those positions of the constriction slow the overall time taken for the test to complete. The position closest to the sample inlet, ‘g’, shows the most deviation from the baseline with the slowest time.

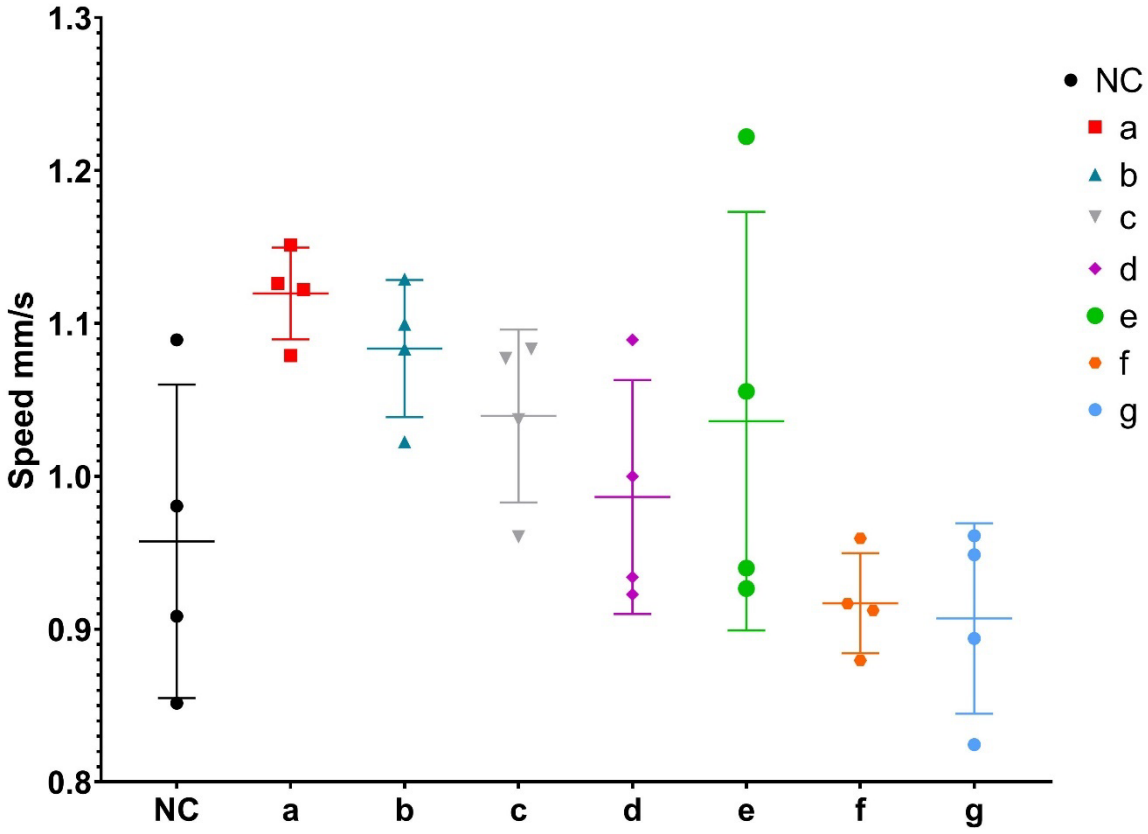

Figure 8.10 – Graph showing the range of the average flow front velocity (mm/s) across the entirety of the LFD for the seven different constriction positions, as well as the LFD with no constriction (NC) for reference. The plotted point shows the mean and error bars represent standard deviation for three repeat measurements.

As seen in Figure 8.10, there is strong negative correlation between the distance of the constriction from the sample inlet (a = 13 mm, g = 1 mm) and the average flow front velocity. There is a general trend of a decrease in the average velocity (mm/s) from position ‘a’ to ‘g’. This is anticipated as the slower flow front velocity leads to an increase in the overall time taken for the test to complete. There is greater variation in the average speed across position ‘e’

The initial experiments to investigate the flow front velocity, were carried out with coloured dye for ease of visualisation and without an immunoassay present on the LFD. This saved time and

cost of the devices for initial testing. The next investigation conducted was to determine how the different constriction positions affected the test line colour intensity of an immunoassay for the detection of PCT.

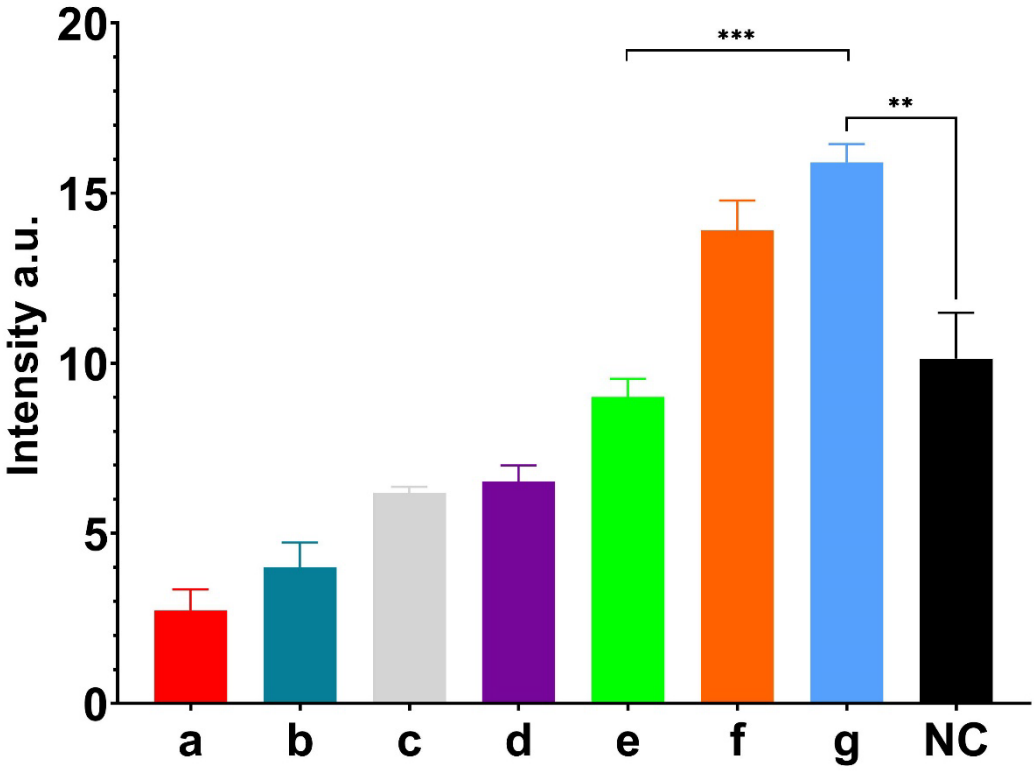

Figure 8.11 - Graph showing the mean test line colour intensity with the mean plotted and error bars representing the standard deviation of three repeat measurements for 7 different constriction positions and a test with no constriction (NC). Differences were considered significant where $p < 0.05$ and calculated from unpaired t-tests. The star rating represents and is proportional to the level of significance of the data.

It was clearly observed that the time taken for the flow front to reach the end of the LFD for the different constriction positions affected the resultant test line colour intensity, and a slower rate of flow produced a higher test line intensity. This is the expected result as the components of the immunoassay have an increased incubation time with the sample prior to arrival at the test line, and the analyte-detection antibody complex will move slower over the test line giving more opportunity for binding and the formation of the analyte-detection antibody-capture complex that is essential for the production of the visible test line. Figure 8.11 shows the test line colour intensity values for each of the seven constriction positions and the LFD with NC.

Statistical analysis performed in GraphPad prism using the unpaired t-test shows that there is significant difference between the test line colour intensity for constriction position ‘g’ and no constriction (NC), shown in Figure 8.11 by the three-star significance rating.

8.3.2 Parameter 2 - Position of the test line within the flow path

The position of the test line within the flow path of the LFD is another parameter that can affect the LOD of the test. The position of the test line defines how long the conjugate/detection antibody and the analyte in the sample have to bind before they reach the test line, and the flow speed at the test line then dictates how much time the analyte-detection antibody complex has to bind to the pre-deposited capture antibody at the test line. In addition, the speed of the sample flow decreases over the length of the LFD; therefore, the flow rate will be slower towards the end of the test so the immunoassay components will have more time to bind. The hypothesis here therefore is that the further the test line is positioned from the sample inlet the higher the test line signal intensity will be. The results of this set of experiments that determine the optimal test line position, as determined by the highest test line colour intensity, are shown in Figure 8.12.

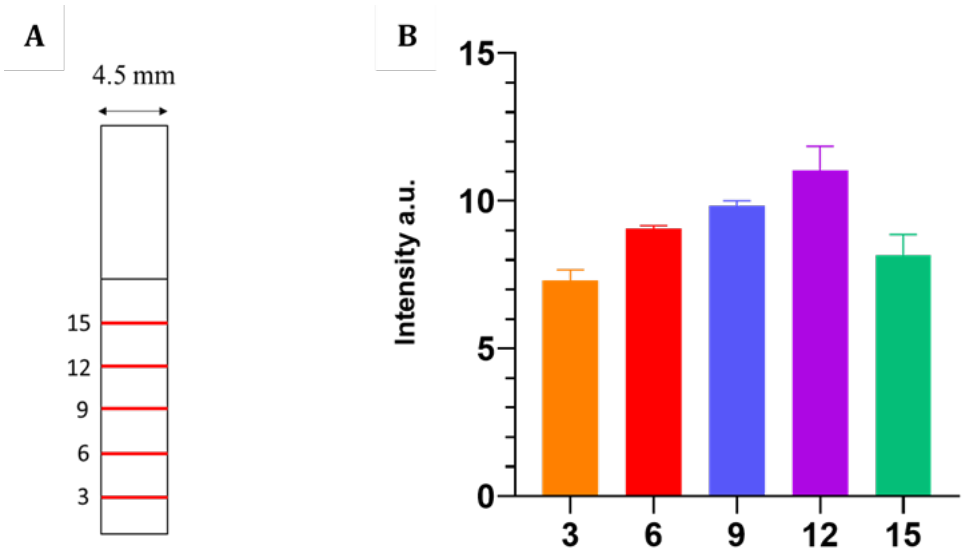

Figure 8.12 - A) Schematic of a non-constricted LFD showing the different positions of the test line that were investigated labelled by their mm distance from the sample inlet. B) Shows the results are seen for the mean test line colour intensity for each different position; the error bars represent the standard deviation of three repeat measurements.

The results show that as the test line was moved further up the test, the test line colour intensity increases, and this is true up until 12 mm from the sample inlet. At 15 mm from the sample inlet,

however, the test line colour intensity is lower, similar to having the test line placed at 3 mm from the sample inlet. This could be a result of the effect that the wicking pad has on the overall flow rate. Once the flow front reaches the wicking pad the flow velocity will increase as the wicking pad has greater absorbent capacity than the nitrocellulose membrane and also acts as a passive pump that accelerates the extraction of the oncoming fluid from the nitrocellulose membrane. In the case when the test line is at 15 mm and relatively close to the wicking pad, when the flow front reaches the wicking pad the rest of the sample which is yet to cross the test line, is wicked across the test line at a higher rate. Therefore, the analyte in the sample has less time to bind to the capture antibodies resulting in lower binding and a decrease in the test line colour intensity. Therefore, the optimal position for the test line was chosen to be 12 mm from the sample inlet.

8.3.3 Parameter 3 - Position of the test line within the constriction

Previously it was determined that the positioning of the test line within the constriction allowed for a greater volume of detection antibody-analyte complexes per unit area, and a 1 mm constriction gave the optimal results without overly compromising on test line visibility [9]. However, the position of the test line within the constriction was not explored and therefore, further to the investigation of test line position within the flow path we investigated the optimal position of the test line placement within the constriction. The constriction is 1 cm long including the angled inlet and outlet. We tested the position of the test line at 1 mm intervals through the length of the constriction to find the optimal position for increased test line colour intensity.

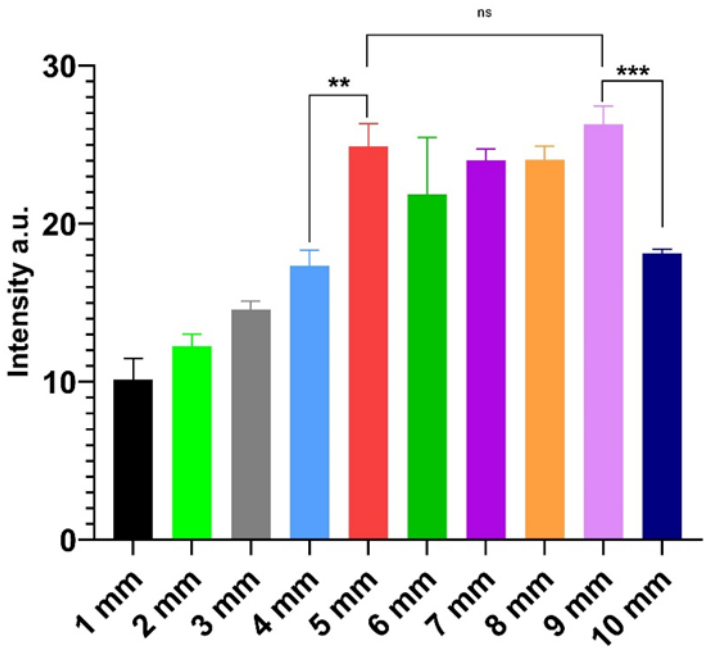

Figure 8.13 - Graph showing the mean test line colour intensity for 10 different test line positions within the constriction characterized by the distance of the test line from the constriction inlet. The error bars represent standard deviation of three repeat measurements. Differences were considered significant where $p < 0.05$ and calculated from unpaired t-tests. The star rating represents and is proportional to the level of significance or no significant (ns) of the data.

The results for this set of experiments are shown in Figure 8.13 and it can be seen that the positions with the highest test line colour intensity fall within the latter half of the constriction, from 5 mm to 9 mm inside the constricted path. When the flow front reaches the end of the constriction and spreads out from the 1 mm channel to the full 4.5 mm test the flow rate is slowed as the sample fills the larger area of nitrocellulose membrane. As the flow front dictates the rate of the subsequent sample flow, once the flow front reaches the end of the constriction the remaining sample will move more slowly through the constriction. It is important that the flow rate, when moving over the test line, is optimal to ensure the maximum binding for the components of the immunoassay. When the flow initially enters the constriction is goes from a wider channel width to a narrower cross-section, leading to an increase in flow rate, which aligns with the results shown here as the test line colour intensity was lowest for the positions closest to the start of the constriction. The peak of test line colour intensity falls at a position of 9 mm from the constriction inlet. However, after statistical analysis was performed for significance levels highlighted in Figure 8.13 with an asterisk rating of significance, it was found that there was no

significant difference in test line colour intensity for the values collected from 5 mm to 9 mm. The difference in test line colour intensity from 4 mm to 5 mm was significant and so was the change from 9 mm to 10 mm. Therefore, the optimal position was chosen as 9 mm.

8.3.4 Parameter 4 - Double constriction

Having performed the experiments to optimize the parameters for a single constriction, the next logical step was to increase the number of constrictions, and so this last set of experiments was performed with two consecutive constrictions. The initial results from the experiments for finding the optimal position of the constriction indicated that the best position for the constriction that has the largest influence on controlling and slowing the flow rate was the position closest to the sample inlet. However, the test line position experiments dictated that the test line would not be ideally positioned near the test inlet but much closer to the end of the device. The additional experimentation described in 1.3.3. indicated that the test line colour intensity was maximized when the test line was placed within the 1 mm constriction and therefore combining this information with acquired results with constriction position a double constriction geometry was developed.

Figure 8.14 shows one such example of a LFD with a double constriction geometry. The initial constriction at position 1 mm, serves to slow the flow rate across the entire test to allow the components of the immunoassay more time to react. The hypothesis here is that the expected enhancement in the intensity at the test line would be a consequence of two combined effects, namely a slower flow rate and increased incubation time of the reagents, and the larger sample volume per unit width of test line within the second constriction at position 13 mm, to increase

the chance of binding and the density of the gold nanoparticles respectively, both leading to increased test line colour intensity.

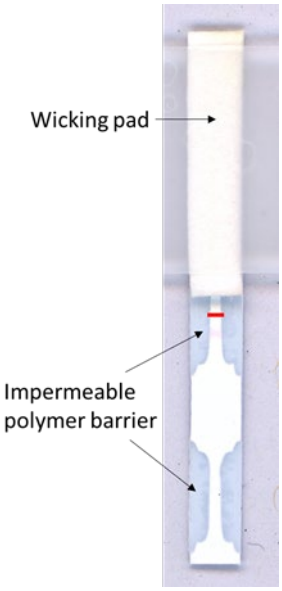

Figure 8.14 - Scanned image of a single LFD with two (double constriction) 1 mm width constrictions in the flow path at positions 1 mm and 13 mm from the inlet with the test and control line.

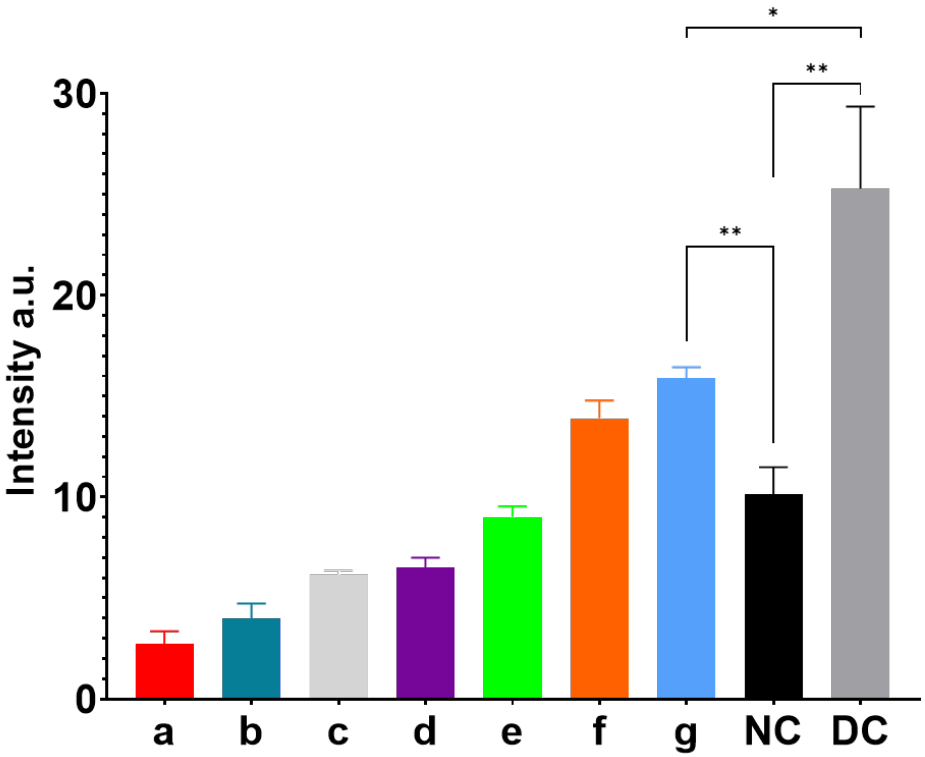

Figure 8.15 - Graph showing the mean time taken for the test to complete for the LFDs with seven different constriction positions, no constriction (NC) and a double constriction (DC). The error bars represent the standard deviation of three repeat measurements Significance levels indicated. Differences were considered significant where $p < 0.05$ and calculated from unpaired t-tests. The star rating represents and is proportional to the level of significance of the data.

Initially, the time for the flow front to travel from the sample inlet position (t = 0) to the end of the nitrocellulose membrane for LFDs with all constriction positions no constriction and double constriction was measured. The results for this can be seen in Figure 8.15. It was observed that the positioning of a constriction close to the sample inlet decreases the flow rate and therefore increases the time for the test to complete. We had shown with previous experiments that 12 mm from the sample inlet was the optimal position for the test line and hence it was this that formed the basis of the next line of experimentation consisting of adding the second constriction to the flow path. The second constriction was added to enhance the effect of both slowing the flow and increasing the signal intensity due to the smaller capture site and concentrated accumulation of analyte-detection antibody complex. Statistical analysis of the data for devices that have the double constriction when compared to those for devices with either a single constriction in position ‘g’ and or those with no constriction, shows a significant increase in time taken for the

test to complete, which was the time taken by flow front in reaching the end of the wicking pad ensuring that all the sample has passed over the entirety of the nitrocellulose membrane.

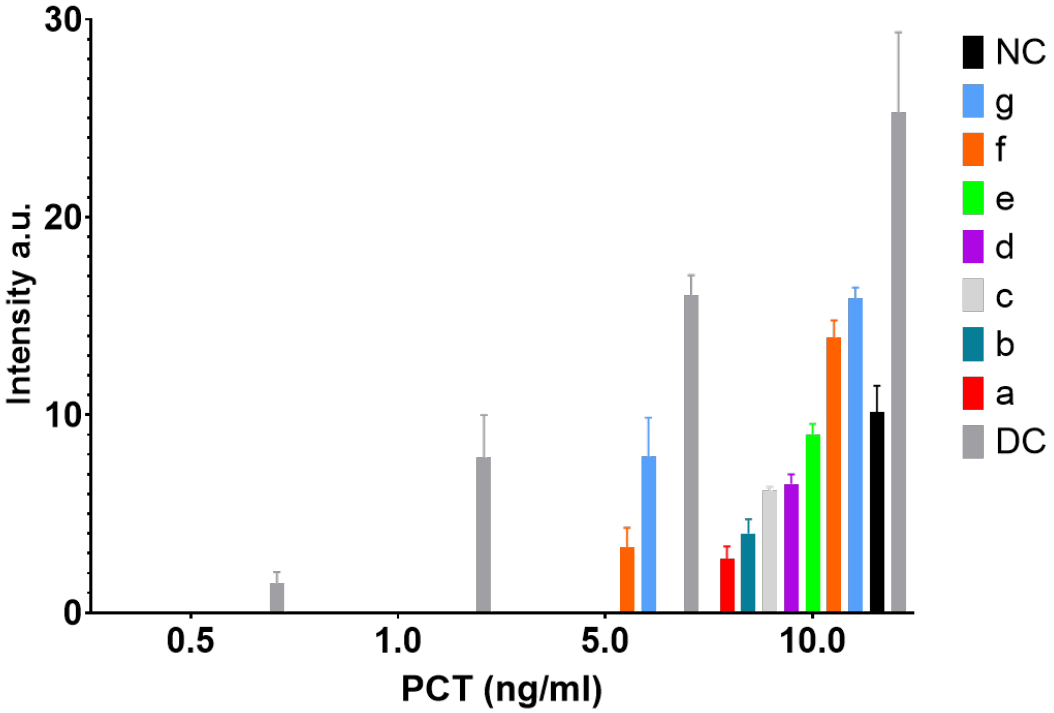

Figure 8.16 - Graph showing the mean test line colour intensity for the seven constriction positions, no constriction (NC) and double constriction (DC). The error bars represent the standard deviation of three repeat measurements.

Finally, the intensity of the test line for serum samples which were spiked with a concentration of PCT ranging from 10-0.5 ng/mL, for all positions of the test line was measured, the results for which can also be seen in Figure 8.16.

The test line colour intensity for the double constriction shows significant improvement, with an increase of 159 % (mean value) compared to the device with no constriction. This equates to an improvement (or reduction) in the LOD from 10 ng/mL to 1 ng/mL when compared to that for devices with no constriction and from 10 ng/mL to 5 ng/mL for devices 'g' with a constriction positioned at 1 mm from the sample inlet. As shown in Figure 8.16, the corresponding test line colour intensity was at 0.5 ng/mL, though faint, it can be picked up with the scanner and can just be viewed with the naked eye and therefore the LOD for the double constriction was 0.5 ng/mL but the limit of quantification (LOQ) for naked eye reading was 1 ng/mL. This is a 10-fold improvement from devices with no constriction and a 5-fold enhancement from devices with a single constriction.

8.3.5 Alternative geometries

An alternative to the double constriction was also investigated. With the knowledge that the flow front will slow down as it enters a wider flow path, a new geometry that moves from a narrow to wider flow path was investigated thereafter. This was explored using a diamond geometry where the test line was positioned within the larger flow path where the flow rate would be reduced, thereby increasing the time available for the analyte and tagged detection antibody complex, to bind to the capture line. The position of the test line within this space was investigated and the shape of the 'diamond' modified to see the effect this would have on test line colour intensity. A schematic with the layout of the different geometric flow paths can be seen in Figure 8.17.

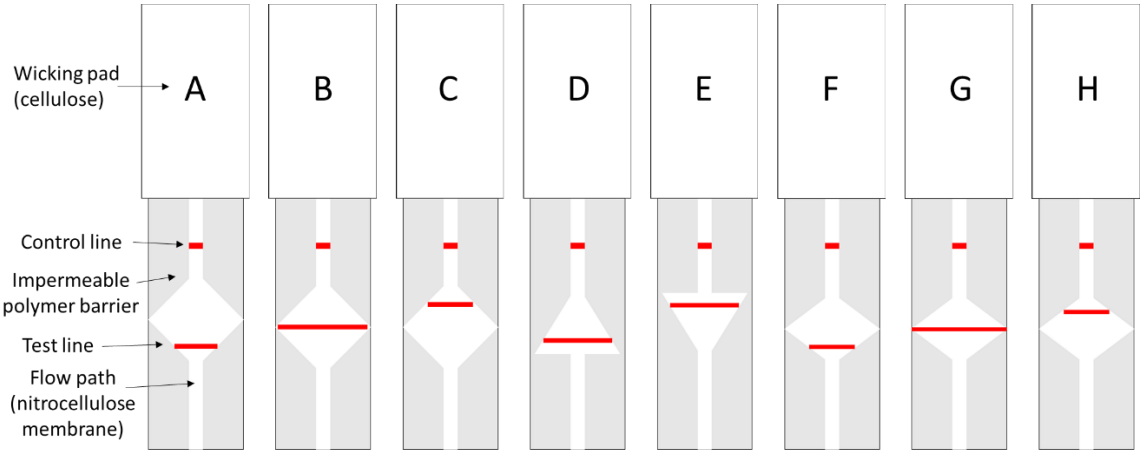

Figure 8.17 – Schematic of eight LFDs labelled A-H with different flow path geometry.

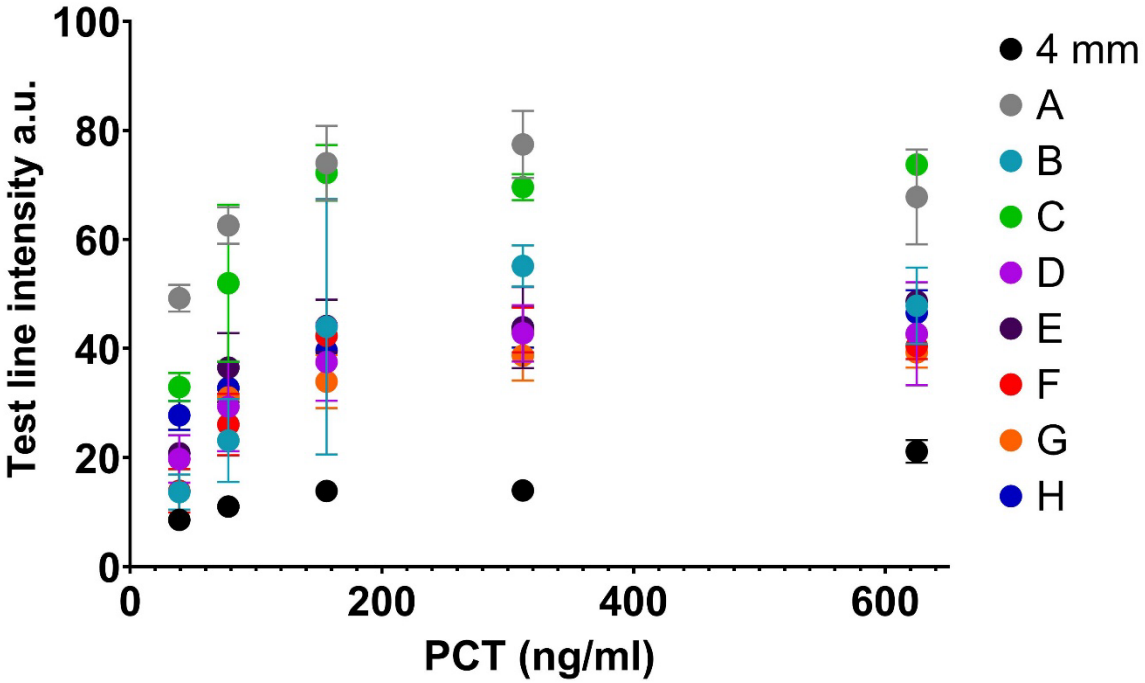

Figure 8.18 – Graph showing the mean test line colour intensity for different geometries labelled A-H and a standard 4 mm LFD for five concentrations of PCT ranging from with the standard deviation being that for three repeat measurements.

The graph in Figure 8.18 shows that the standard LFD with a width of 4 mm has the lowest test line intensity for all concentrations of PCT and that any modification to the flow shows an improvement. The geometry with the highest test line intensity is geometry A, although the results are similar for geometry C similar. Geometries A and F are quite similar however, F has a shorter area of widening in the middle of the test. As the flow front leaves the constricted area it slows down to fill the larger are containing the test line, but once the flow front reaches the next area of constricted flow path it speeds up and due to the incompressibility of the fluid this will mean the subsequent flow will also move faster. As the widened section is shorter for F this could mean that there is more sample yet to cross the test line when the flow front reaches the next constricted section and consequently more sample will move over the test line at a greater velocity compared to geometry A and this leads to a reduced time for the components of the immunoassay to bind at the capture site. Therefore, geometry A was carried forward for comparison with the single constriction geometry to assess whether this geometry would be advantageous to increase the sensitivity of an LFD. Not only does the geometry affect the position of the test line but also the width of the test line and therefore the number of capture sites available to bind to the analyte.

As each assay performs differently it is important to ensure that any potential modifications also show an improvement for the detection of other biomarkers. Therefore additional investigation was carried out with CRP, the results of which can be seen in Figure 8.19.

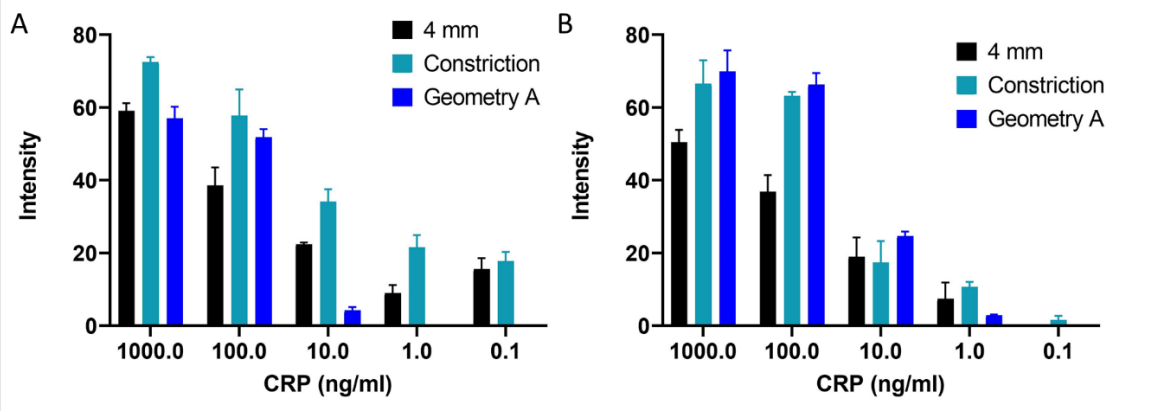

Figure 8.19 – Graphs showing the mean test line colour intensity for five concentrations of CRP, with error bars representing standard deviation for three repeat measurements for A) incubated samples and B) non-incubated samples.

For these experiments and results in Figure 8.19 the samples tested were initially incubated (i.e., the analyte with the detection antibody) for 30 minutes before being added to the test. This gives the analyte more time to bind to the detection antibody and form a complex. In this case geometry A performs only slightly better than a standard 4 mm LFD with the constriction giving superior intensity signals. At the lower concentrations of 1.0 ng/ml and 0.1 ng/ml there is no visible signal for geometry A and it performs worse than the standard LFD. This could be due to the shape of the geometry. As the flow front leaves the constricted area it slows down to fill the larger area containing the test line, however as the flow front reaches the next area of constricted flow path, again, it will speed up and due to the incompressibility of the fluid this will mean the subsequent flow will also move faster. This could mean that some of the sample moves over the test line quicker, leaving less time for the components of the immunoassay to bind at the capture site and this could be more important at the lower concentrations where the number of analyte molecules in the sample is lower. Conversely, in Figure 8.19B where the sample and detection antibody were added directly to the LFD with no prior incubation, as the routine would be for LFD based testing, geometry A performs better than the constriction and standard LFD at higher concentrations, 1000.0, 100.0 and 10 ng/ml. However, below this point, the constriction performs the best giving the lowest LOD of 0.1 ng/ml. This shows that the alternative geometry A could prove advantageous in achieving better sensitivity without the requirement for an additional

incubation step, which would add time to an assay designed to be performed in 5-10 minutes. As the results of the alternative geometries were not conclusive and the single constriction was still shown to be performing as well as, if not better than geometry A it was decided to move forward with the addition of the double constriction and not pursue this further.

8.4 Discussion

The principle of a lateral flow assay is that the analyte in the sample is transported along the test by capillary flow. As it passes through the nitrocellulose membrane which incorporates the reaction zone, the molecules diffuse towards pre-deposited capture sites leading to the formation of the analyte-antibody complex. There are two things occurring, firstly the analyte diffusion through the porous nitrocellulose membrane and then the immunochemical reaction, and the experimental results reported in this chapter show that the time taken for the flow front to traverse the LFD is around 45 seconds but the coupling constants for the antibodies used in this thesis are unknown. Also, as the antibodies used are designed to be used as part of an ELISA which when used in the traditional setting, includes several incubation steps of up to an hour, the analyte-capture and detection antibody complex formation is the limiting step of the process which is key for producing the visible test line [252]. Therefore, controlling and optimizing the sample flow rate is a critical factor in optimizing the antibody binding kinetics and ultimately the sensitivity of the test.

The logic underpinning the work carried out in this chapter stems from several known facts about fluid flow. The nitrocellulose membrane is made up of a network of capillaries that allow for the passive movement of fluid, therefore, here it is assumed that the flow within the nitrocellulose membrane performs the same as within a single capillary. In this instance, flow rate Q is defined as the volume of fluid, V, passing a given location through an area, A, during a period of time, t, which can be written as:

$$Q = \frac{V}{t} \qquad [8.1]$$

The average velocity is:

$$v = \frac{d}{t} \qquad [8.2]$$

Where v is velocity and d is distance travelled. The relationship tells us that flow rate is directly proportional to both the magnitude of the average velocity and the area of the flow path, in this case the diameter of the capillary.

The volume of the capillary is Ad and the average velocity is [8.2] so that the flow rate is:

$$Q = \frac{Ad}{t} = Av \qquad [8.3]$$

As we know equation [1] and equation [2] we can combine these to get a value for flow rate as seen in equation [3].

As Q (flow rate) must remain constant, we know that the flow rate in the first section Q_1 of the LFD must be equal to the flow rate in the second section Q_2:

$$Q_1 = Q_2 \qquad [8.4]$$
$$A_1 v_1 = A_2 v_2$$

Here we show an incompressible fluid flowing along the LFD (capillary) with decreasing radius. Because the fluid is incompressible, the same amount of fluid must flow past any point in the tube in a given time to ensure continuity of flow. In this case, because the cross-sectional area of the pipe decreases, the velocity must increase and then decrease again as it enters the area of wider radius. This logic can be extended to say that the flow rate must be the same at all points along the LFD.

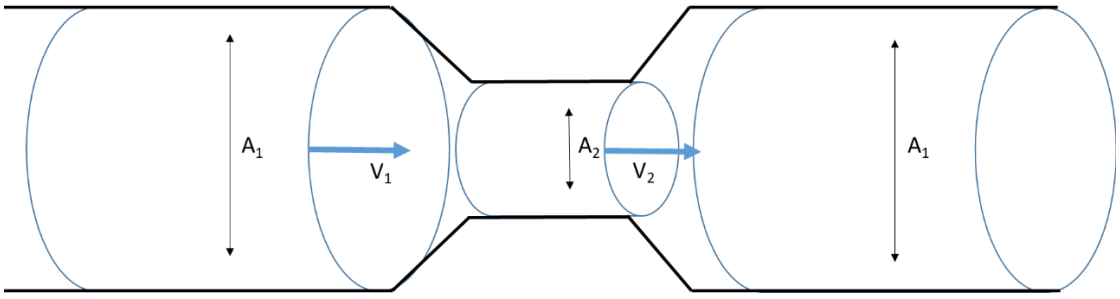

Figure 8.20 – Schematic of a constricted LFD modelled as a constricted capillary; image adapted from [4].

Using the Washburn equation [6]:

$$L = (Dt)^{\frac{1}{2}} \quad [8.5]$$

Where L is the length and D is the diffusion coefficient, we also know that, as the fluid front moves along the length of the lateral flow devices' capillary network the speed of the flow will be reduced. This is also affected by the viscosity of the liquid and surface tension.

From previous work carried out [9] it had been identified that the addition of a constriction to the flow path of a standard LFD can enhance the sensitivity and improve the LOD. This occurs by a two-fold effect: the presence of a constriction in the flow path affects the overall flow rate of the sample within the test, increasing the time taken for the test to complete. Secondly, as the test line placed within the constriction has a smaller area compared to the standard device, it allows more sample to flow per unit area of test line, i.e., there is more sample volume per unit width of the test line. Therefore, the capture antibodies have a greater opportunity to bind to the analyte in the sample, leading to a higher intensity test line colour intensity. This effect is particularly important at low concentrations for standard tests without any constrictions where binding occurs over the full ~ 5mm wide test line would produce a signal that was much less intense.

To build on this finding it was first established that the position of the constriction should be further investigated. Therefore, seven different constriction positions (labelled a-g with 'a' being the design for which the constriction was 13 mms from the inlet point) were trialled. In the first instance each test was run, and the times taken for the flow front to reach several pre-defined positions along the test were recorded. This showed that the position of the constriction has an impact on the time taken for the test to complete. The constrictions in positions 'which to which' closest to the sample inlet showed the most significant slowing of the flow rate, with position 'g' showing an 155% increase in time for the test to complete when compared to not having a constriction in the flow path. This is a highly significant increase, as confirmed by statistical analysis. Next the test line colour intensity was measured for 10 ng/mL of PCT for each constriction position. The results show that the increase in time taken for the test to complete does translate into an increase in test line colour intensity, as position 'g' shows an increase of 157% in intensity compared to the device with no constriction.

The increase in time taken for the test to complete leads to an increase in test line colour intensity due to increased time available for the analyte to bind the detection antibody and for that complex to bind at the capture site. However, as it is known that some of the enhancement in sensitively occurs due to the test line being positioned within the constriction, this became an

issue as the constriction placed so close to the sample inlet would not be a preferable position for the test line due to the time for the interactions between the detection antibody and the analyte in the sample. The flow front velocity decreases across the length of the nitrocellulose membrane until the front reaches the wicking pad, which assists by further drawing the sample through the membrane at a faster rate. When we then investigated the optimal test line position the results showed a position of 12 mm from the sample inlet was preferable, much higher than the ideal position for the constriction, but not completely towards the end of the device. This is because the wicking pad speeds up the flow rate once the front has reached that point meaning subsequent sample would be drawn over the test line much faster and have less time to bind to the capture antibodies. Therefore, to take advantage of both aspects of the constriction enhancement, a second constriction was introduced higher up the device to contain the test line whilst the first constriction in position 'g' acted to slow the overall flow rate of the test.

The addition of a second constriction shows a further decrease in flow rate and therefore increased time for the flow front to reach the end of the LFD. This decreased flow rate further shows improvement in the increased test line colour intensity and consequently the LOD for the PCT assay. This improvement is greatest when comparing an LFD with no constriction to the introduction of a single constriction, however the addition of a second constriction shows significant difference in both decrease of flow rate and increase of test line colour intensity and subsequent LOD both compared to a single constriction and to an LFD with no constrictions.

We were able to see a clear improvement in the LOD from 5 ng/mL for a single constriction to 1 ng/mL for the double constriction. The observed enhancement of LOD is 5x that of a single constriction and although this may seem a small increase, in the context of the use for PCT in sepsis or pneumonia triage, the usefulness of devices with a LOD that is not 5 ng/mL but a lower value of 1 ng/mL is crucial for an effective diagnosis.

8.5 Conclusion

In conclusion, there is clear merit in altering the LFD architecture by adding more than a single constriction within the flow path to produce a sensitivity enhancement and a consequent improvement in the limit of detection. Our reported method employs technologies requiring minimal modification to the LFD structure and thus ensures that scale-up or mass manufacture would be possible with minimal added cost.

Chapter 9 Conclusions and future work

This final chapter provides a summary of all the results collected and described within this thesis. This includes both the optimisation and modification of traditional lateral flow devices to enhance their detection capabilities and the validation of these devices using patient samples for application to solve real world healthcare problems.

9.1 Conclusions

9.1.1 Development of a semi-quantitative and multiplexed LFD

In Chapter 3 a novel three-channel LFD was described with the capability to detect two inflammatory biomarkers, simultaneously, with semi-quantitative analysis, without the need for a reader. This was achieved using the patented LDW patterning technique that allowed for the detection of CRP in the three ranges of (i) below 20 µg/mL, (ii) above 20 µg/mL, but below 100 µg/mL and (iii) above 100 µg/mL, as per the NICE guidelines, defining the clinically relevant range for pneumonia. The test additionally, measured PCT down to a cut-off of 0.5 ng/mL, providing a rapid testing pathway that allows distinguishing between viral and bacterial causative agents.

The combination of these two markers into a single POC diagnostic test that can be used by healthcare professionals would not only improve the speed and accuracy of treatment for patients with pneumonia but would also assist in the campaign for prudent antimicrobial stewardship. The multiple parallel flow-paths within the multichannel CRP-PCT LFD allows for not only the individual detection of different analytes but also their detection at different concentrations without any cross-interference. The device shown in Chapter 3 has excellent potential as a diagnostic tool in the future.

The next stage of this development work is firstly the completion of the test to incorporate the sample and conjugate pad which removes the requirement for any pre-processing of the reagents and would allow the test to be used in under-resourced healthcare settings as well as by healthcare assistants within the community. On completion of the test the final step would be the validation of the LFD for use in pneumonia triage. This would involve the use of the test alongside validated diagnostic methods in a clinical trial with participants who were suffering from suspected pneumonia. The involvement in a clinical trial is a long and expensive process, clearly outside the remit of this thesis, and therefore this would be progression for the future.

9.1.2 Rule-out screening test for Tuberculosis

Chapter 5 presents the results obtained thus far for a multiplexed rule-out screening test for Tuberculosis. The original motivation for this project was to explore the development of a POC test for TB large-scale screening and the results presented here are incredibly promising for future work. The individual LFDs and the multiplexed test have only been explored using a small number of patient samples, but the chosen markers show a great capacity for distinguishing healthy control patients from those with TB infection and their implementation onto the paper-based platform has been successful. Unfortunately, LBP did not perform as expected when transferred to the LFD format and was therefore not included in the multiplex test. It was the ambition to repeat this experiment but due to supply problems the LBP antibodies did not arrive in time and there was also insufficient patient sample available. It was therefore decided to progress forward with the other three markers to produce the three-channel multiplex test and use the remainder of the patient samples to show the proof of concept for this test.

As discussed in the conclusion the proteomics analysis that was carried out to identify the biomarkers investigated in this chapter (CRP, SAA1, LBP and CFHR5) was a part of a larger cohort analysis which is, as yet, incomplete. This means that there is the possibility that other protein biomarkers could be identified that show the ability to distinguish patients with TB from healthy controls. Therefore, any new markers could be added to the LFD or indeed replace any of the current ones. The LFD platform is established and can be easily modified to accommodate further markers or substitute markers with little difficulty, and this could be an option for the future. The next stage after the biomarker panel is finalised in this project would be to further test the multiplexed device on a larger number of samples and for this collection of samples to include an additional cohort of patients from a different population including geographically and that of co-morbidities. Unfortunately, this was also outside the remit of the PhD due to funding and time limitations. Ultimately this multiplexed test is designed for use with a reader and for optimal results and long-term cost efficiency a reader would need to be designed and produced for use with this test.

9.1.3 COVID-19 Test

In Chapter 6 the results are reported for a dual-channel LFD for the simultaneous detection of spike and nucleocapsid proteins for the POC diagnosis of COVID-19. This was developed at the beginning of the pandemic before there was high use and availability of LFDs for large scale population testing. Although the test was successful in that it could detect the coronavirus at

relatively low concentrations the NP alone was sufficiently sensitive and specific, and did not require the addition of the SP. The chapter explores the use of the half LFD with inactivated viral particles and shows that the test still ran effectively with a different medium and the addition of a buffer that was required to cleave the virus open in order to access the NP. This highlights the versatility of LFDs and their future application during a global disaster but also for other POC diagnostic needs. This work will not be continued specifically for the use of SARS-CoV-2 as it has become redundant since the development of many LFDs on a large scale and the slowing down of cases to the point where there is no longer any requirement to test for the infection, nevertheless, this work has reinforced the potential applications of LFDs and usefulness of the LDW patterning technology.

9.1.4 Alzheimer's Disease

In Chapter 7 is presented some preliminary testing for the inflammatory markers ICAM-1, VCAM-1, VAP-1 and characteristic protein amyloid-β. Due to the time constraints of the project and the pandemic this work was not completed and although the full LFDs were developed, they have not been tested on patient samples. The initial testing carried out proved inconclusive and therefore we cannot discern much at this stage however the data suggests that these markers could provide a useful panel of biomarkers for testing and monitoring Alzheimer's disease, moreover this panel could be implemented on an LFD for large scale population screening to maximise speed of treatment initiation to those with high risk of disease onset.

9.1.5 Geometric Flow control

In Chapter 8 a number of geometric flow parameters were investigated to establish the effect that these would have on firstly the flow velocity but also what effect this in turn has on the sensitivity of the assay. This experimentation led onto the use of a double constriction within the flow path of the LFD to enhance the reduction in flow front speed but also improve the LOD. We were able to see a clear improvement in the LOD from 5 ng/mL for a single constriction to 1 ng/mL for the double constriction. The observed enhancement of LOD is 5x that of a single constriction and although this may seem a small increase, in the context of the use for PCT in sepsis or pneumonia triage, the usefulness of devices with a LOD that is not 5 ng/mL but a lower value of 1 ng/mL is crucial for an effective diagnosis.

This test was developed using an immunoassay for PCT which is a common inflammatory marker however as has been observed throughout the course of the work included in this thesis, the LOD and test line colour intensity is assay dependent and therefore to validate that the double constriction can always enhance sensitivity it is pertinent to repeat this testing with other assays to confirm, however due to time restrictions and lack of funding it was not within the scope of this PhD project.

9.2 Future Work

The work detailed in this thesis highlights the great potential for lateral flow devices to tackle real world healthcare problems and explores how these devices can be optimised for wider applications however there is still room for a lot of improvement. Below are detailed some key areas that could be investigated to overcome some of the limitations.

Firstly, and as to be expected, the development work carried out as part of this thesis has been preliminary and therefore the reagents have been bought commercially for ease and to save time however for large scale manufacture this would not be practical or economical. Immediate future work would involve the development of gold conjugation that did not require a commercial kit. This would provide stability of production and a reduction in cost. Similarly, the antibodies that are used for the immunoassays are purchased commercially and this comes with an added issue of batch-to-batch variation and a lack of information that the consumer has access to. This would have to be outsourced to an antibody manufacturer, but the specific design and manufacture of personalised antibodies would give better consistency and higher specificity for the antigen of interest. Due to the increased popularity of LFDs, there are now a wide array of materials and signalling options that were not investigated as part of this thesis that could be included to ensure that the optimal materials are being used. For instance, gold nanoparticles have been exclusively used and there are a number of other newer options that could provide superior sensitivity and would be worth investigating.

Secondly, the development of the multiplexed test for TB screening has the potential for huge global healthcare impact and therefore this is an area that must be pursued. The next stage is a reliability study with a larger number of LFDs, additionally more samples are required for a larger validation of the tests diagnostic capabilities and this would need to include several things: a cohort from a different geographical region, a cohort that included individuals with co-infection with HIV and comparison to individuals with other respiratory diseases (ORDs) as this can cause issues with TB diagnosis and is an important factor for investigating the specificity of the test.

Furthermore, the identification of antibiotic resistant bacteria is becoming increasingly important to tackle antimicrobial resistance that is growing, specifically in the context of TB infection. There are now strains that are completely resistant to all front-line antibiotics which poses a real threat, especially in high burden areas. There are several ways this could be achieved, and there are a number of genes that can be used to identify strains with antimicrobial resistance that does not involve culturing the bacteria and *Mycobactierum tuberculosis* is a slow growing bacterium. Therefore, some form of amplification method such as PCR or LAMP could be implemented onto a LFD.

Appendix A **Publications and conference contributions**

Publications

- **Alice H. Iles,** Peijun J.W. He, Ioannis N. Katis, Peter Horak, Robert W. Eason, Collin L. Sones. (2022) Optimization of flow path parameters for enhanced sensitivity lateral flow devices. Talanta, [123579]. (doi:10.1016/j.talanta.2022.123579).
- **Iles, Alice H**., He, Peijun J.W., Katis, Ioannis N., Galanis, Panagiotis P., John, Anto J.U.K., Elkington, Paul, Eason, Robert W. and Sones, Collin L. (2022) Semi-quantitative detection of inflammatory biomarkers using a laser-patterned multiplexed lateral flow device. Talanta, 237, 1-8, [122944]. (doi:10.1016/j.talanta.2021.122944).
- Galanis, Panagiotis, Katis, Ioannis, He, Peijun, **Iles, Alice**, Kumar, Anto J.U., Eason, R.W. and Sones, Collin (2022) Laser-patterned paper-based flow-through filters and lateral flow immunoassays to enable the detection of C-reactive protein. Talanta, 238, [123056]. (doi:10.1016/j.talanta.2021.123056).
- John, Anto, He, Peijun, Katis, Ioannis, Galanis, Panagiotis, **Iles, Alice**, Eason, R.W. and Sones, Collin (2021) Capillary-based reverse transcriptase loop-mediated isothermal amplification for cost-effective and rapid point-of-care COVID-19 testing. Analytica Chimica Acta, 1185, [339002]. (doi:10.1016/j.aca.2021.339002).
- Galanis, Panagiotis, He, Peijun, Katis, Ioannis, **Iles, Alice**, Kumar, Anto J.U., Eason, R.W. and Sones, Collin (2020) Local photo-polymer deposition-assisted fabrication of multilayer paper-based devices. Sensors and Actuators, B: Chemical, 322, [128574]. (doi:10.1016/j.snb.2020.128574).

Conference Contributions

- **Iles, A.,** He, P., H. F. Schiff, D. J. Garay-Baquero, Ioannis N. Katis, P. Elkington, R. W. Eason, C. L. Sones (2022) Paper-based screening tool for Tuberculosis 'rule-out' test. 7th Annual Conference on Bio-sensing technology. Sitges, Spain 22-25 May 2022. (poster)
- **Iles, A.,** Katis, I., He, P., Galanis, P., Sones, C. & Eason, R. W. (2022) Optimisation of flow path parameters for enhanced sensitivity lateral flow. SPIE Photonics West Optical Diagnostics and Sensing XXII: Toward Point-of-Care Diagnostics. San Francisco, CA, United States. 21-27 February 2022. (oral)
- **Iles, A.,** He, P., Katis, I., Galanis, P., Sones, C. & Eason, R. W., (2022) Monitoring neurodegenerative diseases using paper based lateral-flow devices. SPIE Photonics West Optical Methods for Tumor Treatment and Detection: Mechanisms and

Techniques in Photodynamic and Photobiomodulation Therapy. San Francisco, CA, United States. 21-27 February 2022. (oral)

- **Iles, Alice**, He, Peijun, Hunbert, Maria Victoria Katis, Ioannis, John, Anto, Clark, Tristan, Christodoulides, Myron, Eason, R.W., Mccormick, Christopher and Sones, Collin (2021) Lateral flow device for the dual detection of SARS-COV 2 coronavirus nucleocapsid and spike protein: a rapid, point-of-care testing solution for COVID-19 mass screening. The 25th International Conference on Miniaturized Systems for Chemistry and Life Sciences (MicroTAS 2021), Palm Springs, CA, United States. 10 - 14 Oct 2021. (oral & poster)
- **Iles, A**., He, P., Katis, I., Galanis, P., Sones, C. & Eason, R. W., (2021) Semi-quantitative detection of the inflammatory biomarkers, C-reactive protein and procalcitonin for rapid pneumonia triage. Biosensors and Bioelectronics 30th Anniversary World Congress on Biosensors, Busan, Korea Tuesday 27 – Thursday 29 July 2021. (oral)
- **Iles, A.,** He, P., Hunbert, M. V., Katis, I., Clark, T., John, A., Christodoulides, M., Eason, R. W., McCormick, C. & Sones, C., 2021, Lateral flow device for the dual detection of SARS-CoV 2 Coronavirus Nucleocapsid and Spike protein: A large-scale, rapid, point-of-care testing solution for Covid-19. Biosensors and Bioelectronics 30th Anniversary World Congress on Biosensors, Busan, Korea Tuesday 27 – Thursday 29 July 2021. (oral)
- **Iles, A.,** He, P., Katis, I., Galanis, P., Teeling, J., Sones, C. & Eason, R. W., (2021) Paper-based point-of-care testing for monitoring progression of neurodegenerative disease using laser-patterning multiplex technology. Point-of-Care Diagnostics and Biosensors 2021 SelectBIO, Coronado Island, California on 13-15 December 2021 (oral)
- **Iles, A.,** He, P., Katis, I., Galanis, P., Sones, C. & Eason, R. W., (2020) Laser-patterned lateral-flow devices with multiple flow-paths for semi-quantitative measurement of the inflammatory biomarker, C-reactive protein. SPIE BiOS: SPIE: the International Society for Optics and Photonics San Francisco, CA, United States. 1-6 February 2020. (oral)
- Galanis, P. P., He, P. J. W., Katis, I. N., **Iles, A. H.,** Kumar J, A. J. U., Eason, R. W. & Sones, C. L. (2020) Laser patterned flow-through filters for paper-based immunoassays. Conference on Lasers and Electro-Optics Pacific Rim, CLEO-PR 2020 - Proceedings. Institute of Electrical and Electronics Engineers Inc., 9255968 (oral)

Appendix B **Biodot dispensing system**

Appendix – Biodot Dispensing system

In this appendix is detailed the mechanism and theories behind the Biodot Aspirate/Dispense system.

The BioJet Plus™ implements a combined technology consisting of high-resolution displacement with a syringe pump and a high-speed micro solenoid valve. This combination allows for precise and non-contact dispensing of nanolitre volumes of liquid. A schematic of the system can be seen in Figure 10.1.

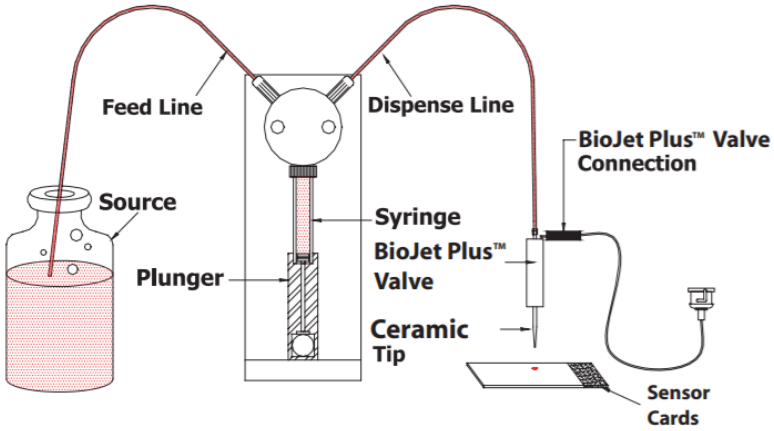

Figure 9.1 – Schematic of the BioJet Plus™ dispensing system

Typically, several of the syringe/solenoid channels are placed together, utilising two methods of liquid handling; Continuous dispensing and the aspirate dispense. During the continuous dispensing the reagent or solvent is pulled into the syringe from a larger reservoir and is then dispensed through the micro solenoid valve. This fills the system with fluid before dipping the tip of the value into the sample, withdrawing the syringe to aspirate the sample then dispensing the aspirated sample completes the aspirate/dispense process.

The dispensing system is a hydraulically driven system that requires fluid to be present from the syringe to the micro solenoid value. The dispensing process involves the following steps:

1) The syringe is displaced by a given amount
2) The value is then opened
3) Fluid is release from the valve that travels to the tip
4) The fluid increases its linear velocity as it leaves the tip and dispenses as a single drop

To ensure accuracy of the volume dispensed the system utilises a steady state pressure (SSP) within the dispensing system. It is achieved by the syringe pump driven displacement of fluid. The SSP is dependent on the displacement (size of the drop) and therefore increases with the displacement. The SSP is determined by the system compliance, which is dominated by entrapped air bubbles. Once the SSP is established, the amount of fluid displaced by the syringe pump will be equal to the volume dispensed.

The plot in Figure 10.2 shows how the SSP fluctuates during the prime, aspirate and dispensing cycle. Taken from [253].

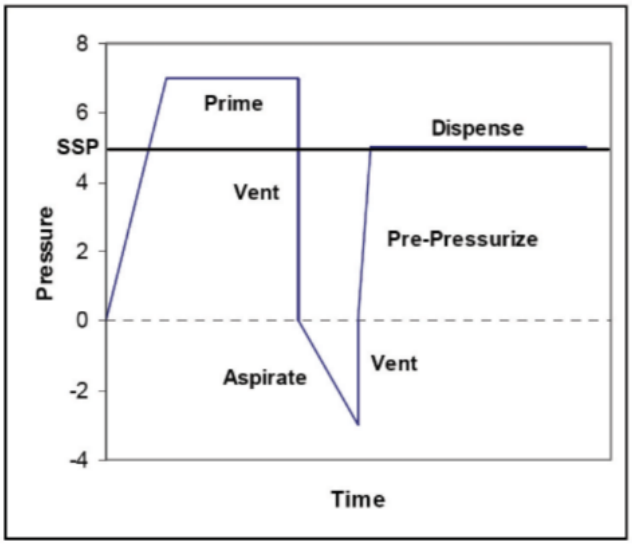

Figure 9.2 - SSP during prime, aspirate and dispensing phases of BioJet™ system.

Priming the system is used to initialize and fill the syringe pumps, micro solenoid valves of the dispense head, and the tubing that connects to the reservoir(s) with fluid. The reservoir fluid is either system fluid for aspirate/dispense of reagent, or sample fluid for continuous (line or dot) dispensing. Once the dispense system is primed, several hundred microlitres of fluid are dispensed as a stream. The resistance to the flow is caused by the valve and tip which causes the pressure within the system to become higher than desired for SSP. To achieve SSP, the valves must be open without displacing fluid (called a vent) to bring the system to ambient (zero) pressure and then the SSP can be achieved.

During aspiration, the sample is drawn from a reservoir, usually a micro-well plate, into the tip of the dispense head. The process relies on several parameters, that are set by using Syringe Speed and Channel Parameter actions. The syringe speed controls the pump dispensers and in general

slower syringe speeds are used during aspiration to prevent a large vacuum which can result in bubbles developing in the system. During aspiration a slightly negative pressure is produced, which is relieved by performing a vent on the valve. When the sample is aspirated the syringe draws fluid to the tip. As with priming SSP must be achieved, usually by venting the system. Venting is typically performed with the tip in the sample to prevent the introduction of air to the system.

AxSys^{TM} is the software program for operation of the BioDot dispensing system. The dispensing process starts with an initial homing of the platform, followed by priming and venting of the system. The prime is used to initialise the syringe pumps and the valves and ensure connection to the reservoir. The valve is vented to ensure an ambient pressure prior to SSP. The next stage is cleaning of the tip, where it is washed, vacuumed and dried. Following cleaning there are two dispensing modes; continuous dispensing and aspirate/dispense which can be chosen according to the application requirements. The experiments discussed in this thesis utilise the aspirate/dispense mode, where an additional step is required to collect the sample from a reservoir into the tip which is followed by cleaning. Next, there are several procedures that are completed prior to dispensing. This includes pre-dispense, pre-pressurisation and cleaning of the tip. This readies the system for accurate and consistent dispensing under the correct SSP. Once the system is ready the dispensing is performed for the pre-programmed volume. The final stage is homing of the platform and the dispensing tip.

Appendix C **APACHE II Score - Acute Physiology and Chronic Health Evaluation II**

Estimates intensive care unit (ICU) mortality based on a number of laboratory values and patient signs taking both acute and chronic disease into account.

It is used in the first 24 hours after patient admission to an ICU. A score from 0 to 71 is computed based on outcome of several different measurements and the higher score corresponds to a higher risk of death. The first APACHE model was presented in 1981 by Knaus et al [254].

The point score is calculated from 12 admission physiologic variables comprising the Acute Physiology Score, the patient's age, and chronic health status:

A. Acute Physiology Score (measured within 24 hours of admission)

1. AaDO2 or PaO2 (for FiO2≥0.5 or <0.5, respectively)

2. body temperature (rectal)

3. mean arterial pressure

4. blood pH

5. heart rate

6. respiratory rate

7. serum sodium

8. serum potassium

9. creatinine (Double point score for acute renal failure)

10. haematocrit

11. white blood cell count

12. Glasgow Coma Scale (15 minus actual GCS)

B. Age points

AGE (yrs)	Points
≤44	0
45-54	2
55-64	3
65-74	5
≥75	6

C. Chronic health points

If the patient has a history of severe organ system insufficiency (i.e. liver cirrhosis, portal hypertension, NYHA class IV heart failure, severe respiratory disease, dialysis dependent) or is immunocompromised (i.e. due to chemotherapy, radiation, high dose steroid therapy, or advanced leukaemia, lymphoma or AIDS) assign points as follows:

a. non-operative or emergency postoperative patients: 5 points

b. elective postoperative patients: 2 points

The score, by definition is an admission score and therefore is not recalculated during the stay, if a patient is discharged from the ICU and later readmitted, a new APACHE II score is calculated.

References

1. Insights, F.B. *Point of Care Diagnostics Market*. 2021 [cited 2022 31/01/2022]; Available from: https://www.fortunebusinessinsights.com/industry-reports/point-of-care-diagnostics-market-101072.
2. World Health Organization. Geneva, S.W., *High priority target product profiles for new tuberculosis diagnostics: report of a consensus meeting*. 2014.
3. FDA, U.S.F.a.D.A. *Aducanumab (marketed as Aduhelm) Information*. 2021 [cited 2022 Feb 2022]; Available from: https://www.fda.gov/drugs/postmarket-drug-safety-information-patients-and-providers/aducanumab-marketed-aduhelm-information#:~:text=Aduhelm%20is%20an%20amyloid%20beta,uncertainty%20about%20the%20clinical%20benefit.
4. Richards, L.A., *CAPILLARY CONDUCTION OF LIQUIDS THROUGH POROUS MEDIUMS.* Physics, 1931. **1**(5): p. 318-333.
5. Fu, E., et al., *Transport in two-dimensional paper networks.* Microfluidics and nanofluidics, 2011. **10**(1): p. 29-35.
6. Washburn, E.W., *The Dynamics of Capillary Flow.* Physical Review, 1921. **17**(3): p. 273-283.
7. Panagiotis, P.G., et al. *Laser-direct-writing to enable filtration in paper-based devices*. in *SPIE Microfluidics, BioMEMS, and Medical Microsystems XVII;*. 2019.
8. Eriksson, E., et al., *Geometric Flow Control Lateral Flow Immunoassay Devices (GFC-LFIDs): A New Dimension to Enhance Analytical Performance.* Research, 2019. **2019**: p. 8.
9. Katis, I.N., et al., *Improved sensitivity and limit-of-detection of lateral flow devices using spatial constrictions of the flow-path.* Biosensors and Bioelectronics, 2018. **113**: p. 95-100.
10. Saias, L., et al., *Design, modeling and characterization of microfluidic architectures for high flow rate, small footprint microfluidic systems.* Lab on a Chip, 2011. **11**(5): p. 822-832.
11. Xia, G., et al., *Effect of sample volume on the sensitivity of lateral flow assays through computational modeling.* Analytical Biochemistry, 2021. **619**: p. 114130.
12. Hecht, L., D. van Rossum, and A. Dietzel, *Femtosecond-laser-structured nitrocellulose membranes for multi-parameter Point-of-Care tests.* Microelectronic Engineering, 2016. **158**: p. 52-58.
13. Nguyen, V.-T., et al., *Recent advances in high-sensitivity detection methods for paper-based lateral-flow assay.* Biosensors and Bioelectronics, 2020. **152**: p. 112015.
14. Zhu, M., et al., *A highly sensitive dual-color lateral flow immunoassay for brucellosis using one-step synthesized latex microspheres.* Analytical Methods, 2019. **11**(22): p. 2937-2942.
15. Posthuma-Trumpie, G.A., et al., *Amorphous carbon nanoparticles: a versatile label for rapid diagnostic (immuno)assays.* Analytical and bioanalytical chemistry, 2012. **402**(2): p. 593-600.
16. Wang, J., et al., *Quantum Dot-Based Lateral Flow Test Strips for Highly Sensitive Detection of the Tetanus Antibody.* ACS Omega, 2019. **4**(4): p. 6789-6795.
17. Pan, M., et al., *Development of Lateral Flow Immunochromatographic Assays Using Colloidal Au Sphere and Nanorods as Signal Marker for the Determination of Zearalenone in Cereals.* Foods (Basel, Switzerland), 2020. **9**(3): p. 281.
18. Britannica, T.E.o.E. *Antibody*. Encyclopædia Britannica, 2020.
19. Lipman, N.S., et al., *Monoclonal Versus Polyclonal Antibodies: Distinguishing Characteristics, Applications, and Information Resources.* ILAR Journal, 2005. **46**(3): p. 258-268.
20. Leng, S.X., et al., *ELISA and multiplex technologies for cytokine measurement in inflammation and aging research.* The journals of gerontology. Series A, Biological sciences and medical sciences, 2008. **63**(8): p. 879-884.
21. Sones, C.L., et al., *Laser-induced photo-polymerisation for creation of paper-based fluidic devices.* Lab Chip, 2014. **14**(23): p. 4567-74.

22. He, P.J., et al., *Laser-based patterning for fluidic devices in nitrocellulose.* Biomicrofluidics, 2015. **9**(2): p. 026503.
23. He, P.J.W., et al., *Engineering fluidic delays in paper-based devices using laser direct-writing.* Lab on a Chip, 2015. **15**(20): p. 4054-4061.
24. He, P.J.W., et al., *Rapid Multiplexed Detection on Lateral-Flow Devices Using a Laser Direct-Write Technique.* Biosensors, 2018. **8**(4): p. 97.
25. He, P.J.W., et al., *Laser direct-write for fabrication of three-dimensional paper-based devices.* Lab on a Chip, 2016. **16**(17): p. 3296-3303.
26. Iles, A.H., et al., *Semi-quantitative detection of inflammatory biomarkers using a laser-patterned multiplexed lateral flow device.* Talanta, 2022. **237**: p. 122944.
27. Iles, A.H., et al., *Optimization of flow path parameters for enhanced sensitivity lateral flow devices.* Talanta, 2022: p. 123579.
28. Baroli, B., *Physicochemical characterization of photopolymerizable PLGA blends.* Adv Exp Med Biol, 2006. **585**: p. 183-96.
29. Martinez, A.W., et al., *FLASH: a rapid method for prototyping paper-based microfluidic devices.* Lab on a chip, 2008. **8**(12): p. 2146-2150.
30. Carrilho, E., A.W. Martinez, and G.M. Whitesides, *Understanding Wax Printing: A Simple Micropatterning Process for Paper-Based Microfluidics.* Analytical Chemistry, 2009. **81**(16): p. 7091-7095.
31. Lu, Y., et al., *Fabrication and characterization of paper-based microfluidics prepared in nitrocellulose membrane by wax printing.* Anal, Chem, 2010. **82**(1): p. 329-335.
32. Preechakasedkit, P., et al., *Development of an automated wax-printed paper-based lateral flow device for alpha-fetoprotein enzyme-linked immunosorbent assay.* Biosensors and Bioelectronics, 2018. **102**: p. 27-32.
33. Rivas, L., et al., *Improving sensitivity of gold nanoparticle-based lateral flow assays by using wax-printed pillars as delay barriers of microfluidics.* Lab Chip, 2014. **14**(22): p. 4406-14.
34. Yamada, K., et al., *Paper-Based Inkjet-Printed Microfluidic Analytical Devices.* Angewandte Chemie International Edition, 2015. **54**(18): p. 5294-5310.
35. Eriksson, E., et al., *Geometric Flow Control Lateral Flow Immunoassay Devices (GFC-LFIDs): A New Dimension to Enhance Analytical Performance.* Research (Washington, D.C.), 2019. **2019**: p. 8079561-8079561.
36. Schenk, F., et al., *Development of a paper-based lateral flow immunoassay for simultaneous detection of lipopolysaccharides of Salmonella serovars.* Anal Bioanal Chem, 2018. **410**(3): p. 863-868.
37. Olkkonen, J., K. Lehtinen, and T. Erho, *Flexographically printed fluidic structures in paper.* Anal Chem, 2010. **82**(24): p. 10246-50.
38. Xiao, G., et al., *A wearable, cotton thread/paper-based microfluidic device coupled with smartphone for sweat glucose sensing.* Cellulose, 2019. **26**(7): p. 4553-4562.
39. Kao, P.-K. and C.-C. Hsu, *One-step rapid fabrication of paper-based microfluidic devices using fluorocarbon plasma polymerization.* Microfluidics and Nanofluidics, 2014. **16**(5): p. 811-818.
40. Altundemir, S., A.K. Uguz, and K. Ulgen, *A review on wax printed microfluidic paper-based devices for international health.* Biomicrofluidics, 2017. **11**(4): p. 041501-041501.
41. Lu, Y., et al., *Rapid prototyping of paper-based microfluidics with wax for low-cost, portable bioassay.* Electrophoresis, 2009. **30**(9): p. 1497-500.
42. Yang, M., et al., *Inkjet-printed barcodes for a rapid and multiplexed paper-based assay compatible with mobile devices.* Lab on a Chip, 2017. **17**(22): p. 3874-3882.
43. Tortorich, R.P. and J.-W. Choi, *Inkjet Printing of Carbon Nanotubes.* Nanomaterials, 2013. **3**(3).

44. Su, W., et al., *Fully inkjet-printed microfluidics: a solution to low-cost rapid three-dimensional microfluidics fabrication with numerous electrical and sensing applications.* Scientific Reports, 2016. **6**(1): p. 35111.
45. Kaigala, G.V., et al., *Rapid prototyping of microfluidic devices with a wax printer.* Lab Chip, 2007. **7**(3): p. 384-7.
46. Hamad, E.M., et al., *Inkjet printing of UV-curable adhesive and dielectric inks for microfluidic devices.* Lab on a Chip, 2016. **16**(1): p. 70-74.
47. Frey, V., et al., *Printed FLCDs on plastic substrates.* Ferroelectrics, 2000. **246**(1): p. 131-141.
48. Al-Jumaili, A., et al., *Chapter 8 - Plasma Treatment of Polymeric Membranes*, in *Non-Thermal Plasma Technology for Polymeric Materials*, S. Thomas, et al., Editors. 2019, Elsevier. p. 211-240.
49. Galanis, P.P., et al., *Local photo-polymer deposition-assisted fabrication of multilayer paper-based devices.* Sensors and Actuators B: Chemical, 2020. **322**: p. 128574.
50. Dundas, C.M., D. Demonte, and S. Park, *Streptavidin–biotin technology: improvements and innovations in chemical and biological applications.* Applied Microbiology and Biotechnology, 2013. **97**(21): p. 9343-9353.
51. Bioquest, A. *Biotin and Streptavidin*. 2022; Available from: https://www.aatbio.com/catalog/biotin-and-streptavidin#System.
52. MacDougall, D. and W.B. Crummett, *Guidelines for data acquisition and data quality evaluation in environmental chemistry.* Analytical Chemistry, 1980. **52**: p. 2242-2249.
53. Armbruster, D.A. and T. Pry, *Limit of blank, limit of detection and limit of quantitation.* The Clinical biochemist. Reviews, 2008. **29** p. S49-S52.
54. Rohr, U.-P., et al., *The Value of In Vitro Diagnostic Testing in Medical Practice: A Status Report.* PloS one, 2016. **11**(3): p. e0149856-e0149856.
55. MR, R., *Lateral flow assay market by application, product, technique, end user—global forecast to 2023.* 2018: https://www.marketsandmarkets.com/Market-Reports/lateral-flow-assay-market-167205133.html.
56. Tsai, T.-T., et al., *Development of a multiplex and sensitive lateral flow immunoassay for the diagnosis of periprosthetic joint infection.* Scientific Reports, 2019. **9**(1): p. 15679.
57. Panhotra, B.R., et al., *Visual detection of multiple viral amplicons by dipstick assay: its application in screening of blood donors a welcome tool for the limited resource settings.* J Clin Microbiol, 2005. **43**(12): p. 6218; author reply 6218-9.
58. Corstjens, P.L.A.M., et al., *Lateral flow assay for simultaneous detection of cellular- and humoral immune responses.* Clinical biochemistry, 2011. **44**(14-15): p. 1241-1246.
59. Huang, H.S., et al., *Multiplex PCR system for the rapid diagnosis of respiratory virus infection: systematic review and meta-analysis.* Clinical Microbiology and Infection, 2018. **24**(10): p. 1055-1063.
60. Zhao, Y., et al., *Rapid multiplex detection of 10 foodborne pathogens with an up-converting phosphor technology-based 10-channel lateral flow assay.* Sci Rep, 2016. **6**: p. 21342.
61. Han, M., et al., *An octuplex lateral flow immunoassay for rapid detection of antibiotic residues, aflatoxin M1 and melamine in milk.* Sensors and Actuators B: Chemical, 2019. **292**: p. 94-104.
62. Taranova, N.A., et al., *Integration of lateral flow and microarray technologies for multiplex immunoassay: application to the determination of drugs of abuse.* Microchimica Acta, 2013. **180**(11): p. 1165-1172.
63. Dincer, C., et al., *Multiplexed Point-of-Care Testing – xPOCT.* Trends in Biotechnology, 2017. **35**(8): p. 728-742.
64. Li, J. and J. Macdonald, *Multiplexed lateral flow biosensors: Technological advances for radically improving point-of-care diagnoses.* Biosens Bioelectron, 2016. **83**: p. 177-92.

65. Hong, W., et al., *Development of an up-converting phosphor technology-based 10-channel lateral flow assay for profiling antibodies against Yersinia pestis.* J Microbiol Methods, 2010. **83**(2): p. 133-40.
66. Fenton, E.M., et al., *Multiplex lateral-flow test strips fabricated by two-dimensional shaping.* ACS Appl Mater Interfaces, 2009. **1**(1): p. 124-9.
67. Li, C.Z., et al., *Paper based point-of-care testing disc for multiplex whole cell bacteria analysis.* Biosens Bioelectron, 2011. **26**(11): p. 4342-8.
68. Zhao, Y.G., et al., *Enteric methane emissions and nitrogen utilisation efficiency for two genotype of hill hoggets offered fresh, ensiled and pelleted ryegrass.* Livestock Science, 2016. **188**: p. 1-8.
69. Zhang, H., et al., *A dye-assisted paper-based point-of-care assay for fast and reliable blood grouping.* Sci Transl Med, 2017. **9**(381).
70. Yu, Q., et al., *Gold nanoparticles-based lateral flow immunoassay with silver staining for simultaneous detection of fumonisin B1 and deoxynivalenol.* Food Control, 2015. **54**: p. 347-352.
71. Noguera, P., et al., *Carbon nanoparticles in lateral flow methods to detect genes encoding virulence factors of Shiga toxin-producing Escherichia coli.* Analytical and bioanalytical chemistry, 2011. **399**(2): p. 831-838.
72. Zhang, X., et al., *Multiplex Lateral Flow Immunoassays Based on Amorphous Carbon Nanoparticles for Detecting Three Fusarium Mycotoxins in Maize.* J Agric Food Chem, 2017. **65**(36): p. 8063-8071.
73. Carter, D.J. and R.B. Cary, *Lateral flow microarrays: a novel platform for rapid nucleic acid detection based on miniaturized lateral flow chromatography.* Nucleic acids research, 2007. **35**(10): p. e74-e74.
74. Gantelius, J., et al., *A Lateral Flow Protein Microarray for Rapid and Sensitive Antibody Assays.* International Journal of Molecular Sciences, 2011. **12**(11).
75. Gantelius, J., et al., *A lateral flow protein microarray for rapid determination of contagious bovine pleuropneumonia status in bovine serum.* Journal of Microbiological Methods, 2010. **82**(1): p. 11-18.
76. Lin, L., et al., *A multiplex lateral flow immunochromatography assay for the quantitative detection of pyraclostrobin, myclobutanil, and kresoxim-methyl residues in wheat.* Food Chemistry, 2022. **377**: p. 131964.
77. Gong, X., et al., *A review of fluorescent signal-based lateral flow immunochromatographic strips.* Journal of Materials Chemistry B, 2017. **5**(26): p. 5079-5091.
78. Song, L.W., et al., *Rapid fluorescent lateral-flow immunoassay for hepatitis B virus genotyping.* Anal Chem, 2015. **87**(10): p. 5173-80.
79. Chen, Z., et al., *Simultaneous quantitation of cytokeratin-19 fragment and carcinoembryonic antigen in human serum via quantum dot-doped nanoparticles.* Biosens Bioelectron, 2017. **91**: p. 60-65.
80. Shao, Y., et al., *Quantum dot nanobead-based multiplexed immunochromatographic assay for simultaneous detection of aflatoxin B(1) and zearalenone.* Anal Chim Acta, 2018. **1025**: p. 163-171.
81. Wu, R., et al., *Quantitative and rapid detection of C-reactive protein using quantum dot-based lateral flow test strip.* Analytica Chimica Acta, 2018. **1008**(30): p. 1-7.
82. Peng, T., et al., *Highly luminescent green-emitting Au nanocluster-based multiplex lateral flow immunoassay for ultrasensitive detection of clenbuterol and ractopamine.* Analytica Chimica Acta, 2018. **1040**: p. 143-149.
83. Wang, Y., et al., *Bio-barcode detection technology and its research applications: A review.* Journal of Advanced Research, 2019. **20**: p. 23-32.

84. Lee, J.H., et al., *Multiplex diagnosis of viral infectious diseases (AIDS, hepatitis C, and hepatitis A) based on point of care lateral flow assay using engineered proteinticles.* Biosens Bioelectron, 2015. **69**: p. 213-25.
85. Wang, W., et al., *Gold nanoparticle-based paper sensor for multiple detection of 12 Listeria spp. by P60-mediated monoclonal antibody.* Food and Agricultural Immunology, 2017. **28**(2): p. 274-287.
86. Chen, Y., et al., *Ultrasensitive Immunochromatographic Strip for Fast Screening of 27 Sulfonamides in Honey and Pork Liver Samples Based on a Monoclonal Antibody.* J Agric Food Chem, 2017. **65**(37): p. 8248-8255.
87. Di Nardo, F., et al., *Colour-encoded lateral flow immunoassay for the simultaneous detection of aflatoxin B1 and type-B fumonisins in a single Test line.* Talanta, 2019. **192**: p. 288-294.
88. Kaur, A. and S. Dhakal, *Recent applications of FRET-based multiplexed techniques.* TrAC Trends in Analytical Chemistry, 2020. **123**: p. 115777.
89. Cha, S.K., et al., *Au–Ag Core–Shell Nanoparticle Array by Block Copolymer Lithography for Synergistic Broadband Plasmonic Properties.* ACS Nano, 2015. **9**(5): p. 5536-5543.
90. Wang, Z., et al., *SERS-Activated Platforms for Immunoassay: Probes, Encoding Methods, and Applications.* Chemical Reviews, 2017. **117**(12): p. 7910-7963.
91. Sánchez-Purrà, M., et al., *Surface-Enhanced Raman Spectroscopy-Based Sandwich Immunoassays for Multiplexed Detection of Zika and Dengue Viral Biomarkers.* ACS Infectious Diseases, 2017. **3**(10): p. 767-776.
92. Wu, Z., *Simultaneous Detection ofListeria monocytogenesandSalmonella typhimuriumby a SERS-Based Lateral Flow Immunochromatographic Assay.* Food Analytical Methods, 2019. **12**(5): p. 1086-1091.
93. Sánchez-Purrà, M., et al., *Design of SERS nanotags for multiplexed lateral flow immunoassays.* Mol Syst Des Eng, 2017. **2**(4): p. 401-409.
94. Huang, Y., et al., *A universal lateral flow biosensor for proteins and DNAs based on the conformational change of hairpin oligonucleotide and its use for logic gate operations.* Biosensors and Bioelectronics, 2014. **61**: p. 598-604.
95. Chen, J., et al., *Computational Lateral Flow Biosensor for Proteins and Small Molecules: A New Class of Strip Logic Gates.* Analytical Chemistry, 2012. **84**(15): p. 6321-6325.
96. Leung, W., et al., *InfectCheck CRP barcode-style lateral flow assay for semi-quantitative detection of C-reactive protein in distinguishing between bacterial and viral infections.* Journal of Immunological Methods, 2008. **336**(1): p. 30-36.
97. Zhang, D., et al., *A naked-eye based strategy for semiquantitative immunochromatographic assay.* Analytica Chimica Acta, 2012. **740**: p. 74-79.
98. Fang, C., et al., *Barcode lateral flow immunochromatographic strip for prostate acid phosphatase determination.* Journal of Pharmaceutical and Biomedical Analysis, 2011. **56**(5): p. 1035-1040.
99. Panferov, V.G., et al., *Setting up the cut-off level of a sensitive barcode lateral flow assay with magnetic nanoparticles.* Talanta, 2017. **164**: p. 69-76.
100. Oh, Y.K., et al., *A three-line lateral flow assay strip for the measurement of C-reactive protein covering a broad physiological concentration range in human sera.* Biosensors and Bioelectronics, 2014. **61**: p. 285-289.
101. Gao, Y., et al., *An aptamer-based hook-effect-recognizable three-line lateral flow biosensor for rapid detection of thrombin.* Biosensors and Bioelectronics, 2019. **133**: p. 177-182.
102. Zangheri, M., et al., *A simple and compact smartphone accessory for quantitative chemiluminescence-based lateral flow immunoassay for salivary cortisol detection.* Biosensors and Bioelectronics, 2015. **64**: p. 63-68.
103. Mudanyali, O., et al., *Integrated rapid-diagnostic-test reader platform on a cellphone.* Lab on a chip, 2012. **12**(15): p. 2678-2686.

104. You, D.J., T.S. Park, and J.-Y. Yoon, *Cell-phone-based measurement of TSH using Mie scatter optimized lateral flow assays.* Biosensors and Bioelectronics, 2013. **40**(1): p. 180-185.
105. Lee, S., G. Kim, and J. Moon, *Performance improvement of the one-dot lateral flow immunoassay for aflatoxin B1 by using a smartphone-based reading system.* Sensors (Basel, Switzerland), 2013. **13**(4): p. 5109-5116.
106. Ruppert, C., et al., *A smartphone readout system for gold nanoparticle-based lateral flow assays: application to monitoring of digoxigenin.* Mikrochimica acta, 2019. **186**(2): p. 119-119.
107. Li, Z., et al., *Rapid and Sensitive Detection of Protein Biomarker Using a Portable Fluorescence Biosensor Based on Quantum Dots and a Lateral Flow Test Strip.* Analytical Chemistry, 2010. **82**(16): p. 7008-7014.
108. Xu, J., et al., *Converting solution viscosity to distance-readout on paper substrates based on enzyme-mediated alginate hydrogelation: Quantitative determination of organophosphorus pesticides.* Analytica Chimica Acta, 2019. **1071**: p. 1-7.
109. Xu, J., et al., *A dual-readout paper-based sensor for on-site detection of penicillinase with a smartphone.* Sensors and Actuators B: Chemical, 2021. **335**: p. 129707.
110. Pandey, A. and A.P. Galvani, *The burden of childhood pneumonia in India and prospects for control.* The Lancet Child & Adolescent Health, 2020. **4**(9): p. 643-645.
111. Silver, K.T.a.L., *Smartphone ownership is growing rapidly around the world, but not always equally*. 2019, Pew Research Center: https://www.pewresearch.org/global/2019/02/05/smartphone-ownership-is-growing-rapidly-around-the-world-but-not-always-equally/
112. Zvereva, E.A., et al., *Cut-off on demand: adjustment of the threshold level of an immunochromatographic assay for chloramphenicol.* Analytical Methods, 2015. **7**(15): p. 6378-6384.
113. Liu, F., et al., *Highly sensitive and selective lateral flow immunoassay based on magnetic nanoparticles for quantitative detection of carcinoembryonic antigen.* Talanta, 2016. **161**: p. 205-210.
114. Wang, L., et al., *A bare-eye-based lateral flow immunoassay based on the use of gold nanoparticles for simultaneous detection of three pesticides.* Microchimica Acta, 2014. **181**(13): p. 1565-1572.
115. Warriner, K., et al., *Developments in nanoparticles for use in biosensors to assess food safety and quality.* Trends in Food Science & Technology, 2014. **40**(2): p. 183-199.
116. Jain S Fau - Self, W.H., R.G. Self Wh Fau - Wunderink, and R.G. Wunderink, *Community-Acquired Pneumonia Requiring Hospitalization.* N. Engl J Med, 2015. **373**(1533-4406 (Electronic)): p. 415-427.
117. Bhuiyan, M.U., et al., *The contribution of viruses and bacteria to community-acquired pneumonia in vaccinated children: a case-control study.* Thorax, 2019. **74**(3): p. 261.
118. Póvoa, P., et al., *C-reactive protein as a marker of infection in critically ill patients.* Clinical Microbiology and Infection, 2005. **11**(2): p. 101-108.
119. Black, S., I. Kushner, and D. Samols, *C-reactive Protein.* J Biol Chem, 2004. **279**(47): p. 48487-90.
120. Meisner, M., *Update on procalcitonin measurements.* Annals of laboratory medicine, 2014. **34**(4): p. 263-273.
121. Le Bel, J., et al., *Diagnostic accuracy of C-reactive protein and procalcitonin in suspected community-acquired pneumonia adults visiting emergency department and having a systematic thoracic CT scan.* Critical Care, 2015. **19**(1): p. 366.
122. Lee, H., *Procalcitonin as a biomarker of infectious diseases.* The Korean journal of internal medicine, 2013. **28**(3): p. 285-291.

123. Schuetz, P., et al., *Procalcitonin to guide initiation and duration of antibiotic treatment in acute respiratory infections: an individual patient data meta-analysis.* Clinical infectious diseases : an official publication of the Infectious Diseases Society of America, 2012. **55**(5): p. 651-662.
124. Simon, L., et al., *Serum procalcitonin and C-reactive protein levels as markers of bacterial infection: a systematic review and meta-analysis.* Clin Infect Dis, 2004. **39**(2): p. 206-17.
125. Harbarth, S., et al., *Diagnostic value of procalcitonin, interleukin-6, and interleukin-8 in critically ill patients admitted with suspected sepsis.* Am J Respir Crit Care Med, 2001. **164**(3): p. 396-402.
126. Holm, A., et al., *Procalcitonin versus C-reactive protein for predicting pneumonia in adults with lower respiratory tract infection in primary care.* Br J Gen Pract, 2007. **57**(540): p. 555-60.
127. Keramat, F., et al., *Association of serum procalcitonin and C-reactive protein levels with CURB-65 criteria among patients with community-acquired pneumonia.* Int J Gen Med, 2018. **11**: p. 217-223.
128. Hedlund, J. and L.O. Hansson, *Procalcitonin and C-reactive protein levels in community-acquired pneumonia: correlation with etiology and prognosis.* Infection, 2000. **28**(2): p. 68-73.
129. Toikka, P.I.A., et al., *Serum procalcitonin, C-reactive protein and interleukin-6 for distinguishing bacterial and viral pneumonia in children.* The Pediatric Infectious Disease Journal, 2000. **19**(7).
130. Koczula, K.M. and A. Gallotta, *Lateral flow assays.* Essays Biochem, 2016. **60**(1): p. 111-20.
131. Kaiser, L., et al., *Small molecule detection with aptamer based lateral flow assays: Applying aptamer-C-reactive protein cross-recognition for ampicillin detection.* Scientific Reports, 2018. **8**(1): p. 5628.
132. Tholen, D., et al. *Protocols for Determination of Limits of Detection and Limits of Quantitation; Approved Guidelines*. 2004.
133. World Health Organization. Geneva, S.W., *Global Tuberculosis Report*. 2020.
134. Dheda, K., et al., *Accelerate investment and action to find the missing patients with tuberculosis.* Lancet, 2022. **399**(10341): p. 2086-2088.
135. Hong, J.M., et al., *Point-of-care diagnostic tests for tuberculosis disease.* Sci Transl Med, 2022. **14**(639): p. eabj4124.
136. Prakash, A.K., et al., *GENE-XPERT gives early diagnosis in early tuberculosis.* European Respiratory Journal, 2016. **48**(suppl 60): p. PA2775.
137. Puri, L., et al., *Xpert MTB/RIF for tuberculosis testing: access and price in highly privatised health markets.* Lancet Glob Health, 2016. **4**(2): p. e94-5.
138. Pai, M. and J. Furin, *Tuberculosis innovations mean little if they cannot save lives.* eLife, 2017. **6**: p. e25956.
139. Organisation, W.H. *Toman's Tuberculosis, Case detection, treatment, and monitoring – questions and answers*. 2004. 11-12.
140. Desikan, P., *Sputum smear microscopy in tuberculosis: is it still relevant?* The Indian journal of medical research, 2013. **137**(3): p. 442-444.
141. Kivihya-Ndugga, L.E., et al., *A comprehensive comparison of Ziehl-Neelsen and fluorescence microscopy for the diagnosis of tuberculosis in a resource-poor urban setting.* Int J Tuberc Lung Dis, 2003. **7**(12): p. 1163-71.
142. World Health Organization. Geneva, S.W. *High-priority target product profiles for new tuberculosis diagnostics: report of a consensus meeting*. 2014.
143. Wallis, R.S., et al., *Biomarkers and diagnostics for tuberculosis: progress, needs, and translation into practice.* Lancet, 2010. **375**(9729): p. 1920-37.
144. Branigan, D., *The Tuberculosis Diagnostics Pipeline Report: Advancing the Next Generation of Tools*. 2020.

145. Frascella, B., et al., *Subclinical Tuberculosis Disease—A Review and Analysis of Prevalence Surveys to Inform Definitions, Burden, Associations, and Screening Methodology.* Clinical Infectious Diseases, 2021. **73**(3): p. e830-e841.
146. Organization, W.H., *Chest radiography in Tuberculosis detection* 2016.
147. Ai4HLTH. *Stop TB Partnership and FIND*. Cited 2022; Available from: https://www.ai4hlth.org/.
148. Saktiawati, A.M.I., et al., *Sensitivity and specificity of an electronic nose in diagnosing pulmonary tuberculosis among patients with suspected tuberculosis.* PloS one, 2019. **14**(6): p. e0217963-e0217963.
149. Williams, C.M., et al., *Exhaled Mycobacterium tuberculosis output and detection of subclinical disease by face-mask sampling: prospective observational studies.* The Lancet Infectious Diseases, 2020. **20**(5): p. 607-617.
150. Garay-Baquero, D.J., et al. *Comprehensive plasma proteomic profiling reveals biomarkers for active tuberculosis*. JCI insight, 2020. **5**, DOI: 10.1172/jci.insight.137427.
151. Achkar, J.M., et al., *Host protein biomarkers identify active tuberculosis in HIV uninfected and co-infected individuals.* EBioMedicine, 2015. **2**(9): p. 1160-1168.
152. Albuquerque, V.V.S., et al., *Plasma levels of C-reactive protein, matrix metalloproteinase-7 and lipopolysaccharide-binding protein distinguish active pulmonary or extrapulmonary tuberculosis from uninfected controls in children.* Cytokine, 2019. **123**: p. 154773.
153. Ahmad, R., et al., *A rapid triage test for active pulmonary tuberculosis in adult patients with persistent cough.* Science Translational Medicine, 2019. **11**(515): p. 82-87.
154. Chegou, N.N., et al., *Diagnostic performance of a seven-marker serum protein biosignature for the diagnosis of active TB disease in African primary healthcare clinic attendees with signs and symptoms suggestive of TB.* Thorax, 2016. **71**(9): p. 785-94.
155. MacLean, E., et al., *A systematic review of biomarkers to detect active tuberculosis.* Nature Microbiology, 2019. **4**(5): p. 748-758.
156. Jacobs, R., et al., *Host biomarkers detected in saliva show promise as markers for the diagnosis of pulmonary tuberculosis disease and monitoring of the response to tuberculosis treatment.* Oncotarget, 2016. **7**(1096-0023): p. 57581-57592.
157. Yong, Y.K., et al., *Immune Biomarkers for Diagnosis and Treatment Monitoring of Tuberculosis: Current Developments and Future Prospects.* Frontiers in Microbiology, 2019. **10**: p. 2789.
158. De Groote, M.A., et al., *Discovery and Validation of a Six-Marker Serum Protein Signature for the Diagnosis of Active Pulmonary Tuberculosis.* Journal of Clinical Microbiology, 2017. **55**(10): p. 3057.
159. Esterhuyse, M.M., et al., *Epigenetics and proteomics join transcriptomics in the quest for tuberculosis biomarkers.* MBio, 2015. **6**(5): p. e01187-15.
160. Zhang, X., et al., *A proteomics approach to the identification of plasma biomarkers for latent tuberculosis infection.* Diagnostic microbiology and infectious disease, 2014. **79**(4): p. 432-437.
161. Xu, D.D., et al., *Discovery and identification of serum potential biomarkers for pulmonary tuberculosis using iTRAQ-coupled two-dimensional LC-MS/MS.* Proteomics, 2014. **14**(2-3): p. 322-331.
162. Agranoff, D., et al., *Identification of diagnostic markers for tuberculosis by proteomic fingerprinting of serum.* The Lancet, 2006. **368**(9540): p. 1012-1021.
163. Zhou, F., et al., *Protein array identification of protein markers for serodiagnosis of Mycobacterium tuberculosis infection.* Scientific reports, 2015. **5**(1): p. 1-10.
164. Xu, D., et al., *Serum protein S100A9, SOD3, and MMP9 as new diagnostic biomarkers for pulmonary tuberculosis by iTRAQ-coupled two-dimensional LC-MS/MS.* Proteomics, 2015. **15**(1): p. 58-67.

165. Penn-Nicholson, A., et al., *Discovery and validation of a prognostic proteomic signature for tuberculosis progression: a prospective cohort study.* PLoS medicine, 2019. **16**(4): p. e1002781.
166. Lawn, S.D., et al., *Resolution of the acute-phase response in West African patients receiving treatment for pulmonary tuberculosis.* Int J Tuberc Lung Dis, 2000. **4**(4): p. 340-4.
167. Schleicher, G., et al., *Procalcitonin and C-reactive protein levels in HIV-positive subjects with tuberculosis and pneumonia.* European Respiratory Journal, 2005. **25**(4): p. 688-692.
168. Polzin, A., et al., *Procalcitonin as a diagnostic tool in lower respiratory tract infections and tuberculosis.* European Respiratory Journal, 2003. **21**(6): p. 939-943.
169. Wilson, D., M. Badri, and G. Maartens, *Performance of serum C-reactive protein as a screening test for smear-negative tuberculosis in an ambulatory high HIV prevalence population.* PLoS One, 2011. **6**(1): p. e15248.
170. Wilson, D., et al., *Diagnosing smear-negative tuberculosis using case definitions and treatment response in HIV-infected adults.* The International Journal of Tuberculosis and Lung Disease, 2006. **10**(1): p. 31-38.
171. Choi, C., et al., *Role of the C-reactive protein for the diagnosis of TB among military personnel in South Korea.* The International Journal of Tuberculosis and lung disease, 2007. **11**(2): p. 233-236.
172. Breen, R., et al., *How good are systemic symptoms and blood inflammatory markers at detecting individuals with tuberculosis?* The international journal of tuberculosis and lung disease, 2008. **12**(1): p. 44-49.
173. Kang, Y.A., et al., *Role of C-reactive protein and procalcitonin in differentiation of tuberculosis from bacterial community acquired pneumonia.* The Korean journal of internal medicine, 2009. **24**(4): p. 337.
174. Sage, E., et al., *Prognostic value of C-reactive protein in HIV-infected patients with Pneumocystis jirovecii pneumonia.* International journal of STD & AIDS, 2010. **21**(4): p. 288-292.
175. Samuels, T.H.A., et al., *Evaluation of the diagnostic performance of laboratory-based c-reactive protein as a triage test for active pulmonary tuberculosis.* PLOS ONE, 2021. **16**(7): p. e0254002.
176. Yoon, C., et al., *Diagnostic accuracy of C-reactive protein for active pulmonary tuberculosis: a meta-analysis.* The international journal of tuberculosis and lung disease : the official journal of the International Union against Tuberculosis and Lung Disease, 2017. **21**(9): p. 1013-1019.
177. Yoon, C., et al., *Point-of-care C-reactive protein-based tuberculosis screening for people living with HIV: a diagnostic accuracy study.* The Lancet. Infectious diseases, 2017. **17**(12): p. 1285-1292.
178. Lawn, S., et al., *Serum C-reactive protein and detection of tuberculosis in persons co-infected with the human immunodeficiency virus.* Transactions of the Royal Society of Tropical Medicine and Hygiene, 2001. **95**(1): p. 41-42.
179. Goovaerts, O., et al., *LPS-binding protein and IL-6 mark paradoxical tuberculosis immune reconstitution inflammatory syndrome in HIV patients.* PloS one, 2013. **8**(11): p. e81856-e81856.
180. Müller, M., et al., *Immune reconstitution inflammatory syndrome in patients starting antiretroviral therapy for HIV infection: a systematic review and meta-analysis.* The Lancet Infectious Diseases, 2010. **10**(4): p. 251-261.
181. Goovaerts, O., et al., *LPS-Binding Protein and IL-6 Mark Paradoxical Tuberculosis Immune Reconstitution Inflammatory Syndrome in HIV Patients.* PLOS ONE, 2013. **8**(11): p. 81856.
182. Malle, E., S. Sodin-Semrl, and A. Kovacevic, *Serum amyloid A: an acute-phase protein involved in tumour pathogenesis.* Cell Mol Life Sci, 2009. **66**(1): p. 9-26.
183. Kedia, K., et al., *Application of multiplexed ion mobility spectrometry towards the identification of host protein signatures of treatment effect in pulmonary tuberculosis.* Tuberculosis, 2018. **112**: p. 52-61.

184. Issaq, H.J., Z. Xiao, and T.D. Veenstra, *Serum and Plasma Proteomics.* Chemical Reviews, 2007. **107**(8): p. 3601-3620.
185. Wang, Q., et al., *A multiplex immunochromatographic test using gold nanoparticles for the rapid and simultaneous detection of four nitrofuran metabolites in fish samples.* Anal Bioanal Chem, 2018. **410**(1): p. 223-233.
186. Sotnikov, D.V., A.V. Zherdev, and B.B. Dzantiev, *Theoretical and experimental comparison of different formats of immunochromatographic serodiagnostics.* Sensors (Switzerland), 2018. **18**(1).
187. Zou, K.H., A.J. O'Malley, and L. Mauri, *Receiver-Operating Characteristic Analysis for Evaluating Diagnostic Tests and Predictive Models.* Circulation, 2007. **115**(5): p. 654-657.
188. Burke, R.M., et al., *Community-based active case-finding interventions for tuberculosis: a systematic review.* The Lancet Public Health, 2021. **6**(5): p. e283-e299.
189. Bujang, M.A. and T.H. Adnan, *Requirements for Minimum Sample Size for Sensitivity and Specificity Analysis.* J Clin Diagn Res, 2016. **10**(10): p. Ye01-ye06.
190. Ariffin, N., et al., *Lateral Flow Immunoassay for Naked Eye Detection of Mycobacterium tuberculosis.* Journal of Sensors, 2020. **2020**: p. 1365983.
191. Carrio, A., et al., *Automated Low-Cost Smartphone-Based Lateral Flow Saliva Test Reader for Drugs-of-Abuse Detection.* Sensors (Basel), 2015. **15**(11): p. 29569-93.
192. Silver, K.T. and Laura, *Smartphone ownership is growing rapidly around the world, but not always equally*. 2019, Pew Research Center: https://www.pewresearch.org/global/2019/02/05/smartphone-ownership-is-growing-rapidly-around-the-world-but-not-always-equally/.
193. Jacobs, R., et al., *Identification of novel host biomarkers in plasma as candidates for the immunodiagnosis of tuberculosis disease and monitoring of tuberculosis treatment response.* Oncotarget, 2016. **7**(36): p. 57581-57592.
194. Bjerrum, S., et al., *Lateral flow urine lipoarabinomannan assay for detecting active tuberculosis in people living with HIV.* Cochrane Database Syst Rev, 2019. **10**(10): p. Cd011420.
195. Organization, W.H., *Lateral flow urine lipoarabinomannan assay (LF-LAM) for the diagnosis of active tuberculosis in people living with HIV. Policy update 2019*. 2019.
196. Zhu, N., et al., *A Novel Coronavirus from Patients with Pneumonia in China, 2019.* New England Journal of Medicine, 2020. **382**(8): p. 727-733.
197. Medema, G., et al., *Presence of SARS-Coronavirus-2 RNA in Sewage and Correlation with Reported COVID-19 Prevalence in the Early Stage of the Epidemic in The Netherlands.* Environmental Science & Technology Letters, 2020. **7**(7): p. 511-516.
198. Huang, C., et al., *Clinical features of patients infected with 2019 novel coronavirus in Wuhan, China.* The Lancet, 2020. **395**(10223): p. 497-506.
199. World Health Organization. Geneva, S.W., *Weekly Operational Update on COVID-19*. 2020: Accessed by https://www.who.int/publications/m/item/weekly-operational-update-on-covid-19---20-november-2020.
200. Zou, L., et al., *SARS-CoV-2 Viral Load in Upper Respiratory Specimens of Infected Patients.* New England Journal of Medicine, 2020. **382**(12): p. 1177-1179.
201. Sharfstein, J.M., S.J. Becker, and M.M. Mello, *Diagnostic Testing for the Novel Coronavirus.* JAMA, 2020. **323**(15): p. 1437-1438.
202. Sun, B., et al., *Kinetics of SARS-CoV-2 specific IgM and IgG responses in COVID-19 patients.* Emerging microbes & infections, 2020. **9**(1): p. 940-948.
203. Pan, Y., et al., *Serological immunochromatographic approach in diagnosis with SARS-CoV-2 infected COVID-19 patients.* Journal of Infection, 2020. **81**(1): p. e28-e32.
204. Liu, W., et al., *Evaluation of Nucleocapsid and Spike Protein-Based Enzyme-Linked Immunosorbent Assays for Detecting Antibodies against SARS-CoV-2.* Journal of Clinical Microbiology, 2020. **58**(6): p. e00461-20.

205. Cassaniti, I., et al., *Performance of VivaDiag COVID-19 IgM/IgG Rapid Test is inadequate for diagnosis of COVID-19 in acute patients referring to emergency room department.* Journal of Medical Virology, 2020. **92**(10): p. 1724-1727.
206. Woelfel, R., et al., *Clinical presentation and virological assessment of hospitalized cases of coronavirus disease 2019 in a travel-associated transmission cluster.* medRxiv, 2020: p. 2020.03.05.20030502.
207. Di, B., et al., *Monoclonal antibody-based antigen capture enzyme-linked immunosorbent assay reveals high sensitivity of the nucleocapsid protein in acute-phase sera of severe acute respiratory syndrome patients.* Clinical and diagnostic laboratory immunology, 2005. **12**(1): p. 135-140.
208. Wu, F., et al., *A new coronavirus associated with human respiratory disease in China.* Nature, 2020. **579**(7798): p. 265-269.
209. Che, X.-Y., et al., *Nucleocapsid protein as early diagnostic marker for SARS.* Emerging infectious diseases, 2004. **10**(11): p. 1947-1949.
210. Che, X.-y., et al., *Sensitive and Specific Monoclonal Antibody-Based Capture Enzyme Immunoassay for Detection of Nucleocapsid Antigen in Sera from Patients with Severe Acute Respiratory Syndrome.* Journal of Clinical Microbiology, 2004. **42**(6): p. 2629.
211. Choi, J.R., et al., *Lateral Flow Assay Based on Paper–Hydrogel Hybrid Material for Sensitive Point-of-Care Detection of Dengue Virus.* Advanced Healthcare Materials, 2017. **6**(1): p. 1600920.
212. Oem, J.K., et al., *Simple and Rapid Lateral-Flow Assay for the Detection of Foot-and-Mouth Disease Virus.* Clinical and Vaccine Immunology, 2009. **16**(11): p. 1660.
213. Lei, C., et al., *On the Calculation of TCID(50) for Quantitation of Virus Infectivity.* Virologica Sinica, 2021. **36**(1): p. 141-144.
214. Alzheimer's, A., *2019 Alzheimer's disease facts and figures.* Alzheimer's & Dementia, 2019. **15**(3): p. 321-387.
215. Mroczko, B., M. Groblewska, and A. Litman-Zawadzka, *The Role of Protein Misfolding and Tau Oligomers (TauOs) in Alzheimer's Disease (AD).* International Journal of Molecular Sciences, 2019. **20**(19).
216. Kumar, A., A. Singh, and Ekavali, *A review on Alzheimer's disease pathophysiology and its management: an update.* Pharmacological Reports, 2015. **67**(2): p. 195-203.
217. van Oostveen, W.M. and E.C.M. de Lange, *Imaging Techniques in Alzheimer's Disease: A Review of Applications in Early Diagnosis and Longitudinal Monitoring.* International Journal of Molecular Sciences, 2021. **22**(4).
218. Henriksen, K., et al., *The future of blood-based biomarkers for Alzheimer's disease.* Alzheimer's & dementia : the journal of the Alzheimer's Association, 2014. **10**(1): p. 115-131.
219. Schindler, S.E., et al., *High-precision plasma beta-amyloid 42/40 predicts current and future brain amyloidosis.* Neurology, 2019. **93**(6).
220. Rowe, C.C., et al., *Predicting Alzheimer disease with β-amyloid imaging: Results from the Australian imaging, biomarkers, and lifestyle study of ageing.* Annals of Neurology, 2013. **74**(6): p. 905-913.
221. Duits, F.H., et al., *Synaptic proteins in CSF as potential novel biomarkers for prognosis in prodromal Alzheimer's disease.* Alzheimer's research & therapy, 2018. **10**(1): p. 5-5.
222. Janelidze, S., et al., *CSF biomarkers of neuroinflammation and cerebrovascular dysfunction in early Alzheimer disease.* Neurology, 2018. **91**(9): p. 867-877.
223. Albert, M.S., et al., *The diagnosis of mild cognitive impairment due to Alzheimer's disease: recommendations from the National Institute on Aging-Alzheimer's Association workgroups on diagnostic guidelines for Alzheimer's disease.* Alzheimers Dement, 2011. **7**(3): p. 270-9.
224. Schjønning Nielsen, M., et al., *Are CSF Biomarkers Useful as Prognostic Indicators in Diagnostically Unresolved Cognitively Impaired Patients in a Normal Clinical Setting.* Dementia and geriatric cognitive disorders extra, 2016. **6**(3): p. 465-476.

225. Leonard, B.E., *Inflammation, depression and dementia: are they connected?* Neurochem Res, 2007. **32**(10): p. 1749-56.
226. Sperling, R.A., C.R. Jack, Jr., and P.S. Aisen, *Testing the right target and right drug at the right stage.* Sci Transl Med, 2011. **3**(111): p. 111cm33.
227. Weller, J. and A. Budson, *Current understanding of Alzheimer's disease diagnosis and treatment.* F1000Research, 2018. **7**: p. F1000 Faculty Rev-1161.
228. Ewers, M., M.M. Mielke, and H. Hampel, *Blood-based biomarkers of microvascular pathology in Alzheimer's disease.* Experimental gerontology, 2010. **45**(1): p. 75-79.
229. Akiyama, H., et al., *Inflammation and Alzheimer's disease.* Neurobiol Aging, 2000. **21**(3): p. 383-421.
230. Xie, J., L. Van Hoecke, and R.E. Vandenbroucke, *The Impact of Systemic Inflammation on Alzheimer's Disease Pathology.* Frontiers in Immunology, 2022. **12**.
231. McGeer, P.L., et al., *Immune system response in Alzheimer's disease.* Can J Neurol Sci, 1989. **16**(4): p. 516-27.
232. Mrak, R.E. and W.S. Griffin, *Common inflammatory mechanisms in Lewy body disease and Alzheimer disease.* J Neuropathol Exp Neurol, 2007. **66**(8): p. 683-6.
233. Tuppo, E.E. and H.R. Arias, *The role of inflammation in Alzheimer's disease.* Int J Biochem Cell Biol, 2005. **37**(2): p. 289-305.
234. Walker, K.A., B.N. Ficek, and R. Westbrook, *Understanding the Role of Systemic Inflammation in Alzheimer's Disease.* ACS Chemical Neuroscience, 2019. **10**(8): p. 3340-3342.
235. Beydoun, M.A., et al., *Clinical and Bacterial Markers of Periodontitis and Their Association with Incident All-Cause and Alzheimer's Disease Dementia in a Large National Survey.* J Alzheimers Dis, 2020. **75**(1): p. 157-172.
236. Sans, M., et al., *VCAM-1 and ICAM-1 mediate leukocyte-endothelial cell adhesion in rat experimental colitis.* Gastroenterology, 1999. **116**(4): p. 874-883.
237. Hua, S., *Targeting sites of inflammation: intercellular adhesion molecule-1 as a target for novel inflammatory therapies.* Frontiers in Pharmacology, 2013. **4**.
238. Elo, P., et al., *Vascular adhesion protein-1 is actively involved in the development of inflammatory lesions in rat models of multiple sclerosis.* Journal of Neuroinflammation, 2018. **15**(1): p. 128.
239. Rentzos, M., et al., *Serum levels of soluble intercellular adhesion molecule-1 and soluble endothelial leukocyte adhesion molecule-1 in Alzheimer's disease.* J Geriatr Psychiatry Neurol, 2004. **17**(4): p. 225-31.
240. Zuliani, G., et al., *Markers of endothelial dysfunction in older subjects with late onset Alzheimer's disease or vascular dementia.* J Neurol Sci, 2008. **272**(1-2): p. 164-70.
241. Drake, J.D., et al., *Peripheral Markers of Vascular Endothelial Dysfunction Show Independent but Additive Relationships with Brain-Based Biomarkers in Association with Functional Impairment in Alzheimer's Disease.* J Alzheimers Dis, 2021. **80**(4): p. 1553-1565.
242. Becchi, S., A. Buson, and B.W. Balleine, *Inhibition of vascular adhesion protein 1 protects dopamine neurons from the effects of acute inflammation and restores habit learning in the striatum.* Journal of Neuroinflammation, 2021. **18**(1): p. 233.
243. Zetterberg, H., et al., *Plasma tau levels in Alzheimer's disease.* Alzheimer's Research & Therapy, 2013. **5**(2): p. 9.
244. Bikkarolla, S.K., et al., *A lateral flow immunoassay with self-sufficient microfluidic system for enhanced detection of thyroid-stimulating hormone.* AIP Advances, 2020. **10**(12): p. 125316.
245. Gong, M.M. and D. Sinton, *Turning the page: advancing paper-based microfluidics for broad diagnostic application.* Chemical reviews, 2017. **117**(12): p. 8447-8480.
246. Parolo, C., et al., *Simple paper architecture modifications lead to enhanced sensitivity in nanoparticle based lateral flow immunoassays.* Lab on a Chip, 2013. **13**(3): p. 386-390.

247. Elizalde, E., R. Urteaga, and C.L.A. Berli, *Rational design of capillary-driven flows for paper-based microfluidics.* Lab on a Chip, 2015. **15**(10): p. 2173-2180.
248. Choi, J.R., et al., *Polydimethylsiloxane-Paper Hybrid Lateral Flow Assay for Highly Sensitive Point-of-Care Nucleic Acid Testing.* Anal Chem, 2016. **88**(12): p. 6254-64.
249. Wang, X., J.A. Hagen, and I. Papautsky, *Paper pump for passive and programmable transport.* Biomicrofluidics, 2013. **7**(1): p. 14107-14107.
250. Chiu, R.Y.T., et al., *Simultaneous concentration and detection of biomarkers on paper.* Lab on a Chip, 2014. **14**(16): p. 3021-3028.
251. Tsai, T.-T., et al., *Development a stacking pad design for enhancing the sensitivity of lateral flow immunoassay.* Scientific Reports, 2018. **8**(1): p. 17319.
252. Kockmann, N., *Transport Phenomena in Micro Process Engineering*. 2008, Springer. p. 163-224.
253. Biodot, I., *AD Systems Reference Manual* 2008: https://www.selectscience.net/downloads/articles/605_biojectquanti.pdf.
254. Knaus, W.A., et al., *APACHE—acute physiology and chronic health evaluation: a physiologically based classification system.* Critical Care Medicine, 1981. **9**(8).